

**Identification and Characterization of the Plasticity-Relevant
Fucose- α (1-2)Galactose Glycoproteome from Mouse Brain**

Thesis by

Heather Elizabeth Murrey

In Partial Fulfillment of the Requirements

for the Degree of

Doctor of Philosophy

California Institute of Technology

Pasadena, California

2009

(Defended 4 August 2008)

© 2009

Heather Elizabeth Murrey

All Rights Reserved

...for my family and friends who have helped me over the years...

Acknowledgments

Without the help and support of many people, both scientific and personal, the work in this thesis would not have been possible. I would first and foremost like to thank my advisor, Professor Linda Hsieh-Wilson, for her advice and guidance throughout my years here at Caltech. She has helped me develop as a scientist in all aspects of research, from experimental design to written and oral communication skills.

I would also like to thank the members of my committee, Professor Dennis Dougherty, Professor David Chan, and Professor Paul Patterson. During my candidacy and yearly meetings, I have received excellent feedback that has furthered my research. I'd also like to thank the rest of the Dougherty lab, especially Erik Rodriguez for help with scientific discussions and experimental troubleshooting. Erik has also been one of my closest friends outside of work and we've shared many memorable (and crazy!) moments together.

I would not be in the position I am in today without the support of my undergraduate advisor, Professor Irwin Levitan, who gave me an opportunity to start working in the lab as a freshman that knew nothing about scientific research. Yi Zhou was a post-doc in the lab who took me under his wing and taught me almost everything I know about molecular biology. We worked together for three and half years, during which time I learned many experimental techniques that I have carried through my graduate career.

I am also indebted to Professor's Peter S. Kim and Harvey F. Lodish at MIT, where I worked for two years after finishing my undergraduate research. I learned almost everything I know about protein biochemistry from my work in the Kim lab. I'd also like

to give a special thanks to Dr. Tsu-Shuen Tsao from the Lodish lab. He was the first person to let me take what I had learned over the years, and apply it to a new area of research. His belief in me and my ideas, built my confidence as a scientist, and our work together led to the publication of multiple papers. In addition to his help in my development as a scientist, he is also a great friend outside of the lab and is still someone I look to for advice.

I'd like to thank all members of the Hsieh-Wilson lab, both past and present, especially Cristal Gama. Cristal has been one of my best friends, and has helped me in the lab as well as outside. We have shared many wonderful as well as difficult times together, and without her help and the help of her family, I would not be where I am today. I'll always remember making tamales (did I spell it right??), eating posole (I'm sure I didn't spell that right...) and spending holidays with her and her family, they always made me feel at home and I really appreciate everything they have done for me over the years. I'd also like to thank past lab members Sarah Tully, Callie Bryan, Katie Saliba, and Tammy Campbell, all of whom I spent many a night with outside of Caltech. I'll miss pumpkin carving at the Bryan household! That was always a lot of fun. I'd like to thank newer lab members Young-In Oh, Arif Wibowo, and especially Chithra Krishnamurthy. They have become my good friends outside of the lab, and Chithra has been a wonderful partner to work with on the fucose project.

I am also indebted to the help from the animal facility here at Caltech, especially Jennifer Alex, Ana Colon, Gwen Williams, Karen Chase, and Janet Baer, all of whom have helped me maintain and care for the animals, as well as learn new experimental

techniques. I also need to thank my collaborators at GNF, Dr. Eric C. Peters and Dr. Scott Ficarro for all the hard work they put in on my experiments.

There are also many people I would like to thank outside of Caltech, including my family. My mother, sisters Kelly and Colleen, as well as my brother-in-law Matt and nephew Brody have always given me their support and have helped me tremendously over the years. In addition, my friend Cynthia Capdeville has been a great friend since high school, and continues to support me throughout my scientific endeavors. Lastly, I'd like to thank Christian St. James, for being there for me during one of the most difficult times in my life, and giving me the love and support I need to be where I am today. Thanks everyone!

Abstract

Fuc α (1-2)Gal carbohydrates have been implicated in cognitive processes such as learning and memory. However, a molecular level understanding of their functions has been lacking. This thesis describes multiple chemical and biological approaches that we have undertaken to elucidate the molecular mechanisms by which fucosyl sugars mediate neuronal communication. We demonstrate that Fuc α (1-2)Gal carbohydrates play an important role in the regulation of synaptic proteins and neuronal morphology. We identify synapsins Ia and Ib as prominent Fuc α (1-2)Gal glycoproteins in rat hippocampus, and fucosylation protects synapsin I from proteolytic degradation by the calcium-activated protease calpain. Synapsin fucosylation has important consequences on neuronal growth and morphology, with defucosylation leading to stunted neurites and delayed synapse formation. In addition, we identify the Fuc α (1-2)Gal proteome from mouse olfactory bulb using lectin affinity chromatography. We discover four major classes of Fuc α (1-2)Gal glycoproteins, including the immunoglobulin superfamily of cell adhesion molecules, ion channels and solute carriers/transporters, ATP-binding proteins, and synaptic vesicle-associated proteins. Protein fucosylation is regulated by FUT1 in mouse olfactory bulb, and olfactory bulb development is impaired in FUT1-deficient mice. In particular, FUT1 KO animals exhibit defects in the olfactory nerve and glomerular layers of olfactory sensory neurons expressing the fucosylated cell adhesion molecules NCAM and OCAM. Lastly, we explore the molecular mechanisms of protein fucosylation by metabolic labeling with alkynyl- and azido-fucose derivatives. We demonstrate that fucosylated glycoconjugates are present along both axons and dendrites

of developing neuronal cultures, as well as in the Golgi body. We identify the fucosylated proteome from cultured cortical neurons, and demonstrate that proteins such as NCAM, the MARCKS family of proteins, and the inositol 1,4,5 triphosphate receptor are fucosylated. In addition, we can label fucosylated glycans *in vivo*, which will have important consequences for studies on the dynamics of protein fucosylation in living animals. Cumulatively, our studies suggest important functional roles for fucosyl-carbohydrates in the nervous system, and implicate an extended role for fucose in the molecular mechanisms that may underlie synaptic plasticity and neuronal development.

Table of Contents

	Acknowledgments.....	iv
	Abstract.....	vii
	Table of Contents.....	ix
	List of Figures.....	x
	List of Abbreviations.....	xiv
Chapter 1	Introduction to the Role of Glycans in the Nervous System.....	1
Chapter 2	Protein Fucosylation Regulates Synapsin I Expression and Neuronal Morphology.....	17
Chapter 3	Identification of the Plasticity-Relevant Fucose α (1-2)Galactose Proteome.....	55
Chapter 4	Investigation of Fucosylation in the Olfactory Bulb of Wild-Type and FUT1 Transgenic Knockout Mice	85
Chapter 5	Investigation of Fucosylation by Metabolic Labeling with Alkynyl- and Azido-Fucose Derivatives	107
Appendix 1	Exploring Synapsin I Regulation and Fucosylation by Small Molecule Inhibitors	143
Appendix 2	Early Efforts for Identification of the Fucose α (1-2)Gal Glycoproteome	172
Appendix 3	Protein Fucosylation in FUT1 and FUT2 Transgenic Knockout Animals	189

List of Figures

Chapter 1		Page
Figure 1.1	Chemical structure of α -L-Fucose and 2'Fucosyllactose	2
Figure 1.2	Fucosyltransferases catalyze diverse fucose structures	5
Figure 1.3	Structure of Sialyl Lewis ^x	6
Figure 1.4	Chemical structures of D-galactose (Gal), 2-deoxy-D-galactose (2-dGal), D-glucose (Glc) and 2-deoxy-D-glucose (2-dGlc)	9
 Chapter 2		
Figure 2.1	Fuca(1-2)Gal glycoproteins are present at different developmental days <i>in vitro</i> (DIV)	18
Figure 2.2	Fuca(1-2)Gal glycoproteins are enriched in presynaptic nerve terminals	21
Figure 2.3	Synapsins Ia and Ib are Fuca(1-2)Gal glycoproteins	23
Figure 2.4	Loss of the fucosylated bands at 75 and 73 kDa in synapsin I KO mice confirms that synapsin I is recognized by antibody A46-B/B10	24
Figure 2.5	Treatment of bovine synapsin I with an α -(1-2)-fucosidase rapidly decreases synapsin I fucosylation levels	25
Figure 2.6	Synapsin I is fucosylated in all subcellular compartments	26
Figure 2.7	2-dGal is used by the Leloir pathway for galactose metabolism	27
Figure 2.8	Treatment of HeLa cells expressing synapsin I with 2-dGal affects synapsin fucosylation and expression levels	28
Figure 2.9	Synapsin I defucosylation decreases its cellular half-life	29
Figure 2.10	Inhibition of the calcium-activated protease calpain with calpain30 inhibitor peptide or calpeptin rescues synapsin from degradation by 2-dGal	
Figure 2.11	Defucosylation leads to synapsin I degradation and stunted neuronal growth	31
Figure 2.12	Concentration-dependence of 2-dGal on neuronal morphology	32
Figure 2.13	2-dGal induces less neurite retraction in synapsin I KO neurons	33
Figure 2.14	Domain organization of the synapsin gene family	34

Figure 2.15	Only Synapsin I is fucosylated	35
Figure 2.16	Determination of synapsin I epitope density	37
Figure 2.17	NTCB cleavage of purified synapsin I	37
Figure 2.18	Determination of synapsin I domains containing the Fuc α (1-2)Gal moiety	38
Figure 2.19	Identification of synapsin I Fuc α (1-2)Gal sites by site-directed point mutagenesis	40

Chapter 3

Figure 3.1	Fuc α (1-2)Gal glycoproteins are enriched in mammalian olfactory bulb	59
Figure 3.2	The mammalian olfactory bulb is highly enriched in expression of Fuc α (1-2)Gal glycoproteins	61
Figure 3.3	Strategy for the isolation and identification of Fuc α (1-2)Gal glycoproteins from mouse olfactory bulb	62
Figure 3.4	Silver stain of proteins isolated from the control protein A agarose-column and the UEAI column	63
Figure 3.5	All four major classes of Fuc α (1-2)Gal glycoproteins identified in MS data are confirmed by immunoblotting lectin column eluates	69

Chapter 4

Figure 4.1	FUT1 regulates expression of Fuc α (1-2)Gal in adult and neonatal mouse olfactory bulb	89
Figure 4.2	UEAI immunohistochemistry of coronal olfactory bulb sections from postnatal mice	92
Figure 4.3	Confocal images of coronal olfactory bulb slices stained with NCAM	94
Figure 4.4	Colocalization of OCAM and UEAI in the developing mouse olfactory bulb	95
Figure 4.5	Confocal fluorescence microscopy of coronal sections of the developing WT and FUT1 KO MOB	97

Chapter 5

Figure 5.1	Biorthogonal chemical reactions	108
------------	---------------------------------	-----

Figure 5.2	Chemical structures of alkynyl- and azido-Fuc with substitutions at the C6 position of the ring	109
Figure 5.3	Alkynyl- or azido-Fuc analogues are metabolized via the fucose salvage pathway and can be incorporated into glycans on the cell surface	111
Figure 5.4	Alkynyl-Fuc labeling of glycoproteins is more specific than azido-Fuc in cultured cortical neurons	112
Figure 5.5	Testing the reactions parameters for the click chemistry with alkynyl-Fuc	115
Figure 5.6	CuSO ₄ induces non-specific protein degradation	117
Figure 5.7	Strategy for the isolation and identification of alkynyl-Fuc-tagged glycoproteins from rat cortical neurons	118
Figure 5.8	Silver stain of proteins isolated from alkynyl-Fuc and Fuc labeled cortical neurons by streptavidin affinity chromatography	120
Figure 5.9	Metabolic labeling with alkynyl-Fuc in labels the cell body and neuronal processes of hippocampal cultures	123
Figure 5.10	Staining with alkynyl-Fuc labels physiologically relevant epitopes	124
Figure 5.11	Alkynyl-Fuc glycoproteins are localized along axons and dendrites, as well as in the Golgi apparatus	126
Figure 5.12	Alkynyl-Fuc glycoproteins are not highly localized to synapses	128
Figure 5.13	Intracranial administration of alkynyl-Fuc leads to direct incorporation into fucosyl glycoproteins <i>in vivo</i>	129
 Appendix 1		
Figure A1.1	Strategy for mapping of Fuc-Gal linkages	145
Figure A1.2	Deoxy-Gal treatment can potentially be used to determine oligosaccharide linkages	147
Figure A1.3	Deoxy-Gal affects Synapsin Ia deletion mutants	148
Figure A1.4	S579A-Synapsin I is degraded by 2-dGal treatment	150
Figure A1.5	GFP-S579A-Synapsin has a defect in localization to synapses	152
Figure A1.6	Autoradiography fails to detect a fucosylated glycan on synapsin I	153
Figure A1.7	Chemical structure of Brefeldin A	155
Figure A1.8	Treatment of 6 DIV cortical neurons with the Golgi trafficking inhibitor Brefeldin A for 1 DIV leads to loss of synapsin I expression and expression of the Fuc α (1-2)Gal epitope on	156

glycoproteins

Appendix 2

Figure A2.1	Optimization of antibody A46-B/B10 affinity column wash conditions	175
Figure A2.2	2-Dimensional gel electrophoresis of embryonic rat forebrain lysates	176
Figure A2.3	Immunoprecipitation confirms that tenascin C is a Fuc α (1-2)Gal glycoprotein	178

Appendix 3

Figure A3.1	Deletion of FUT1 or FUT2 does not affect neurite outgrowth	189
Figure A3.2	Neither FUT1 nor FUT2 regulates the fucose proteome recognized by antibody A46-B/B10	191
Figure A3.3	The adult mouse olfactory bulb is enriched in expression of Fuc α (1-2)Gal disaccharides and the proteome is regulated by FUT1	192
Figure A3.4	The Fuc α (1-2)Gal proteome is regulated by FUT2 in the hippocampus of adult mouse brain	193
Figure A3.5	Immunohistochemistry of adult mouse brain slices from the olfactory bulb and hippocampus	194

List of Tables

Chapter 3		Page
Table 3.1	Table of putative Fuc α (1-2)Gal glycoproteins sorted by functions	64
Table 3.2	Table of all putative Fuc α (1-2)Gal glycoproteins identified	78
 Chapter 5		
Table 5.1	Proteins identified from the alkynyl fucose proteome arranged by molecular weights and functions	120
 Appendix 2		
Table A2.1	Summary of putative Fuc α (1-2)Gal glycoproteins identified from rat cortical neuronal lysates	

List of Abbreviations

1D	one-dimensional
2D	two-dimensional
2-dGal	2-deoxy-D-galactose
2-fucosyllactose	L-fucose α (1-2)galactose β (1-4)glucose
3-dGal	3-deoxy-D-galactose
4-dGal	4-deoxy-D-galactose
6-dGal	6-deoxy-D-galactose
2-dGlc	2-deoxy-D-glucose
AAA	<i>Anguilla anguilla</i> agglutinin
Ab	antibody
Ac	acetyl, acetate
AgNO ₃	silver nitrate
AOB	accessory olfactory bulb
aq	aqueous
ATP	adenosine triphosphate
Baf. A1	bafilomycin A1
BCA	bicinchoninic acid
β -Gal	β -galactosidase
BSA	bovine serum albumin
°C	degree Celsius
CaCl ₂	calcium chloride
Cacna2d1	alpha 2/delta subunit of the dihydropyridine-sensitive channel
cAMP	cyclic adenosine monophosphate
CAMs	cell adhesion molecules
CDG	congenital disorder of glycosylation
CH ₃ CN	acetonitrile
CHCl ₃	chloroform
CHO	Chinese hamster ovary
CMF-HBSS	Calcium and Magnesium Free Hank's Balanced Salt Solution
CNS	central nervous system
CO ₂	carbon dioxide
CRMP-2	collapsin response mediator protein
CV	column volume
ddH ₂ O	double distilled water
D-Gal	D-galactose
DIV	days in vitro
DMEM	Dulbecco's Minimal Eagle's medium
DMSO	dimethylsulfoxide
DNA	deoxyribonucleic acid
DTT	dithiothreitol
E18	embryonic day 18
EBI-IPI	European Bioinformatics Institute-International Protein Index
ECL	enhance chemiluminescence

EDTA	ethylenediaminetetraacetic acid
EGTA	ethylene glycol tetraacetic acid
Endo H	endoglycosidase H
ER	endoplasmic reticulum
FCS	fetal calf serum
Fuc	L-fucose
Fuc α (1-2)Gal	fucose α (1-2) galactose
Fuc α (1-3)Gal	fucose α (1-2) galactose
Fuc α (1-4)Gal	fucose α (1-4) galactose
Fuc α (1-6)GlcNAc	fucose α (1-6) <i>N</i> -acetylglucosamine
FUT1	α (1-2) fucosyltransferase 1
FUT2	α (1-2) fucosyltransferase 2
FUT3	α (1-3,4) fucosyltransferase 3
FUT4	α (1-3,4) fucosyltransferase 4
FUT5	α (1-3) fucosyltransferase 5
FUT6	α (1-3) fucosyltransferase 6
FUT7	α (1-3) fucosyltransferase 7
FUT8	α (1-6) fucosyltransferase 8
FUT9	α (1-6) fucosyltransferase 9
FUT10	putative α (1-3) fucosyltransferase 10
FUT11	putative α (1-3) fucosyltransferase 11
g	gram, gravitational force
Gal	galactose
GalNAc	<i>N</i> -acetylgalactosamine
GDP-fucose	guanosine diphosphatyl-fucose
Glc	glucose
GlcA	D-glucuronic acid
GlcN	D-glucosamine
GlcNAc	<i>N</i> -acetylglucosamine
GluR1	glutamate receptor 1
GTP	guanosine triphosphate
h	hour
H	homogenate
HIO ₄	periodate
hnRNP	heterogeneous ribonucleoprotein
H ₂ O	water
HOAc	acetic acid
HRP	horse-radish peroxidase
Hsc/Hsp 70	heat shock chaperonin/heat shock protein 70
IACUC	institute of animal care and use committee
IgSF	immunoglobulin superfamily
IgG	immunoglobulin
IP	immunoprecipitated
K ⁺	potassium ion
K _{assoc}	association constant

KCl	potassium chloride
kDa	kilodalton
$K_3Fe(CN)_6$	potassium ferricyanide
KO	knockout
L	liter
LAC	lectin affinity chromatography
LAD II	leukocyte adhesion deficiency type II
LC/MS ⁿ	liquid-chromatography mass spectrometry
LTL	<i>Lotus tetragonolobus</i> lectin
LTP	long-term potentiation
LS1	soluble fraction of synaptosome lysis
LS2	crude synaptosol
LP1	insoluble fraction of synaptosome lysis
LP2	crude synaptic vesicle preparation
M	molar
MALDI-TOF	matrix-assisted laser desorption/ionization time-of-flight
Man	mannose
MAP2	microtubule associated protein 2
MEM	Minimal Eagle's Medium
MeOH	methanol
μ g	microgram
MG132	proteasome inhibitor
$MgCl_2$	magnesium chloride
min	minutes
m	milli or meter
μ	micro
μ Ci	micro-Curie
MOB	main olfactory bulb
mol	mole
MS	mass spectrometry
Munc18	syntaxin-binding protein
MWCO	molecular weight cut-off
n	nano
N	normal
Na^+	sodium ion
NaCl	sodium chloride
NaOH	sodium hydroxide
Na_2CO_3	sodium bicarbonate
NaN_3	sodium azide
$Na_2S_2O_3$	sodium thiosulfate
NCAM	neural cell adhesion molecule
NCBI	national center for biotechnology information
NETFD	SDS-neutralization lysis buffer
Neu5Ac	sialic acid
NH_4HCO_3	ammonium bicarbonate
NIH	national institute of health

NP-40	nonidet P-40 detergent
NPI	neuronal pentraxin I
NSF	<i>N</i> -ethylmaleimide sensitive factor
NTCB	2-nitro-5-thiocyanobenzoic acid
OCAM	olfactory cell adhesion molecule
OEt	<i>O</i> -ethyl
ONL	olfactory nerve layer
OSN	olfactory sensory neuron
P0	post-natal day 0 mouse or rat pup
P1	insoluble fraction 1
P2	insoluble fraction 2
P2'	insoluble fraction 2'; crude synaptosomes
P3	post-natal day 3 mouse or rat pup
PAGE	polyacrylamide gel electrophoresis
PBS	phosphate buffered saline
PEPCase	phosphoenolpyruvate carboxylase
PNGase F	<i>N</i> -glycosidase F
POFUT1	<i>O</i> -fucosyltransferase 1
POFUT2	<i>O</i> -fucosyltransferase 2
PSA	polysialic acid
PSD-95	post synaptic density protein 95
PTM	post-translation modification
PVDF	polyvinylidene difluoride
Rab-GDI	Rab guanine-dissociation inhibitor
RNA	ribonucleic acid
rpm	revolutions per minute
rt	room temperature
S1	soluble fraction 1
S2	soluble fraction 2
S2'	soluble fraction 2'
SDS	sodium dodecyl sulfate
Slc12a2	solute carrier family member 2
Sec1	noncatalytic α (1-2) fucosyltransferase
SEM	standard error of the mean
SG	sucrose-gradient purified synaptic vesicles
SNAP-25	synaptosomal-associated protein of 25 kDa
SynI	synapsin I
Syn KO	synapsin knockout
TBST	tris buffered saline with Tween-20
TCEP	tris(2-carboxyethyl)phosphine
TEAA	triethylammonium acetate
Tris-Cl	tris chloride
TRPV5	transient receptor potential cation channel
UEAI	<i>Ulex europeaus</i> agglutinin I
UDP	uridyl-diphosphate
UV	ultraviolet

VDAC1	voltage-dependent anion channel 1
vol	volume
w/v	weight per volume
WGA	wheat germ agglutinin
WT	wild type
Xyl	xylose

Chapter 1: Introduction to the Role of Glycans in the Nervous System¹

Introduction

The cell surface displays a complex array of oligosaccharides, glycoproteins, and glycolipids. This diverse mixture of glycans contains a wealth of information, modulating a wide range of processes such as cell migration, proliferation, transcriptional regulation, and differentiation.¹⁻⁷ Glycosylation is one of the most ubiquitous forms of post-translational modification, with more than 50 percent of the human proteome estimated to be glycosylated.⁸ Glycosylation adds another facet to the complexity of cellular signaling and expands the ability of a cell to modulate protein function. The astonishingly varied structural complexity of glycan modifications ranges from the addition of a single monosaccharide unit to polysaccharides containing hundreds of sugars in branched or linear arrays.⁹ This chemical diversity enables glycans to impart a vast array of functions, including structural stability, proteolytic protection, protein recognition, cell migration, neurite outgrowth and fasciculation, and modulation of cell signaling networks.^{3, 9-13}

Emerging evidence suggests a pivotal role for glycans in regulating nervous system development and function. For instance, glycosylation influences various neuronal processes, such as neurite outgrowth and morphology, and contributes to the molecular events that govern synaptic plasticity, a neurochemical model of learning and memory.^{9, 14, 15} Glycosylation is an efficient modulator of cell signaling and has been

¹ Portions of this chapter were taken from Murrey, H. E., and Hsieh-Wilson, L. C. *Chemical Neurobiology* *Chem. Rev.* **2008**, 108, (5), 1708-1731.

implicated in memory consolidation pathways.¹⁶⁻¹⁸ Genetic ablation of glycosylation enzymes often leads to developmental defects and can influence various organismal behaviors such as stress and cognition.¹⁹⁻²¹ Thus, the complexity of glycan functions help to orchestrate proper neuronal development during embryogenesis, as well as influence adult behaviors.

The importance of glycosylation is further highlighted by defects in glycan structures that often lead to human disease, as exhibited by the congenital disorders of glycosylation (CDG).²²⁻²⁶ These are usually inherited disorders resulting from defects in glycan biosynthesis, which are accompanied by severe developmental abnormalities, mental retardation, and difficulties with motor coordination. Such disorders highlight the importance of glycan biosynthesis in human health and development. As therapeutic treatments are currently limited, investigations into the structure-activity relationships of glycans, as well as disease-associated alterations to glycan structure, are crucial to find new therapeutic targets to treat the pathological conditions associated with GDGs. For

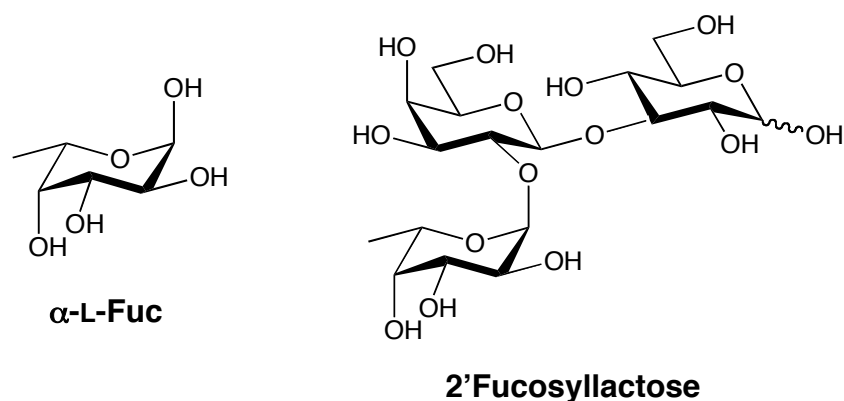


Figure 1.1. Chemical structure of α -L-Fucose and 2'fucosyllactose.

example, current treatments in the congenital disorder that has a defective enzyme that

produces a substrate for mannosyltransferase I is treated orally with mannose.⁹ Another congenital disorder that leads to a reduction in fucose glycoconjugates can also be treated orally with fucose, highlighting the importance of understanding glycan biology to develop the proper treatment for these diseases.

Glycan Biosynthesis

The wide range of glycan structures can be attached to either proteins or lipids. This diversity of structures is specific to cell type and is developmentally regulated. The carbohydrate compositions can change in the monosaccharide content and linkages within oligosaccharide chains. The monosaccharides composing glycan chains include glucose (Glc), galactose (Gal), *N*-acetylglucosamine (GlcNAc), *N*-acetylgalactosamine (GalNAc), fucose (Fuc), sialic acid (Neu5Ac), mannose (Man), glucuronic acid, and xylose (Xyl). These monosaccharides can be linked in different glycosidic bonds at different hydroxyl groups of the monosaccharides, creating significant chemical diversity in oligosaccharide structures.

Oligosaccharides are biosynthesized in the endoplasmic reticulum (ER) and Golgi compartments of the cell and can be either *N*-linked to Asn in the consensus sequence Asn-X-Ser/Thr, (where X cannot be proline), or *O*-linked to Ser and Thr residues.⁹ To date, there is no consensus sequence of *O*-linked glycosylation. *N*-linked glycans are formed by the addition of a core structure synthesized on the lipid dolichol in the ER. This core oligosaccharide is formed by the sequential addition of three Glc, nine Man, and two GlcNAc residues in different linkages where it is transferred to the core Asn on the nascent protein chain. This structure is then trimmed of the Glc residues and one

Man, and the glycoprotein then moves to the Golgi apparatus for terminal processing. This carbohydrate structure gets trimmed and the addition of new monosaccharides are added which leads to the great diversity in composition and chain length of *N*-linked glycans. Glycans in the brain are characterized by core $\alpha(1-6)$ -fucosylation, bisecting GlcNAc residues, and outer-arm $\alpha(1-3)$ -fucosylation.

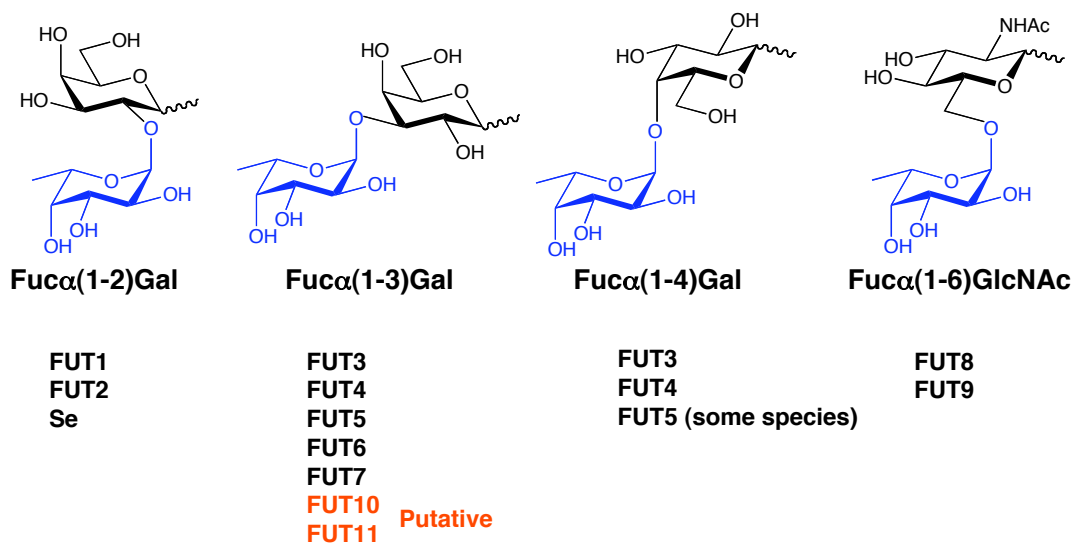
In contrast to *N*-linked glycosylation, *O*-glycosylation occurs in the Golgi apparatus with the attachment of either GalNAc or Man to Ser/Thr residues to nascent proteins.⁹ The monosaccharides are then elongated with GlcNAc, Gal, Fuc, or Neu5Ac in different structures with different linkages creating great diversity in glycan composition. *O*-linked oligosaccharides tend to be much smaller than *N*-linked glycans. However, the structural diversity in both *N*- and *O*-linked glycoconjugates is unfathomable, due to the hundreds of combinations of chain length, composition, and sugar linkages that can be present in each oligo- or polysaccharide.

α -L-Fucose

α -L-Fucose (6-deoxy-L-galactose) is generally expressed as a terminal monosaccharide on *N*- and *O*-linked glycoproteins and glycolipids. As such, it often serves as an important molecular recognition element for proteins. Fucose is distinct from other naturally occurring sugars in that it is a deoxyhexose sugar and exists exclusively in the L-configuration in nature (Figure 1.1). At least 13 human fucosyltransferases have been identified, which are responsible for the synthesis of a structurally diverse array of fucosylated glycans (Figure 1.2). Fucose is often linked to the C-2, C-3, or C-4 positions of the penultimate galactose in glycoconjugates or to the

C-6 position of the core GlcNAc residue of *N*-linked glycans.¹ *O*-Fucosylation, the direct modification of serine and threonine residues by α -L-Fuc, has also been observed on epidermal growth factor (EGF) repeats of glycoproteins such as Notch, a protein involved in cell growth and differentiation.²⁷ While Fuc is not elongated in *N*-linked and *O*-linked glycans, *O*-Fuc can be elongated by other sugars.¹

Given the structural diversity of fucosylated glycans, it is perhaps not surprising that more than a dozen different human enzymes are involved in the formation of Fuc linkages, most of which exist in the terminal Golgi compartments.¹ Two enzymes,



O-fucosyltransferases

POFUT1
POFUT2

Figure 1.2. Fucosyltransferases catalyze diverse fucose structures. Fuc is in blue and Gal or GalNAc is in black. Enzymes known to catalyze the structures are written below. FUT10 and FUT11 are putative α (1-3)fucosyltransferases.

FUT1 and FUT2, are dedicated to the synthesis of $\text{Fuca}(1-2)\text{Gal}$ glycans, an epitope

found on the ABO blood group antigens (Figure 1.2)²⁸⁻³⁰ that has also been implicated in synaptic plasticity.^{14, 31, 32} A gene homologous to FUT1 and FUT2, called Sec1, contains translational frameshifts and stop codons that interrupt potential open reading frames and thus appears to be a pseudogene.²⁸ FUT3 catalyzes the synthesis of both $\alpha(1-3)$ - and $\alpha(1-4)$ -fucosylated glycans and can transfer fucose to both Gal and GlcNAc in an oligosaccharide chain, whereas FUT4-7 form only $\alpha(1-3)$ -fucosylated glycans.^{33, 34} FUT8 and FUT9 generate Fuc $\alpha(1-6)$ GlcNAc structures, with FUT8 generally catalyzing attachment of this structure to the core Asn residue of *N*-linked oligosaccharides³⁵ and FUT9 catalyzing its attachment to a distal GlcNAc of polylactosamine chains.³⁶ FUT10 and FUT11 are putative fucosyltransferases that are reported to synthesize $\alpha(1-3)$ -fucosylated glycans based on sequence homology, although no functional studies have yet been performed.¹ Finally, POFUT1 and POFUT2, also known as *O*-fucosyltransferase 1 and *O*-fucosyltransferase 2, catalyze the direct fucosylation of

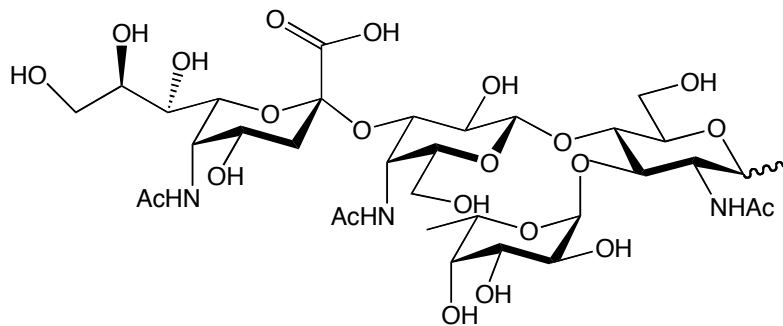


Figure 1.3. Structure of sialyl Lewis^X, an important ligand for selectin interactions.

serine/threonine residues within epidermal growth factor repeats and exist in the ER.^{37, 38}

Neurobiological functions

Fucosylated glycans play pivotal roles in various physiological and pathological processes, including leukocyte adhesion,^{39, 40} host-microbe interactions,^{41, 42} and neuronal development.^{43, 44} They are prevalent on the glycolipids of erythrocytes, where they form the ABO blood group antigens that distinguish specific blood types.³⁰ Aberrant expression of fucosylated glycoconjugates has been associated with cancer,⁴⁵⁻⁴⁸ inflammation,^{39, 49-51} and neoplastic processes.^{52, 53} For instance, the $\alpha(1-3)$ -fucosylated antigens, sialyl Lewis^X (Figure 1.3), sialyl Lewis^Y, and sialyl Lewis^B, are up-regulated in certain cancers and have been associated with advanced tumor progression and poor clinical prognosis.⁵⁴⁻⁵⁷ Moreover, the $\alpha(1-3)$ -fucosylated Lewis^X serves as a marker for neural stem cells⁵⁸ and radial glia cells that differentiate into mainly astrocytes and a small number of cortical neurons.⁵⁹ Furthermore, deficiency in fucose leads to a congenital disorder of glycosylation type IIc in humans, also known as leukocyte adhesion deficiency type II (LAD II). This disorder results in the impairment of leukocyte-vascular epithelium interactions and is characterized by immunodeficiency, developmental abnormalities, psychomotor difficulties, and deficits in mental capabilities.⁶⁰

α -L-Fucose in Neuronal Development

Although their roles in the brain are less well understood, fucosylated glycans have been implicated in neural development, learning, and memory. *O*-Fucosylation is essential for the activity of Notch, a transmembrane receptor protein that controls a broad range of cell-fate decisions during development.^{18, 61-65} Studies suggest that fucose modulates Notch signaling either by inducing a conformational change in the protein or

by interacting directly with Notch ligands.^{64, 66} Notch signaling is believed to be involved in neuronal progenitor maintenance, and governs the cell-fate decision between neuronal and glial lineages. Notch signaling may also contribute to the behavior of differentiated neurons and neuronal migration.⁶⁷ Genetic deletion of the POFUT1 gene is embryonic lethal in mice and causes developmental defects similar to those observed upon deletion of Notch receptors, including abnormal vasculogenesis, somitogenesis, and neurogenesis.^{68, 69} These studies demonstrate the importance of fucose in proper neuronal development and implicate Notch fucosylation as an important mediator of these events.

In addition to Notch, the Lewis^X epitope is reported to play roles in neurite outgrowth and neuronal migration during development of the central nervous system. The Lewis^X epitope is involved in neurite outgrowth of *Xenopus* tadpoles⁷⁰ and participates in several cell-cell interactions in the early neural development of chicks and rats.^{71, 72} Deletion of the FUT9 gene, which synthesizes the Lewis^X epitope, leads to anxiety-related behaviors in mice, suggesting that abnormal neuronal development may have phenotypic effects in the adult organism.^{73, 74}

α -L-Fucose in Learning and Memory

Multiple studies have suggested a role for fucosylation in learning and memory. For instance, incorporation of fucose into glycoconjugates in the brain was significantly enhanced by task-dependent learning in both chicks and rats.^{15, 75-77} Rats were trained in a brightness discrimination task, in which animals learned to enter a bright chamber while avoiding a dark one while chicks learned to avoid pecking a bitter-tasting bead. Trained animals demonstrated an increase in [³H]-labeled fucose incorporation into

glycoconjugates at synapses, the specialized sites of communication between neurons.^{15,}

⁷⁶ Moreover, exogenous application of L-fucose or 2'-fucosyllactose (Figure 1.1) enhanced long-term potentiation (LTP), an electrophysiological model for learning and memory, both *in vivo* and in hippocampal slices.^{78, 79}

Fucose is highly enriched at neuronal synapses,^{14, 80, 81} where the majority of the fucosylated glycoconjugates exist as complex, *N*-linked structures.⁸² Studies indicate that the activity of fucosyltransferases increases during synaptogenesis⁸³ and upon passive-avoidance training in animals.⁸⁴ Moreover, the cellular machinery involved in protein glycosylation can be found within dendrites,⁸⁵ raising the intriguing possibility that local protein synthesis and fucosylation may be occurring at synapses in response to neuronal stimulation.

Further studies have specifically implicated $\text{Fuca}(1-2)\text{Gal}$ (Figure 1.2) linkages in neuronal communication processes. For instance, 2-deoxy-D-galactose (2-dGal; Figure 1.4), which competes with native galactose for incorporation into glycan chains and thus prevents the formation of $\text{Fuca}(1-2)\text{Gal}$ linkages,⁸⁶ has been shown to induce reversible amnesia in animals.^{32, 86, 87} In contrast, other small molecule sugars such as 2-deoxy-D-

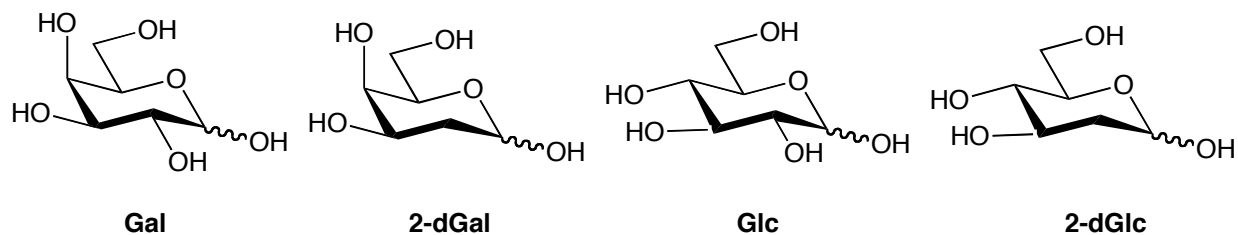


Figure 1.4. Chemical structures of D-galactose (Gal), 2-deoxy-D-galactose (2-dGal), D-glucose (Glc) and 2-deoxy-D-glucose (2-dGlc).

glucose, Gal, or Glc (Figure 1.4) had no effect, suggesting a unique function for Fuc α (1-2)Gal –containing oligosaccharides. 2-dGal has also been reported to interfere with the maintenance of LTP, both *in vitro* and *in vivo*.^{88, 89} Furthermore, a monoclonal antibody specific for Fuc α (1-2)Gal⁹⁰ significantly impaired memory formation in animals, presumably by blocking formation of the Fuc α (1-2)Gal epitope.³¹

Conclusions

Glycan structures are prevalent in the disease pathogenesis that underlies a variety of cognitive problems associated with a range of congenital disorders. Understanding these disorders requires extensive analysis of the molecular mechanisms that perpetuate these diseases. Furthermore, the monosaccharide α -L-Fuc has also been shown to enhance memory formation, especially through the Fuc α (1-2)Gal epitope suggesting that cognitive problems associated with fucose-deficiency may be due to defects in the synthesis of this disaccharide. Despite these intriguing behavioral and molecular responses for α -L-Fuc in disease and cognitive function, the precise mechanisms by which fucosyl carbohydrates exert their functional effects has been largely uncharacterized. This thesis describes our approach to elucidate these mechanisms by identifying and characterizing Fuc α (1-2)Gal glycoproteins from mammalian brain.

References

1. Becker, D. J.; Lowe, J. B., Fucose: biosynthesis and biological function in mammals. *Glycobiology* **2003**, 13, (7), 41-53.
2. Vosseller, K.; Wells, L.; Hart, G. W., Nucleocytoplasmic O-glycosylation: O-GlcNAc and functional proteomics. *Biochimie* **2001**, 83, (7), 575-581.
3. Rexach, J. E.; Clark, P. M.; Hsieh-Wilson, L. C., Chemical approaches to understanding O-GlcNAc glycosylation in the brain. *Nat. Chem. Biol.* **2008**, 4, (2), 97-106.
4. Gama, C. I.; Hsieh-Wilson, L. C., Chemical approaches to deciphering the glycosaminoglycan code. *Curr. Op. Chem. Biol.* **2005**, 9, (6), 609-619.
5. Rampal, R.; Luther, K. B.; Haltiwanger, R. S., Notch signaling in normal and disease states: Possible therapies related to glycosylation. *Curr. Mol. Med.* **2007**, 7, (4), 427-445.
6. Gabius, H. J.; Andre, S.; Kaltner, H.; Siebert, H. C., The sugar code: functional lectinomics. *Biochim. Biophys. Acta* **2002**, 1572, (2-3), 165-177.
7. Nishihira, J., Novel pathophysiological aspects of macrophage migration inhibitory factor (Review). *Int. J. Mol. Med.* **1998**, 2, (1), 17-28.
8. Apweiler, R.; Hermjakob, H.; Sharon, N., On the frequency of protein glycosylation, as deduced from analysis of the SWISS-PROT database. *Biochim. Biophys. Acta* **1999**, 1473, (1), 4-8.
9. Kleene, R.; Schachner, M., Glycans and neural cell interactions. *Nat. Rev. Neurosci.* **2004**, 5, (3), 195-208.
10. Wujek, P.; Kida, E.; Walus, M.; Wisniewski, K. E.; Golabek, A. A., N-glycosylation is crucial for folding, trafficking, and stability of human tripeptidyl-peptidase I. *J. Biol. Chem.* **2004**, 279, (13), 12827-12839.
11. Rudd, P. M.; Merry, A. H.; Wormald, M. R.; Dwek, R. A., Glycosylation and prion protein. *Curr. Op. Struct. Biol.* **2002**, 12, (5), 578-586.
12. Yamaguchi, H., Chaperone-like functions of N-glycans in the formation and stabilization of protein conformation. *Trends Glycosci. Glycotech.* **2002**, 14, (77), 139-151.
13. Wells, L.; Vosseller, K.; Hart, G. W., Glycosylation of nucleocytoplasmic proteins: signal transduction and O-GlcNAc. *Science* **2001**, 291, (5512), 2376-2378.
14. Murrey, H. E.; Gama, C. I.; Kalovidouris, S. A.; Luo, W. I.; Driggers, E. M.; Porton, B.; Hsieh-Wilson, L. C., Protein fucosylation regulates synapsin Ia/lb expression and neuronal morphology in primary hippocampal neurons. *Proc. Natl. Acad. Sci. USA* **2006**, 103, (1), 21-26.
15. McCabe, N. R.; Rose, S. P. R., Passive-avoidance training increases fucose incorporation into glycoproteins in chick forebrain slices in vitro. *Neurochem. Res.* **1985**, 10, (8), 1083-1095.
16. Hanover, J. A., Glycan-dependent signaling: O-linked N-acetylglucosamine. *FASEB J.* **2001**, 15, (11), 1865-1876.

17. Sandi, C.; Rose, S. P. R.; Mileusnic, R.; Lancashire, C., Corticosterone facilitates long-term-Memory formation via enhanced glycoprotein-synthesis. *Neuroscience* **1995**, 69, (4), 1087-1093.
18. Stanley, P., Regulation of Notch signaling by glycosylation. *Curr. Op. Struct. Biol.* **2007**, 17, (5), 530-535.
19. Jaeken, J.; Matthijs, G., Congenital disorders of glycosylation: A rapidly expanding disease family. *Ann. Rev. Genom. Human Gen.* **2007**, 8, 261-278.
20. Ohtsubo, K.; Marth, J. D., Glycosylation in cellular mechanisms of health and disease. *Cell* **2006**, 126, (5), 855-867.
21. Best, T.; Kemps, E.; Bryan, J., Effects of saccharides on brain function and cognitive performance. *Nut. Rev.* **2005**, 63, (12), 409-418.
22. Di Rocco, M.; Hennet, T.; Grubenmann, C. E.; Pagliardini, S.; Allegri, A. E. M.; Frank, C. G.; Aebi, M.; Vignola, S.; Jaeken, J., Congenital disorder of glycosylation (CDG) Ig: Report on a patient and review of the literature. *J. Inher. Metab. Disease* **2005**, 28, (6), 1162-1164.
23. Endo, T.; Toda, T., Glycosylation in congenital muscular dystrophies. *Biol. Pharm. Bulletin.* **2003**, 26, (12), 1641-1647.
24. Lowe, J. B.; Marth, J. D., A genetic approach to mammalian glycan function. *Ann. Rev. Biochem.* **2003**, 72, 643-691.
25. Marquardt, T.; Denecke, J., Congenital disorders of glycosylation: review of their molecular bases, clinical presentations and specific therapies. *Eur. J. Pediat.* **2003**, 162, (6), 359-379.
26. Schachter, H., Congenital disorders involving defective *N*-glycosylation of proteins. *Cell. Mol. Life Sci.* **2001**, 58, (8), 1085-1104.
27. Moloney, D. J.; Shair, L. H.; Lu, F. M.; Xia, J.; Locke, R.; Matta, K. L.; Haltiwanger, R. S., Mammalian Notch1 is modified with two unusual forms of *O*-linked glycosylation found on epidermal growth factor-like modules. *J. Biol. Chem.* **2000**, 275, (13), 9604-9611.
28. Kelly, R. J.; Rouquier, S.; Giorgi, D.; Lennon, G. G.; Lowe, J. B., Sequence and expression of a candidate for the human secretor blood-group alpha(1,2)fucosyltransferase gene (Fut2) - homozygosity for an enzyme-inactivating nonsense mutation commonly correlates with the non-secretor phenotype. *J. Biol. Chem.* **1995**, 270, (9), 4640-4649.
29. Larsen, R. D.; Ernst, L. K.; Nair, R. P.; Lowe, J. B., Molecular-cloning, sequence, and expression of a human GDP-L-fucose - beta-D-galactoside 2-alpha-L-fucosyl-transferase CDNA that can form the H-blood group antigen. *Proc. Natl. Acad. Sci. USA* **1990**, 87, (17), 6674-6678.
30. Lowe, J. B., The blood group-specific human glycosyltransferases. *Baillieres Clin. Haematol.* **1993**, 6, (2), 465-492.
31. Jork, R.; Smalla, K. H.; Karsten, U.; Grecksch, G.; Ruthrich, H. L.; Matthies, H., Monoclonal-antibody specific for histo-blood group antigens-H (type-2 and type-4) interferes with long-term-memory formation in rats. *Neurosci. Res. Comm.* **1991**, 8, (1), 21-27.
32. Rose, S. P. R.; Jork, R., Long-term-memory formation in chicks is blocked by 2-deoxygalactose, a fucose analog. *Behav. Neural Biol.* **1987**, 48, (2), 246-258.

33. Kaneko, M.; Kudo, T.; Iwasaki, H.; Ikehara, Y.; Nishihara, S.; Nakagawa, S.; Sasaki, K.; Shiina, T.; Inoko, H.; Saitou, N.; Narimatsu, H., alpha 1,3-fucosyltransferase IX (Fuc-TIX) is very highly conserved between human and mouse; molecular cloning, characterization and tissue distribution of human Fuc-TIX. *FEBS Lett.* **1999**, 452, (3), 237-242.
34. Natsuka, S.; Lowe, J. B., Enzymes involved in mammalian oligosaccharide biosynthesis. *Curr. Op. Struct. Biol.* **1994**, 4, (5), 683-691.
35. Miyoshi, E.; Noda, K.; Yamaguchi, Y.; Inoue, S.; Ikeda, Y.; Wang, W. G.; Ko, J. H.; Uozumi, N.; Li, W.; Taniguchi, N., The alpha 1-6-fucosyltransferase gene and its biological significance. *Biochim. Biophys. Acta* **1999**, 1473, (1), 9-20.
36. Nishihara, S.; Iwasaki, H.; Kaneko, M.; Tawada, A.; Ito, M.; Narimatsu, H., alpha 1,3-fucosyltransferase 9 (FUT9; Fuc-TIX) preferentially fucosylates the distal GlcNAc residue of polylactosamine chain while the other four alpha 1,3FUT members preferentially fucosylate the inner GlcNAc residue. *FEBS Lett.* **1999**, 462, (3), 289-294.
37. Luo, Y.; Koles, K.; Vorndam, W.; Haltiwanger, R. S.; Panin, V. M., Protein O-fucosyltransferase 2 adds O-fucose to thrombospondin type 1 repeats. *J. Biol. Chem.* **2006**, 281, (14), 9393-9399.
38. Wang, Y.; Shao, L.; Shi, S. L.; Harris, R. J.; Spellman, M. W.; Stanley, P.; Haltiwanger, R. S., Modification of epidermal growth factor-like repeats with O-fucose - Molecular cloning and expression of a novel GDP-fucose protein O-fucosyltransferase. *J. Biol. Chem.* **2001**, 276, (43), 40338-40345.
39. Springer, T. A., Traffic Signals for Lymphocyte Recirculation and Leukocyte Emigration - the Multistep Paradigm. *Cell* **1994**, 76, (2), 301-314.
40. Lowe, J. B., Selectin ligands, leukocyte trafficking, and fucosyltransferase genes. *Kidney Int.* **1997**, 51, (5), 1418-1426.
41. Hooper, L. V.; Gordon, J. I., Glycans as legislators of host-microbial interactions: spanning the spectrum from symbiosis to pathogenicity. *Glycobiol.* **2001**, 11, (2), 1R-10R.
42. Guruge, J. L.; Falk, P. G.; Lorenz, R. G.; Dans, M.; Wirth, H. P.; Blaser, M. J.; Berg, D. E.; Gordon, J. I., Epithelial attachment alters the outcome of *Helicobacter pylori* infection. *Proc. Natl. Acad. Sci. USA* **1998**, 95, (7), 3925-3930.
43. Li, Y. X.; Li, L.; Irvine, K. D.; Baker, N. E., Notch activity in neural cells triggered by a mutant allele with altered glycosylation. *Development* **2003**, 130, (13), 2829-2840.
44. Sasamura, T.; Sasaki, N.; Miyashita, F.; Nakao, S.; Ishikawa, H. O.; Ito, M.; Kitagawa, M.; Harigaya, K.; Spana, E.; Bilder, D.; Perrimon, N.; Matsuno, K., Neurotic, a novel maternal neurogenic gene, encodes an O-fucosyltransferase that is essential for Notch-Delta interactions. *Development* **2003**, 130, (20), 4785-4795.
45. Block, T. M.; Comunale, M. A.; Lowman, M.; Steel, L. F.; Romano, P. R.; Fimmel, C.; Tennant, B. C.; London, W. T.; Evans, A. A.; Blumberg, B. S.; Dwek, R. A.; Mattu, T. S.; Mehta, A. S., Use of targeted glycoproteomics to identify serum glycoproteins that correlate with liver cancer in woodchucks and humans. *Proc. Natl. Acad. Sci. USA* **2005**, 102, (3), 779-784.

46. Wang, J. W.; Ambros, R. A.; Weber, P. B.; Rosano, T. G., Fucosyl-transferase and alpha-L-fucosidase activities and fucose levels in normal and malignant endometrial tissue. *Cancer Res.* **1995**, 55, (16), 3654-3658.
47. Yazawa, S.; Nakamura, J.; Asao, T.; Nagamachi, Y.; Sagi, M.; Matta, K. L.; Tachikawa, T.; Akamatsu, M., Aberrant Alpha-1-]2fucosyltransferases Found in Human Colorectal-Carcinoma Involved in the Accumulation of Le(B) and Y-Antigens in Colorectal L Tumors. *Jpn. J. Cancer Res.* **1993**, 84, (9), 989-995.
48. Thompson, S.; Dargan, E.; Turner, G. A., Increased fucosylation and other carbohydrate changes in haptoglobin in ovarian-cancer. *Cancer Lett.* **1992**, 66, (1), 43-48.
49. Lowe, J. B., Glycan-dependent leukocyte adhesion and recruitment in inflammation. *Curr. Op. Cell Biol.* **2003**, 15, (5), 531-538.
50. Vestweber, D.; Blanks, J. E., Mechanisms that regulate the function of the selectins and their ligands. *Physiol. Rev.* **1999**, 79, (1), 181-213.
51. Butcher, E. C.; Picker, L. J., Lymphocyte homing and homeostasis. *Science* **1996**, 272, (5258), 60-66.
52. Listinsky, J. J.; Siegal, G. P.; Listinsky, C. M., alpha-L-fucose - A potentially critical molecule in pathologic processes including neoplasia. *Am. J. Clin. Pathol.* **1998**, 110, (4), 425-440.
53. Macartney, J. C., Fucose-containing antigens in normal and neoplastic human gastric-mucosa - a comparative-study using lectin histochemistry and blood-group immunohistochemistry. *J. Pathol.* **1987**, 152, (1), 23-30.
54. Kim, Y. J.; Borsig, L.; Varki, N. M.; Varki, A., P-selectin deficiency attenuates tumor growth and metastasis. *Proc. Natl. Acad. Sci. USA* **1998**, 95, (16), 9325-9330.
55. Orntoft, T. F.; Vestergaard, E. M., Clinical aspects of altered glycosylation of glycoproteins in cancer. *Electrophoresis* **1999**, 20, (2), 362-371.
56. Kim, Y. J.; Varki, A., Perspectives on the significance of altered glycosylation of glycoproteins in cancer. *Glycocon. J.* **1997**, 14, (5), 569-576.
57. Miyake, M.; Taki, T.; Hitomi, S.; Hakomori, S., Correlation of expression of H/Le(Y)/Le(B) antigens with survival in patients with carcinoma of the lung. *N. Engl. J. Med.* **1992**, 327, (1), 14-18.
58. Capela, A.; Temple, S., LeX/ssea-1 is expressed by adult mouse CNS stem cells, identifying them as nonependymal. *Neuron* **2002**, 35, (5), 865-875.
59. Mo, Z. C.; Moore, A. R.; Filipovic, R.; Ogawa, Y.; Kazuhiro, I.; Antic, S. D.; Zecevic, N., Human cortical neurons originate from radial glia and neuron-restricted progenitors. *J. Neurosci.* **2007**, 27, (15), 4132-4145.
60. Yakubenia, S.; Wild, M. K., Leukocyte adhesion deficiency II - Advances and open questions. *FEBS J.* **2006**, 273, (19), 4390-4398.
61. Artavanis-Tsakonas, S.; Rand, M. D.; Lake, R. J., Notch signaling: Cell fate control and signal integration in development. *Science* **1999**, 284, (5415), 770-776.
62. Rampal, R.; Arboleda-Velasquez, J. F.; Nita-Lazar, A.; Kosik, K. S.; Haltiwanger, R. S., Highly conserved O-fucose sites have distinct effects on Notch1 function. *J. Biol. Chem.* **2005**, 280, (37), 32133-32140.

63. Lei, L.; Xu, A. G.; Panin, V. M.; Irvine, K. D., An O-fucose site in the ligand binding domain inhibits Notch activation. *Development* **2003**, 130, (26), 6411-6421.
64. Haines, N.; Irvine, K. D., Glycosylation regulates notch signalling. *Nat. Rev. Mol. Cell Biol.* **2003**, 4, (10), 786-797.
65. Okajima, T.; Irvine, K. D., Regulation of notch signaling by O-linked fucose. *Cell* **2002**, 111, (6), 893-904.
66. Kao, Y. H.; Lee, G. F.; Wang, Y.; Starovasnik, M. A.; Kelley, R. F.; Spellman, M. W.; Lerner, L., The effect of O-fucosylation on the first EGF-like domain from human blood coagulation factor VII. *Biochemistry* **1999**, 38, (22), 7097-7110.
67. Louvi, A.; Artavanis-Tsakonas, S., Notch signalling in vertebrate neural development. *Nat. Rev. Neurosci.* **2006**, 7, (2), 93-102.
68. Lu, L. C.; Stanley, P., Roles of O-fucose glycans in notch signaling revealed by mutant mice. In *Functional Glycomics*, 2006; Vol. 417, pp 127-136.
69. Shi, S. L.; Stanley, P., Protein O-fucosyltransferase 1 is an essential component of Notch signaling pathways. *Proc. Natl. Acad. Sci. USA* **2003**, 100, (9), 5234-5239.
70. Yoshida-Noro, C.; Heasman, J.; Goldstone, K.; Vickers, L.; Wylie, C., Expression of the Lewis group carbohydrate antigens during *Xenopus* development. *Glycobiology* **1999**, 9, (12), 1323-1330.
71. Osanai, T.; Chai, W. G.; Tajima, Y.; Shimoda, Y.; Sanai, Y.; Yuen, C. T., Expression of glycoconjugates bearing the Lewis X epitope during neural differentiation of P19 EC cells. *FEBS Letters* **2001**, 488, (1-2), 23-28.
72. Boubelik, M.; Draberova, L.; Draber, P., Carbohydrate-mediated sorting in aggregating embryonal carcinoma cells. *Biochem. Biophys. Res. Comm.* **1996**, 224, (2), 283-288.
73. Kudo, T.; Fujii, T.; Ikegami, S.; Inokuchi, K.; Takayama, Y.; Ikehara, Y.; Nishihara, S.; Togayachi, A.; Takahashi, S.; Tachibana, K.; Yuasa, S.; Narimatsu, H., Mice lacking alpha 1,3-fucosyltransferase IX demonstrate disappearance of Lewis x structure in brain and increased anxiety-like behaviors. *Glycobiology* **2007**, 17, (1), 1-9.
74. Nishihara, S.; Iwasaki, H.; Nakajima, K.; Togayachi, A.; Ikehara, Y.; Kudo, T.; Kushi, Y.; Furuya, A.; Shitara, K.; Narimatsu, H., alpha 1,3-fucosyltransferase IX (Fut9) determines Lewis X expression in brain. *Glycobiology* **2003**, 13, (6), 445-455.
75. Sukumar, R.; Rose, S. P. R.; Burgoyne, R. D., Increased incorporation of [H-3]fucose into chick brain glycoproteins following training on a passive-avoidance task. *J. Neurochem.* **1980**, 34, (4), 1000-1006.
76. Pohle, W.; Acosta, L.; Ruthrich, H.; Krug, M.; Matthies, H., Incorporation of [H-3] fucose in rat hippocampal structures after conditioning by perforant path stimulation and after LTP-producing tetanization. *Brain Res.* **1987**, 410, (2), 245-256.
77. Bullock, S.; Rose, S. P. R.; Zamani, R., Characterization and regional localization of presynaptic and postsynaptic glycoproteins of the chick forebrain showing changed fucose incorporation following passive-avoidance training. *J. Neurochem.* **1992**, 58, (6), 2145-2154.

78. Krug, M.; Wagner, M.; Staak, S.; Smalla, K. H., Fucose and fucose-containing sugar epitopes enhance hippocampal long-term potentiation in the freely moving rat. *Brain Res.* **1994**, 643, (1-2), 130-135.
79. Matthies, H.; Staak, S.; Krug, M., Fucose and fucosyllactose enhance in-vitro hippocampal long-term potentiation. *Brain Res.* **1996**, 725, (2), 276-280.
80. Zanetta, J.-P.; Reeber, A.; Vincendon, G.; Gombos, G., Synaptosomal plasma membrane glycoproteins. II. Isolation of fucosyl-glycoproteins by affinity chromatography on the *Ulex europaeus* lectin specific for L-fucose. *Brain Res.* **1977**, 138, 317-328.
81. Krusius, T.; Finne, J., Structural features of tissue glycoproteins - fractionation and methylation analysis of glycopeptides derived from rat-brain, kidney and liver. *Eur. J. Biochem.* **1977**, 78, (2), 369-379.
82. Taniguchi, T.; Adler, A. J.; Mizuochi, T.; Kochibe, N.; Kobata, A., The structures of the asparagine-linked sugar chains of bovine interphotoreceptor retinol-binding protein - occurrence of fucosylated hybrid-type oligosaccharides. *J. Biol. Chem.* **1986**, 261, (4), 1730-1736.
83. Matsui, Y.; Lombard, D.; Massarelli, R.; Mandel, P.; Dreyfus, H., Surface glycosyltransferase activities during development of neuronal cell-cultures. *J. Neurochem.* **1986**, 46, (1), 144-150.
84. Popov, N.; Schmidt, S.; Schulzeck, S.; Jork, R.; Lossner, B.; Matthies, H., Changes in activities of fucokinase and fucosyl-transferase in rat hippocampus after acquisition of a brightness-discrimination reaction. *Pharmacol. Biochem. Behav.* **1983**, 19, (1), 43-47.
85. Gardiol, A.; Racca, C.; Triller, A., Dendritic and postsynaptic protein synthetic machinery. *J. Neurosci.* **1999**, 19, (1), 168-179.
86. Bullock, S.; Potter, J.; Rose, S. P. R., Effects of the amnesic agent 2-deoxygalactose on incorporation of fucose into chick brain glycoproteins. *J. Neurochem.* **1990**, 54, (1), 135-142.
87. Lorenzini, C. G. A.; Baldi, E.; Bucherelli, C.; Sacchetti, B.; Tassoni, G., 2-deoxy-D-galactose effects on passive avoidance memorization in the rat. *Neurobiol. Learn Mem.* **1997**, 68, (3), 317-324.
88. Matthies, H.; Kretlow, J.; Smalla, K. H.; Staak, S.; Krug, M., Glycosylation of proteins during a critical time window is necessary for the maintenance of longterm potentiation in the hippocampal CA1 region. *Neuroscience* **1999**, 91, (1), 175-183.
89. Krug, M.; Jork, R.; Reymann, K.; Wagner, M.; Matthies, H., The Amnesic substance 2-deoxy-D-galactose suppresses the maintenance of hippocampal LTP. *Brain Res.* **1991**, 540, (1-2), 237-242.
90. Karsten, U.; Pilgrim, G.; Hanisch, F. G.; Uhlenbruck, G.; Kasper, M.; Stosiek, P.; Papsdorf, G.; Pasternak, G., A new monoclonal-antibody (A46-B/B10) highly specific for the blood group-H type-2 epitope - generation, epitope analysis, serological and histological-evaluation. *Brit. J. Cancer* **1988**, 58, (2), 176-181.

Chapter 2: Protein Fucosylation Regulates Synapsin I Expression and Neuronal Morphology¹

Background

Experimental studies suggest that protein fucosylation can be regulated in response to synaptic activity. Both task-specific learning and LTP have been shown to induce the fucosylation of proteins at the synapse.^{1, 2} Furthermore, the activity of fucosyltransferases, enzymes involved in the transfer of fucose to glycoproteins, has also been demonstrated to increase substantially during synaptogenesis³ and upon passive avoidance training in animals.⁴ Together, these studies suggest that protein fucosylation may be a highly regulated process in the brain and may contribute to neuronal development and synaptic plasticity. Despite these intriguing observations, little is known about the molecular mechanisms by which Fuc α (1-2)Gal sugars influence neuronal communication. Moreover, no Fuc α (1-2)Gal glycoproteins had been characterized from the brain, and the precise roles of this sugar in regulating the structure and function of neuronal proteins was unknown.

¹ Portions of this chapter were taken from Murrey, HE,; Gama, CI,; Kalovidouris, SA,; Luo, WI,; Driggers, EM,; Porton, B,; and Hsieh-Wilson, LC,; Protein fucosylation regulates synapsin Ia/Ib expression and neuronal morphology in primary hippocampal neurons. *Proc. Natl. Acad. Sci. USA* **2006**, 103, (1), 21-26.

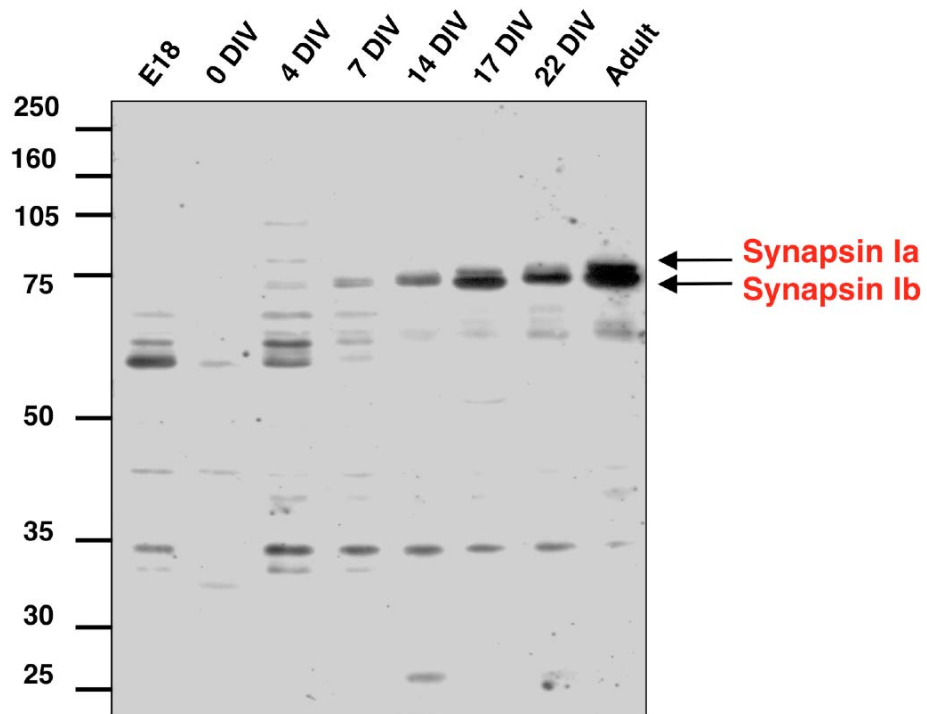


Figure 2.1. Fuc α (1-2)Gal glycoproteins are present at different developmental days *in vitro* (DIV). Expression of fucosylated glycoproteins changes during the course of neuronal development. Synapsins Ia and Ib the predominant glycoproteins expressed in mature neuronal cultures and adult hippocampus.

Here, we show that Fuc α (1-2)Gal carbohydrates are expressed on several glycoproteins during neuronal development. We demonstrate that synapsin Ia and Ib are the predominant Fuc α (1-2)Gal glycoproteins expressed in the adult rat hippocampus. We also present molecular insights into the function of the Fuc α (1-2)Gal epitope in regulating neuronal proteins, demonstrating that fucosylation increases the cellular half-life of synapsin in cells and modulates neurite outgrowth. Our studies suggest important

roles for the Fuc α (1-2)Gal epitope in the regulation of synaptic proteins and the morphological changes that may underlie synaptic plasticity.

Expression of Fuc α (1-2)Gal on Glycoproteins in the Hippocampus

We investigated whether Fuc α (1-2)Gal glycoproteins are present in the hippocampus, a brain structure important for spatial learning and memory.⁵ Cell lysates from adult rat hippocampus, embryonic day 18 (E18) hippocampus, and cultured embryonic hippocampal neurons were analyzed by Western blotting using an antibody (A46-B/B10) selective for Fuc α (1-2)Gal.⁶ Antibody A46-B/B10 has been shown to induce amnesia in animals,^{6,7} suggesting that it recognizes one or more physiologically relevant epitopes. We found that the Fuc α (1-2)Gal epitope is present on several different proteins during neuronal development (Figure 2.1). In E18 hippocampal tissue, three major glycoproteins of approximately 35, 60, and 65 kDa are prominently observed, whose expression is significantly reduced in the adult hippocampus. In contrast, glycoproteins of approximately 73 and 75 kDa are found in mature cultured neurons and in adult brain tissue. Interestingly, expression of Fuc α (1-2)Gal is observed on multiple proteins in developing neurons cultured for 4 and 7 days *in vitro* (DIV), periods when axons, dendrites and functional synapses are being formed, suggesting a putative role for these glycoproteins in the regulation of these processes. Thus, expression and/or fucosylation of Fuc α (1-2)Gal glycoproteins appears to change dramatically during the course of neuronal development.

Fuc α (1-2)Gal Is Enriched at Synapses

In collaboration with Cristal Gama, we next investigated the subcellular localization of Fuc α (1-2)Gal sugars in neurons. Hippocampal neurons were cultured for 14 DIV to allow for synapse formation and were subsequently fixed, permeabilized and co-immunostained with antibody A46-B/B10 and an antibody against the neuronal marker tubulin. The Fuc α (1-2)Gal epitope exhibited a punctate pattern consistent with enriched localization to neuronal synapses (Figure 2.2A). To examine whether the sugar was present at pre- or postsynaptic terminals, neurons were co-immunostained for Fuc α (1-2)Gal and the presynaptic marker synapsin I or the postsynaptic marker spinophilin. We observed Fuc α (1-2)Gal labeling in a subpopulation of the synapses ($58 \pm 2\%$; $n = 350$), overlapping with synapsin-positive puncta (Figure 2.2B) and generally apposing spinophilin-positive puncta (Figure 2.2C). Membrane de-lipidation did not alter the immunostaining pattern, which confirms the staining of glycoproteins rather than glycolipids (data not shown). These findings indicate that Fuc α (1-2)Gal sugars are enriched on glycoproteins in presynaptic nerve terminals. The lack of complete co-localization of synapsin I-positive puncta with antibody A46-B/B10 may suggest that only a certain subset of synapses contain Fuc α (1-2)Gal glycoproteins.

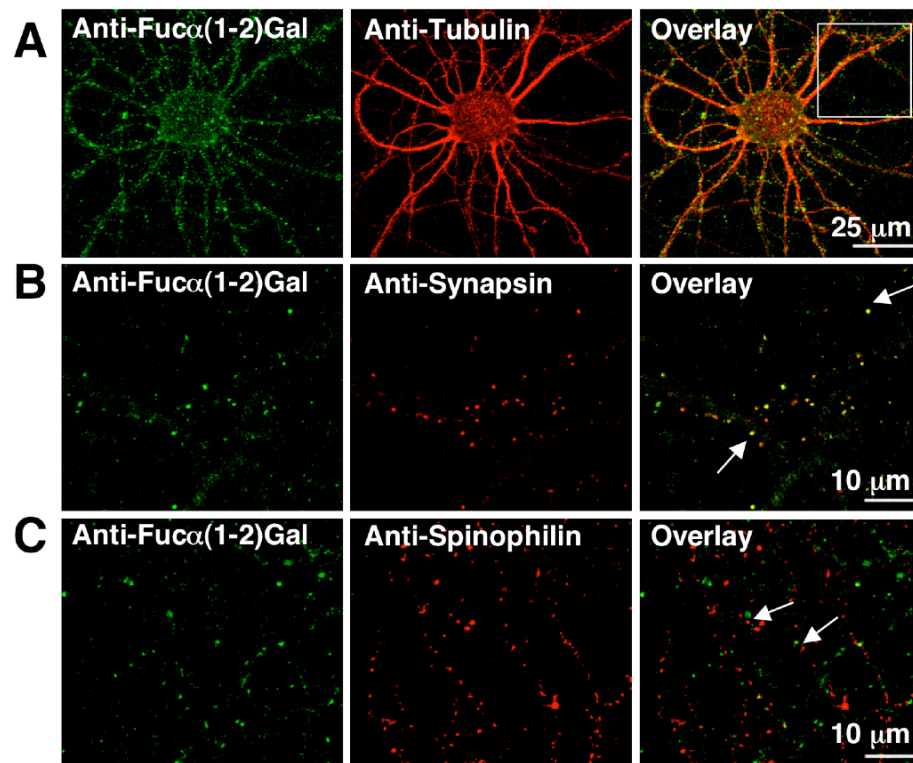


Figure 2.2. Fuc α (1-2)Gal glycoproteins are enriched in presynaptic nerve terminals. Co-immunostaining of 14 DIV neurons with antibody A46-B/B10 (green) and tubulin (red, A), the presynaptic marker synapsin I (red, B), and the postsynaptic marker spinophilin (red, C). B and C are equivalent in area to the white rectangle in A. White arrows point to overlap of Fuc α (1-2)Gal with synapsin (B) or apposition to the postsynaptic marker spinophilin (C). Image courtesy of Cristal Gama.

Synapsin Ia and Ib Are the Major Fuc α (1-2)Gal Glycoproteins in the Hippocampus

We next sought to identify neuronal glycoproteins modified by the Fuc α (1-2)Gal epitope. Attempts to purify Fuc α (1-2)Gal glycoproteins from brain extracts using antibody A46-B/B10 were unsuccessful due to the relatively weak binding affinity of the antibody for the carbohydrate epitope (data not shown). In collaboration with Wen-I. Luo, we circumvented these challenges, by identifying potential glycoproteins using a

combination of subcellular fractionation, gel electrophoresis, and matrix-assisted laser desorption/ionization time-of-flight mass spectrometry (MALDI-TOF MS). Adult rat hippocampal lysates were enriched in synaptic proteins using standard subcellular fractionation procedures. The crude synaptosomal fractions were resolved by 1-D or 2-D gel electrophoresis and analyzed by Western blotting with antibody A46-B/B10 or stained with Coomassie Brilliant Blue. As observed previously, two major glycoproteins of approximately 73 and 75 kDa were recognized by antibody A46-B/B10. Proteins of interest were identified by immunoblotting and the corresponding bands were excised from a Coomassie-stained gel, digested with trypsin, and identified by matrix-assisted laser desorption/ionization time-of-flight mass spectrometry (MALDI-TOF MS). MS analysis revealed three potential Fuc α (1-2)Gal-containing glycoproteins: synapsin Ia, synapsin Ib, and *N*-ethylmaleimide-sensitive factor (NSF). Eleven measured peptides matched the masses calculated from the National Center for Biotechnology Information (NCBI) non-redundant database for both synapsins Ia and Ib with greater than 50 ppm accuracy, and the unmodified matching peptides covered 11.2% of the amino acid sequence (data not shown). For NSF, 24 peptides were detected within 50 ppm, which provided 29.7% overall sequence coverage (data not shown).

To establish whether synapsin Ia/ Ib and NSF were indeed recognized by antibody A46-B/B10, each protein was immunoprecipitated and examined by Western blotting with antibody A46-B/B10 in collaboration with Wen-I. Luo. Upon immunoprecipitation, synapsins Ia and Ib were specifically detected by the antibody, whereas NSF was not recognized (Figure 2.3A). In addition, loss of the fucosylated bands corresponding to synapsins Ia and Ib was observed by Western blot analysis of adult hippocampal lysates

from synapsin I-deficient mice, confirming that synapsin Ia and Ib are the predominant Fuc α (1-2)Gal glycoproteins (Figure 2.4). Treatment of purified synapsin I with PNGaseF and EndoH, enzymes that cleave *N*-linked oligosaccharides from proteins, did not abolish the interaction with antibody A46-B/B10, which suggests that the Fuc α (1-

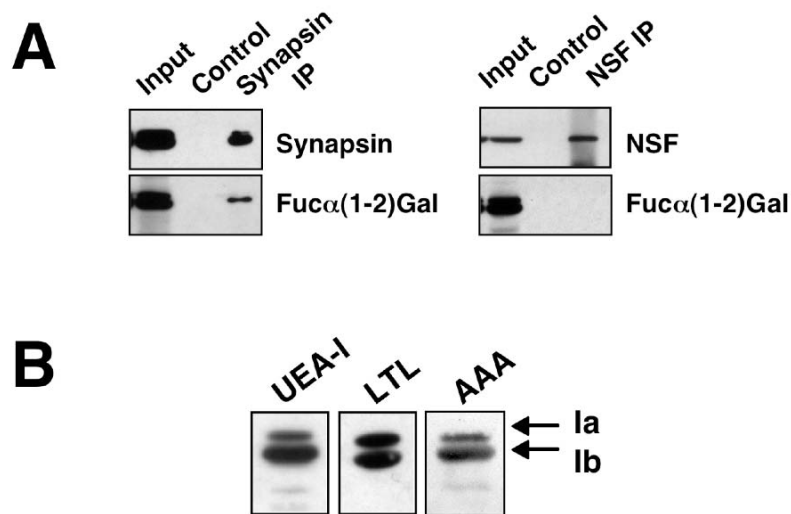


Figure 2.3. Synapsins Ia and Ib are Fuc α (1-2)Gal glycoproteins. (A) Immunoprecipitation of synapsin and NSF demonstrates that synapsin is specifically recognized by antibody A46-B/B10. (B) Lectin immunoblotting with fucose-specific lectins confirms the presence of a fucosyl oligosaccharide on synapsins Ia and Ib. Figure 2.3 (A) courtesy of Wen-I. Luo.

2)Gal moiety is present on an *O*-linked glycan (data not shown). Together, these studies suggest that synapsin Ia and Ib are glycosylated with an *O*-linked fucosyl oligosaccharide.

Characterization of the Carbohydrate Structure on Synapsin

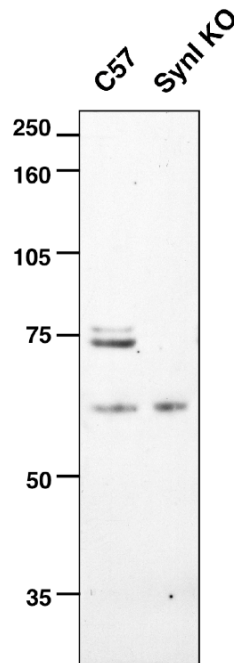


Figure 2.4. Loss of the fucosylated bands at 75 and 73 kDa in synapsin I KO mice confirms that synapsin I is recognized by antibody A46-B/B10.

Having identified the synapsins, we turned our attention to establishing the presence of the $\text{Fuca}(1-2)\text{Gal}$ epitope. As an independent confirmation to recognition by antibody A46-B/B10, we examined the ability of α -L-fucose-specific lectins to bind to synapsin. *Lotus tetragonolobus* lectin (LTL) and *Ulex europeaus* agglutinin lectin (UEA-I) have been reported to interact strongly with terminal $\text{Fuca}(1-2)\text{Gal}$ carbohydrates, whereas *Anguilla anguilla* lectin (AAA) prefers $\text{Fuca}(1-3)\text{Gal}$ carbohydrates and interacts only weakly with $\text{Fuca}(1-2)\text{Gal}$.⁸ Consistent with the presence of a $\text{Fuca}(1-2)\text{Gal}$ moiety on synapsin, both LTL and UEA-I readily detected synapsins Ia and Ib (Figure 2.3B). However, AAA also recognized synapsin, indicating that lectins cannot be used to determine the nature of the fucose-galactose linkage on synapsin.

As fucosidases have been shown to hydrolyze specific glycosidic linkages, we next treated synapsins Ia and Ib with an α -(1-2)-fucosidase or an α -(1-3,4)-fucosidase

from *Xanthomonas manihotis*. Rapid deglycosylation of synapsin was observed upon treatment with the α -(1-2)-fucosidase (Figure 2.5). In contrast, the α -(1-3,4)-fucosidase, which hydrolyzes both $\text{Fuca}(1-3)$ and $\text{Fuca}(1-4)$ linkages, had no effect on the fucosylation levels of synapsin, even after 6 h of treatment (Figure 2.5 and data not shown). Together, these results provide strong evidence that synapsin Ia and Ib are covalently modified by the critical $\text{Fuca}(1-2)\text{Gal}$ epitope.

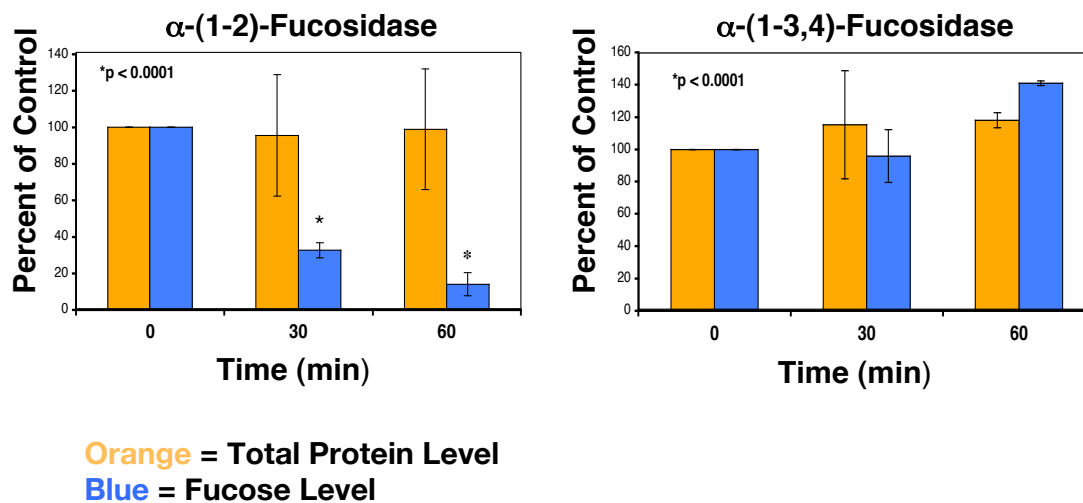


Figure 2.5. Treatment of bovine synapsin I with an α -(1-2)-fucosidase rapidly decreases synapsin I fucosylation levels as determined by immunoblotting and densitometry analysis with anti-synapsin and antibody A46-B/B10 (left panel). In contrast, an α -(1-3,4)-fucosidase failed to remove fucose from synapsin I (right panel), confirming the presence of a $\text{Fuca}(1-2)\text{Gal}$ epitope on synapsin.

Synapsin I Is Fucosylated in Various Subcellular Compartments

We next investigated the extent of fucosylation on neuronal synapsin I. Subcellular fractions of rat forebrain lysates were analyzed for the levels of fucosylated or total synapsin (Figure 2.6A). Fucosylated synapsin was present in all subcellular fractions containing synapsin. Moreover, the relative level of fucosylated synapsin to

total synapsin was equivalent in the fractions examined. Quantitative analysis revealed that the membrane-associated to soluble ratio (LP2:LS2) of fucosylated synapsin was similar to that of synapsin (39:1 and 38:1 for fucosylated synapsin and synapsin, respectively; Figure 2.6B). These results suggest that neuronal synapsin is extensively fucosylated in various subcellular compartments and that fucosylation does not alter the subcellular localization of synapsin.

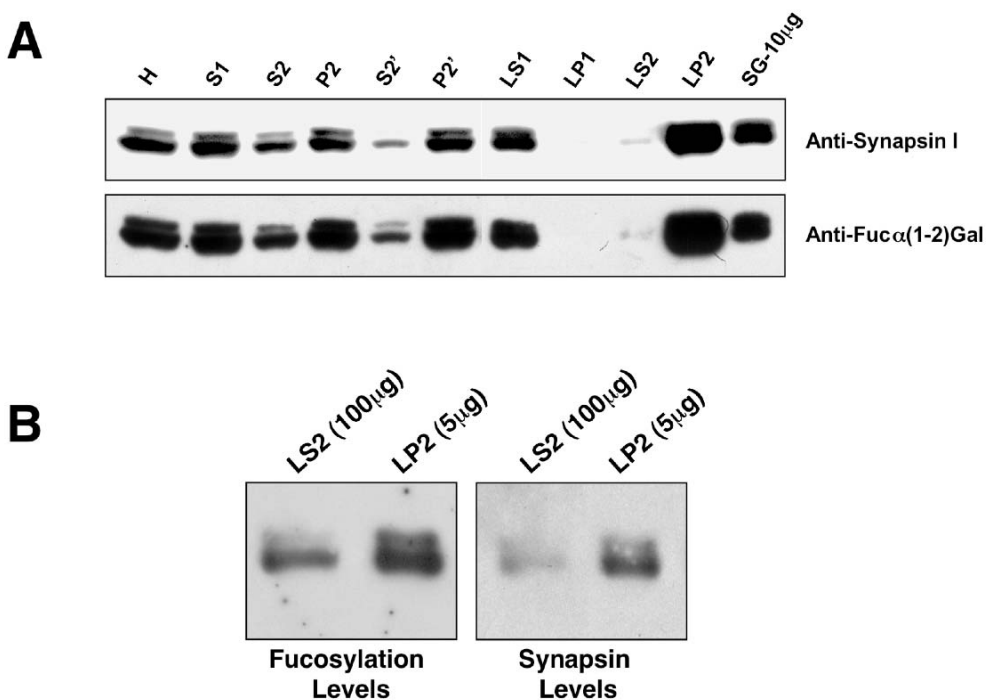


Figure 2.6. (A) Synapsin I is fucosylated in all subcellular compartments. 100 μ g of total fractions were loaded H=homogenate, S1, S2, S2' are soluble fractions, P2=insoluble fraction, P2'=crude synaptosomes LS1=soluble fraction from synaptosome lysis, LP1=insoluble fraction from synaptosome lysis, LS2=synaptosol, LP2=crude synaptic vesicles, SG=synaptic vesicles after sucrose gradient purification (B) Densitometry analysis of soluble (LS2) versus membrane-associated (LP2) suggests that synapsin I is fucosylated to equivalent degrees in these subcellular fractions.

Inhibiting Synapsin Fucosylation Significantly Decreases Its Cellular Half-Life

To investigate the impact of fucosylation on the functional properties of synapsin, we inhibited the fucosylation of synapsin in cells using 2-dGal. 2-dGal has previously been shown to prevent the fucosylation of glycoproteins.⁹ Upon cellular uptake, 2-dGal is converted via the Leloir pathway to the corresponding activated uridyl diphosphate (UDP) analogue (Figure 2.7A).^{9, 10} UDP-2-deoxy-galactose competes with UDP-galactose for incorporation into glycan chains and thereby terminates the chain by preventing formation of the $\text{Fuca}(1-2)\text{Gal}$ linkage.⁹

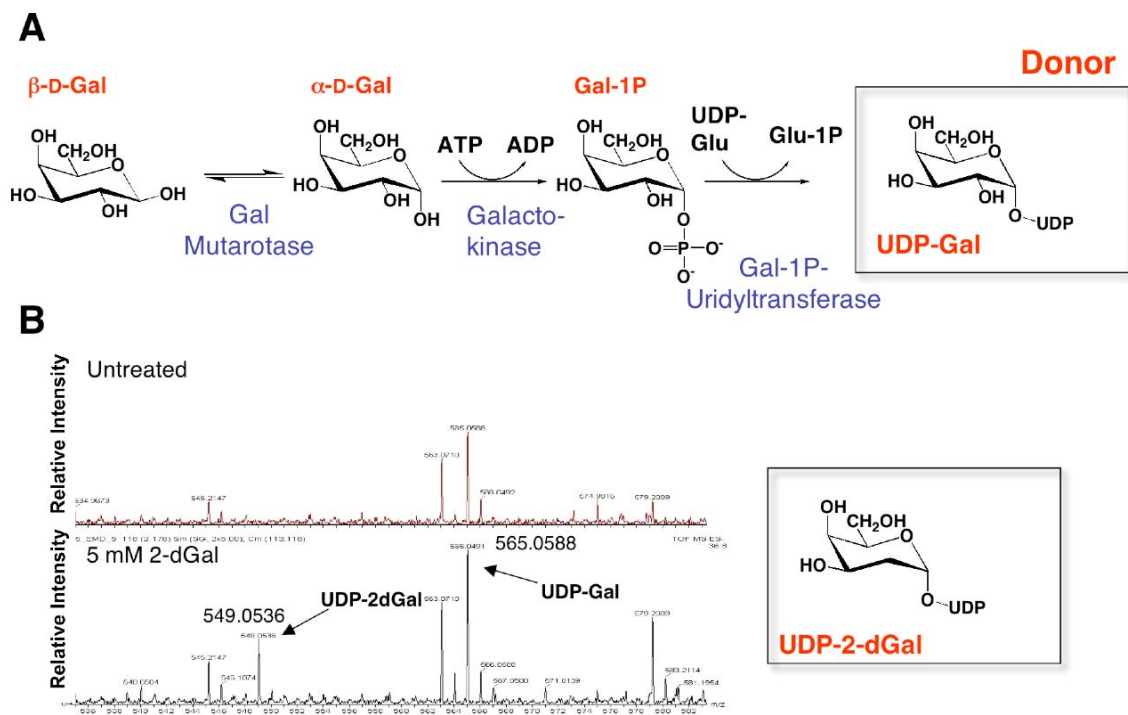


Figure 2.7. (A) Leloir pathway for galactose metabolism. (B) UDP-2-dGal is formed in cells treated with 2-dGal as determined by LC-MS.

We first established that incubation of HeLa cells with 2-dGal leads to the biosynthesis of UDP-2-deoxy-galactose. Sugars were extracted from HeLa cells treated with 2-dGal, and analyzed by liquid chromatography MS (LC-MS). We observed significant formation of UDP-2-deoxy-galactose by LC-MS analysis of sugar extracts,

demonstrating that 2-dGal is an efficient unnatural substrate for the Leloir pathway enzymes (Figure 2.7B). We next investigated the effects of 2-dGal on synapsin I expressed in HeLa cells. Cell lysates containing equivalent amounts of transfected

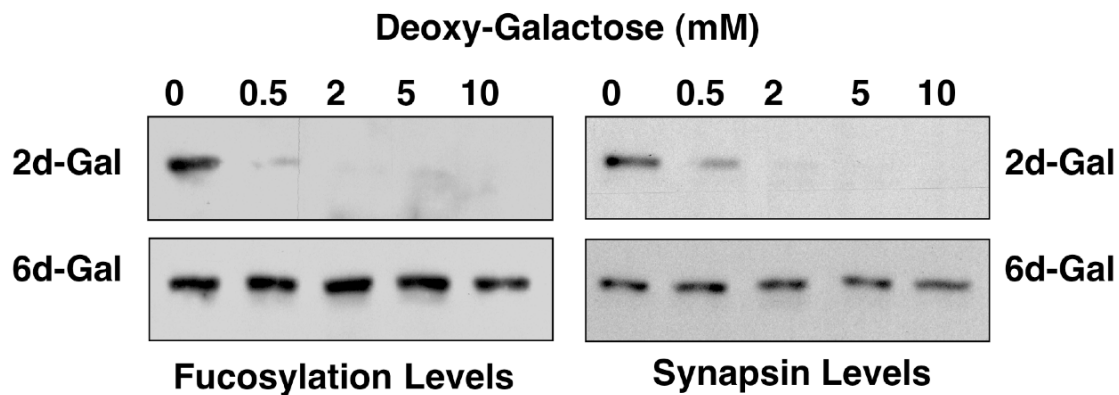


Figure 2.8. Treatment of HeLa cells expressing synapsin I with 2-dGal affects synapsin fucosylation and expression levels (top panels). Treatment with 6-dGal has no effect (bottom panels).

protein were resolved by SDS-PAGE, and the fucosylation and protein levels of synapsin were measured by immunoblotting. Consistent with the presence of a $\text{Fuc}\alpha(1-2)\text{Gal}$ epitope on synapsin, 2-dGal had a dramatic effect on the fucosylation level of synapsin (Figure 2.8). Surprisingly, the 2-dGal treatment also led to a significant decrease in the level of synapsin protein. The effects appear to be specific to 2-dGal, as treatment with other deoxy-galactose sugars, including 6-deoxy-D-galactose (6-dGal), had no effect on either the fucosylation or protein levels of synapsin (Figure 2.8 and data not shown). Thus, 2-dGal was found to specifically affect synapsin levels and fucosylation specifically through the C2 position of galactose.

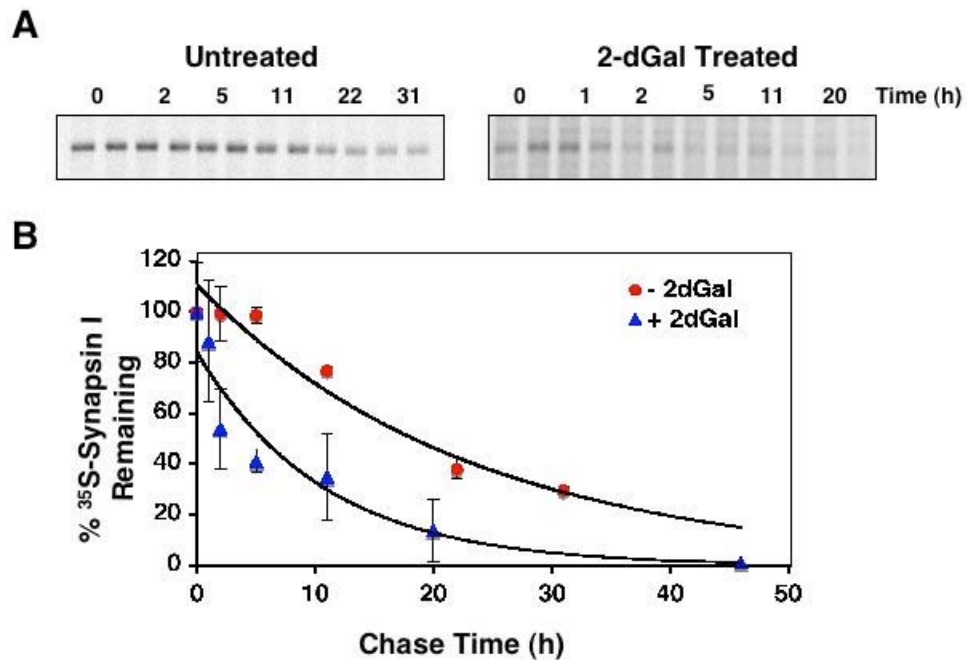


Figure 2.9. Synapsin I defucosylation decreases its cellular half-life. (A) ³⁵S-labeled synapsin I after indicated chase periods, samples are in duplicate. (B) Graphical representation of densitometry analysis of synapsin I remaining.

Based on these results, we postulated that fucosylation might be critical for modulating the half-life and turnover of synapsin in cells. We conducted pulse-chase experiments of synapsin Ia expressed in HeLa cells in the presence or absence of 2-dGal. Cells were pulse labeled with ³⁵S- L-cysteine and ³⁵S- L-methionine and then incubated for various times in the absence of radioisotopes. After the indicated chase times, synapsin Ia was immunoprecipitated from the cell lysates. A relatively long half-life of 18 h was observed for synapsin Ia (Figure 2.9), consistent with previous studies of endogenous synapsin I in cultured hippocampal neurons ($t_{1/2} \approx 20$ h)¹¹. In contrast, treatment of the cells with 2-

dGal led to a dramatic reduction in synapsin half-life to 5.5 h. These results indicate that de-fucosylation of synapsin induces its degradation in cells.

Synapsin Degradation Is Mediated by the Calcium-Dependent Protease Calpain

To investigate the molecular mechanisms responsible for synapsin turnover, cells expressing synapsin were treated with various inhibitors of protein degradation in the presence or absence of 2-dGal. Specifically, we used the lysosomal inhibitors bafilomycin A1 and ammonium chloride, the proteasome inhibitor MG132, and two inhibitors of the calcium-dependent protease calpain. With the exception of MG132, the inhibitors had minimal effects on synapsin expression levels in the absence of 2-dGal (Figure 2.10). As before, 2-dGal treatment of the cells significantly reduced the levels of synapsin expression. Notably, inhibition of the protease calpain using a calpain inhibitor

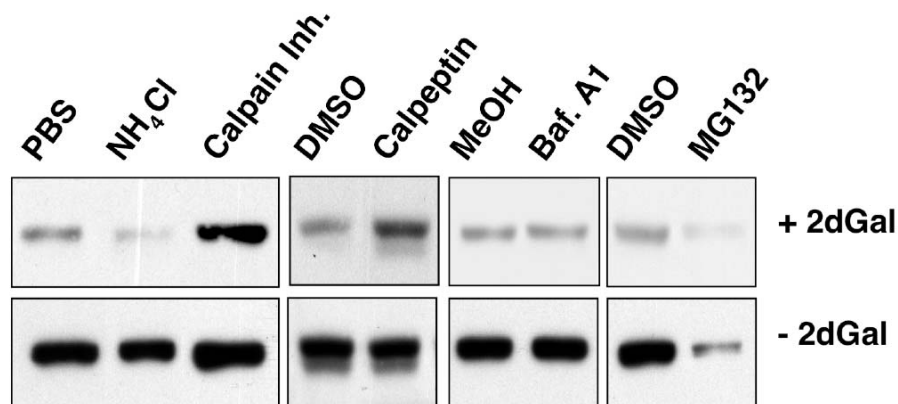


Figure 2.10. Inhibition of the calcium-activated protease calpain with calpain inhibitor peptide or calpeptin rescues synapsin from degradation by 2-dGal. The lysosome was inhibited with ammonium chloride and bafilomycin A1. The proteasome was inhibited with MG132.

peptide or calpeptin rescued the effects of 2-dGal, significantly attenuating the loss of synapsin, whereas the lysosomal and proteasomal inhibitors could not rescue synapsin from degradation. These data suggest that fucosylation protects synapsin from rapid degradation mediated at least in part by the Ca^{2+} -activated protease calpain.

Fucosylation Modulates the Expression of Synapsin in Neurons and Neurite Outgrowth

To examine the effects of 2-dGal on synapsin fucosylation in neurons, neurons were cultured for 7 DIV to allow for adequate expression of synapsin and subsequently treated with either 2-dGal or 6-dGal for 3 days. 2-dGal dramatically reduced the expression of synapsin I in cultured neurons (Figure 2.11A). Importantly, the effects of

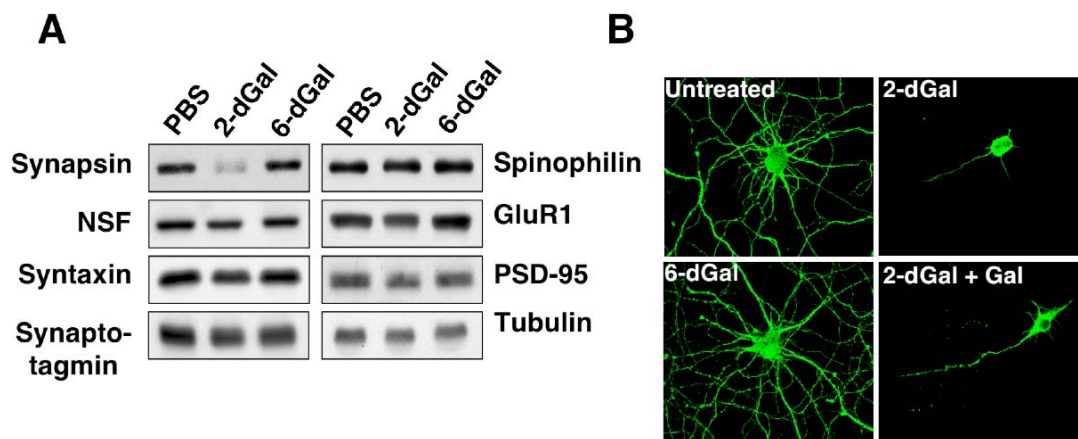


Figure 2.11. (A) 2-dGal reduces synapsin I expression whereas 6-dGal has no effect. Other pre- and postsynaptic proteins, as well as tubulin, are unaffected by 2-dGal treatment. (B) E18 cortical neurons were cultured for 7 DIV and treated with 2-dGal or 6-dGal for 3 days. 2-dGal led to a dramatic collapse of synapses and reduction in neurite length (top panels) whereas 6-dGal had no effect (bottom, left panel). The effects were partially rescued by subsequent treatment with Gal. Figure 2.11 (B) courtesy of C. Gama.

2-dGal appear to be selective as treatment with another deoxy sugar, 6-dGal, did not alter the expression of synapsin. Moreover, the effects of 2-dGal were specific to synapsin as

the expression of other synaptic proteins, including NSF, synaptotagmin, syntaxin, PSD-95, the AMPA receptor GluR1 subunit, and spinophilin, was unchanged by the 2-dGal treatment.

As the synapsins play important roles in neuronal development and synaptogenesis,^{12, 13} we next investigated whether 2-dGal might influence neuronal growth and morphology in collaboration with Cristal Gama. Hippocampal neurons were cultured for 7 DIV as above to establish functional synapses and subsequently incubated for 3-5 days with 2-dGal at various concentrations. Treatment with 2-dGal induced a

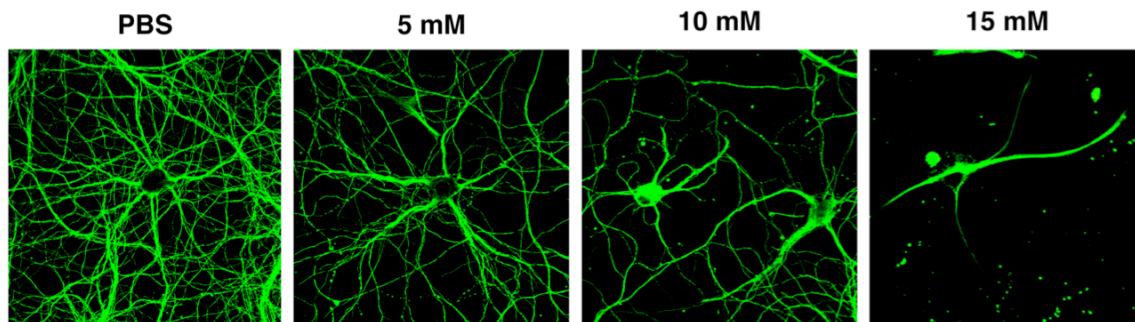


Figure 2.12. Concentration-dependence of 2-dGal on neuronal morphology. Neurons were cultured for 7 DIV and treated for 3 days with the indicated amounts of 2-dGal. Image courtesy of C. Gama.

dramatic retraction of neurites and collapse of synapses, whereas 6-dGal had no effect (Figure 2.11B). The effects of 2-dGal could be partially rescued by subsequent incubation of the neurons with D-Gal, which is expected to re-establish the Fuc α (1-2)Gal linkage (Figure 2.11B, 2.06 ± 0.14 fold rescue; $n = 50$; $p < 0.0001$). These results suggest that disruption of the Fuc α (1-2)Gal linkage on neuronal glycoproteins has a profound impact on neurite outgrowth and neuronal morphology.

One potential mechanism by which 2-dGal might influence neuronal morphology is by regulating the function and/or expression of synapsin in presynaptic terminals.

Notably, the phenotypic effects of 2-dGal on neurite outgrowth at 5 mM concentration are similar to deletion of the synapsin I gene, which results in retarded neurite outgrowth and delayed synapse formation¹² (Figure 2.12). However, because other neuronal proteins bear the Fuc α (1-2)Gal modification (Figure 1A), these proteins might also contribute to the morphological effects observed upon de-fucosylation.

To examine the relative contribution of synapsin I to the effects of 2-dGal, neurons were cultured from synapsin I-deficient or wild-type mice for 2 days in collaboration with Cristal Gama, treated in the presence or absence of 2-dGal for 3 days and examined by confocal fluorescence microscopy. Top panels (Figure 2.13A) are representative images of untreated wild-type and synapsin I-deficient neurons after 5 days in culture, respectively. Neurons from wild-type mice treated with 2-dGal had shorter neurites relative to their untreated wild-type counterparts (left panels in Figure 2.13A). The

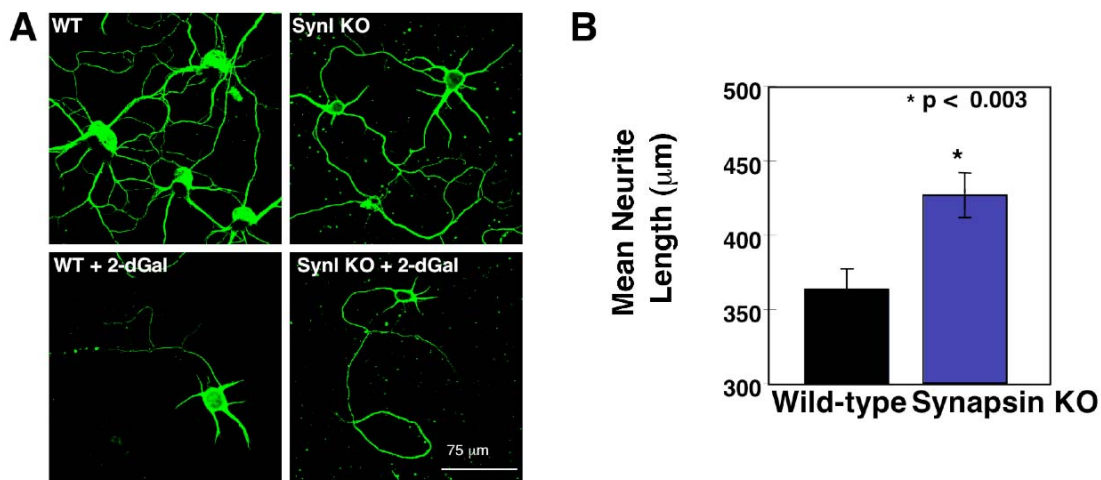


Figure 2.13. 2-dGal induces less neurite retraction in synapsin I KO neurons. (A) Neurons from synapsin I KO or wild-type neonatal pups were cultured for 2 DIV and treated for 3 days with PBS (top panels) or 2-dGal (bottom panels). (B) Quantification of neurite lengths of 2-dGal treated wild-type and synapsin I hippocampal neurons.

effects of de-fucosylation at a concentration of 15 mM 2-dGal were more pronounced than elimination of the synapsin I gene (Figure 2.13A). Finally, treatment with 2-dGal induced a more dramatic neurite retraction in wild-type relative to synapsin-deficient neurons (bottom panels in Figure 2.13A). Although the length and extensive overlap among processes for untreated wild-type neurons precluded a quantitative analysis of neurite length, 2-dGal treatment led to neurite retraction and enabled quantification. We found that synapsin-deficient neurons displayed longer neurites than wild-type neurons upon treatment with 2-dGal (bar graph in Figure 2.13B).

Synapsin I Is the Only Synapsin Gene Fucosylated

Synapsin I is a member of a multigene family of neuronal phosphoproteins that regulate neurotransmitter release.¹⁴ They are encoded by three genes termed synapsin I, II, and III with different splice variants creating distinct isoforms.¹⁵

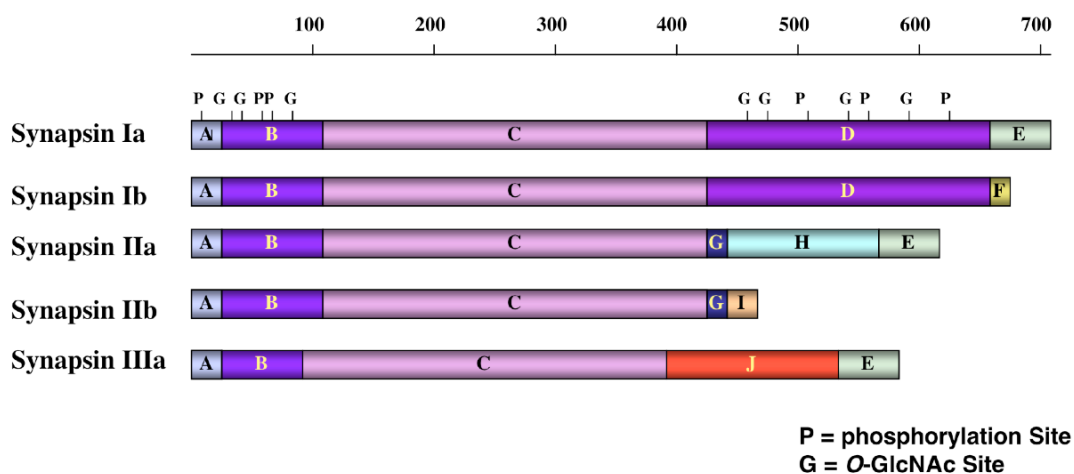


Figure 2.14. Domain organization of the synapsin gene family.

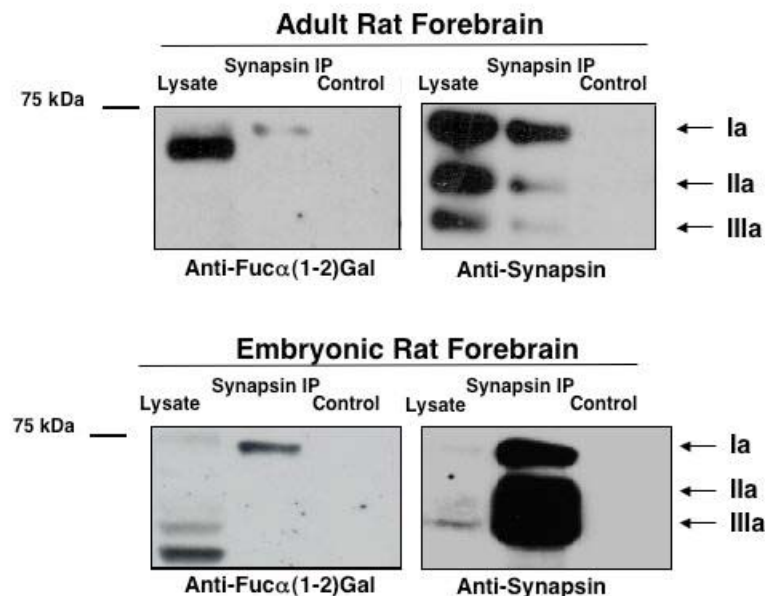


Figure 2.15. Only synapsin I is fucosylated. The synapsins were immunoprecipitated from adult (top panels) and embryonic (bottom panels) rat forebrain. Immunoprecipitates were probed with antibody A46-B/B10 (left panels) and an anti-synapsin (right panels) antibody.

Synapsins Ia and Ib are both splice variants of the same gene. The synapsins are highly conserved at the N-terminal region in domains A-C, and differ at the C-terminal domains (Figure 2.14). Domain C, which is the most conserved domain amongst all synapsin isoforms, is important for interaction with synaptic vesicles, via insertion of a small peptide directly into the lipid bilayer of the vesicles.¹⁶ Due to the extensive sequence conservation between genes, we next investigated whether other synapsin family members were fucosylated. Synapsins Ia, IIa, and IIIa were immunoprecipitated with antibody G304,¹⁷ which recognizes the E domain of the three synapsin genes, from rat

forebrain lysates of adult and embryonic rats. In adult rats, expression of synapsin Ia is highest, and in embryonic tissues, expression of synapsins IIa and IIIa is more prominent. Immunoprecipitates were probed with antibody A46-B/B10 to determine whether other synapsins were fucosylated. Synapsin Ia was fucosylated in both embryonic and adult rat brain as indicated by the band present in the immunoprecipitated lanes. Surprisingly, neither synapsins IIa or IIIa were found to be fucosylated. This is most evident from the blot of embryonic lysates, where synapsins IIIa and IIa have greater expression, but no bands were detected by the anti-Fuc α (1-2)Gal antibody. (Figure 2.15). Due to the high degree of sequence conservation at the N-terminal regions of the of synapsin gene family, these data implicate the D domain of synapsin I as containing the potential Fuc α (1-2)Gal epitope.

Synapsin I Contains 1.5 - 3.2 Fucosylation Sites

To gain insight into the stoichiometry of fucosylation, we compared synapsin I purified from bovine brain against a fucosylated bovine serum albumin (BSA) standard (Figure 2.16). 2'-Fucosyllactose (Fuc α (1-2)Gal β (1-4)GlcNAc) was conjugated to BSA using reductive amination chemistry, and an epitope density of approximately 3.0 ± 0.8 moles of fucose per BSA molecule was determined using the Habeeb assay.¹⁸ Comparison of the relative binding of antibody A46-B/B10 to synapsin I versus this standard revealed a stoichiometry of approximately 1.5 - 3.2 Fuc α (1-2)Gal epitopes per synapsin molecule.

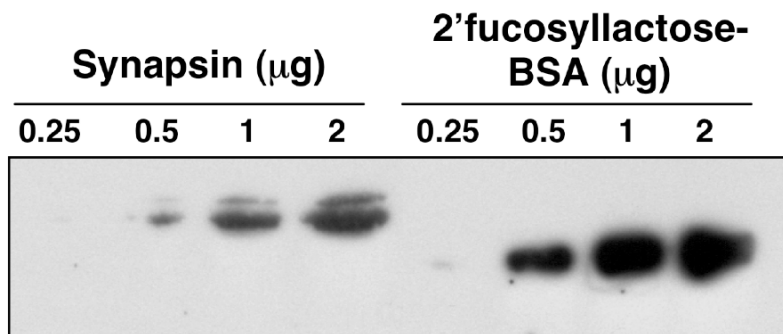


Figure 2.16. Bovine synapsin I and BSA conjugated to 2'fucosyllactose were resolved by SDS-PAGE and examined by densitometry analysis to determine the extent of synapsin I fucosylation. Analysis reveals a stoichiometry of 1.5 – 3.2 Fuc α (1-2)Gal epitopes per synapsin molecule.

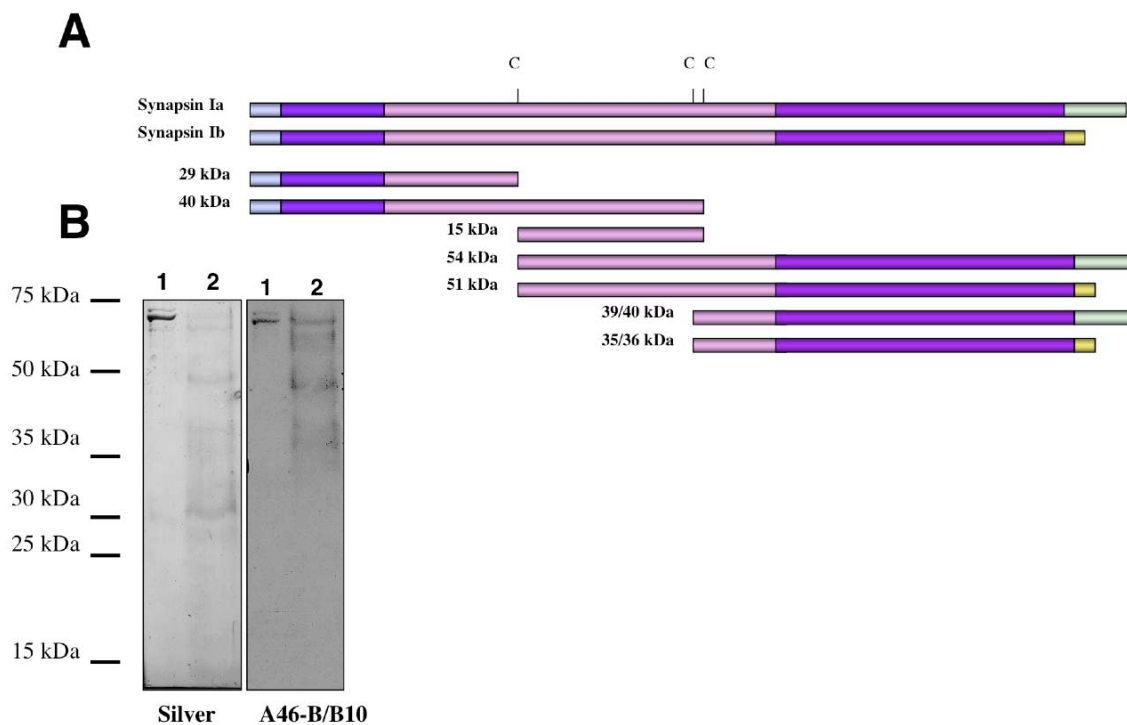


Figure 2.17. NTCB cleavage of purified synapsin I. Bovine synapsin I was cleaved with NTCB under alkaline conditions. (A) Expected fragments observed after NTCB cleavage. (B) Left panel is a silver stain of undigested (lane 1) and digested (lane 2) to observe all peptide fragments. Right panel is a Western blot to demonstrate fragments labeled by the Fuc α (1-2)Gal antibody.

Synapsins Ia and Ib are Fucosylated in Domain D via an *O*-Linkage

As immunoprecipitation studies implicated the D domain of synapsin I as containing a $\text{Fuc}\alpha(1-2)\text{Gal}$ moiety, we sought to address whether this was the case. Purified bovine synapsins Ia and Ib were subjected to cleavage by the small molecule reagent 2-nitro-5-thiocyanobenzoic acid (NTCB). This reagent will cleave proteins after cysteine residues under alkaline conditions.¹⁹ Synapsins Ia and Ib contain 3 cysteine residues at amino acids 222, 360, and 370. Figure 2.17 shows a map of synapsins Ia and Ib cleavage products obtained after NTCB treatment. Products from the cysteines at positions 360 and 370 resulted in peptides indistinguishable by SDS-PAGE, and thus are represented as one peptide in the figure. After NTCB treatment, proteins were separated by SDS-PAGE, and either transferred to PVDF for immunoblotting, or stained with silver

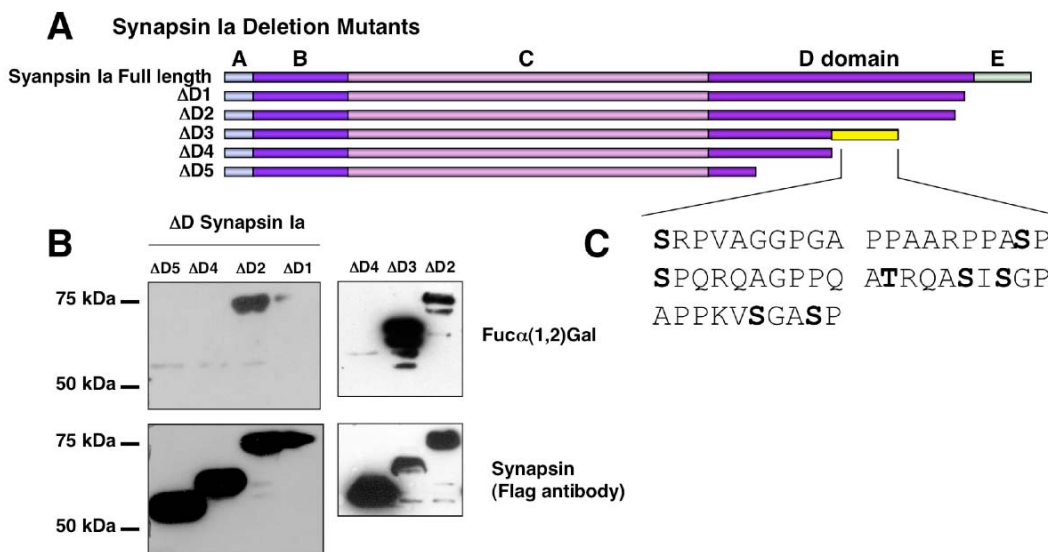


Figure 2.18. (A) Deletion mutants created from the Flag-synapsin I construct. (B) Western blot analysis reveals that the $\text{Fuc}\alpha(1-2)\text{Gal}$ antibody recognizes domains ΔD3 , ΔD2 , and ΔD1 (top panels) but not domains ΔD4 and ΔD5 . (C) Sequence of amino acids in the region narrowed down by deletion mutagenesis that should contain a $\text{Fuc}\alpha(1-2)\text{Gal}$ moiety.

nitrate to identify all cleavage fragments. Transferred proteins were immunoblotted with antibody A46-B/B10. The smallest fragments recognized by the Fuc α (1-2)Gal antibody were the 39/40 kDa fragment of synapsin Ia and the 35/36 kDa fragment corresponding to synapsin Ib (data not shown). These fragments contain a short segment of domain C, along with domain D in its entirety, confirming the presence of a Fuc α (1-2)Gal epitope in domain D of synapsins Ia and Ib.

To identify the region of glycosylation within the D domain, we created a series of deletion mutants of this region (Figure 2.18A). We first subcloned the cDNA of synapsin I into the pFLAG-CMV vector (Sigma) to place an N-terminal Flag tag on the protein. The construct allows for expression in heterologous host cells, and the Flag-tag facilitates immunoprecipitation and Western blot analyses. We next created truncation mutants by PCR, and subsequently expressed the deletion mutants in HeLa cells to examine fucosylation levels with antibody A46-B/B10. All truncation mutants were successfully expressed, and the Fuc α (1-2)Gal-specific antibody was able to detect fucose on deletion mutants Δ D1 - Δ D3 (Figure 2.18B). The antibody did not detect any fucose on deletion mutants Δ D4 - Δ D5. This suggests that there is at least one Fuc α (1-2)Gal epitope between residues 531 and 658. As there are no asparagine residues within this region, the modification is attached via an *O*-linkage to either a serine or threonine residue within this domain (Figure 2.18C).

Synapsin I Contains a Putative Fuc α (1-2)Gal Site at Ser579

To determine the exact site of fucosylation, we created a series of point-mutants corresponding to serine and threonine residues within amino acids 531-590 of the Flag-synapsin I construct. The Flag-synapsin I point mutants were transiently expressed in HeLa cells and examined for their expression and recognition by $\text{Fuc}\alpha(1-2)\text{Gal}$ -specific

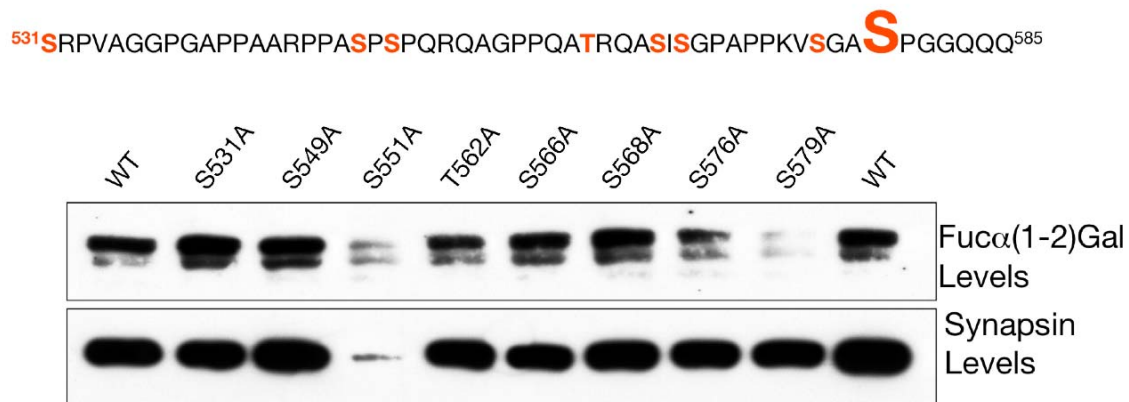


Figure 2.19. Identification of synapsin I $\text{Fuc}\alpha(1-2)\text{Gal}$ sites by site-directed point mutagenesis. Only Ser579 has an appreciable decrease in fucosylation levels as detected with antibody A46-B/B10.

antibody A46-B/B10. All point mutants were capable of being expressed, however the S531A mutant did not express as well as the other point mutants (Figure 2.19). However, we observed a significant decrease in fucosylation of point mutant S579A, whereas fucosylation of other mutants appeared to be unaffected. There was still some detection by antibody A46-B/B10 of the S579A mutant, suggesting the presence of another site of fucosylation consistent with densitometry analysis. These data suggest that synapsin I contains a putative $\text{Fuc}\alpha(1-2)\text{Gal}$ moiety at Ser 579, and another site of fucosylation may exist in the protein.

To determine whether another fucosylation site exists in synapsin I, we created a series of double mutants using the S579A construct, of all Ser and Thr residues between

amino acids 531 and 705. Furthermore, despite our data suggesting that the $\text{Fuca}(1-2)\text{Gal}$ moiety is on an *O*-linked glycan in the D domain, we also created double mutants of three Asn residues at amino acids 661, 668, and 671 as well as Ser and Thr residues in the E domain of synapsin I. All mutants were capable of being expressed, and all mutants appeared to be recognized by antibody A46-B/B10 to a similar degree. To date we have not been able to identify a second site with the double mutants (data not shown). However, experiments are still in progress to identify the sites.

UEA1 Lectin Recognizes a Different $\text{Fuca}(1-2)\text{Gal}$ Moiety on Synapsins Ia and Ib than Antibody A46-B/B10

To facilitate our identification of fucosylation sites, we employed lectin immunoblotting with UEA1. Surprisingly, UEA1 recognizes the S579A mutant as well as wild-type synapsin I, suggesting that UEA1 lectin recognizes a different epitope on synapsin I. To identify the region that UEA1 interacts with, we used the ΔD deletion mutants to narrow down the site of fucosylation. Interestingly, UEA1 only interacts with deletion mutants ΔD1 and ΔD2 and not with ΔD3 , which antibody A46-B/B10 interacts with (data not shown). This suggests that UEA1 recognizes a $\text{Fuca}(1-2)\text{Gal}$ moiety between amino acids 591 and 659. We are currently exploring the ability of UEA1 lectin to bind to synapsin I double mutants, however, results have been inconclusive to date.

Conclusions

Increasing evidence has linked synaptic activity with changes in the levels of protein fucosylation in the brain. For instance, both task-specific learning and LTP have

been shown to enhance protein fucosylation at the synapse.^{1,2} Moreover, the activity of fucosyltransferases increases substantially during synaptogenesis³ and upon passive avoidance training in animals.⁴ Together, these studies suggest that protein fucosylation may relate to the dynamic regulation of synaptic proteins. Studies have implicated a particular carbohydrate, Fuc α (1-2)Gal, in cognitive processes such as learning and memory. Although Fuc α (1-2)Gal has been postulated to covalently modify synaptic glycoproteins, the identity of such proteins has remained elusive. In this study, we identify synapsins Ia and Ib as the major Fuc α (1-2)Gal glycoproteins in maturing neuronal cultures and the adult rat hippocampus. Our results provide the first molecular insights into the functions of Fuc α (1-2)Gal and demonstrate that these carbohydrates play a critical role in the regulation of synaptic proteins.

The synapsins are a family of neuron-specific phosphoproteins that are associated with synaptic vesicles, and are homologous at their *N*-terminal region.¹⁴ Studies indicate that these proteins regulate multiple aspects of neuronal function including neurotransmitter release by regulating the supply of releasable vesicles during periods of high activity,^{14, 26} and controlling synaptic vesicle dynamics in developing neurons via a cAMP-dependent pathway.²⁷ Accordingly, synapsin knock-out mice show reduced numbers of synaptic vesicles within nerve terminals and exhibit significant alterations in neurotransmitter release and synaptic depression.^{14, 28} The synapsins have also been implicated in diverse aspects of neuronal development, including axonal outgrowth, nerve terminal development, synapse formation, and synapse maintenance.^{12, 29, 30}

Our studies indicate that fucosylation of synapsin critically impacts its expression and turnover in presynaptic nerve terminals. The potential to modulate the expression

level of synapsin is expected to have important consequences for neuronal function. For instance, the addition of exogenous synapsin I to embryonic *Xenopus* spinal neurons has been shown to accelerate structural and functional maturation of neuromuscular synapses, including the early compartmentalization of synaptic vesicles into nerve terminals and a mature form of quantal secretion.^{31, 32} Conversely, reduction in synapsin expression levels also has profound effects: synapsin-deficient mice exhibit significant delays in axonal extension, neuronal differentiation, and synapse formation.

We found that de-fucosylation of synapsin promoted its degradation by calcium-activated calpain proteases, which are a family of non-lysosomal, neutral cysteine proteases. These observations corroborate and extend recent findings suggesting a role for calpain in the regulation of both synaptic transmission and neuronal morphology.^{33, 34} Interestingly, calpain has been suggested to be critical for refilling depleted vesicle stores in sensory motor synapses of *Aplysia* via a mechanism involving the cleavage of potential substrates such as synapsin.³⁵ In addition, calpain was found to degrade SNAP-25 (synaptosomal-associated protein of 25 kDa), a protein essential for neurotransmitter release, in a calcium-dependent manner.³⁶ The proteolytic activity of calpain has also been shown to induce cytoskeletal rearrangements, leading to both facilitation and inhibition of neurite outgrowth.^{34, 37, 38} Although further studies will be necessary to understand more fully the mechanisms of calpain-mediated synapsin degradation, our results suggest an expanded role for this protease family in presynaptic nerve terminals and reveal that fucosylation has profound effects on the half-life of synapsin, possibly preventing synapsin from calcium-activated degradation.

In this study, we investigated the role of synapsin fucosylation on neuronal growth and morphology. 2-dGal, a small molecule inhibitor of $\text{Fuc}\alpha(1-2)\text{Gal}$ linkages, served as a valuable tool to de-fucosylate synapsin and dissect the role of the carbohydrate in modulating synapsin function. Treatment of neurons with 2-dGal led to stunted neurite outgrowth and delayed synapse formation. Moreover, significant differences were observed between wild-type and synapsin-deficient neurons upon treatment with 2-dGal. We believe that the extent of neurite retraction in synapsin-deficient mice is less pronounced because the primary target of 2-dGal, synapsin I, is missing. Indeed, the bar graph shown in Figure 2.13 likely represents a lower estimate of the contribution of synapsin as neurites from synapsin-deficient neurons are shorter than those from wild-type neurons prior to treatment with 2-dGal. Based on these results, we propose that de-fucosylation may disrupt synapsin function, leading to its degradation and neurite retraction. Although further studies will be needed to resolve whether synapsin fucosylation stimulates or inhibits neurite outgrowth, these results strongly support the notion that synapsin fucosylation plays a role in modulating neuronal growth and morphology.

Our data also implicate other $\text{Fuc}\alpha(1-2)\text{Gal}$ glycoproteins in the regulation of neuronal morphology. We demonstrate that $\text{Fuc}\alpha(1-2)\text{Gal}$ carbohydrates are not limited to synapsin, but are found on several additional proteins in developing neurons. Expression of the sugar and/or these glycoproteins changes dramatically during the course of neuronal development. We found that disruption of synapsin fucosylation contributed, but was not fully sufficient, to account for the striking neurite retraction induced by 2-dGal. For instance, 2-dGal had stronger effects on neurite outgrowth at

high concentrations relative to deletion of the synapsin I gene, suggesting that 2-dGal may disrupt the fucosylation of other Fuc α (1-2)Gal glycoproteins that influence neuronal morphology. Moreover, 2-dGal was still capable of inducing partial neurite retraction in synapsin-deficient neurons and young cultured neurons where synapsin expression is low.²⁰ Thus, Fuc α (1-2)Gal sugars appear to modulate the functions of multiple proteins involved in neuronal morphology and exert their effects via several distinct molecular mechanisms.

Finally, our findings may shed light on behavioral and electrophysiological studies implicating Fuc α (1-2)Gal in long-term memory storage. Alterations in neuronal morphology, such as dynamic changes in dendritic spine number and shape, occur during memory consolidation and LTP.^{39, 40} Future studies will investigate whether Fuc α (1-2)Gal sugars and their associated glycoproteins contribute to structural remodeling events that underlie synaptic plasticity.

Materials and Methods

Neuronal Cultures and Immunocytochemistry. Hippocampal and cortical neurons were cultured and immunostained as described previously.²⁰ Synapsin I knockout mice¹² were generously provided by Drs. H.T. Kao and P. Greengard (The Rockefeller University, New York, NY). Antibody A46-B/B10⁶ was a generous gift from Dr. U. Karsten (Max-Delbruck Centre for Molecular Medicine, Berlin-Buch, Germany) and was incubated in 3% BSA (2.5 μ g/mL) overnight at 4 °C. The anti-tubulin (1:500; Sigma), anti-synapsin (1:5000; Molecular Probes) and anti-spinophilin (1:10000; ²¹) antibodies

were added in 3% BSA for 2 h at 37 °C. Goat anti-mouse IgM-AlexaFluor 488 or goat anti-rabbit IgG AlexaFluor 568 (1:250; Molecular Probes) was added for 1 h at 37 °C in 3% BSA.

Adult Rat Hippocampal Dissection, Lysis, and Immunoprecipitation. The hippocampi of adult male Sprague-Dawley rats (100-150 g) were homogenized in 50 mM Tris-HCl pH 8.0, 150 mM NaCl, 0.2% sodium deoxycholate, 1% NP-40 supplemented with protease inhibitors with a glass Dounce homogenizer and sonicated briefly. Supernatants were clarified by centrifugation at 12,000× g for 10 min, and protein concentrations were determined using the BCA protein assay method (Pierce). Immunoprecipitations were performed at approximately 2 mg/mL lysate using an anti-synapsin (Chemicon) or anti-NSF (Synaptic Systems) antibody.

Synaptic Vesicle Purification from Adult Rat Brain. Synaptic vesicles were purified using a sucrose density gradient as described previously.²²

Treatment of Cells with Deoxy-Galactose Analogues. Rat neuronal cultures were treated after 7 days as described.²⁰ Neuronal cultures from C57BL/6 E16 mice were treated after 7 DIV with 2-dGal (0, 5, 10, or 15 mM) in PBS for 5 days. Neurons from C57BL/6 and synapsin I knockout P0 mice were cultured for 2 days and then treated for 3 days with 15 mM 2-dGal. HeLa cells were seeded at 6×10^5 cells per 60 mm dish in Dulbecco's Modified Eagle Medium (DMEM) supplemented with 10% fetal calf serum (FCS) and incubated at 37 °C / 5% CO₂ for 24 h. After pretreatment with the deoxy-galactose analogues (0.5 - 10 mM) for 1 h, the cells were transfected at ~60% confluence with the plasmid pCMV-FLAG-Synapsin Ia and pSV-β-galactosidase (Promega) using Lipofectamine 2000 (Invitrogen). After 22 h, the cells were harvested, resuspended in

PBS, and either lysed in 1% boiling SDS (70% of the cells) or analyzed for transfection efficiency using a β -galactosidase assay (30% of the cells). For synapsin degradation experiments, cells were treated with 2-dGal or PBS as above, followed by treatment 4 h post-transfection with bafilomycin A1 (100 nM, Acros), MG132 (5 μ M, Sigma), ammonium chloride (25 mM, Fisher), calpain inhibitor peptide (33 μ M, Sigma), or calpeptin (2 μ M, Alexis Biochemicals). Cells were lysed as above after 15 h of treatment, resolved by SDS-PAGE, and analyzed by immunoblotting with chemiluminescence detection (Pierce).

Pulse-Chase Analysis. HeLa cells were transfected and treated with 2-dGal as above with the following modifications. Cells were transfected at ~95% confluence with pCMV-FLAG-Synapsin Ia. Sixteen hours post-transfection, cells were washed with PBS and starved in DMEM (without L-cysteine and L-methionine) supplemented with 10% FCS for 1 h. Cells were pulse labeled with 100 μ Ci/mL EasytagTM Express Protein Labeling Mix (Perkin Elmer) for 1 h, washed with DMEM, and chased in conditioned medium collected from the cells prior to the starvation period. Cells were lysed in 1% boiling SDS and neutralized with an equal volume of NETFD (50 mM Tris-HCl pH 7.4, 100 mM NaCl, 5 mM EDTA, 50 mM NaF, 6% NP-40 supplemented with protease inhibitors). Synapsin was immunoprecipitated using anti-FLAG M2 affinity agarose (Sigma), resolved by SDS-PAGE, fixed with destain, treated with Amplify (Amersham), and dried. ³⁵S-labeled protein was measured using a Typhoon 8600 Variable Mode Imager (Molecular Dynamics, Amersham).

Molecular Cloning. The synapsin Ia gene was subcloned into the vector pFLAG-CMV (Sigma) using the restriction enzymes KpnI and BglII to place an N-terminal

FLAG tag on the protein. Synapsin I deletion mutants were created by PCR mutagenesis from the pFLAG-CMV-Synapsin Ia construct with the following antisense primers: Δ D1 5'-CGAGGTACCTCAGGTCAGAGACTGGGATTTG-3'; Δ D2 5'-CGAGGTACCTCAGAG-CTGGGGGTGCGG-3'; Δ D3 5'-CGAGGTACCTCACGTGACTGGCGGCCTTGA-3'; Δ D4 5'-CGAGGTACCTCACTGGCGCTGAGGTCCTGG-3'. Each fragment was created with the sense primer: 5'-AAATGTCGTAATAACCCCGCCCCCGTTGAACGC-3'. The fragments were subcloned into the pFLAG-CMV vector with KpnI and BglII.

Synapsin I point mutants were created by site directed mutagenesis of the Flag-Synapsin I construct using the QuickChange strategy (Stratagene) with the indicated primer pairs. Mutant S531A sense primer 5'-AGGCCGCCAGGCACGGCCAGTGG-3' and the antisense primer 5'-CCACTGGCCGTGCCTGGCGGCCT-3'. Mutant S549A sense primer 5'-CCCGCCGGCCGCCCATCTCCAC-3' and the antisense primer 5'-GTGGAGATGGGGCGGCCGGCGGG-3'. Mutant S551A sense primer 5'-GGCCTCCCCAGCTCCACAGCGTC-3' and the antisense primer 5'-GACGCTGTGGAGCTGGGGAGGCC-3'. Mutant T562A sense primer 5'-CCCCACAGGCTGCCCGTCAGGCATC-3' and the antisense primer 5'-GATGCCTGACGGGCAGCCTGTGGGG-3'. Mutant S566A sense primer 5'-CCCGTCAGGCAGCTATCTCTGGTCCAG-3' and the antisense primer 5'-CTGGACCAGAGATAGCTGCCTGACGGG-3'. Mutant S568A sense primer 5'-GTCAGGCATCTATCGCTGGTCCAGCTCCA-3' and the antisense primer 5'-TGGAGCTGGACCAGCGATAGATGCCTGAC-3'. Mutant S576A sense primer 5'-CACCGAAGGTCGCAGGAGCCTCACC-3' and the antisense primer 5'-

GGTGAGGCTCCTGCGACCTTCGGTG-3'. Mutant S579A sense primer 5'-CTCAGGAGCCGCACCCGGAGGGC-3' and the antisense primer 5'-GCCCTCCGGGTGCGGCTCCTGAG-3'.

Synapsin I double mutants were created on the S579A-Flag-Synapsin I construct. A second round of QuickChange was performed with all the aforementioned primers and the indicated new primer pairs. Mutant S579A/S603A sense primer 5'-CATTCGTCAGGCCGCCAGGCAGGTC-3' and the antisense primer 5'-GACCTGCCTGGGCGGCCTGACGAATG-3'. Mutant S579A/T611A sense primer 5'-CGGACCTCGCGCTGGCGGACCC-3' and the antisense primer 5'-GGGTGGCCCAGCGCGAGGTCCG-3'. Triple mutant S579A/T615A/T616A sense primer 5'-GGGCCACCCGCCGCACAGCAGCCCCGG-3' and the antisense primer 5'-CCGGGGCTGCTGTGCGGCGGGTGGCCC-3'. Mutant S579A/S622A sense primer 5'-GCCCCGGCCCCGCCGGCCCAGGTC-3' and the antisense primer 5'-GACCTGGGCCGGCGGGCCGGGGC-3'. Mutant S579A/T631A sense primer 5'-GCTGGACGTCCCGCCAAACCACAG-3' and the antisense primer 5'-CTGTGGTTTGGCGGGACGTCCAGC-3'. Mutant S579A/S640A sense primer 5'-GCTCAGAAACCCGCCAGGATGTGCC-3' and the antisense primer 5'-GGCACATCCTGGGCGGGTTTCTGAGC-3'. Mutant S579A/S662A sense primer 5'-CCCAGCTCAACAAAGCCCAGTCTCTGACC-3' and the antisense primer 5'-GGTCAGAGACTGGGCTTTGTTGAGCTGGG-3'. Mutant S579A/S664A sense primer 5'-CAAATCCCAGGCTCTGACCAATGCCTTC-3' and the antisense primer 5'-GAAGGCATTGGTCAGAGCCTGGGATTTG-3'. Mutant S579A/T666A sense primer 5'-CCCAGTCTCTGGCCAATGCCTTCAACC-5' and the antisense primer 5'-

CGTTGAAGGCATTGGCCAGAGACTGGG-3'. Mutant S579A/S680A sense primer 5'-GCCAGGCCCGGCCTTAGCCAGG-3' and the antisense primer 5'-CCTGGCTAAGGCCGGGCCTGGGC-3'. Mutant S579A/S682A sense primer 5'-GGCCAGCCTTGGCCAGGATGAGG-3' and the antisense primer 5'-CCTCATCCTGGCCAAGGCTGGGCC-3'. Mutant S579A/T691A sense primer 5'-GGTGAAAGCTGAGGCCATCCGCAGCCTG-3' and the antisense primer 5'-CAGGCTGCGGATGGCCTCAGCTTTCACC-3'. Mutant S579A/S693A sense primer 5'-GAGACCATCCGCGGCCTGAGGAAG-3' and the antisense primer 5'-CTTCCTCAGGCCGCGGATGGTCTC-3'. Mutant S579A/S697A sense primer 5'-GCAGCCTGAGGAAGGCTTTCGCCAGC-3' and the antisense primer 5'-GCTGGCGAAAGCCTTCCTCAGGCTGC-3'. Mutant S579A/S700A sense primer 5'-GAAGTCTTTCGCCGGCCTCTTCTCCG-3' and the antisense primer 5'-CGGAGAAGAGGCCGGCGAAAGACTTC. Mutant S579A/S705A sense primer 5'-CCAGCCTCTTCGCCGACTGAGGTACC-3' and the antisense primer 5'-GGTACCTCAGTCGGCGAAGAGGCTGG-5'.

Asn point mutants were created on the S579A-Flag-Synapsin construct with the indicated primers. Mutant S579A/N661A sense primer 5'-CCCCAGCTCGCCAAATCCCAGTC-3' and the antisense primer 5'-GACTGGGATTTGGCGAGCTGGGGG-3'. Mutant S579A/N668A sense primer 5'-CCAGTCTCTGACCGCTGCCTTCAACCTTCC-3' and the antisense primer 5'-GGAAGGTTGAAGGCAGCGGTCAGAGACTGG-3'. Mutant S579A/N671A sense primer 5'-CCAATGCCTTCGCCCTTCCAGAGCC-3' and the antisense primer 5'-GGCTCTGGAAGGGCGAAGGCATTGG-3'.

Western Blotting. PVDF membranes were blocked for 1 h at rt in 5% milk/TBST (50 mL, 50 mM Tris-HCl pH 7.4, 150 mM NaCl, 0.1% Tween-20) except when used with antibody A46-B/B10, which was blocked in 3% periodated BSA in PBS.²³ Primary antibodies were added overnight at 4 °C at the following concentrations: anti-synapsin (Chemicon) at 0.5 µg/mL, anti-synapsin (G143)²⁴ at 0.2 µg/mL, anti-NSF (Synaptic Systems) at 1:1000, anti-synaptotagmin 1 (Synaptic Systems) at 1:3000, anti-spinophilin²¹ at 1:5000, anti-syntaxin (Synaptic Systems) at 1:3000, anti-PSD-95 (Synaptic Systems) at 1:3000, anti-tubulin (Sigma) at 1:50,000, anti-GluR1 (Santa Cruz) at 1:1000, and A46-B/B10 at 0.5 µg/mL in TBS. Membranes were washed with TBST, incubated with the appropriate horseradish peroxidase-conjugated secondary antibody (Pierce), and visualized by chemiluminescence (Pico Chemiluminescent Substrate, Pierce).

Characterization of Synapsin with Lectins and Glycosidases. Bovine synapsin Ia/b (500 ng) was resolved by SDS-PAGE, transferred to PVDF membrane, and detected by blotting with horseradish peroxidase-conjugated lectins according to the manufacturer's protocol (EY Laboratories). For glycosidase analyses, purified bovine synapsin Ia/b (100 ng) was denatured in boiling 1% SDS for 1 min and neutralized by an equivalent volume of NETFD buffer (50 mM Tris-HCl pH 7.4, 100 mM NaCl, 5 mM EDTA, 50 mM NaF, 6% NP-40 supplemented with protease inhibitors). Reactions were performed in 50 µL fractions using α -(1-2)-fucosidase or α -(1-3,4)-fucosidase (400 µU/100 ng synapsin; Calbiochem) in 50 mM sodium acetate buffer at pH 5.0 at 37 °C. Samples were resolved by SDS-PAGE and analyzed by immunoblotting and densitometry with NIH Image 1.62 software. Statistical analysis was performed using StatView (SAS Institute Inc.).

Morphometric Analysis. For quantitative analysis of neurite length, 50 cells were analyzed per experimental condition for three separate experiments. Only cells with neurites longer than one cell body diameter were measured. The length of the longest neurite was measured using NIH Image 1.52 software, and mean neurite lengths were compared by the ANOVA test using the statistical analysis program Stat View 4.0.

Extraction of UDP-Gal and UDP-2-dGal from Cells. HeLa cells were treated in the presence or absence of 2-dGal (5 mM) as described above. The sugar nucleotides were extracted as reported previously,²⁵ and the samples (100 μ L) were diluted with ice-cold isopropanol (900 μ L), and centrifuged at 13,000 rpm for 15 min at 4 °C. The resulting supernatant was evaporated to dryness, dissolved in 100 mM HEPES, pH 8.5 (200 μ L), and extracted with chloroform (200 μ L). The aqueous phase was removed, evaporated to dryness, re-dissolved in 0.1 mM aqueous triethylammonium acetate (TEAA), pH 7.4 (20 μ L), 15 μ L of which was injected directly onto the LC-MS. Chromatography was performed using a C18-capillary column (Waters Xterra MS-C18 CapLC column (300 μ m I.D. \times 15 cm)). The chromatographic profile was from 95% solvent A (8.3 mM triethylamine/100 mM hexafluoroisopropanol, pH 7.4) to 55% methanol in 10 min at a flow rate of 5 μ L/min; the UDP compounds eluted in 95% solvent A. MS analysis was performed on a Waters Q-ToF-API US (Milford, MA), and negative mode ESI data was collected at 1 s/scan, from 400-2000 m/z . Spectra were processed only by smoothing (5 \times 2 Savitsky-Golay). Identical sets of MS scans were summed from each chromatographic trace to enable comparison between samples.

References

1. McCabe, N. R.; Rose, S. P. R., Passive-avoidance training increases fucose incorporation into glycoproteins in chick forebrain slices in vitro. *Neurochem. Res.* **1985**, 10, (8), 1083-1095.
2. Pohle, W.; Acosta, L.; Ruthrich, H.; Krug, M.; Matthies, H., Incorporation of [³H] fucose in rat hippocampal structures after conditioning by perforant path stimulation and after LTP-producing tetanization. *Brain Res.* **1987**, 410, (2), 245-256.
3. Matsui, Y.; Lombard, D.; Massarelli, R.; Mandel, P.; Dreyfus, H., Surface glycosyltransferase activities during development of neuronal cell-cultures. *J. Neurochem.* **1986**, 46, (1), 144-150.
4. Popov, N.; Schmidt, S.; Schulzeck, S.; Jork, R.; Lossner, B.; Matthies, H., Changes in activities of fucokinase and fucosyl-transferase in rat hippocampus after acquisition of a brightness-discrimination reaction. *Pharmacol. Biochem. Behav.* **1983**, 19, (1), 43-47.
5. Frankland, P. W.; Bontempi, B., The organization of recent and remote memories. *Nat. Rev. Neurosci.* **2005**, 6, 119-130.
6. Karsten, U.; Pilgrim, G.; Hanisch, F. G.; Uhlenbruck, G.; Kasper, M.; Stosiek, P.; Papsdorf, G.; Pasternak, G., A New monoclonal-antibody (A46-B/B10) highly specific for the blood group-H type-2 epitope - generation, epitope analysis, serological and histological-evaluation. *Brit. J. Cancer* **1988**, 58, (2), 176-181.
7. Jork, R.; Smalla, K. H.; Karsten, U.; Grecksch, G.; Ruthrich, H. L.; Matthies, H., Monoclonal-antibody specific for histo-blood group antigens-H (type-2 and type-4) interferes with long-term-memory formation in rats. *Neurosci. Res. Comm.* **1991**, 8, (1), 21-27.
8. Alonso, E.; Saez, F. J.; Madrid, J. F.; Hernandez, F., Lectin histochemistry shows fucosylated glycoconjugates in the primordial germ cells of *Xenopus* embryos. *J. Histochem. Cytochem.* **2003**, 51, (2), 239-243.
9. Bullock, S.; Potter, J.; Rose, S. P. R., Effects of the amnesic agent 2-deoxygalactose on incorporation of fucose into chick brain glycoproteins. *J. Neurochem.* **1990**, 54, (1), 135-142.
10. Holden, H., M.; Rayment, I.; Thoden, J. B., Structure and function of enzymes of the Leloir pathway for galactose metabolism. *J. Biol. Chem.* **2003**, 278, (45), 43885-43888.
11. Daly, C.; Ziff, E. B., Post-transcriptional regulation of synaptic vesicle protein expression and the developmental control of synaptic vesicle formation. *J. Neurosci.* **1997**, 17, (7), 2365-2375.
12. Chin, L. S.; Li, L.; Ferreira, A.; Kosik, K. S.; Greengard, P., Impairment of Axonal Development and of Synaptogenesis in Hippocampal-Neurons of Synapsin I-Deficient Mice. *Proc. Natl. Acad. Sci. USA* **1995**, 92, (20), 9230-9234.
13. Ferreira, A.; Li, L.; Chin, L. S.; Greengard, P.; Kosik, K. S., Postsynaptic element contributes to the delay in synaptogenesis in synapsin I-deficient neurons. *Mol. Cell. Neurosci.* **1996**, 8, (4), 286-299.

14. Hilfiker, S.; Pieribone, V. A.; Czernik, A. J.; Kao, H. T.; Augustine, G. J.; Greengard, P., Synapsins as regulators of neurotransmitter release. *Phil. Tran. Royal Soc.* **1999**, 354, (1381), 269-279.
15. Kao, H. T.; Porton, B.; Hilfiker, S.; Stefani, G.; Pieribone, V. A.; DeSalle, R.; Greengard, P., Molecular evolution of the synapsin gene family. *J. Exp. Zool.* **1999**, 285, (4), 360-77.
16. Cheetham, J. J.; Hilfiker, S.; Benfenati, F.; Weber, T.; Greengard, P.; Czernik, A. J., Identification of synapsin I peptides that insert into lipid membranes. *Biochem. J.* **2001**, 354, 57-66.
17. Kao, H. T.; Porton, B.; Czernik, A. J.; Feng, J.; Yiu, G.; Haring, M.; Benfenati, F.; Greengard, P., A third member of the synapsin gene family. *Proc. Natl. Acad. Sci. USA* **1998**, 95, (8), 4667-4672.
18. Habeeb, A. F. S., Determination of free amino groups in proteins by trinitrobenzenesulfonic acid. *Anal. Biochem.* **1966**, 14, (3), 328-336.
19. Wu, J.; Watson, J. T., Optimization of the cleavage reaction for cyanylated cysteinyl proteins for efficient and simplified mass mapping. *Anal. Biochem.* **1998**, 258, (2), 268-276.
20. Kalovidouris, S. A.; Gama, C. I.; Lee, L. W.; Hsieh-Wilson, L. C., A role for fucose alpha(1-2) galactose carbohydrates in neuronal growth. *J. Am. Chem. Soc.* **2005**, 127, (5), 1340-1341.
21. Allen, P. B.; Ouimet, C. C.; Greengard, P., Spinophilin, a novel protein phosphatase 1 binding protein localized to dendritic spines. *Proc. Natl. Acad. Sci. USA* **1997**, 94, (18), 9956-9961.
22. Huttner, W. B.; Schiebler, W.; Greengard, P.; Decamilli, P., Synapsin-I (protein-I), a nerve terminal-specific phosphoprotein . Its association with synaptic vesicles studied in a highly purified synaptic vesicle preparation. *J. Cell Biol.* **1983**, 96, (5), 1374-1388.
23. Glass, W. F.; Briggs, R. C.; Hnilica, L. S., Use of lectins for detection of electrophoretically separated glycoproteins transferred onto nitrocellulose sheets. *Analytical Biochemistry* **1981**, 115, (1), 219-224.
24. Pieribone, V. A.; Shupliakov, O.; Brodin, L.; Hilfiker-Rothenfluh, S.; Czernik, A. J.; Greengard, P., Distinct pools of synaptic vesicles in neurotransmitter release. *Nature* **1995**, 375, (6531), 493-497.
25. Tomiya, N.; Ailor, E.; Lawrence, S. M.; Betenbaugh, M. J.; Lee, Y. C., Determination of nucleotides and sugar nucleotides involved in protein glycosylation by high-performance anion-exchange chromatography: Sugar nucleotide contents in cultured insect cells and mammalian cells. *Anal. Biochem.* **2001**, 293, (1), 129-137.
26. Chi, P.; Greengard, P.; Ryan, T. A., Synapsin dispersion and reclustering during synaptic activity (vol 4, pg 1187, 2001). *Nature Neuroscience* **2001**, 4 (12), 1187-1193.
27. Bonanomi, D.; Menegon, A.; Miccio, A.; Ferrari, G.; Corradi, A.; Kao, H. T.; Benfenati, F.; Valtorta, F., Phosphorylation of synapsin I by cAMP-dependent protein kinase controls synaptic vesicle dynamics in developing neurons. *J. Neurosci.* **2005**, 25, (32), 7299-7308.
28. Gitler, D.; Feng, J.; Ren, Y.; Rodriguiz, R. M. W., W. C.

- Greengard, P.; Augustine, G. J., Different presynaptic roles of synapsins at excitatory and inhibitory synapses. *J. Neurosci.* **2004**, 24, (50), 11368-11380.
29. Ferreira, A.; Rapoport, M., The synapsins: beyond the regulation of neurotransmitter release. *Cell. Mol. Life Sci.* **2002**, 59, (4), 589-595.
30. Li, L.; Chin, L. S.; Shupliakov, O.; Brodin, L.; Sihra, T. S.; Hvalby, O.; Jensen, V.; Zheng, D.; McNamara, J. O.; Greengard, P.; Andersen, P., Impairment of synaptic vesicle clustering and of synaptic transmission, and increased seizure propensity, in synapsin I-deficient mice. *Proceedings of the National Academy of Sciences of the United States of America* **1995**, 92, (20), 9235-9239.
31. Lu, B.; Greengard, P.; Poo, M. M., Exogenous synapsin I promotes functional maturation of developing neuromuscular synapses. *Neuron* **1992**, 8, (3), 521-529.
32. Valtorta, F.; Iezzi, N.; Benfenati, F.; Lu, B.; Poo, M. M.; Greengard, P., Accelerated structural maturation induced by synapsin I at developing neuromuscular synapses of *Xenopus laevis*. *The European journal of neuroscience* **1995**, 7, (2), 261-270.
33. Denny, J. B.; Polancurtain, J.; Ghuman, A.; Wayner, M. J.; Armstrong, D. L., Calpain inhibitors block long-term potentiation. *Brain Res.* **1990**, 534, (1-2), 317-320.
34. Shea, T. B.; Cressman, C. M.; Spencer, M. J.; Beermann, M. L.; Nixon, R. A., Enhancement of neurite outgrowth following calpain inhibition is mediated by protein-kinase-C. *J. Neurochem.* **1995**, 65, (2), 517-527.
35. Khoutorsky, A.; Spira, M. E., Calcium-activated proteases are critical for refilling depleted vesicle stores in cultured sensory-motor synapses of *Aplysia*. *Learn. Mem.* **2005**, 12, (4), 414-422.
36. Ando, K.; Kudo, Y.; Takahashi, M., Negative regulation of neurotransmitter release by calpain: a possible involvement of specific SNAP-25 cleavage. *J. Neurochem.* **2005**, 94, (3), 651-658.
37. Robles, E.; Huttenlocher, A.; Gomez, T. M., Filopodial calcium transients regulate growth cone motility and guidance through local activation of calpain. *Neuron* **2003**, 38, (4), 597-609.
38. Wilson, M. T.; Kisaalita, W. S.; Keith, C. H., Glutamate-induced changes in the pattern of hippocampal dendrite outgrowth: A role for calcium-dependent pathways and the microtubule cytoskeleton. *J. Neurobiol.* **2000**, 43, (2), 159-172.
39. Luscher, C.; Nicoll, R. A.; Malenka, R. C.; Muller, D., Synaptic plasticity and dynamic modulation of the postsynaptic membrane. *Nat. Neurosci.* **2000**, 3, (6), 545-550.
40. Trachtenberg, J. T.; Chen, B. E.; Knott, G. W.; Feng, G. P.; Sanes, J. R.; Welker, E.; Svoboda, K., Long-term in vivo imaging of experience-dependent synaptic plasticity in adult cortex. *Nature* **2002**, 420, (6917), 788-794.

Chapter 3: Identification of the Plasticity-Relevant Fucose- α (1-2)Galactose Proteome

Background

The human genome project led to the striking revelation that the number of proteins necessary for human function and development is only 20-25,000 genes, much less than the anticipated 100,000 genes thought to be discovered.¹ While genomics has produced a wealth of information on the genes encoded by DNA, it provides little information on the protein products themselves. Proteomics has emerged as an important new field to annotate the functions of proteins and provide valuable information that expedites the characterization of these proteins. Numerous large-scale approaches have been developed to characterize proteins, such as protein microarray technologies,^{2, 3} large-scale yeast two-hybrid screens,⁴ and high-throughput protein production and crystallization.⁵ In these approaches, mass spectrometry has emerged as the main method for analysis of protein functions from native biological systems.⁶⁻⁹

Mass spectrometry is a powerful approach to analyze complex proteomes because of its unparalleled ability to acquire quantitative information from samples of enormous complexity. Recent advances in instrumentation, data acquisition, and analysis have yielded this methodology amenable to a variety of proteomics techniques such as the characterization of functional protein complexes, protein pathways, and proteins modified by post-translational modifications. Furthermore, the ability to directly sequence peptides has facilitated the high-throughput identification and characterization of phosphorylation and glycosylation sites, problems that would normally take weeks of

molecular cloning, site-directed mutagenesis, and analysis through in-direct methods to establish the modified sites. More recently, mass-spectrometry-based proteomics has yielded the ability to quantitatively analyze changes in proteins during disease states.^{10, 11} Such experiments enable the identification of biomarkers for disease progression such as in cancer, diabetes, and other metabolic diseases.

With the acceleration of mass-spectrometry-based proteomics methods, it is no wonder the current literature is full of proteomic identifications and characterizations. However, despite this wealth of information, the ability to characterize proteomes by post-translation modifications (PTMs) has remained technically challenging. The lability of phosphorylation and glycosidic linkages on the mass spectrometer has hindered efforts to identify proteomes with these modifications. In addition, PTMs are often present in the cell in substoichiometric abundance, further complicating their analysis. Despite these limitations for identification of glycoproteomes, we report a successful mass-spectrometry-based proteomics method involving lectin affinity chromatography to identify the first comprehensive Fuc α (1-2)Gal proteome from adult rat cortex and murine neonatal olfactory bulb.

We employed the use of the Fuc α (1-2)Gal-binding lectin *Ulex europaeus* agglutinin (UEAI), which is reported to interact specifically with Fuc α (1-2)Gal epitopes.^{12, 13} The key binding interactions between UEAI and Fuc α (1-2)Gal disaccharides involve the hydroxyls at C2, C3, and C4 of the α -L-Fuc unit and the C3 hydroxyl of the β -D-Gal unit.^{13, 14} The key polar interactions come from the C3 and C4 of α -L-Fuc and are necessary for the interaction.¹³ The carbohydrate recognition domain of UEAI is comprised of residues Glu44, Thr86, Asp87, Arg102, Ala103, Gly104,

Gly105, Tyr106, Ile129, Val133, Asn134, Trp136, Tyr219, and Arg222.¹⁵ In addition to the key polar interactions with hydroxyl groups, Thr86 is reported to make an important hydrophobic interaction with the C5-methyl of α -L-Fuc. Thus, due to the high specificity of UEAI for Fuc α (1-2)Gal disaccharides, we chose to exploit this lectin to identify the Fuc α (1-2)Gal proteome.

We identify four major functional classes of Fuc α (1-2)Gal glycoproteins from murine olfactory bulb: the cell adhesion molecules, ion channels and solute transporters/carriers, ATP-binding proteins, and synaptic vesicle-associated proteins. We demonstrate that these proteins involved in neurotransmitter release, neurite outgrowth, and synaptic plasticity. Their identification suggests extended roles for protein fucosylation in mediating neuronal communication processes.

Results

Identification of Brain Fractions Enriched in Fuc α (1-2)Gal Glycoproteins

Identification of proteins modified by carbohydrates is especially challenging from a proteomics perspective. Lectins and antibodies that are used to capture proteins often suffer from low binding affinities, precluding the isolation of large quantities of proteins for LC-MS studies. For example, a recent proteomics study necessitated the use of a 39-foot lectin column to enrich desired glycoproteins.¹⁶ In addition, fucose is present in low cellular abundance, further complicating the isolation and identification of proteins modified by this monosaccharide. Despite these limitations for protein capture and identification, we have developed a novel method to identify the first comprehensive

Fuc α (1-2)Gal proteome from murine olfactory bulb using lectin affinity chromatography (LAC).

Previous studies have indicated that Fuc α (1-2)Gal are present in the adult and developing hippocampus.¹⁷ However, we first sought to address whether other brain regions might be further enriched in expression of Fuc α (1-2)Gal glycoproteins to facilitate isolation of glycoproteins for proteomics studies. Postnatal day 3 (P3) and adult rat brains were isolated and dissected into major brain regions including the cortex, cerebellum, hippocampus, hypothalamus, olfactory bulb, striatum, and thalamus. Brain substructures were analyzed by SDS-PAGE and Western blotting with UEAI lectin

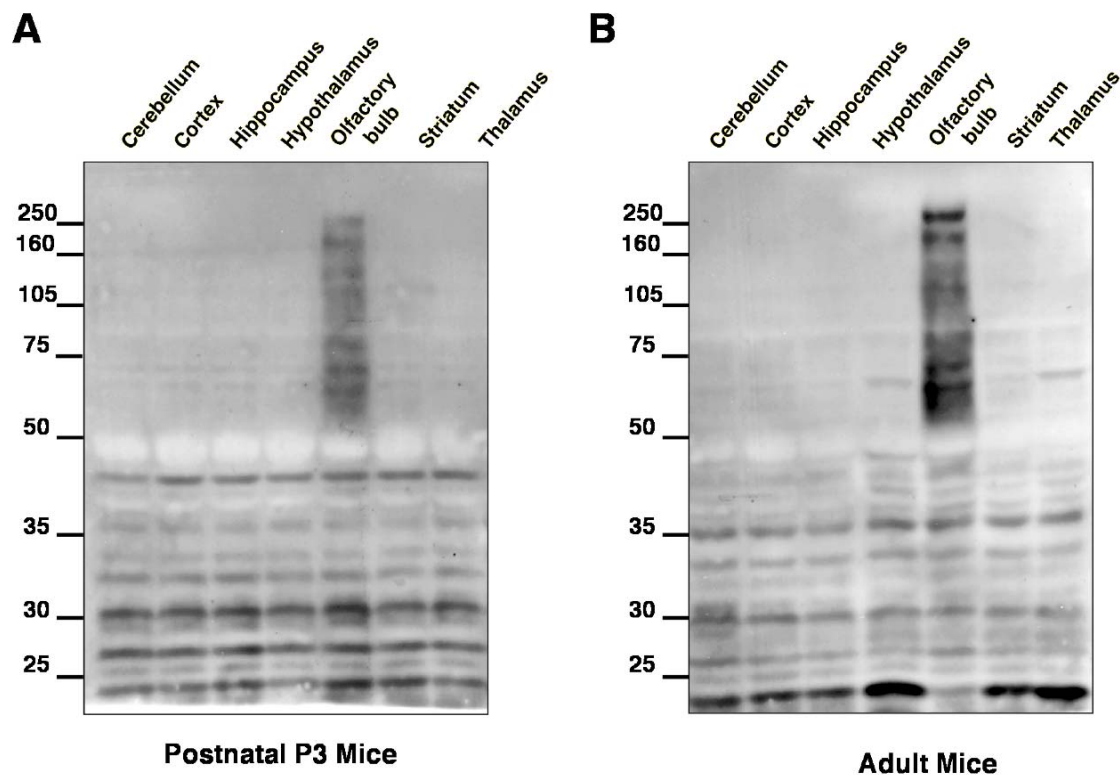


Figure 3.1. Fuc α (1-2)Gal glycoproteins are enriched in mammalian olfactory bulb. Western blot of neonatal rat brain homogenates demonstrates enrichment of Fuc α (1-2)Gal glycoproteins in postnatal (A) and adult (B) olfactory bulb. Blots were probed with UEAI.

Significant labeling of proteins was observed in olfactory bulb homogenates of both adult and neonatal rats, suggesting that Fuc α (1-2)Gal glycoproteins are highly enriched in this brain regions (Figure 3.1). Furthermore, Fuc α (1-2)Gal staining suggests the presence of many Fuc α (1-2)Gal glycoproteins between 50 and 200 kilodaltons (kDa) of rat olfactory bulb. The presence of low molecular weight proteins between 20 and 50 kDa of all brain substructures may reflect Fuc α (1-2)Gal glycoproteins expressed to a similar degree in each brain subfraction. Alternatively, these proteins may be non-specifically recognized by the Fuc α (1-2)Gal-binding lectin UEAI. In addition, there is an enriched Fuc α (1-2)Gal glycoprotein expressed at approximately 60 kDa in the adult thalamus and hypothalamus. Darker exposures of brain subfractions demonstrate that the olfactory bulb appears to contain significantly more labeling than hippocampus, another brain substructure with high expression of Fuc α (1-2)Gal glycoproteins (Figure 3.2). Finally, expression of Fuc α (1-2)Gal was significantly enhanced in neonatal mice when compared to adult olfactory bulb (data not shown), consistent with our studies suggesting that Fuc α (1-2)Gal glycoproteins are enriched during periods of neuronal growth.¹⁷ Thus, the mammalian olfactory bulb of P3 neonatal mice contains the highest expression of Fuc α (1-2)Gal glycoproteins in the brain.

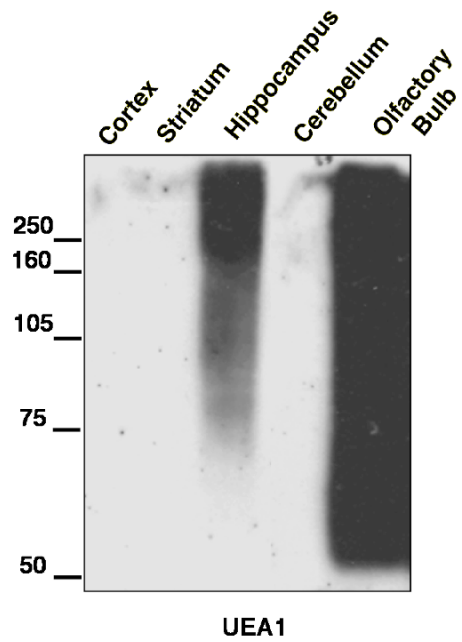


Figure 3.2. The mammalian olfactory bulb is highly enriched in expression of Fuc α (1-2)Gal glycoproteins. Rat adult brain fractions were resolved by SDS-PAGE and analyzed by immunoblotting with lectin UEA1. The olfactory bulb contains the highest expression of Fuc α (1-2)Gal glycoproteins while the hippocampus is the next region enriched.

Identification of the Fuc α (1-2)Gal Proteome from Mouse Olfactory Bulb

As the olfactory bulb of neonatal mice contained significantly higher expression of Fuc α (1-2)Gal glycoproteins, we optimized a method for the enrichment of these proteins from olfactory bulb lysates by UEA1 lectin affinity chromatography (Figure 3.3).

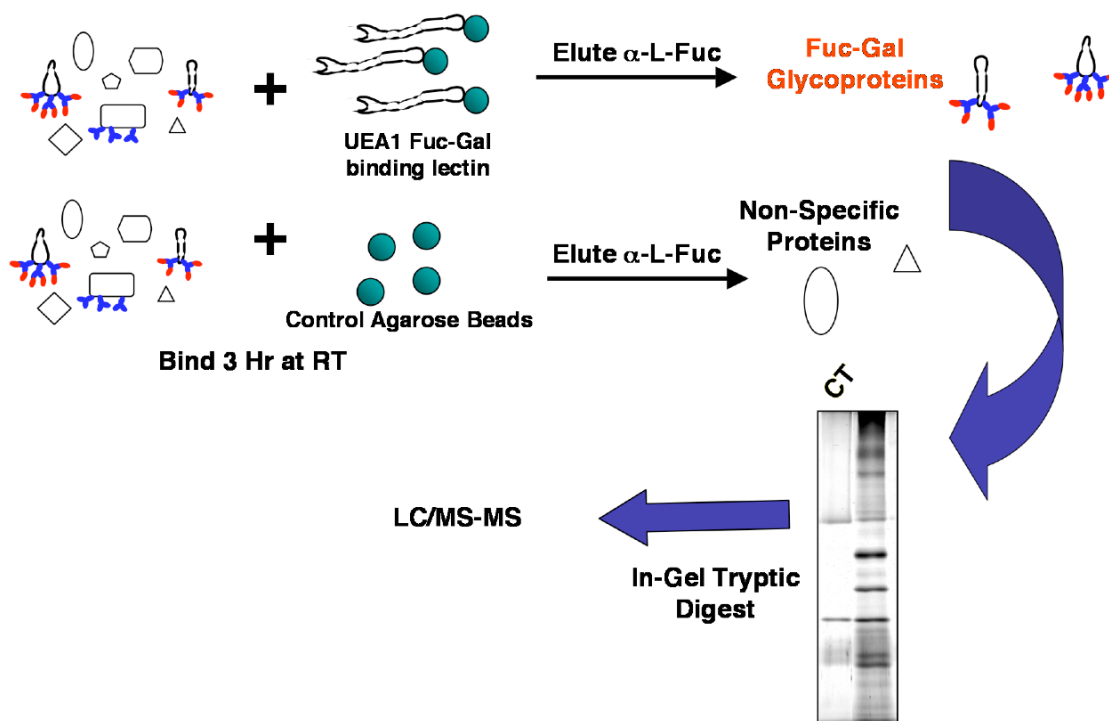


Figure 3.3. Strategy for the isolation and identification of Fuc α (1-2)Gal glycoproteins from mouse olfactory bulb.

Our approach utilizes an empirically determined buffer that maximizes lectin-carbohydrate binding while minimizing non-specific interactions, and the counter-intuitive incubation of the columns with protein lysates at room temperature to enhance glycoprotein recognition. Furthermore, the use of control protein A-agarose columns

aided in the identification of non-specific proteins that bind to the agarose beads (Figure 3.3). Using these optimized conditions and Fuc α (1-2)Gal-enriched olfactory bulb lysates, we identify a large number of proteins that were specifically captured in the UEA1 lectin affinity column from C57BL/6 P3 mice with respect to the control column (Figure 3.4).

To determine protein identities, 33 bands from each lane were excised, digested

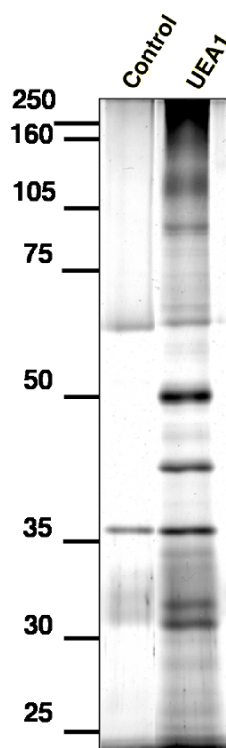


Figure 3.4. Silver stain of proteins isolated from the control protein A agarose-column (left lane) and the UEA1 column (right lane).

in-gel by trypsin and subjected to LC-MS/MS for peptide identification. Peptides were searched using a SEQUEST 3.0 search algorithm against the European Bioinformatics Institute-International Protein Index (EBI-IPI) database. The search results were compiled and filtered using Scaffold 2.0. Each series of bands was analyzed for the

presence of the protein in the agarose control columns to eliminate false positives, and putative glycoproteins between columns were compared using the Scaffold viewer. Proteins were considered potential Fuc α (1-2)Gal glycoproteins when at least 2 unique peptides were identified, which gives $\geq 99\%$ probability that the protein is present in the sample. Proteins were considered non-specific if any peptides were isolated from the control protein A-agarose column. As lectin affinity chromatography can also suffer from the purification of protein complexes due to the mild lysis conditions, other proteins that associate with the Fuc α (1-2)Gal glycoproteins may also be isolated. Thus, we implemented a stringent peptide cut-off of 7 peptides to reduce the number of non-specific proteins identified by this technique. The proteins meeting the search criteria were sorted by functions and are listed in Table 3.1. For a list of all proteins identified, see the supplemental table after the Materials and Methods section.

Proteins	Accession Number	MW	Peptides
Cell Adhesion Molecules			
Ncam1 neural cell adhesion molecule 1 isoform 1	IPI:IPI00831465.1	93474.6	35
Ncam1 Isoform N-CAM 180 of Neural cell adhesion molecule 1, 180 kDa isoform precursor	IPI:IPI00122971.1	119333.5	26
Igsf3 Immunoglobulin superfamily, member 3	IPI:IPI00420589.2	134605.2	24
L1cam L1 cell adhesion molecule	IPI:IPI00406778.3 IPI:IPI00785371.1 IPI:IPI00831568.1	140413.3	15
Cntn1 Contactin-1 precursor	IPI:IPI00123058.1	113372.8	11
Nrcam Isoform 6 of Neuronal cell adhesion molecule precursor	IPI:IPI00120564.5 IPI:IPI00338880.3 IPI:IPI00395042.1 IPI:IPI00403536.1	122736	8
Ncam2 Isoform Long of Neural cell adhesion molecule 2 precursor	IPI:IPI00127556.1 IPI:IPI00322617.1	93187.3	7

Ion Channels and Solute Transporters/ Carrier Proteins			
Slc12a2 solute carrier family 12, member 2	IPI: IPI00135324.2	130654.7	20
Cacna2d1 Isoform 2B of Dihydropyridine-sensitive L-type calcium channel subunits alpha-2/delta precursor	IPI: IPI00230013.3 IPI: IPI00319970.1 IPI: IPI00407868.1 IPI: IPI00410982.1 IPI: IPI00626793.3	122505.5	16
Slc25a12 Calcium-binding mitochondrial carrier protein Aralar1	IPI: IPI00308162.3	74553.8	12
Slc3a2 CD98 heavy chain	IPI: IPI00114641.2	58805.6	11
Slc7a5 Solute carrier family 7 (Cationic amino acid transporter, y+ system), member 5	IPI: IPI00331577.3	55856	7
ATP Synthase/ ATPase/ Transporters			
Atp1a1 Sodium/potassium-transporting ATPase subunit alpha-1 precursor	IPI: IPI00311682.5	112967.3	51
Atp5a1 ATP synthase subunit alpha, mitochondrial precursor	IPI: IPI00130280.1	59736.1	14
Atp1a3 Sodium/potassium-transporting ATPase subunit alpha-3	IPI: IPI00122048.2	111676.4	11
Atp1b1 Sodium/potassium-transporting ATPase subunit beta-1	IPI: IPI00121550.2	35771.2	10
Synaptic Vesicle Proteins			
Stxbp1 Isoform 1 of Syntaxin-binding protein 1	IPI: IPI00415402.3	67553.8	14
Syt1 Synaptotagmin-1	IPI: IPI00129618.1 IPI: IPI00750142.1	47400.9	10
Nsf Vesicle-fusing ATPase	IPI: IPI00656325.2	82598.5	8
Receptors			
Plxnb2 14 days pregnant adult female placenta cDNA, RIKEN full-length enriched library, clone: M5C1068G03 product: plexin B2, full insert sequence	IPI: IPI00405742.6 IPI: IPI00666301.1 IPI: IPI00752396.1	206212.3	16
Igf1r Insulin-like growth factor 1 receptor precursor	IPI: IPI00120225.1	155772.7	8
Cytoskeletal Remodeling/			

Binding/ Dynamics			
Dpysl3 Dihydropyrimidinase-related protein 3	IPI: IPI00122349.1	61918.9	11
Dpysl2 Dihydropyrimidinase-related protein 2	IPI: IPI00114375.2	62259.9	7
Heat Shock Proteins/ Chaperonins			
Hsp90ab1 Heat shock protein 84b	IPI: IPI00229080.7	83266.3	15
Endoplasmin precursor	IPI: IPI00129526.1	92460.6	7
Transcription/ Translation/ Ribosomal			
Eef1a1 Elongation factor 1-alpha 1	IPI: IPI00307837.5	50736.9	9
Eef2 Elongation factor 2	IPI: IPI00466069.3	95298	7
Rps3 40S ribosomal protein S3	IPI: IPI00134599.1	26656.5	7
GTPase-binding/ Cell Signaling			
Gnao1 Guanine nucleotide-binding protein G(o) subunit alpha 2	IPI: IPI00115546.4	40019.4	10
Rab3a Ras-related protein Rab-3A	IPI: IPI00122965.1	24952.3	9
Ywhaz 14-3-3 protein zeta/delta	IPI: IPI00116498.1	27753.9	8
Rab14 Ras-related protein Rab-14	IPI: IPI00126042.3	23879.6	7
Other			
Npepps Aminopeptidase puromycin sensitive	IPI: IPI00608097.1	103310.1	9
Psm2 26S proteasome non-ATPase regulatory subunit 2	IPI: IPI00123494.3	100187.1	9
Phb2; Grc10 Prohibitin-2	IPI: IPI00321718.4	33279.6	7
Phb; EG665511 Prohibitin	IPI: IPI00133440.1	29802.6	7
LOC100042349; LOC100041325; Gapdh; LOC100046067; LOC100048291; LOC100042025; LOC100040053; LOC100042746 Glyceraldehyde-3-phosphate dehydrogenase	IPI: IPI00273646.9 IPI: IPI00462008.5 IPI: IPI00620663.3	35792.1	7
Ldha L-lactate dehydrogenase A chain	IPI: IPI00319994.6 IPI: IPI00751369.1	36480.9	7

Table 3.1. Table of all putative proteins Fuca(1-2)Gal glycoproteins identified by LAC and LC-MS/MS with the number of peptides in the sample ≥ 7 . Accession numbers are from the European Bioinformatics Institute-International Protein Index (EBI-IPI).

Based on these criteria, we identified 39 putative Fuc α (1-2)Gal glycoproteins from the UEAI lectin enrichment column (Table 3.1). The major protein hit was the identification of 51 peptides corresponding to the Na⁺/K⁺ ATPase α 1 subunit. Importantly, we also identified 35 peptides for NCAM, a protein previously reported to be modified by Fuc α (1-2)Gal in mammalian olfactory bulb,¹⁸ providing validation of our methodology for the identification of Fuc α (1-2)Gal glycoproteins. In addition to this known Fuc α (1-2)Gal glycoprotein, our approach identifies 38 novel proteins. The major protein hits (greater than 10 peptides) can be categorized into four major functional classes: the cell adhesion molecules, ion channels and solute carriers/transporters, ATP-binding proteins, and synaptic vesicle-associated proteins. Thus, these studies have significantly expanded the repertoire of known Fuc α (1-2)Gal glycoproteins, from 2 to almost 40. Furthermore, identification of novel classes of Fuc α (1-2)Gal glycoproteins such as ion channels, solute transporters, and ATP-binding proteins suggests an extended role for Fuc α (1-2)Gal glycoproteins in mediating membrane excitability and ATP metabolism. In addition to these novel classes, the all of the cell adhesion molecules identified are members of the immunoglobulin superfamily (IgSF) of cell adhesion molecules, which may suggest an important functional role for fucosylation of these proteins in mediating olfactory bulb development.

Confirmation of Fuc α (1-2)Gal Glycoproteins

We next sought to confirm the presence of the four major classes of Fuc α (1-2)Gal glycoproteins identified in the MS by immunoblotting lectin column eluates. The presence of many cell adhesion molecules such as NCAM, NCAM L1, and NCAM2

(more commonly known as NCAM) was independently confirmed by immunoblotting UEAI column eluates with the appropriate antibodies (Figure 3.5). The proteins were specifically recognized by UEAI and were absent from the control column suggesting that these proteins are definitely present in the sample. We next examined eluates for the presence of synaptic vesicle proteins synaptotagmin I and munc18 (syntaxin-binding protein 1), which were also found to be specifically present (Figure 3.5). In addition, we demonstrate that the ATP-binding protein $\alpha 1$ subunit of the Na^+K^+ ATPase, which was the best protein hit by MS analysis, is conclusively present in the sample. We observed other interesting proteins with peptides less than 7 of the four major classes identified, and verified the presence of two of them by immunoblotting. The cell adhesion molecule N-cadherin is a calcium-dependent cell adhesion molecule that is not a member of the IGSF family.¹⁹⁻²² However, the presence of N-cadherin in UEAI column eluates, suggests that other classes of cell adhesion molecules can be fucosylated. We also demonstrate binding of the voltage-dependent anion channel 1 (VDAC1), which is an ion channel normally found in the mitochondrial membrane that is present in post-synaptic density preparations with unknown function.²³ Therefore, we were able to validate a number of putative $\text{Fuc}\alpha(1-2)\text{Gal}$ glycoproteins from the MS data, including proteins from all four major functional classes identified. Abundant cellular proteins such as tubulin and hsp/hsc 70 were found to bind non-specifically to the control columns, consistent with our MS data, and demonstrating the importance of the control column in eliminating false positives (Figure 3.5).

NCAM and synaptotagmin were found to run as multiple bands, which is consistent with the presence of multiple fucosylated glycoforms. In fact, NCAM has

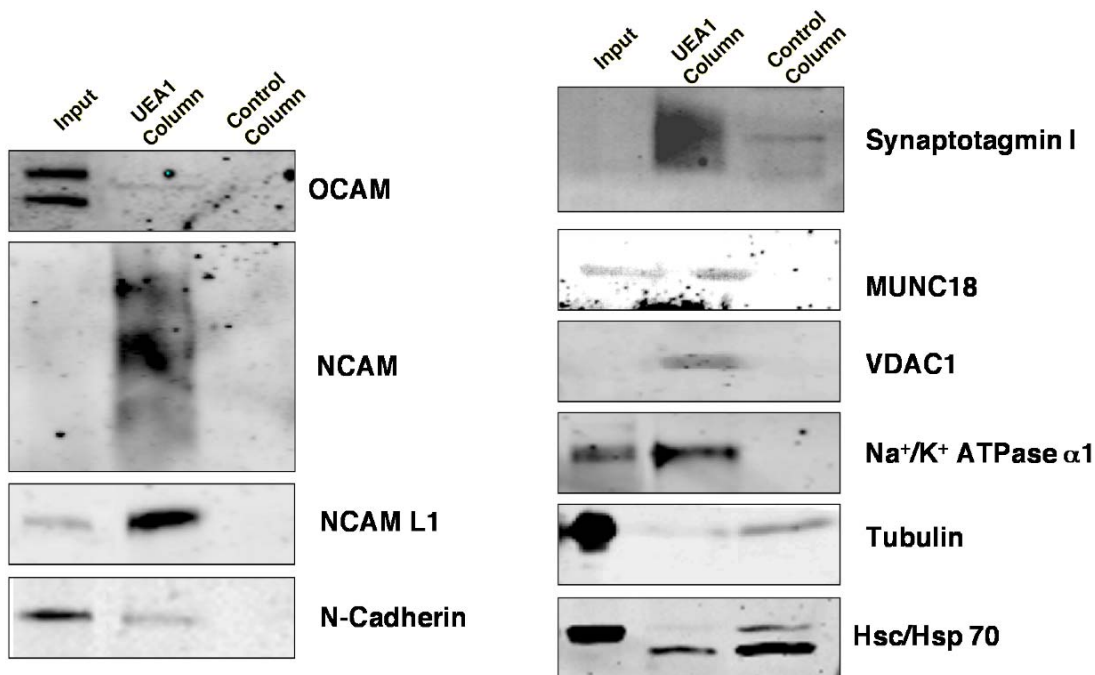


Figure 3.5. All four major classes of Fuc α (1-2)Gal glycoproteins identified in MS data are confirmed by immunoblotting lectin column eluates. We demonstrate the presence of OCAM, NCAM, NCAM L1, N-cadherin, synaptotagmin I, MUNC18, VDAC1, and the Na⁺/K⁺ ATPase α 1 subunit as specific in MS sample. Tubulin and Hsc/Hsp 70 were present in the control column eluates, consistent with MS data.

previously been reported to exist in multiple glycoforms,²⁴ thus raising the intriguing possibility that different combinations of glycans may differentially affect NCAM function. We also immunoprecipitated NCAM to confirm fucosylation by immunoblotting with UEA1 and antibody A46-B/B10 (data not shown).

Discussion

Herein we report the first comprehensive proteome of the plasticity-relevant Fuc α (1-2)Gal epitope. The proteins were identified by an optimized lectin affinity

chromatography approach coupled to mass spectrometry. This study isolates the largest number of Fuc α (1-2)Gal glycoproteins reported, and indicates specific roles for the Fuc α (1-2)Gal epitope in synaptic vesicle cycling, membrane excitability, and synaptic remodeling.

In contrast to previous studies which suggest that the cell adhesion molecule NCAM is the only Fuc α (1-2)Gal glycoprotein present in murine olfactory bulb,¹⁸ our results indicate the presence of numerous Fuc α (1-2)Gal glycoproteins in both murine neonatal olfactory bulb and adult cortex. Expression of these proteins is enhanced during periods of development. We exploited this period of increased Fuc α (1-2)Gal expression to identify the Fuc α (1-2)Gal proteome from neonatal olfactory bulb. Our studies significantly expand the number of known Fuc α (1-2)Gal glycoproteins from 2 to almost 40. Our approach identifies four major classes of these glycoproteins in murine olfactory bulb, including the cell adhesion molecules, ion channels and solute carriers/transporters, ATP-binding proteins, and synaptic vesicle-associated proteins.

The cell adhesion molecules represent the largest class of Fuc α (1-2)Gal glycoproteins identified. They are known to be involved in development and synaptic plasticity. Of the 7 proteins discovered fitting our search criteria, all are members of the immunoglobulin (Ig) superfamily of cell adhesion molecules, suggesting an important functional role for fucosylation of this subclass of proteins in mediating olfactory bulb development. Many of these proteins are already known to regulate development of the olfactory bulb. For example, NCAM is responsible for axonal fasciculation and targeting of OSNs in the olfactory bulb.^{25,26} NCAM is differentially glycosylated, and it's possible that these glycoforms help distinguish subsets of axons and aid in neuronal pathfinding.

Two of these cell adhesion molecules, contactin and OCAM, have previously been reported to play important roles in development of the accessory olfactory bulb (AOB). Contactin is highly expressed in the AOB and is involved in neurite outgrowth,²⁷ while OCAM may be involved in setting up functional subdivisions and defining patterns of connectivity in the AOB.²⁸

Several solute carriers/transporters were identified in this study, including the chloride transporter solute carrier family 12 member 2 protein (Slc12a2) and the calcium-binding mitochondrial carrier protein aralar1 (Slc25a12). Slc12a2 controls the accumulation of chloride in cells, and Slc12a2 knockout mice exhibit a loss of GABA-receptor-mediated currents in dorsal root ganglion neurons (DRGs).²⁹ In accordance with this observation, Slc12a2 KO mice exhibit alterations in locomotion and pain perception. The mitochondrial carrier protein aralar1 is expressed in neurons of the CNS where it undergoes enrichment during maturation of neuronal cultures³⁰ and may be involved in neurodegenerative conditions such as Alzheimer's disease.³¹

We identify the ion channel alpha2/delta subunit of the dihydropyridine-sensitive L-type calcium channel (Cacna2d1) as a putative Fuc α (1-2)Gal glycoprotein. In addition, we observed a known glycosylated ion channel, the transient receptor potential cation channel (TRPV5), with less than 7 peptides in the MS data, and we discuss it here. Identification of Cacna2d1 and the TRPV5 suggests a role for protein fucosylation in regulating ion channel function. Calcium signaling plays a pivotal role in regulating intracellular signaling cascades that underlie synaptic plasticity,³²⁻³⁵ and the identification of Cacna2d1 may suggest that protein fucosylation is involved in these processes. The TRP family of cation channels is expressed by sensory neurons and mediates a variety of

sensory functions such as thermal sensitivity and nociception.^{36, 37} TRP channels of mice are also used in pheromone-sensing to distinguish male mice from females,³⁸ supporting a role for the Fuc α (1-2)Gal epitope in regulating murine olfaction. *N*-linked glycosylation of the first extracellular loop of TRPV5 regulates channel function and targeting of TRP channels.^{39, 40} As TRPV5 is a putative Fuc α (1-2)Gal glycoprotein, it will be intriguing to learn whether fucosylation occurs on this *N*-linked glycan, and the specific roles of the Fuc α (1-2)Gal epitope in regulating TRPV5 channel functions.

We also discovered 11 ATP-binding proteins, including 4 subunits of the Na⁺/K⁺-ATPase, 5 subunits of ATP synthases, and 2 other ATP-driven transport proteins. The Na⁺/K⁺-ATPase is critical for maintenance of the electrochemical gradient of these ions across the plasma membrane,^{41, 42} and the beta1 subunit has previously been reported to contain *N*-linked fucosylated glycans.⁴³ While the precise fucose linkage was previously uncharacterized, our studies suggest that the beta1 glycans contain the plasticity-relevant Fuc α (1-2)Gal epitope. In addition to ATPases, we also identify various ATP synthases, which implicates the Fuc α (1-2)Gal epitope in cellular energy production.

Our identification of several synaptic vesicle-associated proteins suggests an important role for the Fuc α (1-2)Gal epitope in regulating synaptic vesicle cycling. Our previous report identifies synapsin I as a Fuc α (1-2)Gal glycoprotein,¹⁷ and these studies suggest that other proteins such as munc18 and synaptotagmin are also fucosylated. Some of the proteins identified are on the cytosolic face of the membrane, and raises the intriguing possibility that protein fucosylation may occur in the cytoplasm. Although, no known cytosolic fucosyltransferases have been discovered in higher eukaryotes to date, cytosolic fucosylation exists in the lower eukaryote *Dictyostelium discoideum*.⁴⁴⁻⁴⁶

Identification of the Fucc α (1-2)Gal glycoproteome reveals molecular insights into the functions of the Fucc α (1-2)Gal epitope. We uncover proteins involved in development, neurite outgrowth, and synaptic plasticity. These results are consistent with an important role for the Fucc α (1-2)Gal epitope in modulating the molecular mechanisms involved in neuronal communication and development.

Materials and Methods

Animals, Tissue Isolation and Homogenization

C57BL/6 wild-type animals and Sprague-Dawley rats were maintained in accordance with proper Institute of Animal Care and Use Committee (IACUC) procedures. Adult male mice ages 3-4 months and post-natal day 3 (P3) pups were anesthetized with CO₂ and dissected to remove the cerebellum, cortex, hippocampus, hypothalamus, olfactory bulb, striatum, and thalamus. For Western blotting, dissected tissues were cut into small pieces and placed immediately on ice, then lysed in boiling 1% SDS with sonication until homogeneous (5V:W). For lectin affinity chromatography, the olfactory bulbs from 30-50 P3 pups were isolated and homogenized in lectin binding buffer (100 mM Tris pH 7.5/ 150 mM NaCl/ 1mM CaCl₂/ 1 mM MgCl₂/ 0.5% NP-40/ 0.2% Na deoxycholate plus protease inhibitors) by passing through a 26G needle 5 times, then sonicated to homogeneity. Samples were clarified by centrifugation at 12,000g \times 10 min. Lysates were between 6 to 10 mg/mL total protein concentration as determined by the BCA protein assay (Pierce) for lectin affinity chromatography. Alternatively, the olfactory bulbs from 12-16 rat pups were used for lectin affinity chromatography experiments followed by immunoblotting with different antibodies.

Lectin Affinity Chromatography and SDS-PAGE

One mL bed volume of *Ulex europaeus* agglutinin I (UEAI) conjugated to agarose (Vector Labs,) and control Protein A conjugated to agarose (Vector Labs) columns were packed ~333 μ L into 3 minicolumns run in parallel (BioRad). The resin was equilibrated with 10 column volumes (CV) lectin binding buffer. 3 mLs of olfactory bulb lysate at 6-10 mg/mL was bound in batch at RT for 4 hours. Columns were repacked and the flowthrough was passed 3 additional times over the column. Columns were washed with 40 CV of lectin binding buffer, followed by 10 CV of lectin binding buffer lacking detergent (NP-40 and Na deoxycholate). Proteins were eluted in 10 CV of lectin binding buffer lacking detergent supplemented with 200 mM α -L-Fuc and protease inhibitors.

Protein eluates were concentrated in 10,000 molecular weight cut-off (MWCO) centricons (Millipore) followed by 10,000 MWCO microcons (Millipore) to 100 μ L. Following concentration, samples were boiled with 35 μ L of 4X SDS loading dye and loaded onto 10% SDS gels for electrophoresis as described previously.⁴⁷

Silver Staining, Peptide Extraction, and In-Gel Tryptic Digests

All silver staining reagents were prepared fresh. Gels were fixed in 50% MeOH/ 10% acetic acid for 30 min at RT, followed by 5% MeOH/ 1% for 15 min. Gels were rinsed 1x in 50% MeOH for 1min, then washed 6 \times 10 min in ddH₂O. Following fixation, gels were sensitized in 20 mg/100 mL Na₂S₂O₃•5H₂O for 90 s, rinsed 3 x 30 s in

ddH₂O and stained in 200mg/100 mL AgNO₃ for 30 min. Gels were washed 3 x 60 s in ddH₂O, and developed in 6g in 100 mL Na₂CO₃/ 50 µL in 100 mL 37% formaldehyde/ 2mL of 20 mg/100 mL Na₂S₂O₃•5H₂O for up to 10 min, as required. Staining was stopped by 6% acetic acid for 10 min and then washed in ddH₂O. Gels were destained in 0.4 g K₃Fe(CN)₆/ 200 mL Na₂S₂O₃•5H₂O (0.2g/L) for 15 min or until no bands were visible then washed 6 × 15 min in ddH₂O to overnight. Gel pieces were excised and reduced in 150 µL of 8 mM TCEP in 80 mM ammonium bicarbonate buffer, pH 7.8/ 150 µL CH₃CN. Gel pieces were reduced for 20 min at RT. The solution was discarded and cysteines were alkynylated in 150 µL of 10 mM iodoacetamide in 80 mM ammonium bicarbonate buffer, pH 7.8/ 150 µL CH₃CN. Reactions were incubated in the dark for 20 min at RT. The supernatant was discarded and gel pieces were rehydrated in 500 µL of 50 mM ammonium bicarbonate for 10 min at RT. The supernatant was removed and gel pieces were speed vac'd for 15 min. Gel pieces were resuspended in 40 µL H₂O/ 5 µL 500 mM ammonium bicarbonate, pH 7.8/ and 5 µL of 0.2 mg/mL trypsin (promega), and left on ice for 30 min. Tubes were then incubated overnight at 37 °C. The following day, excess trypsin solution not absorbed was removed and saved in a new tube. Gel pieces were washed with 500 µL of H₂O by vortexing for 20 min. The solution was removed and combined with the tryptic digests. Peptides were extracted at 2 × 200 µL of 5% formic acid/ 50% CH₃CN by vortexing for 20 min and combined with the tryptic and wash fractions. Samples were concentrated in a speed vac down to 20 µL for MS analysis.

Orbitrap LC-MS Analysis

Approximately 50% of gel extractions were loaded onto a 360 μm O.D. X 75 μm precolumn packed with 4 cm of 5 μm Monitor C18 particles (Column Engineering) as described previously.⁴⁸

Western Blotting

10% SDS gels were transferred to PVDF, blocked in 3% HIO₄⁻ BSA,¹⁷ and incubated with HRP-conjugated UEAI (Sigma) at 50 $\mu\text{g}/\text{mL}$ in TBST for 2 h at RT. Membranes were washed 3 \times 10 min in TBST, then developed as described previously.¹⁷ For immunoblotting to confirm proteome hits, proteins from lectin affinity chromatography were separated on Bis-Tris 4-12% NuPage gradient gels (Invitrogen) according to the manufacturer's protocol in MOPS running buffer. Gels were transferred to PVDF, blocked in infrared blocking buffer (Rockland), and incubated with the following primary antibodies overnight in TBST: mouse anti-tubulin at 1:50,000 (Sigma), mouse anti-hsc/hsp 70 at 1:2000 (Stressgen), rabbit anti-munc18 at 1:2000 (Synaptic Systems), goat anti-VDAC1 at 1:1000 (Santa Cruz), mouse $\alpha 5$ anti-Na⁺/K⁺ ATPase alpha subunits at 5 $\mu\text{g}/\text{mL}$ (Iowa Hybridoma Bank), mouse anti-OCAM at 1:100 (R&D Systems), mouse 5e anti-NCAM at 10 $\mu\text{g}/\text{mL}$ (Iowa Hybridoma Bank), mouse ASCS4 anti-NCAM L1 at 2 $\mu\text{g}/\text{mL}$ (Iowa Hybridoma Bank), mouse anti-N-cadherin at 1:1000 (Chemicon), and rabbit anti-synaptotagmin I at 1:2000 (Synaptic Systems). Following incubation, blots were washed in TBST 3 times by 10 min, then incubated with secondary antibodies for 1h at 1:5000 in TBST plus 0.02% SDS. The following secondary antibodies were used: Alexa 680-conjugated donkey anti-mouse (Molecular Probes), Alexa 800-conjugated

donkey anti-rabbit (Rockland Immunochemicals), and Alexa 680-conjugated donkey anti-goat (Molecular Probes). Membranes were washed in TBST 3 times by 10 min, and imaged on the Odyssey Infrared imager (Licor).

Antibody Purification

500 μ L of mouse ascites from the $\alpha 5$ Na⁺/K⁺ ATPase alpha subunit, 5e NCAM, and ASCS4 NCAM L1 were purified over 300 μ L Immunopure Protein-A agarose columns following the manufacturer's protocol (Pierce). Eluted antibodies were dialyzed into PBS, concentrations were determined by the A_{280} , and normalized to 1 mg/mL.

Protein name	Accession	MW	C57	UEA1FUT1	KO
LHW_HM_P and Q Samples			Uncategorized Sample	Uncategorized Sampl	
Atp1a1 Sodium/potassium-transporting ATPase subunit alpha	IPI: IPI00311682.5	112967.3	51		0
Ncam1 neural cell adhesion molecule 1 isoform 1	IPI: IPI00831465.1	93474.6	35		0
Tubb5 Tubulin beta-5 chain	IPI: IPI00117352.1	49652.6	28		0
Ncam1 Isoform N-CAM 180 of Neural cell adhesion molecule 1	IPI: IPI00122971.1	119333.5	26		0
Igsf3 Immunoglobulin superfamily, member 3	IPI: IPI00420589.2	134605.2	24		0
Tuba1a Tubulin alpha-1A chain	IPI: IPI00110753.1, IPI	50117.7	24		3
Hspa8 Heat shock cognate 71 kDa protein	IPI: IPI00323357.3, IPI	70854.7	22		6
Slc12a2 solute carrier family 12, member 2	IPI: IPI00135324.2	130654.7	20		0
Actb Actin, cytoplasmic 1	IPI: IPI00110850.1, IPI	41719.8	20		3
Alb Serum albumin precursor	IPI: IPI00131695.3	68674.9	18		14
Plxn2 14 days pregnant adult female placenta cDNA, RIKEN	IPI: IPI00405742.6, IPI	206212.3	16		0
Cacna2d1 Isoform 2B of Dihydropyridine-sensitive L-type calc	IPI: IPI00230013.3, IPI	122505.5	16		0
Tuba1b Tubulin alpha-1B chain	IPI: IPI00117348.4	50133.7	16		3
L1cam L1 cell adhesion molecule	IPI: IPI00406778.3, IPI	140413.3	15		0
Hsp90ab1 Heat shock protein 84b	IPI: IPI00229080.7	83266.3	15		0
Tubb2c Tubulin beta-2C chain	IPI: IPI00169463.1	49812.7	15		0
Stxbp1 Isoform 1 of Syntaxin-binding protein 1	IPI: IPI00415402.3	67553.8	14		0
Atp5a1 ATP synthase subunit alpha, mitochondrial precursor	IPI: IPI00130280.1	59736.1	14		0
Tubb2b Tubulin beta-2B chain	IPI: IPI00109061.1, IPI	49935.1	14		0
Hspa5 78 kDa glucose-regulated protein precursor	IPI: IPI00319992.1	72405.6	13		0
Slc25a12 Calcium-binding mitochondrial carrier protein Aralar	IPI: IPI00308162.3	74553.8	12		0
Atp5b ATP synthase subunit beta, mitochondrial precursor	IPI: IPI00468481.2	56283.2	12		0
Tubb3 Tubulin beta-3 chain	IPI: IPI00112251.1	50400.7	12		0
Cntn1 Contactin-1 precursor	IPI: IPI00123058.1	113372.8	11		0
Atp1a3 Sodium/potassium-transporting ATPase subunit alpha	IPI: IPI00122048.2	111676.4	11		0
Dpysl3 Dihydropyrimidinase-related protein 3	IPI: IPI00122349.1	61918.9	11		0
Slc3a2 CD98 heavy chain	IPI: IPI00114641.2	58805.6	11		0
Syt1 Synaptotagmin-1	IPI: IPI00129618.1, IPI	47400.9	10		0
Gnao1 Guanine nucleotide-binding protein G(o) subunit alpha	IPI: IPI00115546.4	40019.4	10		0
Atp1b1 Sodium/potassium-transporting ATPase subunit beta-	IPI: IPI00121550.2	35771.2	10		0
Npepps Aminopeptidase puromycin sensitive	IPI: IPI00608097.1	103310.1	9		0
Psm2 26S proteasome non-ATPase regulatory subunit 2	IPI: IPI00123494.3	100187.1	9		0
Eef1a1 Elongation factor 1-alpha 1	IPI: IPI00307837.5	50736.9	9		0
LOC100042651 similar to Tubulin, beta 4	IPI: IPI00458204.4	49767.5	9		0
Rab3a Ras-related protein Rab-3A	IPI: IPI00122965.1	24952.3	9		0
Gap43 Neuromodulin	IPI: IPI00128973.1	23614.3	9		5
Igf1r Insulin-like growth factor 1 receptor precursor	IPI: IPI00120225.1	155772.7	8		0
Nrcam Isoform 6 of Neuronal cell adhesion molecule precursor	IPI: IPI00120564.5, IPI	122736	8		0
Nsf Vesicle-fusing ATPase	IPI: IPI00656325.2	82598.5	8		0
Tpm3 Isoform 2 of Tropomyosin alpha-3 chain	IPI: IPI00230044.5	29003.2	8		2
Ywhaz 14-3-3 protein zeta/delta	IPI: IPI00116498.1	27753.9	8		0
Eef2 Elongation factor 2	IPI: IPI00466069.3	95298	7		0
Ncam2 Isoform Long of Neural cell adhesion molecule 2 precu	IPI: IPI00127556.1, IPI	93187.3	7		0
Hsp90b1 Endoplasmic precursor	IPI: IPI00129526.1	92460.6	7		0
Dpysl2 Dihydropyrimidinase-related protein 2	IPI: IPI00114375.2	62259.9	7		0
Slc7a5 Solute carrier family 7 (Cationic amino acid transporte	IPI: IPI00331577.3	55856	7		0
Ldha L-lactate dehydrogenase A chain	IPI: IPI00319994.6, IPI	36480.9	7		0
LOC100042349; LOC100041325; Gapdh; LOC100046067; LOC1	IPI: IPI00273646.9, IPI	35792.1	7		0

Rab5c Ras-related protein Rab-5C	IPI: IPI00224518.2, IPI	23394.7	5	0
Prdx2 Peroxiredoxin-2	IPI: IPI00117910.3	21761.1	5	0
Atp7a Cation-transporting ATPase	IPI: IPI00830169.1	162013.2	4	0
Adcy3 Adenylate cyclase type 3	IPI: IPI00128323.3	129026.7	4	0
Pcdh17 Protocadherin 17	IPI: IPI00356667.4	126116.7	4	0
Slc12a7 Solute carrier family 12 member 7	IPI: IPI00331175.5	119465.7	4	0
Slc8a1 Sodium/calcium exchanger 1 precursor	IPI: IPI00109213.1	108019.5	4	0
Ctnna2 Isoform II of Catenin alpha-2	IPI: IPI00119870.2, IPI	105269.1	4	0
Pygb Glycogen phosphorylase, brain form	IPI: IPI00229796.3	96714.5	4	0
Trpv2 Transient receptor potential cation channel subfamily V	IPI: IPI00322698.6	86305.7	4	0
Ctnnb1 Catenin beta-1	IPI: IPI00125899.1, IPI	85452.9	4	0
Hsp90aa1 Heat shock protein HSP 90-alpha	IPI: IPI00330804.4	84773.2	4	0
Hadha Hydroxyacyl-Coenzyme A dehydrogenase/3-ketoacyl-C	IPI: IPI00223092.4	82627.3	4	0
Gars Glycyl-tRNA synthetase	IPI: IPI00112555.3	81861.1	4	0
Ndufs1 NADH-ubiquinone oxidoreductase 75 kDa subunit, mit	IPI: IPI00308882.4	79731.6	4	0
BC005764 CDNA sequence BC005764	IPI: IPI00117580.7	79143.5	4	0
Ncstn Nicastrin precursor	IPI: IPI00118674.7	78473	4	0
Trf Serotransferrin precursor	IPI: IPI00139788.2	76706.2	4	0
Slc24a2 solute carrier family 24 (sodium/potassium/calcium e	IPI: IPI00225530.1, IPI	74225.6	4	0
Lingo2 Adult male hippocampus cDNA, RIKEN full-length enric	IPI: IPI00341267.4	68054.1	4	0
Igsf8 Immunoglobulin superfamily member 8 precursor	IPI: IPI00321348.3, IPI	64991.6	4	0
Sucla2 Succinyl-CoA ligase [ADP-forming] beta-chain, mitoch	IPI: IPI00261627.1	50096.7	4	0
Tuba4a Tubulin alpha-4A chain	IPI: IPI00117350.1	49906.6	4	0
Idh1 0 day neonate lung cDNA, RIKEN full-length enriched lib	IPI: IPI00135231.2, IPI	47528.7	4	0
ENSMUSG00000075591; Got2 Aspartate aminotransferase, mi	IPI: IPI00117312.1, IPI	47394.3	4	0
Dnaja1 DnaJ homolog subfamily A member 1	IPI: IPI00132208.1, IPI	44850.6	4	0
Acat1 Acetyl-CoA acetyltransferase, mitochondrial precursor	IPI: IPI00154054.1	44798.4	4	0
Tardbp TAR DNA-binding protein 43	IPI: IPI00121758.1, IPI	44529.5	4	0
Kcnab2 Voltage-gated potassium channel subunit beta-2	IPI: IPI00315359.1	41004.4	4	0
Fdps Farnesyl pyrophosphate synthetase	IPI: IPI00120457.1	40565.2	4	0
Atp6v0d1 Vacuolar ATP synthase subunit d 1	IPI: IPI00313841.1	40284.8	4	0
Lgals9 Isoform Long of Galectin-9	IPI: IPI00114396.1, IPI	40017.4	4	0
Ahsa1 Activator of 90 kDa heat shock protein ATPase homolog	IPI: IPI00153740.1	38099.3	4	0
Gnb2i1 Guanine nucleotide-binding protein subunit beta 2-like	IPI: IPI00317740.5	35059	4	0
Slc25a4 ADP/ATP translocase 1	IPI: IPI00115564.5	32887.4	4	0
Vdac1 Isoform PI-VDAC1 of Voltage-dependent anion-selectiv	IPI: IPI00122549.1, IPI	32334.7	4	0
Ywhaq Isoform 1 of 14-3-3 protein theta	IPI: IPI00408378.4, IPI	27761.4	4	0
Etfb Electron transfer flavoprotein subunit beta	IPI: IPI00121440.4	27605.2	4	0
Rab8b Ras-related protein Rab-8B	IPI: IPI00411115.1	23586.9	4	0
Atp5o; LOC100047429 ATP synthase O subunit, mitochondrial	IPI: IPI00118986.1	23346.4	4	0
Snap25 Isoform SNAP-25b of Synaptosomal-associated protei	IPI: IPI00125635.1	23297.4	4	0
Prdx1 Peroxiredoxin-1	IPI: IPI00121788.1, IPI	22159.5	4	0
Basp1 Brain acid soluble protein 1	IPI: IPI00129519.3	22068.6	4	0
Fasn Fatty acid synthase	IPI: IPI00113223.2	272411.3	3	0
Sdk1 Isoform 1 of Protein sidekick-1 precursor	IPI: IPI00420682.5, IPI	240922.5	3	0
Cand1 TBP-interacting protein isoform 1	IPI: IPI00420562.5, IPI	158958.3	3	0
Atp6v0a1 Isoform A1-II of Vacuolar proton translocating ATPe	IPI: IPI00130187.1, IPI	96486.8	3	0
Gsn Isoform 1 of Gelsolin precursor	IPI: IPI00117167.2, IPI	85923.9	3	0
Sv2a Synaptic vesicle glycoprotein 2A	IPI: IPI00465810.3, IPI	82630.9	3	0
Sv2c similar to synaptic vesicle glycoprotein 2c isoform 1	IPI: IPI00751719.1, IPI	82463.2	3	0
Sv2b Synaptic vesicle glycoprotein 2B	IPI: IPI00221456.1	77442	3	0
Cnga2 Cyclic nucleotide-gated olfactory channel	IPI: IPI00330727.2, IPI	76194.7	3	0

3110004L20Rik Adult male brain UNDEFINED_CELL_LINE cDN	IPI: IPI00380443.4	74309.8	3	0
Cnm4 Ancient conserved domain protein 4	IPI: IPI00120783.3	73273.9	3	0
Yars Tyrosyl-tRNA synthetase	IPI: IPI00314153.4, IPI	62985	3	0
Cct6a T-complex protein 1 subunit zeta	IPI: IPI00116281.3	57987.5	3	0
Hmgcs1; LOC100040592 Hydroxymethylglutaryl-CoA synthase	IPI: IPI00331707.1	57552.2	3	0
Dars Aspartyl-tRNA synthetase, cytoplasmic	IPI: IPI00122743.1, IPI	57099.7	3	0
Kcna2 Potassium voltage-gated channel subfamily A member	IPI: IPI00129774.1, IPI	56684.5	3	0
Camkv CaM kinase-like vesicle-associated protein	IPI: IPI00122486.3	54801.8	3	0
Dld Dihydrolipoamide dehydrogenase	IPI: IPI00331564.2	54580.6	3	0
Vim Vimentin	IPI: IPI00227299.6	53670.7	3	0
Hnrpk Isoform 1 of Heterogeneous nuclear ribonucleoprotein	IPI: IPI00223253.1, IPI	50960.5	3	0
Tufm Isoform 1 of Elongation factor Tu, mitochondrial precurs	IPI: IPI00274407.1, IPI	49490.8	3	0
Psmc4 26S protease regulatory subunit 6B	IPI: IPI00108895.1, IPI	47264.7	3	0
Actr2 Actin-like protein 2	IPI: IPI00177038.1, IPI	44743.7	3	0
Cnp Isoform CNPI of 2',3'-cyclic-nucleotide 3'-phosphodiester.	IPI: IPI00229598.4, IPI	44638	3	0
Psmc6 26S protease regulatory subunit S10B	IPI: IPI00125971.1	44156.9	3	0
Pa2g4 Proliferation-associated protein 2G4	IPI: IPI00119305.3	43680.7	3	0
Ckb Creatine kinase B-type	IPI: IPI00136703.1	42696.1	3	0
Actr1a Alpha-centractin	IPI: IPI00113895.1	42597.2	3	0
Ndufa10 NADH dehydrogenase [ubiquinone] 1 alpha subcomp	IPI: IPI00116748.1	40586.7	3	0
Cxadr Isoform 1 of Coxsackievirus and adenovirus receptor hc	IPI: IPI00270376.6, IPI	39930.2	3	0
LOC100048637; Tmod2 Isoform 1 of Tropomodulin-2	IPI: IPI00402982.2	39493.9	3	0
Hnrpd Isoform 1 of Heterogeneous nuclear ribonucleoprotein	IPI: IPI00330958.2, IPI	38336.5	3	0
Mdh1 Malate dehydrogenase, cytoplasmic	IPI: IPI00336324.11	36494.1	3	0
Rpl5; LOC100043295 60S ribosomal protein L5	IPI: IPI00308706.4, IPI	34383.4	3	0
Set; LOC671392 Isoform 1 of Protein SET	IPI: IPI00111560.3, IPI	33360.4	3	0
Vdac2 Voltage-dependent anion-selective channel protein 2	IPI: IPI00122547.1	31715.6	3	0
Rpl7 60S ribosomal protein L7	IPI: IPI00311236.1	31403.6	3	0
Calb2 Calretinin	IPI: IPI00119346.1	31356.6	3	0
Capzb Isoform 2 of F-actin capping protein subunit beta	IPI: IPI00269481.7, IPI	30611.7	3	0
Rps3a 40S ribosomal protein S3a	IPI: IPI00331345.5, IPI	29867.3	3	0
Rps4x 40S ribosomal protein S4, X isoform	IPI: IPI00331092.7	29581.3	3	0
Tpi1 Triosephosphate isomerase	IPI: IPI00467833.5	26694.2	3	0
Slc25a22 25 kDa protein	IPI: IPI00756073.1	24622.5	3	0
Rps18 40S ribosomal protein S18	IPI: IPI00317590.5, IPI	17701.3	3	0
Mrc1 Macrophage mannose receptor 1 precursor	IPI: IPI00126186.1	165051	2	0
Acly Adult male testis cDNA, RIKEN full-length enriched librar	IPI: IPI00126248.3, IPI	120780.5	2	0
Ephb2 Isoform 1 of Ephrin type-B receptor 2 precursor	IPI: IPI00108870.2, IPI	110743.2	2	0
Tmprss6 type II transmembrane serine protease 6	IPI: IPI00173181.6	90959.4	2	0
Plaa Phospholipase A-2-activating protein	IPI: IPI00226234.5, IPI	87219.3	2	0
Aco2 Aconitate hydratase, mitochondrial precursor	IPI: IPI00116074.1	85447.9	2	0
Cntn4 Isoform 2 of Contactin-4 precursor	IPI: IPI00228295.2, IPI	78406.6	2	0
Rpn2 Dolichyl-diphosphooligosaccharide--protein glycosyltran	IPI: IPI00475154.1, IPI	69045.6	2	0
Kcna5 Ventricular potassium channel Kv1.5	IPI: IPI00163025.1	66563.6	2	0
Dclk1 Doublecortin-like protein	IPI: IPI00119762.4	58625.1	2	0
Sept3 53 kDa protein	IPI: IPI00761331.1, IPI	53260.6	2	0
Cadm1 Isoform 1 of Cell adhesion molecule 1 precursor	IPI: IPI00322447.4, IPI	49770.5	2	0
Eif4a1 Eukaryotic initiation factor 4A-1	IPI: IPI00118676.3, IPI	46137.3	2	0
Acta1 Actin, alpha skeletal muscle	IPI: IPI00110827.1, IPI	42034.1	2	4
Taldo1 Transaldolase	IPI: IPI00124692.1	37370.5	2	0
Slc25a5 ADP/ATP translocase 2	IPI: IPI00127841.3	32914.6	2	0
Rpl28; LOC100042670; LOC100047349 60S ribosomal protein	IPI: IPI00222547.6, IPI	15715.7	2	0
RP23-24J10.5; Uba52 Uba52 protein	IPI: IPI00108590.2, IPI	14710.9	2	0
Dclk1 Doublecortin-like protein	IPI: IPI00468380.4, IPI	0	2	0
Dsp desmoplakin isoform 1	IPI: IPI00553419.3, IPI	332901.9	0	6
Myh1 Myosin-1	IPI: IPI00380896.1	223329.7	0	7
Krt13 Isoform 1 of Keratin, type I cytoskeletal 13	IPI: IPI00136056.1	47737.8	0	3
Anxa1 Annexin A1	IPI: IPI00230395.5, IPI	38717.7	0	3

References

1. Collins, F. S.; Lander, E. S.; Rogers, J.; Waterston, R. H., Finishing the euchromatic sequence of the human genome. *Nature* **2004**, 431, (7011), 931-945.
2. Hall, D. A.; Ptacek, J.; Snyder, M., Protein microarray technology. *Mech. Ageing and Dev.* **2007**, 128, (1), 161-167.
3. MacBeath, G., Protein microarrays and proteomics. *Nat. Genet.* **2002**, 32, 526-532.
4. Causius, B., Studying the interactome with the yeast two-hybrid system and mass spectrometry. *Mass Spectrom. Rev.* **2004**, 23, 350-367.
5. Stevens, R. C.; Yokoyama, S.; Wilson, I. A., Global efforts in structural genomics. *Science* **2001**, 294, (5540), 89-92.
6. Yates, J. R., Mass spectral analysis in proteomics. *Annu. Rev. Biophys. Biomol. Struct.* **2004**, 33, 297-316.
7. Aebersold, R.; Mann, M., Mass spectrometry-based proteomics. *Nature* **2003**, 422, (6928), 198-207.
8. Domon, B.; Aebersold, R., Review - Mass spectrometry and protein analysis. *Science* **2006**, 312, (5771), 212-217.
9. Cravatt, B. F.; Simon, G. M.; Yates, J. R., The biological impact of mass-spectrometry-based proteomics. *Nature* **2007**, 450, (7172), 991-1000.
10. Klegeris, A.; Li, J.; Bammler, T. K.; Jin, J.; Zhu, D.; Kashima, D. T.; Pan, S.; Hashioka, S.; Maguire, J.; McGeer, P. L.; Zhang, J., Prolyl endopeptidase is revealed following SILAC analysis to be a novel mediator of human microglial and THP-1 cell neurotoxicity. *Glia* **2008**, 56, (6), 675-685.
11. Yocum, A. K.; Busch, C. M.; Felix, C. A.; Blair, I. A., Proteomics-based strategy to identify biomarkers and pharmacological targets in leukemias with t(4;11) translocations. *J. Prot. Res.* **2006**, 5, (10), 2743-2753.
12. Lemieux, R. U.; Baker, D. A.; Weinstein, W. M.; Switzer, C. M., Artificial antigens - antibody preparations for the localization of Lewis determinants in tissues. *Biochemistry* **1981**, 20, (1), 199-205.
13. Hindsgaul, O.; Khare, D. P.; Bach, M.; Lemieux, R. U., Molecular recognition .3. the binding of the H-type-2 human-blood group determinant by the lectin-I of *Ulex-europaeus*. *Can. J. Chem.* **1985**, 63, (10), 2653-2658.
14. Spohr, U.; Paszkiewicz-natiw, E.; Morishima, N.; Lemieux, R. U., Molecular recognition. 11. The synthesis of extensively deoxygenated derivatives of the H-type-2 human blood-group determinant and their binding by an anti-H-type-2 monoclonal-antibody and the lectin-1 of *Ulex-europaeus*. *Can. J. Chem.* **1992**, 70, (1), 254-271.

15. Audette, G. F.; Olson, D. J. H.; Ross, A. R. S.; Quail, J. W.; Delbaere, L. T. J., Examination of the structural basis for O(H) blood group specificity by Ulex europaeus Lectin I. *Can. J. Chem.* **2002**, 80, (8), 1010-1021.
16. Vosseller, K.; Trinidad, J. C.; Chalkley, R. J.; Specht, C. G.; Thalhammer, A.; Lynn, A. J.; Snedecor, J. O.; Guan, S.; Medzihradzky, K. F.; Maltby, D. A.; Schoepfer, R.; Burlingame, A. L., O-linked N-acetylglucosamine proteomics of postsynaptic density preparations using lectin weak affinity chromatography and mass spectrometry. *Mol. Cell. Proteomics* **2006**, 5, (5), 923-34.
17. Murrey, H. E.; Gama, C. I.; Kalovidouris, S. A.; Luo, W. I.; Driggers, E. M.; Porton, B.; Hsieh-Wilson, L. C., Protein fucosylation regulates synapsin Ia/lb expression and neuronal morphology in primary hippocampal neurons. *Proc. Natl. Acad. Sci. USA* **2006**, 103, (1), 21-26.
18. Pestean, A.; Krizbai, I.; Bottcher, H.; Parducz, A.; Joo, F.; Wolff, J. R., Identification of the Ulex-europaeus agglutinin-I-binding protein as a unique glycoform of the neural cell-adhesion molecule in the olfactory sensory axons of adult-rats. *Neurosci. Lett.* **1995**, 195, (2), 117-120.
19. Bamji, S. X., Cadherins: Actin with the cytoskeleton to form synapses. *Neuron* **2005**, 47, (2), 175-178.
20. Troyanovsky, S., Cadherin dimers in cell-cell adhesion. *Eur. J. Cell Biol.* **2005**, 84, (2-3), 225-233.
21. Goodwin, M.; Yap, A. S., Classical cadherin adhesion molecules: coordinating cell adhesion, signaling and the cytoskeleton. *J. Mol. Histol.* **2004**, 35, (8-9), 839-844.
22. Huntley, G. W.; Gil, O.; Bozdagi, O., The cadherin family of cell adhesion molecules: Multiple roles in synaptic plasticity. *Neuroscientist* **2002**, 8, (3), 221-233.
23. Moon, J. I.; Jung, Y. W.; Ko, B. H.; De Pinto, V.; Jin, I.; Moon, I. S., Presence of a voltage-dependent anion channel 1 in the rat postsynaptic density fraction. *Neuroreport* **1999**, 10, (3), 443-447.
24. Storan, M. J.; Magnaldo, T.; Biol-N'Garagba, M. C.; Zick, Y.; Key, B., Expression and putative role of lactoseries carbohydrates present on NCAM in the rat primary olfactory pathway. *J. Comp. Neurol.* **2004**, 475, (3), 289-302.
25. Au, W. W.; Treloar, H. B.; Greer, C. A., Sublaminar organization of the mouse olfactory bulb nerve layer. *J. Comp. Neurol.* **2002**, 446, (1), 68-80.
26. Gong, Q. Z.; Shipley, M. T., Expression of extracellular matrix molecules and cell surface molecules in the olfactory nerve pathway during early development. *J. Comp. Neurol.* **1996**, 366, (1), 1-14.
27. Ogawa, J.; Lee, S.; Itoh, K.; Nagata, S.; Machida, T.; Takeda, Y.; Watanabe, K., Neural recognition molecule NB-2 of the contactin/F3 subgroup in rat: Specificity in neurite outgrowth-promoting activity and restricted expression in the brain regions. *J. Neurosci. Res.* **2001**, 65, (2), 100-110.
28. vonCampenhausen, H.; Yoshihara, Y.; Mori, K., OCAM reveals segregated mitral/tufted cell pathways in developing accessory olfactory bulb. *Neuroreport* **1997**, 8, (11), 2607-2612.
29. Sung, K. W.; Kirby, M.; McDonald, M. P.; Lovinger, D. M.; Delpire, E., Abnormal GABA(A) receptor-mediated currents in dorsal root ganglion neurons

- isolated from Na-K-2Cl cotransporter null mice. *J. Neurosci.* **2000**, 20, (20), 7531-7538.
30. Ramos, M.; del Arco, A.; Pardo, B.; Martinez-Serrano, A.; Martinez-Morales, J. R.; Kobayashi, K.; Yasuda, T.; Bogonez, E.; Bovolenta, P.; Saheki, T.; Satrustegui, J., Developmental changes in the Ca²⁺-regulated mitochondrial aspartate-glutamate carrier aralar1 in brain and prominent expression in the spinal cord. *Dev. Brain Res.* **2003**, 143, (1), 33-46.
 31. Wishart, T. M.; Paterson, J. M.; Short, D. M.; Meredith, S.; Robertson, K. A.; Sutherland, C.; Cousin, M. A.; Dutia, M. B.; Gillingwater, T. H., Differential proteomics analysis of synaptic proteins identifies potential cellular targets and protein mediators of synaptic neuroprotection conferred by the slow Wallerian degeneration (Wld(s)) gene. *Mol. Cell. Proteomics* **2007**, 6, (8), 1318-1330.
 32. Yamauchi, T., Neuronal Ca²⁺/calmodulin-dependent protein kinase II - Discovery, progress in a quarter of a century, and perspective: Implication for learning and memory. *Biol. Pharm. Bull.* **2005**, 28, (8), 1342-1354.
 33. Groth, R. D.; Dunbar, R. L.; Mermelstein, P. G., Calcineurin regulation of neuronal plasticity. *Biochem. Biophys. Res. Comm.* **2003**, 311, (4), 1159-1171.
 34. Cammarota, M.; Bevilacqua, L. R. M.; Viola, H.; Kerr, D. S.; Reichmann, B.; Teixeira, V.; Bulla, M.; Izquierdo, I.; Medina, J. H., Participation of CaMKII in neuronal plasticity and memory formation. *Cell. Mol. Neurobiol.* **2002**, 22, (3), 259-267.
 35. Gnegy, M. E., Ca²⁺/calmodulin signaling in NMDA-induced synaptic plasticity. *Crit. Rev. Neurobiol.* **2000**, 14, (2), 91-129.
 36. Moran, M. M.; Xu, H. X.; Clapham, D. E., TRP ion channels in the nervous system. *Curr. Op. Neurobiol.* **2004**, 14, (3), 362-369.
 37. Clapham, D. E., TRP channels as cellular sensors. *Nature* **2003**, 426, (6966), 517-524.
 38. Stowers, L.; Holy, T. E.; Meister, M.; Dulac, C.; Koentges, G., Loss of sex discrimination and male-male aggression in mice deficient for TRP2. *Science* **2002**, 295, (5559), 1493-1500.
 39. Cohen, D. M., Regulation of TRP channels by N-linked glycosylation. *Sem. Cell Devel. Biol.* **2006**, 17, (6), 630-637.
 40. Chang, Q.; Hoefs, S.; van der Kemp, A. W.; Topala, C. N.; Bindels, R. J.; Hoenderop, J. G., The beta-glucuronidase klotho hydrolyzes and activates the TRPV5 channel. *Science* **2005**, 310, (5747), 490-493.
 41. Scheiner-Bobis, G., The sodium pump - Its molecular properties and mechanics of ion transport. *Eur. J. Biochem.* **2002**, 269, (10), 2424-2433.
 42. Doris, P. A., Regulation of Na,K-ATPase by Endogenous ouabain-like materials. *Proc. Soc. Exp. Biol. Med.* **1994**, 205, (3), 202-212.
 43. Treuheit, M. J.; Costello, C. E.; Kirley, T. L., Structures of the complex glycans found on the beta-subunit of (Na,K)-ATPase. *J. Biol. Chem.* **1993**, 268, (19), 13914-13919.
 44. Gonzalezyanes, B.; Cicero, J. M.; Brown, R. D.; West, C. M., Characterization of a cytosolic fucosylation pathway in Dictyostelium. *J. Biol. Chem.* **1992**, 267, (14), 9595-9605.

45. West, C. M.; ScottWard, T.; Tengumnuay, P.; vanderWel, H.; Kozarov, E.; Huynh, A., Purification and characterization of an alpha 1,2-L-fucosyltransferase, which modifies the cytosolic protein FP21, from the cytosol of Dictyostelium. *J. Biol. Chem.* **1996**, 271, (20), 12024-12035.
46. Trinchera, M.; Bozzaro, S., Dictyostelium cytosolic fucosyltransferase synthesizes H type 1 trisaccharide in vitro. *FEBS Lett.* **1996**, 395, (1), 68-72.
47. Tai, H.-C.; Khidekel, N.; Ficarro, S. B.; Peters, E. C.; Hsieh-Wilson, L. C., Parallel identification of O-GlcNAc-modified proteins from cell lysates. *J. Am. Chem. Soc.* **2004**, 126, 10500-10501.
48. Khidekel, N.; Ficarro, S. B.; Clark, P. M.; Bryan, M. C.; Swaney, D. L.; Rexach, J. E.; Sun, Y. E.; Coon, J. J.; Peters, E. C.; Hsieh-Wilson, L. C., Probing the dynamics of O-GlcNAc glycosylation in the brain using quantitative proteomics. *Nat. Chem. Biol.* **2007**, 3, (6), 339-348.

Chapter 4: Investigation of Fucosylation in the Olfactory Bulb of Wild-Type and FUT1 Transgenic Knockout Mice

Background

$\alpha(1-2)$ Fucosyltransferases (GDP-L-fucose: β -D-galactosyl-R 2- α -L-fucosyltransferase) catalyze the transfer of α -L-Fuc to the C2 position of terminal β -D-galactose residues in glycoconjugates. The Fuc $\alpha(1-2)$ Gal epitope is important for the synthesis of the ABO blood group antigens, microbe adhesion, morphogenesis, and metastasis of cancerous cells.^{1,2} The carbohydrate structure is synthesized by two known catalytically active enzymes called FUT1 (*H* gene) and FUT2 (secretor or *Se* gene). The *SECI* pseudogene is homologous to FUT2 but is catalytically inactive due to a frameshift mutation.³ Substrate specificity and specific activity differs between FUT1 and FUT2 towards different oligosaccharide acceptor substrates.

FUT1 and FUT2 transgenic knockout animals have been created by homologous recombination using a targeting vector that inserts the *E. coli* β -galactosidase coding sequence in frame proximal to the transmembrane coding segment.⁴ The resultant transgenic mice exhibit no gross anatomical or behavioral abnormalities. Fuc $\alpha(1-2)$ Gal has been implicated in blastocyst adhesion required for murine implantation. However, deletion of the FUT1 and FUT2 loci appeared to be non-essential to blastocyst-uterine epithelial interactions and exhibit normal fertility. These knockout animals have also been examined in formation of glycolipids in the epithelial tissues of the gastrointestinal tract, where they act as receptors for bacteria and are implicated in the immune response.⁵

Interestingly, targeted deletion of either gene had no effect on loss of Fuc α (1-2)Gal glycolipids, which suggests either compensation or redundancy of the α (1-2)fucosyltransferase genes in these tissues. Thus, FUT1 and FUT2 genes may act individually in specific tissues, retain a redundant function, or have compensatory mechanisms when the other gene is knocked out.

As previously discussed in Chapters 1 through 3, Fuc α (1-2)Gal glycoproteins have been implicated in cognitive processes such as learning, memory and development. Thus, we chose to investigate the roles fucosylation mediated by FUT1 and FUT2 in the brain. Recent reports suggest that Fuc α (1-2)Gal glycoconjugates are expressed in the developing and adult olfactory bulb and may be part of a "glycocode" that helps direct axonal pathfinding of olfactory sensory neurons (OSNs).⁶⁻⁹ The glycocode hypothesis suggests that differential expression of glycan structures may act as chemotactic agents to help axonal targeting of OSNs to discrete areas of the olfactory bulb. This would provide a largely uncharacterized mechanism for OSN pathfinding. OSNs each express one of over 1000 different odorant receptors, whose axons connect onto topographically fixed positions in the olfactory bulb.¹⁰⁻¹² While the cell bodies of the OSNs are arranged in a mosaic distribution within one of four zones in the mammalian olfactory epithelium, their axons converge onto one to three glomeruli for neurons expressing a single type of odorant receptor.¹¹⁻¹⁶ The sorting of these axons appears to be controlled by the coordinated spatial and temporal expression of cell adhesion molecules such as the neural cell adhesion molecule (NCAM) and their cognate guidance receptors. However, these molecules alone are not sufficient for the highly specific topographical arrangement of OSNs and glomeruli in the olfactory bulb. Different glycan structures are also expressed

in a selective spatiotemporal arrangement, suggesting their potential involvement in axonal pathfinding of OSNs.

Previous work using lectin immunohistochemistry for $\text{Fuc}\alpha(1-2)\text{Gal}$, Gal, galactosamine (GalNAc), and *N*-acetylglucosamine (GlcNAc) reveals a distinct labeling of OSNs for each glycan that is spatially and temporally regulated in the vomeronasal system and accessory olfactory bulb of mice.^{17, 18} In addition, $\text{Fuc}\alpha(1-2)\text{Gal}$ and GalNAc glycoconjugates display distinct patterns of expression in OSNs of the adult olfactory bulb, consistent with the notion that a glycode contributes to the complex topographical arrangement of OSNs in mammalian olfactory bulb.⁸ A genetic knockout of FUT1^{4, 19, 20} leads to impaired development of the olfactory nerve and glomerular layers of the olfactory bulb in transgenic knockout animals,⁷ suggesting an important role for fucosyl-oligosaccharides in regulating proper olfactory bulb development. However, despite the intriguing possibility for the existence of a glycode, the molecular mechanisms and proteins modified by $\text{Fuc}\alpha(1-2)\text{Gal}$ disaccharides and other glycans were previously uncharacterized (see Chapter 3 of this thesis).

Here, we examine regulation of $\text{Fuc}\alpha(1-2)\text{Gal}$ glycoproteins by FUT1 and FUT2 transgenic knockout animals. We demonstrate that fucosylation of these proteins is synthesized by FUT1 in the olfactory bulb. FUT1 mice exhibit developmental defects in the olfactory nerve and glomerular layers expressing the $\text{Fuc}\alpha(1-2)\text{Gal}$ glycoproteins NCAM (neural cell adhesion molecule) and OCAM (olfactory cell adhesion molecule). $\text{Fuc}\alpha(1-2)\text{Gal}$ glycoproteins are localized to the olfactory nerve and glomerular layers of wild-type mice, where they are expressed in all aspects of the main olfactory bulb (MOB). This staining is completely absent in FUT1 knockout (KO) mice but present in

FUT2 KO mice. In the accessory olfactory bulb (AOB), $\text{Fuc}\alpha(1-2)\text{Gal}$ expression is localized to a distinct region that colocalizes with NCAM. The spatiotemporal expression of $\text{Fuc}\alpha(1-2)\text{Gal}$ is consistent with the existence of a glycode in the developing olfactory bulb. These data suggest that fucosylation of multiple proteins plays an important role in regulating olfactory bulb development and may be part of a glycode regulating OSN targeting.

Results

Regulation of the $\text{Fuc}\alpha(1-2)\text{Gal}$ proteome by FUT1

We first examined the expression of $\text{Fuc}\alpha(1-2)\text{Gal}$ on glycoproteins in the olfactory bulb of wild-type C57/BL6. We identified different patterns of expression for $\text{Fuc}\alpha(1-2)\text{Gal}$ glycoproteins from adult and the developing olfactory bulb (Figure 4.1A, lanes 1 and 4). In adult animals, we observe a smear of glycoproteins recognized by UEAI lectin between 160 and over 250 kDa, as well as prominent bands at ~ 25, 28, and 30 kDa. In the developing postnatal day 3 (P3) olfactory bulb, we detect strong labeling of $\text{Fuc}\alpha(1-2)\text{Gal}$ on glycoproteins between 50 and over 250 kDa, as well as ~ 24, 25, 28, 30, 32, and 45 kDa. In addition, expression of the $\text{Fuc}\alpha(1-2)\text{Gal}$ epitope is significantly upregulated in the developing P3 olfactory bulb, as we observed significantly more labeling with UEAI lectin (Figure 4.1A, lanes 1 and 4).

We also examined expression of $\text{Fuc}\alpha(1-2)\text{Gal}$ on glycoproteins from FUT1 and FUT2 transgenic knockout mice. Deletion of the FUT1 gene led to a significant reduction in detection of $\text{Fuc}\alpha(1-2)\text{Gal}$ glycoproteins from both adult and the developing olfactory bulb (Figure 4.1A). Surprisingly, deletion of the FUT2 gene appeared to have

little effect on protein fucosylation in the olfactory bulb, suggesting that FUT1 is the active enzyme for synthesis of $\text{Fuca}(1-2)\text{Gal}$ glycoproteins in both adult and neonatal mouse tissues. All proteins below 50 kDa as well as proteins at 70 and ~ 120 kDa in both P3 and adult mice showed little to no change in protein fucosylation from either FUT1 or FUT2 KO mice. Thus, fucosylation appears to be regulated primarily by the FUT1 enzyme in the developing and mature olfactory bulb.

Since FUT1 was found to regulate the majority of $\text{Fuca}(1-2)\text{Gal}$ expression in

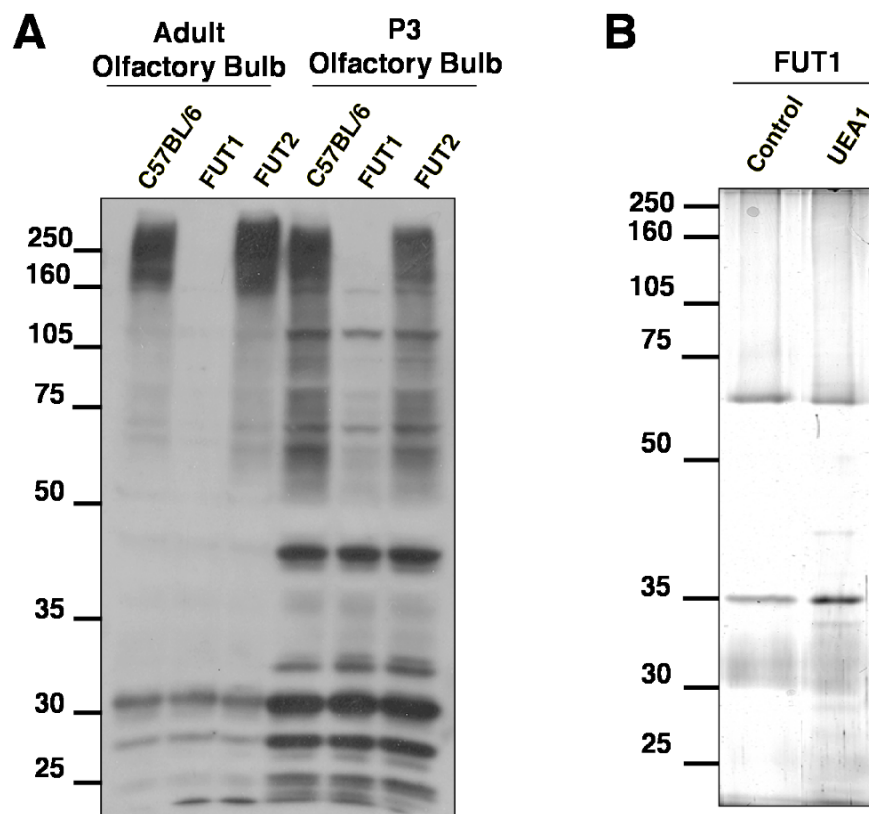


Figure 4.1. FUT1 regulates expression of $\text{Fuca}(1-2)\text{Gal}$ in adult and neonatal mouse olfactory bulb. (A) Western blot with UEA1 lectin of the olfactory bulb from C57BL/6, FUT1 and FUT2 mice. (B) Silver stain of glycoproteins isolated by UEA1 lectin affinity chromatography from P3 mouse olfactory bulb. Proteins in (B) were excised, digested with trypsin, and subjected to LC-MS² analysis for identification.

this brain region, we sought to identify the subset of glycoproteins specifically regulated by the FUT1 enzyme. Using our lectin affinity chromatography approach (see Chapter 3), we isolated and identified proteins from FUT1 olfactory bulb lysates. Consistent with the observation that FUT1 regulates expression of the majority of Fuc α (1-2)Gal glycoproteins, very few proteins were isolated from the UEAI lectin affinity chromatography in FUT1 mice (Figure 4.1B). Of the proteins that were purified from FUT1 olfactory bulb, most were under 50 KDa. This is consistent with the observation that fucosylated proteins at these molecular weights are unaffected by deletion of the FUT1 gene (Figure 4.1A). To determine protein identities, 33 bands were excised from each lane in the gel, and processed as described in Chapter 3. We implemented the same search criteria and stringent peptide cut-off of 7 peptides. Using these criteria, we identified essentially no specific proteins from FUT1 olfactory bulb (data not shown). In Chapter 3, we identified four major classes of Fuc α (1-2)Gal glycoproteins from mouse olfactory bulb: the cell adhesion molecules, ion channels and solute transporters/carriers, ATP-binding proteins, and synaptic vesicle-associated proteins. Notably, none of the proteins identified from FUT1 animals was identified in the proteome from wild-type C57BL/6 mice (see Chapter 3, Table 3.1 and data not shown). This provides strong validation for identification of the Fuc α (1-2)Gal proteome in Chapter 3, and is consistent with regulation of the proteome by FUT1 in mouse olfactory bulb.

Mapping of Fuc α (1-2)Gal Staining in the MOB and AOB: Evidence for a Glycocode

The glycocode hypothesis suggests that glycans should be expressed in regulated spatiotemporal patterns. Thus, we mapped Fuc α (1-2)Gal expression in the developing olfactory bulb and compared it to staining of adult animals. Sections were labeled with UEA1 and examined by confocal fluorescence microscopy. We observe labeling of both the glomerular layer and olfactory nerve layer (ONL) in the developing mouse olfactory bulb, the same areas labeled in adult animals. While Fuc α (1-2)Gal was found to be present only on a subset of OSN axons in adult brain,⁸ we observed extensive labeling of the ONL and greater numbers of glomeruli on all aspects of the developing olfactory bulb. In addition, strong UEA1 labeling of the medial, lateral, and ventral faces was observed from the anterior to posterior regions of the MOB. While strong labeling of the dorsal-lateral OSNs and glomeruli was observed in the anterior region, labeling became weaker to non-existent in the posterior region (Figure 4.2). Furthermore, UEA1-positive glomeruli displayed variations in staining intensity, ranging from strong labeling especially of glomeruli in the medioventral face, to weaker or no labeling of glomeruli in the dorsal-lateral face of the olfactory bulb (Figure 4.2). Lastly, Fuc α (1-2)Gal glycoconjugates were highly localized to the AOB, a structure involved in secondary detection of a particular class of chemical signals involved in regulating sexual behaviors and detecting pheromones.^{21, 22} We also examined the labeling of UEA1 in the olfactory bulb of FUT1 P3 mouse pups. Consistent with our observation that FUT1 regulates the murine Fuc α (1-2)Gal proteome in the olfactory bulb, we observed no labeling of the

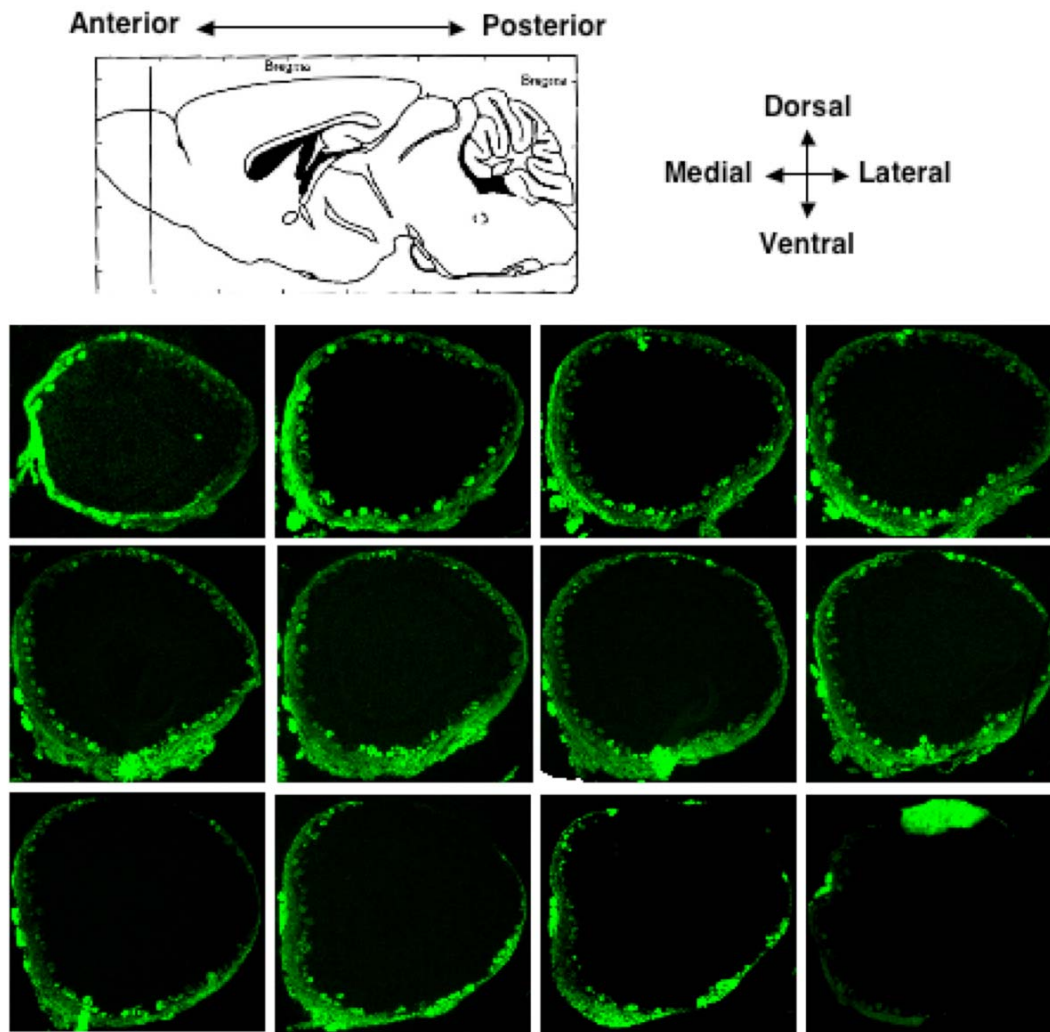


Figure 4.2. UEAI immunohistochemistry of coronal olfactory bulb sections from postnatal mice. Slices are from the anterior (upper left) to posterior (bottom right) of the olfactory bulb. There is strong labeling of the ONL and the glomerular layers in all aspects of the MOB, with the strongest labeling at the medioventral face. There is also strong labeling of the AOB (bottom right panel).

glomerular or ONL in either the MOB or AOB in FUT1 transgenic KO mice (data not shown). Together, these studies demonstrate that $Fuca(1-2)Gal$ glycoconjugates are spatiotemporally regulated, and these expression patterns are consistent with the notion of a glycodecode for axonal targeting of OSNs.

Colocalization of Fuc α (1-2)Gal Glycoproteins NCAM and OCAM with UEAI in the Developing Mouse Olfactory Bulb

We next examined the colocalization of two Fuc α (1-2)Gal glycoproteins identified in Chapter 3 with UEAI in the developing mouse olfactory bulb. We chose to investigate the cell adhesion molecules NCAM (neural cell adhesion molecule) and OCAM (olfactory cell adhesion molecule), which were identified as abundant fucosylated proteins from the largest class of Fuc α (1-2)Gal glycoproteins (Table 3.1). NCAM and OCAM have both previously been shown to label the olfactory nerve and glomerular layers of mouse olfactory bulb. NCAM is ubiquitously expressed throughout these layers, while OCAM expression is localized to the ventral surface. Thus, we examined their colocalization with UEAI to determine the extent of fucosylation of these proteins and their localization in the developing olfactory bulb.

We first examined colocalization between NCAM and OCAM in the developing MOB. NCAM was only partially colocalized with UEAI in the glomerular and olfactory nerve layer of the MOB, consistent with the observation that many other Fuc α (1-2)Gal glycoproteins are present in mammalian olfactory bulb (Figure 4.3). There were many regions where NCAM staining did not colocalize with UEAI, suggesting that NCAM may be differentially fucosylated. NCAM and UEAI overlap was most prevalent in the ventromedial aspect of the developing olfactory bulb from both anterior to posterior regions (data not shown). As expected, OCAM labeling was also partially colocalized with UEAI in the MOB. However, while most OCAM-positive glomeruli were stained by UEAI, there was little colocalization in the anterior portion of the olfactory nerve layer. (Figure 4.4A and B). In the mid-posterior region of the olfactory bulb, there was

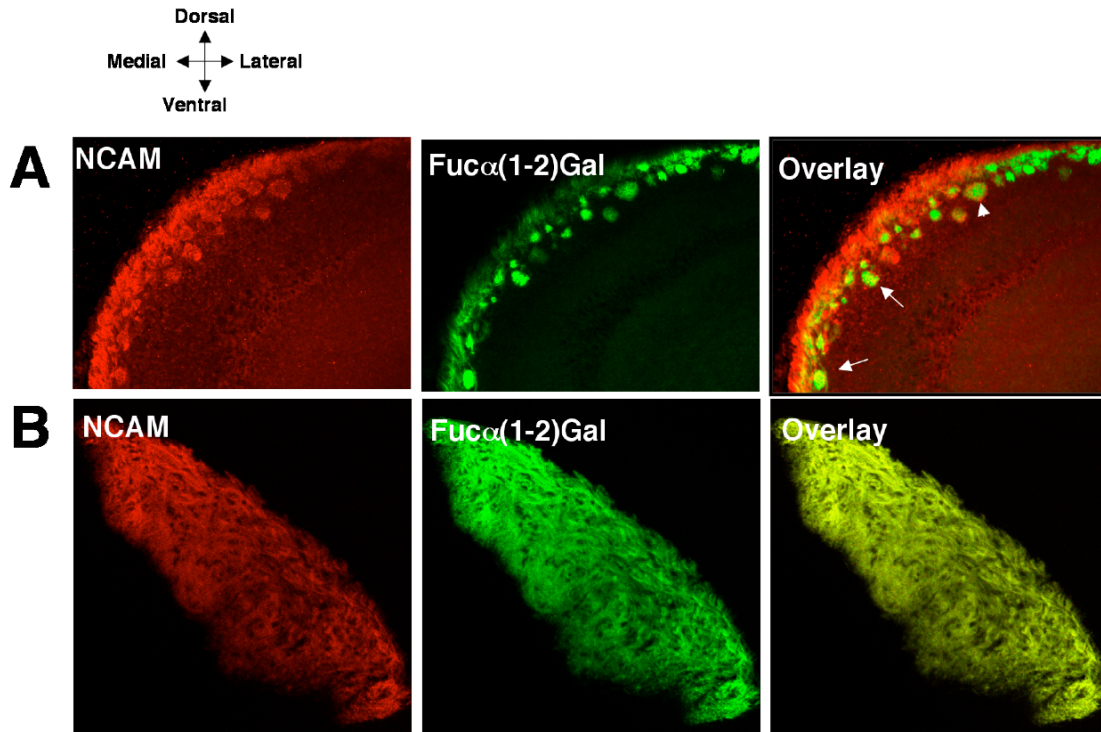


Figure 4.3. Confocal images of coronal olfactory bulb slices. (A) Immunohistochemical analysis demonstrates that NCAM (red) colocalizes with some glomeruli and a portion of the olfactory nerve layer stained by UEAI (green) in the MOB. White arrows point to glomeruli that overlay strongly with UEAI. White arrowhead points to glomerulus with NCAM staining on the outside and UEAI labeling on the inside, demonstrating the diversity in labeling of glomeruli. (B) In the AOB, NCAM is extensively colocalized with UEAI in the olfactory bulb.

significant overlap between NCAM and UEAI in the olfactory nerve layer (Figure 4.4B). These data suggest that both NCAM and OCAM are likely differentially fucosylated in discrete areas of the MOB and the extent of colocalization is consistent with proteomic identification of these proteins as Fuc α (1-2)Gal glycoproteins.

While both NCAM and OCAM colocalize with UEAI in the MOB, only NCAM colocalizes well with UEAI in the AOB (Figures 4.3B and 4.4C), suggesting that OSNs from both the olfactory epithelium and vomeronasal organ are labeled with fucosylated NCAM. Furthermore, lack of significant colocalization of OCAM OSNs from the

vomeronasal organ with UEAI suggests that OCAM is not a primary $\text{Fuc}\alpha(1-2)\text{Gal}$ glycoprotein present on these neurons (Figure 4.4C). Cumulatively, these data suggest that both NCAM and OCAM are differentially fucosylated in the MOB and AOB, consistent with the notion of a glycodecode involving these proteins, as fucosylation at this stage of development is spatially distinct on different $\text{Fuc}\alpha(1-2)\text{Gal}$ glycoproteins.

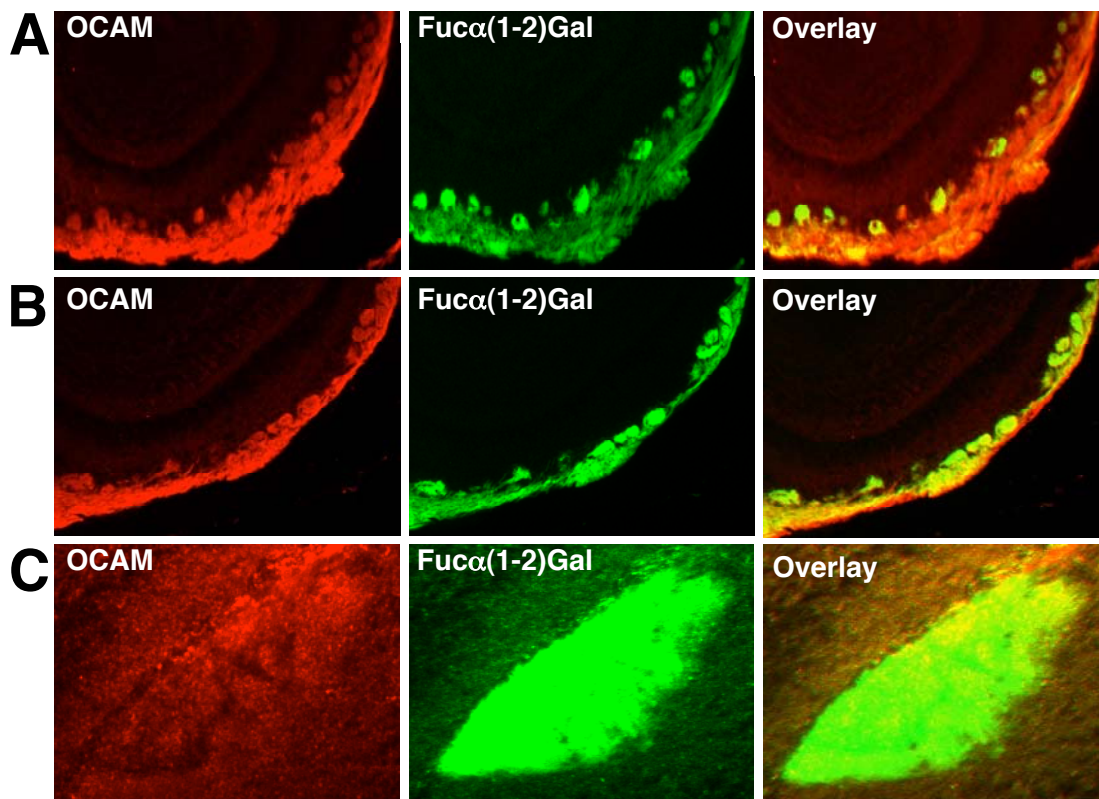


Figure 4.4. Colocalization of OCAM and UEAI in the developing mouse olfactory bulb. Fluorescence microscopy of OCAM (red) colocalizes with UEAI labeling (green) in the ONL and glomerular layers of the anterior MOB (A) and posterior MOB (B). (C) Overlay of OCAM (red) and UEAI (green) from sagittal sections of the AOB.

Development of the Olfactory Nerve Layer and Glomerular Layer is Defective in the Olfactory Bulb of FUT1 KO Mice in Areas Expressing the Fuc α (1-2)Gal Glycoproteins NCAM and OCAM

Having identified the Fuc α (1-2)Gal proteome and its regulation by FUT1, we next explored olfactory bulb development in areas expressing two Fuc α (1-2)Gal glycoproteins, NCAM and OCAM, in FUT1-deficient mice. The olfactory nerve layer (ONL) and glomerular layers of FUT1 postnatal mice are reported to be thinner, with less large glomeruli than wild-type mice.⁷ We examined whether NCAM- and OCAM-expressing OSNs display developmental defects in FUT1 transgenic knockout animals. Olfactory bulbs from wild-type (WT) and FUT1-deficient mice were fixed, cryogenically sliced in coronal sections, stained with either NCAM or OCAM antibodies, and imaged by confocal fluorescence microscopy. We observed moderate defects in the thickness of the ONL and severe defects in the number and demarcation of glomeruli for NCAM-expressing regions of the olfactory bulb (Figure 4.5A). These deficits were most pronounced in the ventromedial surface of the posterior MOB, consistent with areas containing high expression of the Fuc α (1-2)Gal epitope (Figure 4.2). We did not observe any obvious defects in development of NCAM-expressing OSNs in the AOB of FUT1 KO animals (data not shown). While the ONL of NCAM-expressing areas exhibited a decrease in thickness, we did not observe any significant defects in the thickness of the ONL of OCAM-expressing OSNs (Figure 4.5B). However, there was also a significant decrease of large glomeruli expressing OCAM in both the anterior and posterior ventral MOB (Figure 4.5B). The localization and defects in NCAM- and OCAM-positive glomeruli suggest fucosylation may be important for regulating the function of these

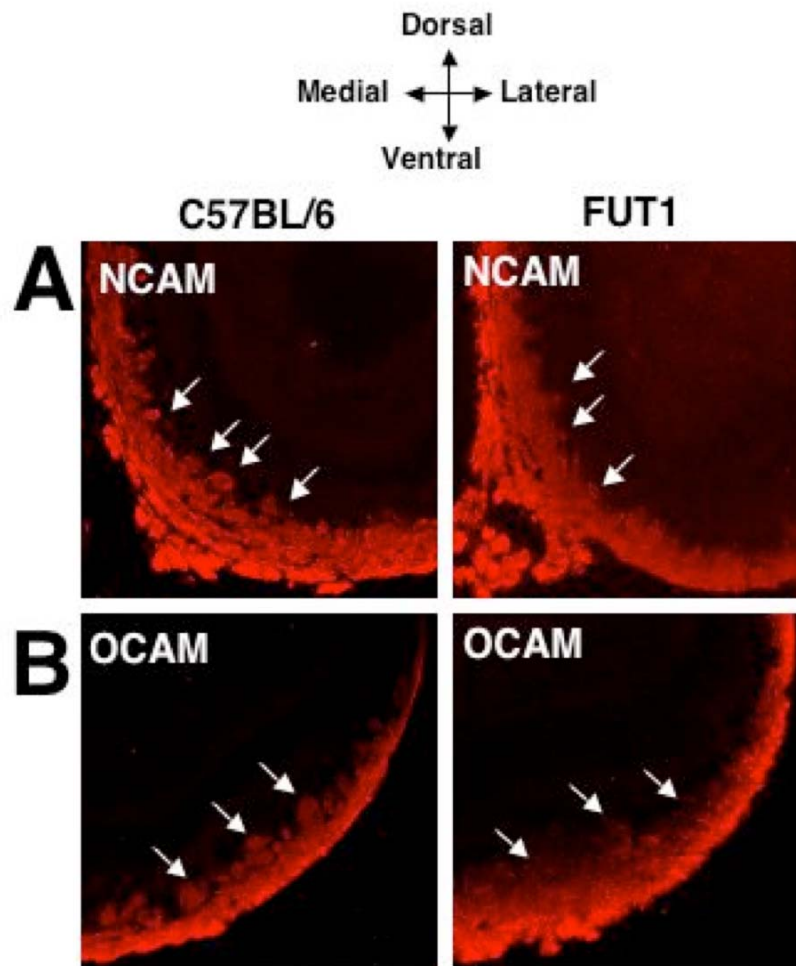


Figure 4.5. Confocal fluorescence microscopy of coronal sections of the developing WT and FUT1 KO MOB. (A) NCAM (red) expressing OSNs exhibit defects in the thickness of the ONL and in the demarcation and number of large glomeruli from FUT1 KO animals (white arrows). (B) OCAM expressing OSNs exhibit a similar thickness in the ONL. However, they also have severe defects in the presence of large glomeruli in FUT1 KO mice (white arrows).

proteins. Both proteins play functional roles in olfactory bulb development and these data suggest that fucosylation of these proteins may also be important.

Discussion

We previously identified the Fuc α (1-2)Gal proteome from mouse olfactory bulb (Chapter 3) and demonstrate here that FUT1 regulates expression of the proteome in mouse olfactory bulb. These results validate identification of the proteome in Chapter 3 and suggest that FUT1 is the dominant enzyme for expression of Fuc α (1-2)Gal in this tissue. The cell adhesion molecules NCAM and OCAM are important for olfactory bulb development, and their fucosylation is regulated by FUT1. We further explored fucosylation of these proteins by examining their colocalization with UEAI in the developing olfactory bulb. Both proteins were found to colocalize with Fuc α (1-2)Gal to varying degrees in the MOB and AOB. NCAM expressing OSNs had a high degree of colocalization in the medioventral aspect of the olfactory bulb in both the olfactory nerve layer and a subset of glomeruli. OCAM expressing glomeruli strongly colocalized with UEAI staining in the lateroventral face of the olfactory bulb. The lack of complete localization of NCAM and OCAM with UEAI in the MOB suggests that other glycoproteins contain the Fuc α (1-2)Gal moiety, consistent with our proteomics studies. In the AOB, NCAM and UEAI staining were highly colocalized, suggesting that NCAM is the predominant Fuc α (1-2)Gal glycoprotein present in the AOB.

We observed a modest defect in the ONL and glomerular layers expressing NCAM and OCAM in FUT1 neonatal mice. These mice exhibit significantly less glomeruli expressing OCAM and NCAM, especially in the medioventral area of the olfactory bulb. In addition, we observed a thinner ONL for OSNs expressing NCAM. Such defects in OSNs stained by these fucosylated cell adhesion molecules suggests that the Fuc α (1-2)Gal carbohydrate epitope of both NCAM and OCAM is important for proper olfactory bulb development. Previous studies have suggested that only NCAM

fucosylation is important in olfactory bulb development, as NCAM was the only known Fuc α (1-2)Gal glycoprotein.⁷ However, an actual investigation of NCAM fucosylation had been lacking. Our studies expand on what was previously hypothesized, and demonstrate that NCAM and OCAM, as well as other Fuc α (1-2)Gal glycoproteins, are important for proper development of the olfactory bulb. Interestingly, NCAM-180 knockout mice are reported to display similar defects in glomerular formation as FUT1 deficient mice.²³ While the olfactory bulb of these mutants appears relatively normal, there are fewer and smaller glomeruli in NCAM-180 KO mice when compared with wild-type mice. This indicates that NCAM-180 is essential for the proper development of glomeruli in the olfactory bulb. This is consistent with a role for NCAM fucosylation in mediating proper olfactory bulb development.

The developmental abnormalities in the nerve fiber layer and glomerular formation appear to recover in adult FUT1 knockouts.⁷ This may suggest that other targeting mechanisms can take over to ensure proper olfactory bulb development. While there are no obvious defects in the topology of adult murine olfactory bulb, it is still possible that some OSNs may fail to make the proper connections to appropriate glomeruli.

Our data also lends support to the existence of a glycode for OSN pathfinding. While UEAI labeling was present throughout the ONL and glomerular layers of the MOB in the developing olfactory bulb, we observed a differential fucosylation of both NCAM and OCAM, suggesting that fucosylation may help mark OSNs to target to appropriate glomeruli. This spatiotemporal fucosylation is consistent with the glycode hypothesis. UEAI labeling was strongest in the medioventral area of the olfactory bulb, where the

largest defect in OSNs and glomerular formation occurred. This suggests that the Fuc α (1-2)Gal epitope may be extremely important for development of this region, whereas areas of weaker UEAI staining may depend on another glycan structure for proper development. Cumulatively, our studies suggest that Fuc α (1-2)Gal labeling displays a unique spatiotemporal expression consistent with a glycode for OSN targeting.

Materials and Methods

Animals, Tissue Isolation and Homogenization.

C57BL/6 wild-type, FUT1 and FUT2 transgenic knockout animals crossed to a C57BL/6 background were a gift from Prof. Stephen Domino and maintained in accordance with proper IACUC procedures. Adult male mice ages 3-4 months and post-natal day 3 (P3) pups were anesthetized with CO₂ and dissected to remove the cerebellum, cortex, hippocampus, hypothalamus, olfactory bulb, striatum, and thalamus. For Western blotting, dissected tissues were cut into small pieces and placed immediately on ice, then lysed in boiling 1% SDS with sonication until homogeneous (5V:W). For lectin affinity chromatography, the olfactory bulbs from 30-50 P3 pups were isolated and homogenized in lectin binding buffer (100 mM Tris pH 7.5/ 150 mM NaCl/ 1mM CaCl₂/ 1 mM MgCl₂/ 0.5% NP-40/ 0.2% Na deoxycholate plus protease inhibitors) by passing through a 26G needle 5 times, then sonicated to homogeneity. Samples were clarified by centrifugation at 12,000g \times 10 min. Lysates were between 6 to 10 mg/mL total protein concentration as determined by the BCA protein assay (Pierce) for lectin affinity chromatography.

Lectin Affinity Chromatography and SDS-PAGE

One mL bed volume of *Ulex europaeus* agglutinin I (UEAI) conjugated to agarose (Vector Labs) and control protein A conjugated to agarose (Vector Labs) columns were packed ~333 μ L into 3 minicolumns run in parallel (BioRad). The resin was equilibrated with 10 column volumes (CV) lectin binding buffer. 3 mL of olfactory bulb lysate at 6-10 mg/mL was bound in batch at RT for 4 hours. Columns were repacked and the flowthrough was passed 3 additional times over the column. Columns were washed with 40 CV of lectin binding buffer, followed by 10 CV of lectin binding buffer lacking detergent (NP-40 and Na deoxycholate). Proteins were eluted in 10 CV of lectin binding buffer lacking detergent supplemented with 200 mM α -L-Fuc and protease inhibitors.

Protein eluates were concentrated in 10,000 MWCO centricons (Millipore) followed by 10,000 MWCO microcons (Millipore) to 100 μ L. Following concentration, samples were boiled with 35 μ L of 4 \times SDS loading dye and loaded onto 10% SDS gels for electrophoresis as described previously.²⁴

Silver Staining, Peptide Extraction, and In-Gel Tryptic Digests

All silver staining reagents were prepared fresh. Gels were stained as described in Chapter 3. Gels were destained in 0.4 g $K_3Fe(CN)_6$ / 200 mL $Na_2S_2O_3 \cdot 5H_2O$ (0.2g/L) for 15 min or until no bands were visible then washed 6 \times 15 min in ddH₂O overnight. Gel pieces were excised and reduced in 150 μ L of 8 mM TCEP in 80 mM ammonium bicarbonate buffer, pH 7.8 / 150 μ L CH₃CN. Gel pieces were reduced for 20 min at RT.

The solution was discarded and cysteines were alkylated in 150 μL of 10 mM iodoacetamide in 80 mM ammonium bicarbonate buffer, pH 7.8 / 150 μL CH_3CN . Reactions were incubated in the dark for 20 min at RT. The supernatant was discarded and gel pieces were rehydrated in 500 μL of 50 mM ammonium bicarbonate for 10 min at RT. The supernatant was removed and gel pieces were concentrated in a speed vac for 15 min. Gel pieces were resuspended in 40 μL H_2O / 5 μL 500 mM ammonium bicarbonate, pH 7.8/ and 5 μL of 0.2 mg/mL trypsin (promega), and left on ice for 30 min. Tubes were then incubated overnight at 37 $^\circ\text{C}$. The following day, excess trypsin solution not absorbed was removed and saved in a new tube. Gel pieces were washed with 500 μL of H_2O by vortexing for 20 min. The solution was removed and combined with the tryptic digests. Peptides were extracted at 2 \times 200 μL of 5% formic acid/ 50% CH_3CN by vortexing for 20 min and combined with the tryptic and wash fractions. Samples were concentrated in a speed vac down to 20 μL for MS analysis.

Orbitrap LC-MS Analysis

Approximately 50% of gel extractions were loaded onto a 360 μm O.D. \times 75 μm precolumn packed with 4 cm of 5 μm Monitor C18 particles (Column Engineering) as described previously.²⁵

Western Blotting

10% SDS gels were transferred to PVDF, blocked in 3% HIO_4^- BSA,²⁶ and incubated with HRP-conjugated UEAI (Sigma) at 50 $\mu\text{g}/\text{mL}$ in TBST for 2 h at RT or

antibody A46-B/B10 at 5 $\mu\text{g}/\text{mL}$. Membranes were washed 3×10 min in TBST, then developed as described previously.²⁶

Immunohistochemistry

Adult mice (3-4 months) were anesthetized with sodium pentobarbital (100 mg/kg) and then fixed by transcardiac perfusion with PBS (pH 7.4), followed by a 4% paraformaldehyde in PBS solution. Brain tissue was removed, and immersion fixed overnight at 4 °C in the same solution. P3 mouse pups were killed by decapitation, the brain was removed and immersion fixed overnight in 4% paraformaldehyde in PBS at 4 °C. The following day, the solution was replaced with an ice-cold solution of 15% sucrose in PBS at 4 °C until the brains sunk, followed by 30% sucrose in PBS. The brain tissue was mounted in OCT medium (Tissue Tek), and frozen in a dry ice/ MeOH bath. Frozen brains were stored at -80 °C until processed for sectioning. Fixed tissues were cryogenically sliced on a Leica, CM1800 cryostat in coronal sections, 20 μm thick sections for P3 pups and 50 μm thick for adult tissues. Sections were dried at 37 °C for 20 min, then blocked in 10% donkey serum/ 0.3% Triton X-100 in PBS for OCAM immunohistochemistry and 10% goat serum/ 0.3% Triton X-100 in PBS for NCAM immunohistochemistry for 1 h at RT. Sections were incubated with mouse anti-NCAM (Sigma) diluted 1:100 in 2% donkey serum/ 0.1% Triton X-100 in PBS, or goat anti-OCAM (R&D Systems) diluted 1:100 in 2% goat serum/ 0.1% Triton X-100 in PBS at RT for 2 h. Sections were washed three times in PBS for 10 min and then incubated with a cocktail of Alexa-568-conjugated donkey anti-goat with UEA1 conjugated to fluorescein (Sigma) at 50 $\mu\text{g}/\text{mL}$ for 1 h at 37 °C.

References

1. Gorelik, E.; Xu, F.; Henion, T.; Anaraki, F.; Galili, U., Reduction of metastatic properties of BL6 melanoma cells expressing terminal fucose alpha 1-2-galactose after alpha 1,2-fucosyltransferase cDNA transfection. *Cancer Res.* **1997**, *57*, (2), 332-336.
2. Bry, L.; Falk, P. G.; Midtvedt, T.; Gordon, J. I., A model of host-microbial interactions in an open mammalian ecosystem. *Science* **1996**, *273*, (5280), 1380-1383.
3. Kelly, R. J.; Rouquier, S.; Giorgi, D.; Lennon, G. G.; Lowe, J. B., Sequence and expression of a candidate for the human secretor blood-group alpha(1,2)fucosyltransferase gene (Fut2) - homozygosity for an enzyme-inactivating nonsense mutation commonly correlates with the non-secretor phenotype. *J. Biol. Chem.* **1995**, *270*, (9), 4640-4649.
4. Domino, S. E.; Zhang, L.; Gillespie, P. J.; Saunders, T. L.; Lowe, J. B., Deficiency of reproductive tract alpha(1,2)fucosylated glycans and normal fertility in mice with targeted deletions of the FUT1 or FUT2 alpha(1,2)fucosyltransferase locus. *Mol. Cell. Biol.* **2001**, *21*, (24), 8336-8345.
5. Iwamori, M.; Domino, S. E., Tissue-specific loss of fucosylated glycolipids in mice with targeted deletion of alpha(1,2)fucosyltransferase genes. *Biochem. J.* **2004**, *380*, 75-81.
6. Chehrehasa, F.; Key, B.; St John, J. A., The cell surface carbohydrate blood group A regulates the selective fasciculation of regenerating accessory olfactory axons. *Brain Res.* **2008**, *1203*, 32-38.
7. St John, J. A.; Claxton, C.; Robinson, M. W.; Yamamoto, F.; Domino, S. E.; Key, B., Genetic manipulation of blood group carbohydrates alters development and pathfinding of primary sensory axons of the olfactory systems. *Dev. Biol.* **2006**, *298*, (2), 470-484.
8. Lipscomb, B. W.; Treloar, H. B.; Klenoff, J.; Greer, C. A., Cell surface carbohydrates and glomerular targeting of olfactory sensory neuron axons in the mouse. *J. Comp. Neurol.* **2003**, *467*, (1), 22-31.
9. St John, J. A.; Key, B., Expression of galectin-1 in the olfactory nerve pathway of rat. *Dev. Brain Res.* **1999**, *117*, (2), 171-178.
10. Nagao, H.; Yoshihara, Y.; Mitsui, S.; Fujisawa, H.; Mori, K., Two mirror-image sensory maps with domain organization in the mouse main olfactory bulb. *Neuroreport* **2000**, *11*, (13), 3023-3027.
11. Ressler, K. J.; Sullivan, S. L.; Buck, L. B., Information coding in the olfactory system - evidence for a stereotyped and highly organized epitope map in the olfactory-bulb. *Cell* **1994**, *79*, (7), 1245-1255.
12. Vassar, R.; Chao, S. K.; Sitcheran, R.; Nunez, J. M.; Vosshall, L. B.; Axel, R., Topographic organization of sensory projections to the olfactory-bulb. *Cell* **1994**, *79*, (6), 981-991.
13. Treloar, H. B.; Feinstein, P.; Mombaerts, P.; Greer, C. A., Specificity of glomerular targeting by olfactory sensory axons. *J. Neurosci.* **2002**, *22*, (7), 2469-2477.

14. Mombaerts, P.; Wang, F.; Dulac, C.; Chao, S. K.; Nemes, A.; Mendelsohn, M.; Edmondson, J.; Axel, R., Visualizing an olfactory sensory map. *Cell* **1996**, 87, (4), 675-686.
15. Vassar, R.; Ngai, J.; Axel, R., Spatial segregation of odorant receptor expression in the mammalian olfactory epithelium. *Cell* **1993**, 74, (2), 309-318.
16. Ressler, K. J.; Sullivan, S. L.; Buck, L. B., A zonal organization of odorant receptor gene-expression in the olfactory epithelium. *Cell* **1993**, 73, (3), 597-609.
17. Salazar, I.; Quinteiro, P. S., Differential development of binding sites for four lectins in the vomeronasal system of juvenile mouse: from the sensory transduction site to the first relay stage. *Brain Res.* **2003**, 979, (1-2), 15-26.
18. Salazar, I.; Quinteiro, P. S.; Lombardero, M.; Cifuentes, J. M., Histochemical identification of carbohydrate moieties in the accessory olfactory bulb of the mouse using a panel of lectins. *Chem. Senses* **2001**, 26, (6), 645-652.
19. Domino, S. E.; Zhang, L.; Lowe, J. B., Molecular cloning, genomic mapping, and expression of two secretor blood group alpha(1,2)fucosyltransferase genes differentially regulated in mouse uterine epithelium and gastrointestinal tract. *J. Biol. Chem.* **2001**, 276, (26), 23748-23756.
20. Domino, S. E.; Hiraiwa, N.; Lowe, J. B., Molecular cloning, chromosomal assignment and tissue-specific expression of a murine alpha(1,2)fucosyltransferase expressed in thymic and epididymal epithelial cells. *Biochem. J.* **1997**, 327, 105-115.
21. Bigiani, A.; Mucignat-Caretta, C.; Montani, G.; Tirindelli, R., Pheromone reception in mammals. *Rev. Physiol. Biochem. Pharmacol.* **2005**, 154, 1-35.
22. Baxi, K. N.; Dorries, K. M.; Eisthen, H. L., Is the vomeronasal system really specialized for detecting pheromones? *Trends Neurosci.* **2006**, 29, (1), 1-7.
23. Treloar, H.; Tomasiewicz, H.; Magnuson, T.; Key, B., The central pathway of primary olfactory axons is abnormal in mice lacking the N-CAM-180 isoform. *J. Neurobiol.* **1997**, 32, (7), 643-658.
24. Tai, H.-C.; Khidekel, N.; Ficarro, S. B.; Peters, E. C.; Hsieh-Wilson, L. C., Parallel identification of O-GlcNAc-modified proteins from cell lysates. *J. Am. Chem. Soc.* **2004**, 126, 10500-10501.
25. Khidekel, N.; Ficarro, S. B.; Clark, P. M.; Bryan, M. C.; Swaney, D. L.; Rexach, J. E.; Sun, Y. E.; Coon, J. J.; Peters, E. C.; Hsieh-Wilson, L. C., Probing the dynamics of O-GlcNAc glycosylation in the brain using quantitative proteomics. *Nat. Chem. Biol.* **2007**, 3, (6), 339-348.
26. Murrey, H. E.; Gama, C. I.; Kalovidouris, S. A.; Luo, W. I.; Driggers, E. M.; Porton, B.; Hsieh-Wilson, L. C., Protein fucosylation regulates synapsin Ia/lb expression and neuronal morphology in primary hippocampal neurons. *Proc. Natl. Acad. Sci. USA* **2006**, 103, (1), 21-26.

Chapter 5: Investigation of Fucosylation by Metabolic Labeling with Alkynyl- and Azido-Fuc Derivatives

Background

The cell surface can be modified by abiotic functionalities to introduce unnatural sugars into cellular glycans, a process known as oligosaccharide engineering. This metabolic labeling with unnatural sugars has become an important tool to incorporate chemical probes into glycan chains within a cellular environment. These studies exploit the biosynthetic machinery within a cell to incorporate unnatural sugar analogues into glycoconjugates. The unnatural sugars often contain chemical functionalities not normally present within a cell such as the azide or alkyne groups, making them “bioorthogonal”. Incorporation of such unnatural sugars enables the researcher to place a chemical handle on glycoconjugates of interest, which can then be reacted with other functional groups to install a tag or chemical reporter. Since azides and alkynes are not normally present on biomolecules within a cell, insertion of abiotic functional groups enables chemoselective labeling of glycoconjugates in a cellular context.

In addition to requiring a bioorthogonal chemical functionality, metabolic labeling necessitates a fast chemoselective ligation strategy that can be applied in a biological environment, at physiological pH and temperature. These reactions must be robust enough to avoid non-specific chemical reactions or metabolic side-effects. Such reactions include the Staudinger ligation of a triarylphosphine with an azide to form an amide bond (Figure 5.1A),^{1, 2} Cu(I)-catalyzed [3+2] cycloaddition chemistry with an alkyne-azide pair via “click chemistry” (Figure 5.1B)³⁻⁵, or strain-promoted cycloaddition

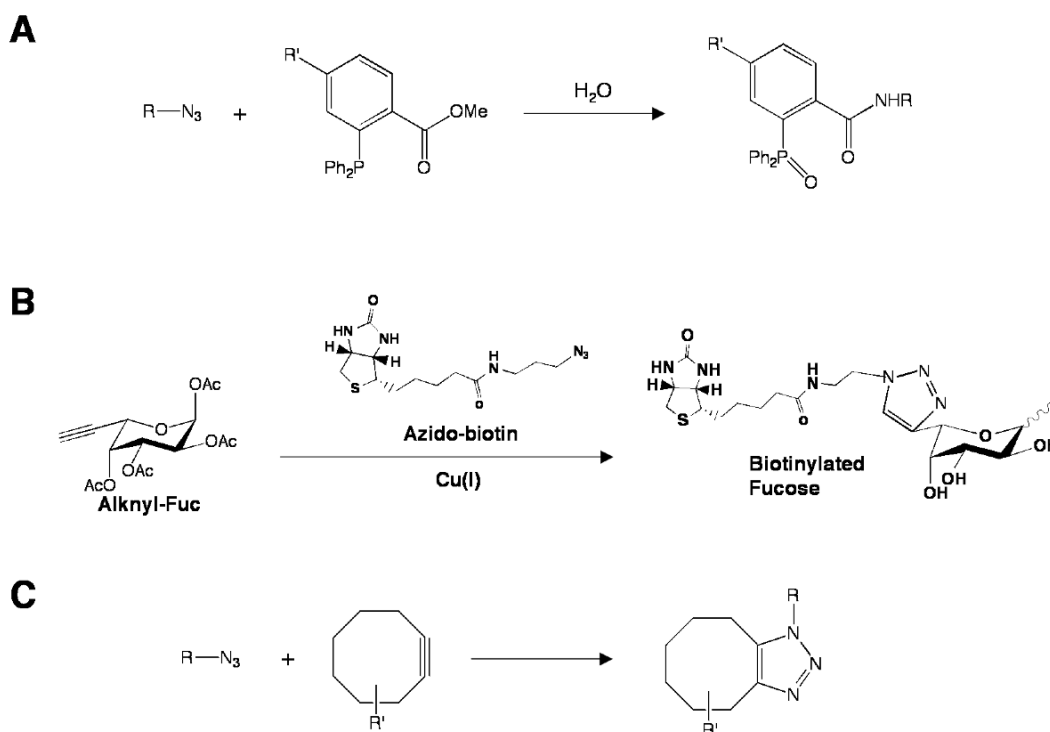


Figure 5.1. Biorthogonal chemical reactions. (A) Staudinger ligation. (B) Click chemistry reaction. (C) Strain-promoted-cycloaddition.

reactions between a cyclooctyne and azide which removes the necessity of a Cu(I) catalyst for click chemistry reactions (Figure 5.1C).⁶

The chemical labeling of glycan chains with unnatural sugars has played a key role in expanding the knowledge of sugar function. Recently, the Bertozzi and Wong groups independently demonstrated that alkynyl- or azido-containing fucose analogues (Figure 5.2) could be exploited to selectively label and image fucosylated glycans in mammalian cells.^{7, 8} Their strategy exploits the fucose salvage pathway to convert unnatural fucose sugars into the corresponding GDP-fucose analogues, which then serve as donors for fucosyltransferases (Figure 5.3). Once the azido or alkynyl fucose analogue is incorporated into glycans, it can be reacted with fluorescent dyes, biotin or peptides via the Staudinger ligation or strain-promoted cycloadditions for incorporation of an azide, or

it can be reacted via click chemistry for incorporation of both azides and alkynes. Bertozzi and co-workers synthesized fucose derivatives with azido groups at the C2, C4, and C6 positions.⁷ Only the C6 azido fucose analogue (Figure 5.2) was successfully incorporated into the glycans of Jurkat cells, consistent with earlier observations that some fucosyltransferases tolerate substitutions at the C6 position of the pyranose ring. Wong and colleagues demonstrated that both azido and alkynyl-modified C6-fucose derivatives (Figure 5.2) could be incorporated into the glycans of hepatoma cells,

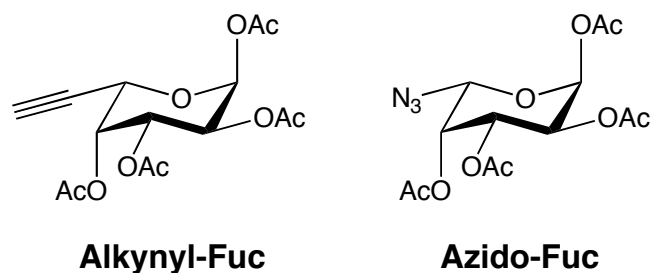


Figure 5.2. Chemical structures of alkynyl- and azido-Fuc with substitutions at the C6 position of the ring.

allowing for fluorescent imaging of fucosylated glycoconjugates.⁸ Interestingly, the alkynyl fucose analogue was shown to be significantly less toxic to cells than the azido fucose analogue.⁸

While metabolic labeling has been extensively used in cell culture experiments for investigation of cancerous cell lines, an in-depth investigation of these compounds in other cell-types has not been performed. Thus, we envisioned using the azido- and alkynyl-fucose analogues to investigate the role of fucosylation in the brain. The brain is especially challenging to study as neurons are post-mitotic, and fucose (Fuc) is present in low cellular abundance. Despite these challenges, we have successfully employed the

use of alkynyl- and azido-Fuc analogues for the investigation of protein fucosylation in the brain. We report that fucosylated glycoconjugates are present in neurons, and a number of glycoproteins can be modified by this technique. In particular, we developed a method to identify the Fuc glycoproteome from cultured cortical neurons by a gel-based LC-MS² approach. Recently, the Wong lab used metabolic labeling to identify the sialylated *N*-linked proteome in prostate cancer cells. Their approach uses a synthetic alkynyl-*N*-acylmannosamine (ManNAcyne) that can be utilized by the sialic acid biosynthetic machinery in an analogous manner as the fucose derivatizes.⁹ They developed a glycoproteomic strategy for saccharide-selective glycoprotein identification (ID) and glycan mapping (GIDmap) that tags alkynyl-sialic acid-modified glycoproteins. These studies corroborate our finding that metabolic labeling can successfully be used for proteomics studies. We demonstrate that proteins such as the neural cell adhesion molecule (NCAM), the voltage-gated calcium channel alpha2/delta subunit (Cacna2d2), and the myristoylated-alanine rich protein kinase C substrate (MARCKS) proteins are fucosylated. Furthermore, we show that various neuronal substructures contain fucosyl glycans, such as the Golgi body, axons, and dendrites. Lastly, we are able to chemoselectively tag fucosylated glycans *in vivo*, which will enable future studies investigating fucosylation in living animals.

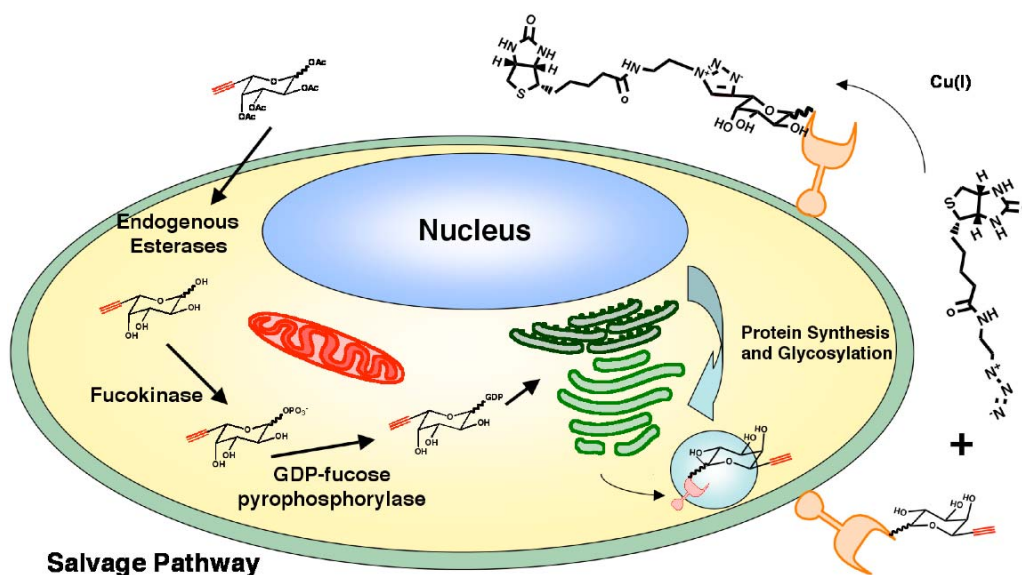


Figure 5.3. Alkynyl- or azido-Fuc analogues are metabolized via the fucose salvage pathway and can be incorporated into glycans on the cell surface.

Results

Alkynyl-Fucose Labels Glycoproteins in Cultured Neurons

We first examined the ability of alkynyl- and azido-Fuc analogues to chemoselectively label glycoconjugates in cultured cortical and hippocampal neurons in collaboration with the Wong lab. All synthetic molecules were provided by the Wong lab at the Scripps Research Institute. Cortical neurons were cultured for 1 day *in vitro* (DIV) and treated with either the acetylated alkynyl-Fuc, azido-Fuc or the Fuc analogue. After treatment, cell lysates were labeled by click chemistry with the corresponding azido- or alkynyl-biotin tag (Figure 5.1B) to determine the ability to selectively label individual glycoproteins. Neurons treated with the azido-Fuc derivative had an appreciable amount of cell death, consistent with the notion that the azido-Fuc compound

is more toxic to the cells than the alkynyl-Fuc sugar.¹⁰ We observed significant labeling of fucosylated glycoproteins in both the alkynyl- and azido-Fuc treated cells (Figure 5.4). However, the azido-Fuc control exhibited labeling of proteins, whereas the alkynyl-Fuc control showed minimal signal by Western blotting. This suggests that the alkynyl-Fuc compound is more specific for labeling of fucosylated glycoproteins. We observed prominent bands at 50, 35, 30 and 28 kDa. The 50 kDa band was present in all samples, suggesting that the protein may be an endogenous biotinylated protein detected by streptavidin. Surprisingly, the 35, 30, and 28 kDa bands were present in the azido-Fuc control but not the alkynyl-Fuc control, suggesting that these proteins may be non-specifically labeled by the click reaction. In addition to these prominent bands, we

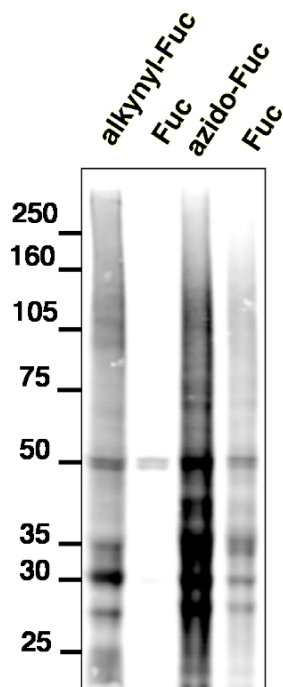


Figure 5.4. Alkynyl-Fuc labeling of glycoproteins is more specific than azido-Fuc in cultured cortical neurons. Neurons were cultured for 1 DIV and treated for three days with the alkynyl-Fuc, azido-Fuc, or Fuc derivatizes. Lanes 1 and 2 were click labeled with azido-biotin and lanes 3 and 4 were labeled with alkynyl-biotin, lysates were resolved by SDS-PAGE, and immunoblotted with streptavidin for visualization.

observe a number of fucosylated proteins between 50 and 250 kDa that appear to be specifically labeled in the alkynyl-Fuc lane, demonstrating the ability to selectively label individual glycoproteins. Due to the toxicity of the azido-Fuc compound and the extensive labeling of the control reaction, we turned our attention toward labeling with alkynyl-Fuc for further experiments.

Optimization of Click Reaction Conditions in Cortical Lysate

In order to effectively label fucosylated glycoproteins in neuronal lysates, we optimized the click chemistry conditions for the incorporation of alkynyl-fucose into cultured rat cortical neurons. These experiments are in collaboration with Chithra Krishnamurthy in the lab. Neurons at 8 DIV were treated with alkynyl-Fuc for 3 days. The cells were lysed at 11 DIV and chemoselectively labeled with the azido-biotin reporter using click chemistry. The original click reaction conditions used included 50 mM CuSO₄ as the source of copper catalyst, 2 mM sodium ascorbate as the Cu(II) reducing agent, 0.1 mM trisriazoleamine ligand (triazole) and 0.1 mM of the azido-biotin.¹¹ The reaction mixture was incubated for 2 h at room temperature and the extent of labeling was visualized by Western blotting with streptavidin. We examined the labeling reactions in absence of each of the reagents to examine selectivity of the alkynyl-Fuc probe for labeling fucosylated glycoproteins (Figure 5.5). These click reaction conditions often gave indistinct labeling and caused extensive protein degradation of alkynyl-fucose-treated neuronal glycoproteins (Figure 5.6). We examined the source of Cu catalyst as well as the incubation conditions in order to optimize the conditions for

efficient labeling of fucosylated glycoconjugates with minimal non-specific background. Protein degradation was significantly decreased by incubation of the reaction at 4 °C for 3h. We determined that CuBr was the optimal copper source under these conditions instead of the commonly used CuSO₄, consistent with previous reports (Figure 5.6).^{8, 12} Because Cu(I) is the active copper species in the click reaction, using CuBr may have precluded the use of reducing agent. However, the use of CuBr with sodium ascorbate ensured the copper catalyst remained as the active Cu(I) species, due to possible endogenous oxidants in the lysate. This reaction gave much more distinct labeling of fucosylated glycoproteins than the use of CuSO₄, which seemed to induce protein degradation (Figure 5.6). However, as CuBr is insoluble in water, the freshly prepared suspension of CuBr needed constant agitation to ensure delivery of the correct amount of CuBr to the reaction mixture, which was determined to be 0.5 mM CuBr (data not shown).

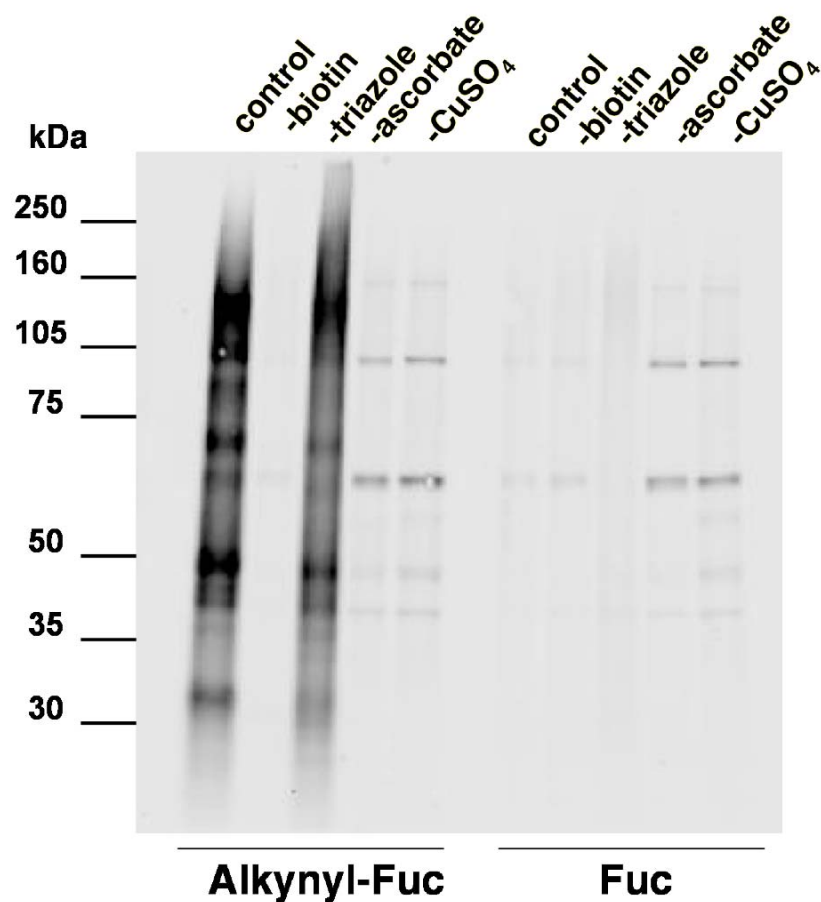


Figure 5.5. Testing the reactions parameters for the click chemistry with alkynyl-Fuc. Neuronal lysates were click labeled under the following conditions. Control reaction is all components needed for click chemistry including 50 mM CuSO₄, 2mM sodium ascorbate, 0.1 mM tris-triazolamine (triazole), and 0.1 mM azido-biotin. Every other lane contains the components from the control reaction minus the reagent indicated above the lane. Image courtesy of C. Krishnamurthy.

Optimization of Fucosylated Glycoprotein Isolation by Streptavidin

Affinity Chromatography

In addition to optimizing click chemistry conditions, fellow lab member Chithra Krishnamurthy developed a protocol for the purification of fucosylated glycoproteins by streptavidin chromatography. Neuronal lysates were cultured for 8 days and treated with

Fuc or alkynyl-Fuc for 3 more days. Lysates were click labeled with the azido-biotin reporter, and we attempted to isolate them by streptavidin affinity chromatography. Protein was first precipitated by a methanol/chloroform extraction to remove the excess biotin from the labeling reaction that would compete for binding sites on the streptavidin column. Protein was resolubilized and incubated with streptavidin resin for one hour at 4 °C. We optimized the binding and wash conditions and found that washing with 40 CV high salt buffer, 40 CV low salt buffer, 30 CV 4M Urea in 1% SDS, 40 CV phosphate buffered saline (PBS) and 40 CV of water was most effective in decreasing non-specific binding. We eluted bound proteins in 6 M urea, 2 M thiourea, 30 mM biotin, 2% SDS at pH 12 to achieve a quantitative elution.¹³

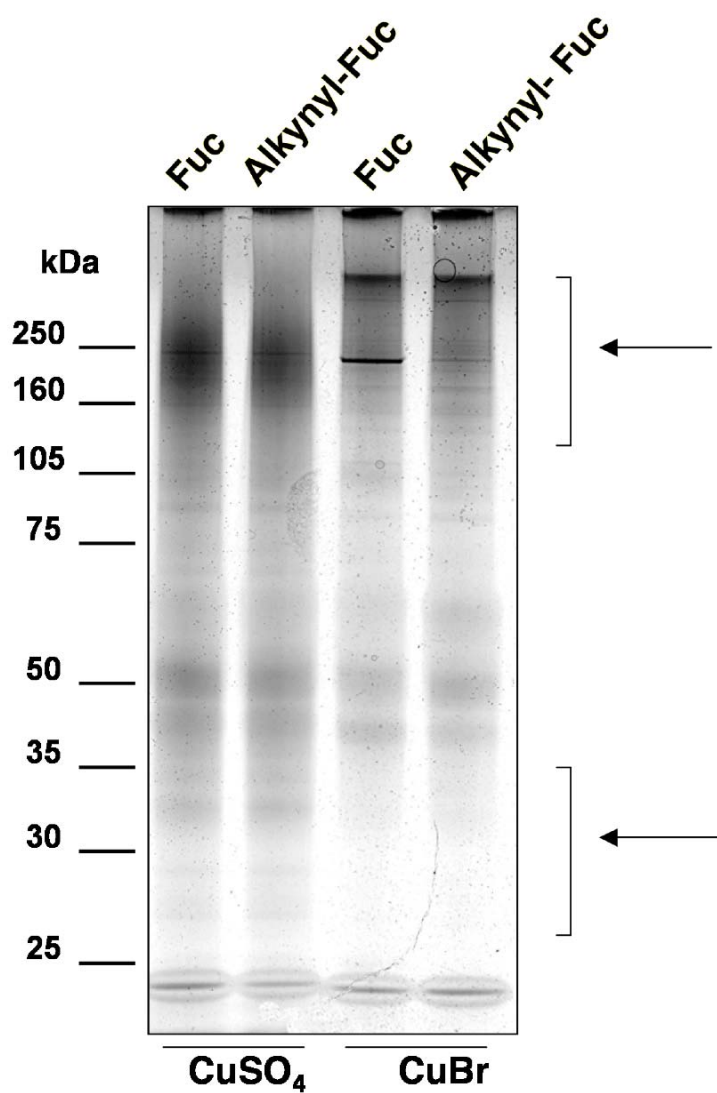


Figure 5.6. CuSO_4 induces non-specific protein degradation. Neuronal lysates were click labeled with either CuSO_4 or CuBr , then analyzed by silver stain to look at total protein levels. In both samples treated with the CuSO_4 catalyst, we observed extensive degradation of proteins between 105 and over 250 kDa as well as between 25 to ~32 kDa (as indicated by arrows). In contrast, proteins treated with the CuBr catalyst had labeling of distinct protein bands and no obvious smears of degraded proteins, suggesting that CuBr is the optimal catalyst. Arrows point to areas of protein degradation. Image courtesy of C. Krishnamurthy.

Identification of the Fucose Proteome

After optimizing the click reaction and streptavidin isolation conditions, fellow lab member Chithra Krishnamurthy began experiments to identify the fucose proteome in neurons using LC/MS/MS. The approach involves labeling cortical neurons in culture with Fuc or alkyne-Fuc, chemically tagging the cellular lysates with azido-biotin, and isolating biotinylated glycoproteins by streptavidin affinity chromatography. Lysates were then resolved by SDS-PAGE and silver stained to identify specific proteins present in the alkyne-Fuc but not the control sample. Individual bands present were excised and subjected to in-gel tryptic digests and LC-MS/MS analysis (Figure 5.7). While there was some labeling in the control fucose column, we saw significantly more proteins eluted from the alkyne-Fuc column. Specifically, we observed fucosylated glycoproteins at ~

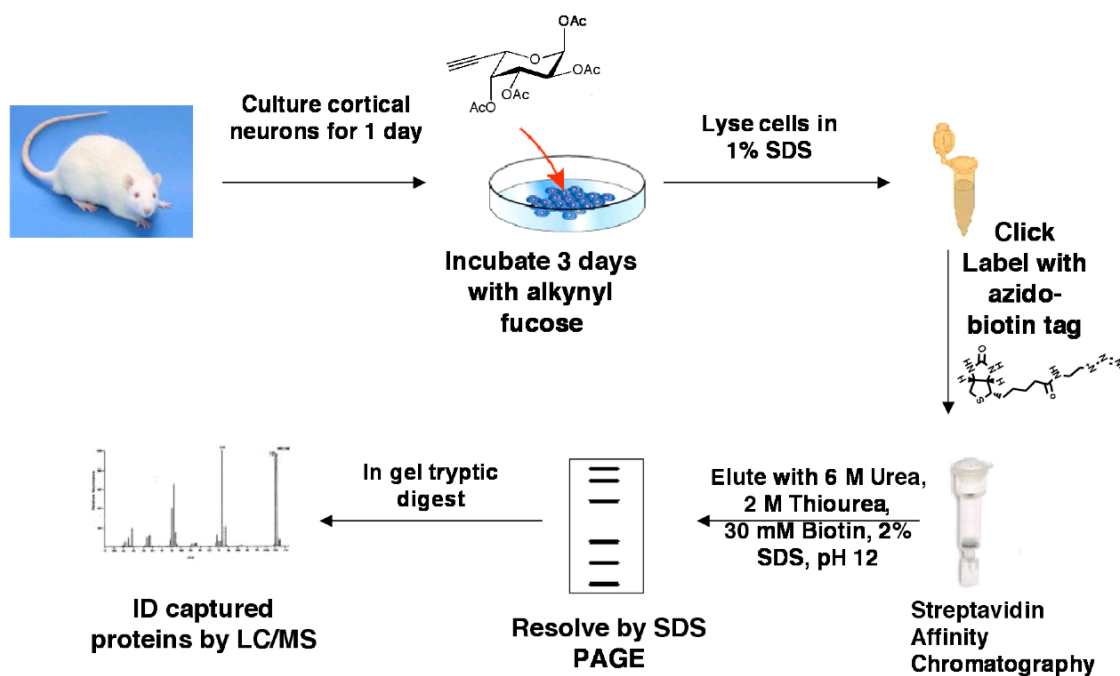


Figure 5.7. Strategy for the isolation and identification of alkyne-Fuc-tagged glycoproteins from rat cortical neurons.

120, 110, 105, 90, 76, 75, 65, 60, 55, 45, 43, 40, 37, and 36 kDa (Figure 5.8). 17 bands from each lane were analyzed by LC-MS/MS in collaboration with Dr. Scott Ficarro and Dr. Eric Peters at the Genomics Institute of the Novartis Research Foundation. The proteins were searched against the NCBI non-redundant database and each individual sample was analyzed in Bioworks (Table 5.1). Proteins were considered putative Fuc-glycoproteins when we observed at least 3 unique peptides, which gives 99% probability that the protein is present in the sample. We observed significant protein degradation in the sample, as many of the proteins identified ran lower than their true molecular weights. This problem may be due to non-specific protein degradation induced by the click reaction and our harsh elution conditions. We are currently in the process of trying to resolve this phenomenon. Despite these problems, we successfully identified numerous fucosyl glycoproteins including cell adhesion molecules such as NCAM and the cell-fate determining protein Notch, two proteins that have previously been reported to be fucosylated. In addition, we identified proteins involved in ion transport and calcium signaling such as voltage-gated calcium channel alpha2/delta subunit and those involved in dendritic cell morphology such as several myristolated alanine-rich protein kinase C substrate (MARCKS) proteins.

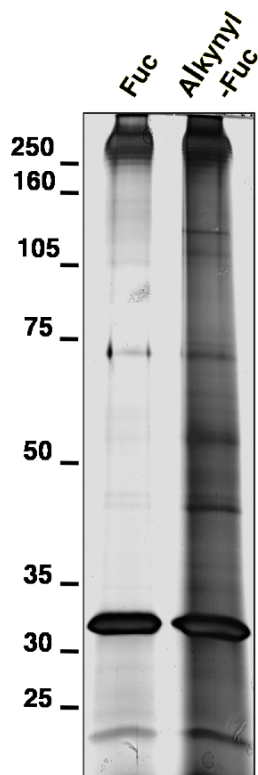


Figure 5.8. Silver stain of proteins isolated from alkynyl-Fuc and Fuc labeled cortical neurons by streptavidin affinity chromatography. Eluted proteins were resolved by SDS-PAGE. The alkynyl-Fuc sample contains significantly more labeling than the control-Fuc sample.

Protein	MW	Accession	Function
Nesprin 1	1010433	29839561	Nuclear scaffold protein
Similar to Low Density Lipoprotein Receptor-Related Protein	504556	109482078	Regulates lipid metabolism and neural development
Homeotic Discs 1	331123	73622271	Histone methylation; maintain active transcription
Type 3 Inositol 1,4,5-Triphosphate Receptor	303842	483831	Intracellular calcium release channels; regulates calcium signaling
Notch Homolog 4	205936	46237578	Cell fate assignment and pattern formation in development

Golgi Sialoglycoprotein MG-160	134504	17376711	Trafficking and processing of fibroblast growth factor (FGF)
NCAM L1	126395	109462307	Cell adhesion*
Voltage-gated Calcium Channel Alpha2/Delta Subunit	124551	1905817	Ion channel, calcium signaling*
Neural Cell Adhesion Molecule (NCAM)	117508	817988	Cell adhesion*
Similar to Vacuolar Proton Translocating ATPase 116 Kda Segment	95061	109473276	Acidification of synaptic vesicles; neurotransmitter release
Potassium Channel	93560	3929231	Ion channel
Cell Adhesion Molecule	75679	2181948	Cell adhesion
Hsc70-ps1	70884	56385	Synaptic vesicle cycling, uncoats clathrin-coated vesicles
Similar to Cadherin-like 24	66351	94398073	Desmosome adhesion
Elongation Factor 1-alpha	50072	74204203	Translation regulation
Lysosomal Membrane Glycoprotein 1 (LAMP1)	43941	6981144	Cellular protein degradation
14-3-3 Gamma Isoform	35074	74215924	Regulation of cell signaling cascades
Similar to Myristoylated Alanine-Rich C-Kinase Substrate	30186	109510177	Maintain dendritic spine morphology
Myristoylated Alanine Rich Protein Kinase C Substrate	29643	6678768	Maintain dendritic spine morphology
14-3-3 Eta Isoform	28288	83754700	Regulation of cell signaling cascades
AMP-activated Protein Kinase, Noncatalytic Gamma-1 Subunit Isoform 2	28267	47132575	Cell signaling*
Growth Associated Protein 43 (GAP-43)	23589	8393415	Axonal growth, development and plasticity*
MARCKS-like 1	19835	51858596	Maintain dendritic spine morphology

Table 5.1. Proteins identified from the alkynyl fucose proteome arranged by molecular weights with their functions. Starred proteins were identified in the Fucc α (1-2)Gal proteome from chapter 3.

In addition to the gel labeling approach, we attempted to use the GID-map strategy developed by the Wong laboratory which involves an off-bead tryptic digest followed by elution of bound peptides with PNGase F, an enzyme that cleaves off *N*-linked sugars.⁹ The eluate was analyzed by multidimensional protein identification (MudPit) MS. However, despite their success with this methodology for identifying sialic acid glycoproteins,⁹ we were never able to successfully isolate fucosyl glycoproteins in significant quantities over the control column. This likely reflects the lower abundance of fucosylated relative to sialylated glycoproteins. This also suggests that our gel-based approach may be the optimal experiment to identify and isolate fucosylated glycoproteins. Due to the low abundance of fucosylated peptides and the high abundance of non-specific proteins, the wash conditions were not stringent enough for us to see differences in the alkylnl-Fuc versus Fuc control when using the GID-map approach (data not shown).

Alkynyl-Fuc Labels Different Neuronal Substructures

We next investigated the ability to chemoselectively label fucosylated glycoconjugates in cultured hippocampal neurons for fluorescence microscopy. Cells were treated with 50 μ M alkynyl-Fuc at 8 days *in vitro* (DIV) for 3 more days. Cells were fixed, permeabilized, and subjected to click labeling conditions with azido-biotin. Fucosylated glycoconjugates were visualized by fluorescence microscopy with streptavidin conjugated to fluorescein. We optimized the labeling conditions by testing the reaction at different temperatures and for different lengths of time. Labeling at 4 $^{\circ}$ C overnight provided the most specific labeling (data not shown) and all subsequent hippocampal cultures were labeled under these parameters. We observed extensive staining of the cell body, as well as labeling of neuronal processes in the alkynyl-Fuc

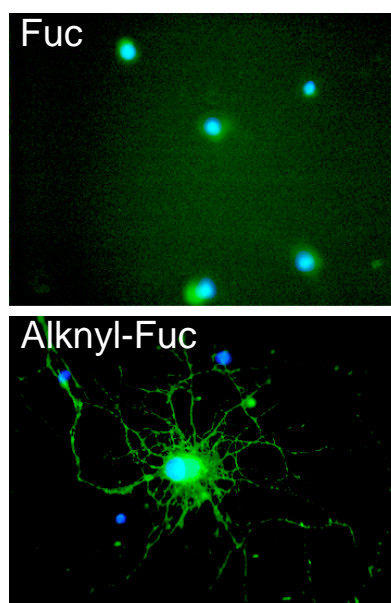


Figure 5.9. Metabolic labeling with alkynyl-Fuc in labels the cell body and neuronal processes of hippocampal cultures. Hippocampal neurons were cultured for 8 DIV and treated with alkynyl-Fuc or Fuc for 3 more days. Cells were fixed, permeabilized, and click labeled with azido-biotin. Fucosylated proteins were visualized with streptavidin conjugated to alexa fluor 488. Nuclei were stained with DAPI.

treated neurons (Figure 5.9). There was minimal background in the control, mostly localized to the cell body. Thus, we are capable of specifically labeling fucosylated glycoproteins in the cell body as well as along neuronal processes of hippocampal cultures.

Identification of Neuronal Substructures Labeled by Alkynyl-Fuc

We next sought to address the neuronal localization of fucosylated glycoconjugates in developing hippocampal neurons in culture. We first examined the colocalization of the known fucosylated glycoprotein NCAM (the neural cell adhesion

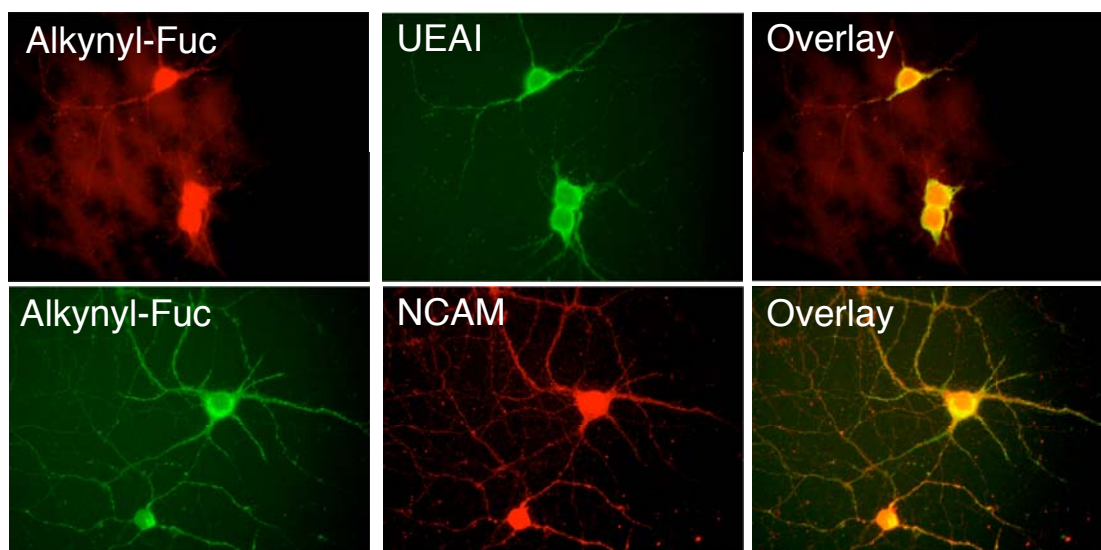


Figure 5.10. Staining with alkynyl-Fuc labels physiologically relevant epitopes. 11 DIV cultures were treated for 3 days with alkynyl-Fuc or Fuc (14 DIV). The neurons were click labeled with azido biotin, and stained with streptavidin (red, top panel) and UEAI conjugated to fluorescein. In the bottom panels, cells were labeled with streptavidin (green and fucosylated NCAM (red)). Both have some extent of colocalization suggesting that alkynyl-Fuc is labeling fucosylated glycans in hippocampal neurons.

molecule), and the fucose binding lectin UEAI to determine whether we are labeling physiologically relevant glycoconjugates. There was some colocalization between NCAM and alkynyl-Fuc, as well as extensive colocalization with UEAI (Figure 5.10), suggesting that we are chemically labeling fucosyl glycans. We examined young neurons that have begun developing axons, as well as older neuronal cultures that have functional synapses. Cells were treated for 3 days with alkynyl-Fuc or Fuc, then fixed, permeabilized, and chemoselectively labeled with a biotin reporter using click chemistry. We investigated the localization of fucosylated glycans with the axonal marker tau, the dendritic marker map2, and the Golgi marker giantin by confocal fluorescence microscopy (Figure 5.11). We observed extensive overlay of the alkynyl-Fuc probe with the Golgi marker giantin, suggesting that most fucosyl glycans reside in the Golgi apparatus (Figure 5.11A). In addition, we identified specific labeling of both axons (Figure 5.11B) and dendrites (Figure 5.11C) in 4 DIV neuronal cultures. We observed similar labeling of older neuronal cultures (data not shown), suggesting that fucosylated glycoconjugates are localized in these neuronal substructures throughout development.

In collaboration with Chithra Krishnamurthy, we examined alkynyl-Fuc labeling in mature 14 DIV hippocampal neurons. We observed the strongest labeling of fucose within the Golgi compartment of mature 14 DIV hippocampal neurons (data not shown). In addition, we examined the colocalization of fucose to synapses with the synaptic marker synapsin. There was some colocalization to synapses indicated by yellow puncta; however, the majority of alkynyl-Fuc-labeled protein did not appear to be highly localized to synapses (Figure 5.12).

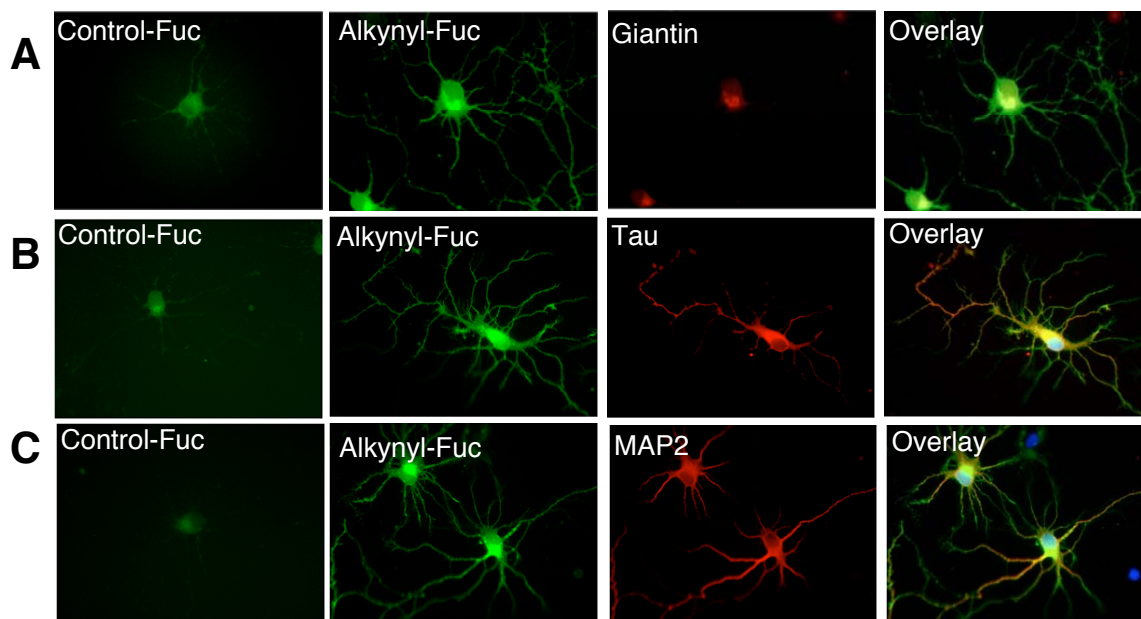


Figure 5.11. Alkynyl-Fuc glycoproteins are localized along axons and dendrites, as well as in the Golgi apparatus. Hippocampal cultures were treated at 1 DIV for 3 days with Fuc or alkynyl-Fuc. Cells were biotinylated with azido biotin via click chemistry and detected with streptavidin conjugates to fluorescein (green). Cells were costained with (A) giantin (red, Golgi marker), (B) tau (red, axonal marker), and (C) map2 (red, dendritic marker).

***In Vivo* Labeling of Fucosylated Glycans**

Having demonstrated the ability to chemoselectively label fucosyl oligosaccharides *in vitro*, we recently began exploring the potential to label fucosylated glycans *in vivo*. Such experiments significantly decrease the amount of molecule needed per experiment and expand our ability to monitor fucosylation in living animals. Since fucose and other sugars do not cross the blood-brain barrier, we needed to develop a protocol involving direct injection into the brain. We began our pilot studies in mouse pups, in which the Fuc α (1-2)Gal epitope is highly up-regulated (Chapter 3). Using a stereotaxic device and a microinjector, we injected alkynyl-Fuc and Fuc into the

forebrain of early postnatal mouse pups using coordinates 2 mm posterior to Bregma, 2 mm lateral to midline, and 2 mm ventral to the top of the skull. We next determined the optimal amount of fucose for injections. Notably, only minute quantities (2 μ L) were needed for injections, minimizing the amount of molecule needed per experiment. After injection, the cortices were removed, lysed, and click labeled with azido-biotin. Lysates were resolved by SDS-PAGE and visualized by blotting with streptavidin conjugated to a fluorophore (Figure 5.13). We were able to detect specific labeling of fucosylated glycoconjugates in the alkynyl-Fuc-injected animals, whereas there was very little labeling in control-Fuc-injected animals. However, we are still in the process of optimizing the gel procedure. All non-specific labeling occurred between 25 – 50 kDa, and may represent endogenous biotinylated proteins. In addition, the two prominent bands at 50 and ~40 kDa were present in the control sample. We observed a number of fucosylated glycoproteins between 50 and over 250 kDa that were only labeled in the alkynyl-Fuc-injected animals, suggesting that we can successfully incorporate the alkynyl-Fuc tag into fucosyl oligosaccharides *in vivo* via metabolic labeling. We are currently optimizing the *in vivo* injection procedures for immunohistochemical experiments. We observe strong background fluorescence in the control injections (data not shown), and are working towards a method for clean labeling. Immunohistochemical studies will enable us to investigate the subcellular distribution of fucosyl-oligosaccharides in the brain, and monitor changes in their distribution in response to learning paradigms in living animals.

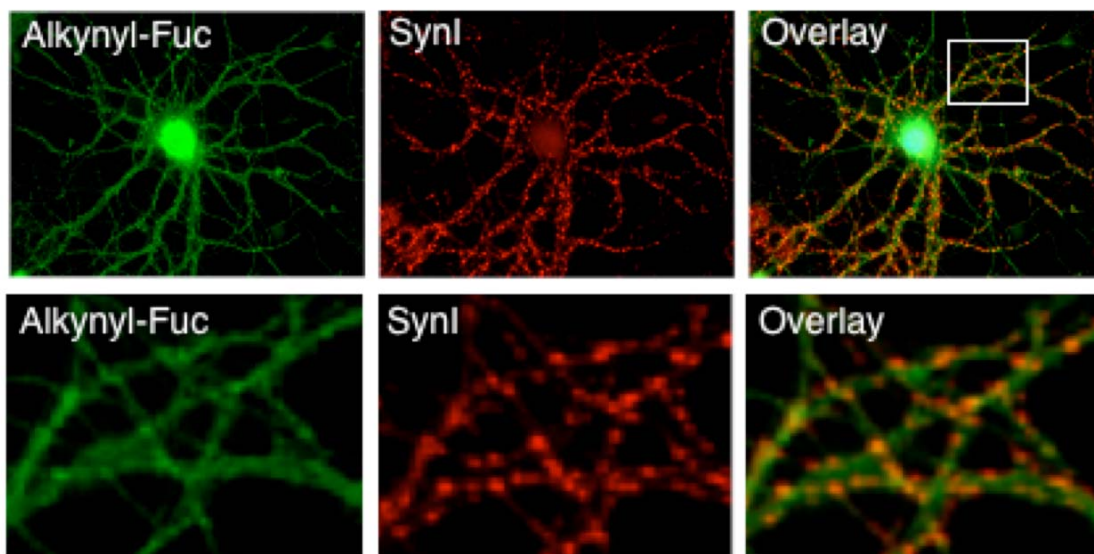


Figure 5.12. Alkynyl-Fuc glycoproteins are not highly localized to synapses. Hippocampal neurons were cultured for 11 days and treated with Fuc or alkynyl-Fuc for 3 days (14 DIV). Cells were click labeled with azido-biotin and visualized with streptavidin (green), or synapsin I (red). Bottom panels are equivalent in size to the white box in the top panels.

Discussion

Metabolic labeling has emerged as an important chemical tool to enhance our understanding of glycobiology. Toward this end, multiple chemical probes have been synthesized for incorporation into various glycoconjugates including such sugars as fucose, sialic acid, and mannose. These chemical probes exploit the biosynthetic machinery of the cell to install bioorthogonal chemical functionalities onto glycoproteins of interest. These versatile chemical tools have previously been investigated in cultured cell lines. Here, we explored the ability to monitor fucose in the brain. Tagging fucose in neurons will facilitate a molecular level understanding of the role that fucosyl oligosaccharides play in learning and memory. Investigation of neurons is especially

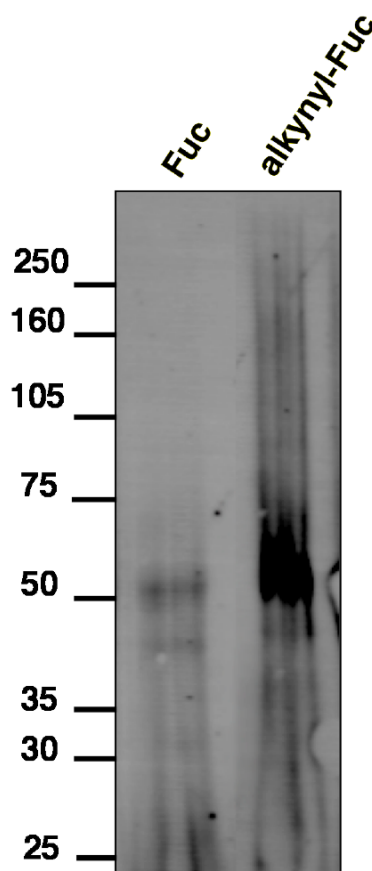


Figure 5.13. Intracranial administration of alkynyl-Fuc leads to direct alkynyl incorporation into fucosyl glycoproteins *in vivo*. Postnatal day 3 mice were injected unilaterally with Fuc or alkynyl-Fuc and tissue was harvested 2 days post-injection. Lysates were click labeled with azido-biotin, resolved by SDS-PAGE and probed with streptavidin conjugated to a fluorophore. There was significant labeling in the alkynyl-Fuc lane when compared to Fuc injected animals. In particular, there was significant labeling of fucosylated glycoproteins between 50 and over 250 kDa, suggesting that intracranial drug administration can label fucosylated glycoproteins *in vivo*.

challenging to study as the cells are post-mitotic and fucose is present in low cellular abundance. Here, we explored the ability to metabolically label fucosylated glycans in cultured neuronal cells and *in vivo*. In addition, we explored the fucosylated proteome in cultured cortical neurons.

Metabolic labeling with alkynyl-Fuc analogues in cultured cortical neurons enabled selective labeling of fucosylated glycans as visualized by Western blotting and

fluorescence microscopy. Fucosylated glycoproteins were highly localized to the Golgi apparatus of both developing and mature neuronal cultures. However, there was also some background staining of the Golgi body in the control click reaction, suggesting that some of the Golgi labeling is non-specific (data not shown). The terminal Golgi apparatus contains the fucosyltransferases necessary for fucosylation of glycoconjugates, thus extensive labeling of the Golgi body was expected and is consistent with previous studies of cancerous cell lines. In addition, we examined the localization of alkynyl-Fuc labeled glycoconjugates in developing hippocampal neurons. Fucosylated glycoconjugates were present in both the axons and dendrites of young and mature neuronal cultures. Interestingly, in older neuronal cultures with functional synapses, we did not observe strong localization to synaptic compartments of the cell, in contrast to our previous studies that $\text{Fuc}\alpha(1-2)\text{Gal}$ glycoproteins are highly localized to presynaptic terminals (Chapter 2).¹⁴ This suggests that the predominant glycoproteins labeled may not be $\text{Fuc}\alpha(1-2)\text{Gal}$, but are likely fucose present in other linkages. We examined the binding of lectin UEAI and found alkynyl-Fuc treated cells bound with lower avidity than the control, most likely due to the change of a methyl group on Fuc to the bulky alkynyl-group, consistent with a previous report.¹⁰ There was also some colocalization between alkynyl-Fuc labeling and UEAI in the cell soma and along neuronal processes, suggesting that we are labeling physiologically relevant epitopes. We observed that NCAM, a protein previously been reported to be fucosylated¹⁵⁻¹⁷ and identified in proteomics studies done in this report, colocalized strongly with alkynyl-Fuc labeling. We did not observe complete colocalization, suggesting that we are labeling NCAM as well as other fucose-containing glycoproteins within mature neuronal cultures. Cumulatively, these

data suggest that fucosylated glycans can be metabolically labeled *in vitro* in neuronal cultures. In addition, we observe alkynyl-Fuc staining along both axons and dendrites, which suggests that the modified glycoconjugates are being successfully trafficked along neuronal processes.

We next explored the fucosylated proteome in cultured cortical neurons through metabolic labeling with alkynyl-Fuc. We identified 23 fucosyl glycoproteins, some of which are novel and some that have been previously characterized. Identification of known fucosyl glycoproteins validates the metabolic labeling approach to label fucosylated glycoproteins. We identify NCAM and NCAM L1, which are cell adhesion molecules involved in cell adhesion, neuronal migration, axonal fasciculation, and synaptogenesis.¹⁸⁻²¹ Both of these proteins were identified as Fuc α (1-2)Gal glycoproteins in Chapter 3 of this thesis. We also identified the voltage-gated calcium channel alpha2/delta subunit which was previously identified as a putative Fuc α (1-2)Gal glycoprotein (Chapter 3). In addition, we identify the notch homolog 4 protein as a fucosylated glycoprotein. The notch family of proteins is involved in cell fate determination and differentiation.²² Notch is known to be fucosylated directly on serines of epidermal growth factor repeats known as *O*-fucosylation.²³ Fucosylation of notch modulates its interaction with ligands, and can have important consequences for cell fate determination.^{24, 25}

Interestingly, we also identify several novel cytosolic fucosylated proteins, such as several members of the MARCKS family of proteins and GAP-43. The MARCKS family of proteins regulates dendritic spine morphology and are myristoylated, so they can be membrane bound.²⁶⁻³¹ These proteins influence cell morphology, cell motility,

and are important for the maintenance of dendritic spines and synaptic plasticity.³² GAP-43 is palmitoylated, and can also interact with membranes.^{33, 34} It is involved in regulating axonal growth, guidance, development, and plasticity.^{35, 36} GAP-43-deficient animals display defects in motor skills and sensory impairments.³⁷ Identification of cytosolic proteins that associate with membranes supports a role for fucosylation in development and other nervous system functions, and supports the notion that soluble cytosolic proteins may be fucosylated like synapsin I.

Ion transport and calcium signaling proteins were identified such as the voltage-gated calcium channel alpha2/delta subunit and the type 3 inositol 1,4,5, triphosphate receptor. The voltage-gated calcium channel alpha2/delta subunit has been shown to bind the drug pregabalin, which helps prevent seizure activity, reduce pain-related behaviors, and anxiety disorders.³⁸ The type 3 inositol 1,4,5, triphosphate receptor regulates calcium currents important for GABAergic signaling.³⁹ Interestingly, the Huntingtin protein influences neuronal calcium signaling through this channel which may affect glutamate-induced Ca^{2+} signals leading to neuronal dysfunction and apoptosis.⁴⁰ Identification of these proteins suggests that fucose may be involved in various neuropathological processes and disease progression.

The ability to label fucose *in vivo* opens new avenues where we can monitor fucosylation in living animals. Using intracranial injections, we detected numerous glycoproteins from *in vivo* alkynyl-Fuc labeling between 50 and over 250 kDa. We are currently attempting to identify the fucosylated proteome from these *in vivo* labeling studies. We are also developing methods for immunohistological analysis of brain slices, with the future intent of training animals in learning and behavioral paradigms, then

monitoring changes in localization or synthesis of fucosylated glycoproteins. These studies will help elucidate the proteins involved in learning and memory consolidation. While click chemistry using a copper catalyst is not amenable to *in vivo* labeling, Bertozzi and colleagues have developed a method to click label glycoproteins *in vivo* utilizing copper free chemistry.⁴¹ They developed difluorinated cyclooctyne (DIFO) reagents to activate the alkyne and eliminate the copper catalyst, which allows click chemistry to work in living animals. They have recently demonstrated the ability to label zebrafish *in vivo*,⁴² suggesting that we could potentially use these reagents to monitor fucosylation dynamics in living mice. Such studies will reveal molecular insights into learning and memory that have been unattainable by conventional biochemical approaches.

Cumulatively, our studies reveal exciting new insights into the molecular mechanisms that govern fucosyl oligosaccharides. We demonstrated that fucosylated glycoproteins are found along both axons and dendrites, as well as in the Golgi apparatus. Identification of proteins involved in regulating neuronal morphology and dendritic spine numbers suggest important roles for fucose in the molecular events that may underlie synaptic plasticity. Identification of the fucosyl proteome enables our investigation of fucose function in the nervous system. We hope to pursue metabolic labeling of fucose in living animals to investigate the roles these individual proteins may play in memory consolidation, development, and synaptic plasticity.

Materials and Methods

Embryonic Hippocampal Dissection

Timed-pregnant Sprague-Dawley rats were purchased from Charles River Laboratories (Kingston, Mass) and housed at the Caltech laboratory animal facilities. Timed-pregnant rats at embryonic day 18 (E18) were euthanized in accordance with proper IACUC protocols. Neurons were cultured as described in Chapter 2.

Embryonic Cortical Dissection

Timed-pregnant rats (E18) were dissected as described above. After the brain was removed from the decapitated embryos, the cortices were cut out and the meninges removed. The cortices were placed in ice-cold HBSS and trypsinized with 0.25% trypsin for 15 minutes at 37 °C and triturated to dissociate individual cells. Cortical neurons were evenly plated out on ten 10-cm petri dishes, coated with poly-D-ornithine., in 5 mL of DMEM. After 30 minutes, the DMEM was removed and replaced with supplemented neurobasal media.

Click Labeling Conditions and Protein Precipitation

Cortical neurons were lysed by sonication in boiling 1% SDS and the protein quantified with the BCA Protein Assay (Pierce). The cell lysate was neutralized with an equal volume of neutralization buffer (6% NP-40, 100 mM Na₂PO₄, 150 mM NaCl) and labeled at 2 mg/mL protein with 0.1 mM azido-biotin (5 mM stock in DMSO, stored at -20 °C), 0.1 mM trisiazoleamine catalyst (5 mM stock in DMSO, stored at -20 °C), 2 mM sodium ascorbate (100 mM stock in water, freshly prepared) and 0.5 mM CuBr (50

mM stock in water, freshly prepared) in a microtube. The reaction tube was allowed to rotate at 4 °C overnight. The protein was precipitated using the SDS-PAGE Clean Up Kit (GE Healthcare) to remove excess reagents and resolubilized in boiling 1% SDS, then normalized to 2 mg/mL.

Isolation by Streptavidin Column, Resolution SDS-PAGE gel and Tryptic Digest

Streptavidin resin (Pierce) was equilibrated in a 1:1 neutralization buffer: 1% SDS solution. Labeled lysate was neutralized with an equal volume of neutralization buffer and allowed to incubate with 100 μ L of streptavidin resin, rotating, overnight at 4°C. After binding, the resin was washed with 40 column volumes (CV) of Low Salt Buffer (0.1 M Na₂PO₄ pH 7.5/ 0.15 M NaCl/ 1% Triton-X100/ 0.5% sodium deoxycholate/ 0.1% SDS), 40 CV of High Salt Buffer (0.1 M Na₂PO₄ pH 7.5/ 0.5 M NaCl/ 0.2% Triton X-100), 30 CV of 4 M Urea/ 1% SDS in H₂O, 40 CV of PBS and 40 CV of H₂O in 2 mL BioSpin Chromatography Columns (BioRad). Alternative wash conditions used were 40 CV Low Salt Buffer, 40 CV High Salt Buffer, 30 CV 2% SDS in PBS, 30 CV 8M Urea in H₂O, 30 CV 1 M KCl and 40 CV H₂O. After washing, streptavidin resin was removed and incubated in a microtube, rotating at RT, in one CV of elution buffer (6 M urea, 2 M thiourea, 30 mM biotin, 2% SDS, pH 12) for 15 minutes. The resin was then boiled for 15 minutes in the elution buffer, vortexing every 5 minutes. The tube was spun down and the eluate was removed. The eluate was diluted 10 times with PBS and concentrated to 50 μ L in Amicon-4mL Ultra concentrators (Millipore).

Tryptic Digest

The eluate was resolved on a 10% acrylamide-SDS gel and visualized by silver stain. The gel was destained and the bands cut out before the in gel tryptic digest as described in Chapter 3. The resulting tryptic peptides were acidified in 0.1% HOAc before MS analysis. A tryptic digest was performed in solution on the eluate as described previously. The tryptic peptides were acidified with 0.1% HOAc before MS analysis.

Western Blotting

Labeled lysates were resolved on a 4-12% acrylamide-SDS gel and proteins were transferred to PVDF membrane (Millipore) for 2 h.

Immunocytochemistry of Hippocampal Neuronal Cultures treated with Fucose and Alkynyl-fucose

After 11 days in culture, hippocampal neurons on coverslips were treated with 50 μ M fucose or alkynyl-fucose for three days. At 14 days in culture, media was aspirated and cells were rinsed once with PBS, fixed in 4% paraformaldehyde for 20 minutes at room temperature, washed twice with PBS, permeabilized in 0.3% Triton X-100 for five minutes at room temperature and washed twice with PBS. Non-specific binding was blocked with 3% BSA in PBS for 1 h at room temperature and then the coverslips were rinsed once with PBS. The click reaction was carried out on the coverslip with 100 μ L of 0.05 mM azido-biotin, 0.05 mM tris-triazoleamine catalyst, 1 mM sodium ascorbate and 0.5 mM CuSO_4 in PBS added to the top of each coverslip, overnight at 4 $^{\circ}\text{C}$. After rinsing twice with PBS, primary antibody: anti-synapsin (rabbit, 1:100; Sigma), anti-

PSD-95 (mouse, 1:250; Affinity BioReagents), anti-giantin (Santa Cruz, 1:100), anti-NCAM (mouse, 1:100, Sigma) and UEAI conjugated to fluorescein (50 μ L/mL, Sigma) was added in 3% BSA in PBS, overnight at 4 °C. After the coverslips were washed three times with PBS, fluorophore conjugated secondary antibodies (goat anti-rabbit; 1:500 and goat anti-mouse; 1:500) were added in 3% BSA in PBS for one hour at 37 °C. Alkynyl-fucose was detected with streptavidin conjugated to AlexaFluor 488 (1:100; Molecular Probes) or AlexaFluor 546 (1:100, Molecular Probes) added together with the secondary antibodies. The coverslips were washed three times with PBS and mounted onto slides with Vectashield with DAPI (Vector Labs) and sealed with clear nail polish. Cells were then subjected to fluorescence and confocal microscopy.

***In Vivo* Labeling of Fucosylated Glycans in Mice**

All procedures were approved by IACUC and animals were handled according to the IACUC guidelines. For injection into neonatal rat pups, individual animals P1-P8 were removed from the dam and cryogenically anesthetized by placing them in a latex sleeve and gently submerging them in an ice bath until they appear anesthetized. A toe pinch was used to determine if the anesthesia was sufficient. The skin on the head at the site of injection was cleaned with chlorhexidine. The skull of the rat pup is cartilaginous at this age, and thus injections can proceed without the need of a surgical incision. The pup was injected with a Hamilton syringe using a 33-gauge needle attached to a microinjector. The compounds were injected based on stereotaxic coordinates previously published, and were injected at 0.1 μ L/min for a total volume of 1-2.5 μ L unilaterally into the cortex. As a control, unmodified L-fucose will also be injected into the hippocampus.

After insertion of the needle, a one-min resting period preceded the injection. The injection needle was withdrawn over a 2 min period. The puncture wounds were sealed with surgical glue. Pups were tattooed to identify alkynyl-fucose vs. control fucose injections by using a 29-gauge needle to inject a small quantity of tattoo ink into one of the digits or footpad. After injection the pups were warmed on a water circulating heating pad until they began moving. They were returned to the dam where they will be maintained on a heat pad until the pups begin nursing. The rump of each pup was exposed to a small amount of urine from the dam to mask any odors that may be associated with the handling and injection procedure. Pups were observed for 4-6 hours post-surgery, and any pups that did not appear to be nursing by lack of a milk spot, or appeared cold, dehydrated, or exhibited neurological symptoms were euthanized immediately. The pups were euthanized 1-3 days post-injection by CO₂, and the cortex was isolated.

For pain relief, the dam of the injected pups was given 2 mg/kg ketoprofen subcutaneously just prior to the surgery in hopes that the pup receives the analgesic and anti-inflammatory effects of the drug through nursing. The pups were not treated post-operatively for pain relief as there is no information on a safe dosage to be administered directly to neonates, and the use of such drugs may induce aberrant behavior in the pups and can increase the chance of cannibalization.

References

1. Agard, N. J.; Baskin, J. M.; Prescher, J. A.; Lo, A.; Bertozzi, C. R., A comparative study of bioorthogonal reactions with azides. *ACS Chem. Biol.* **2006**, 1, (10), 644-648.
2. Kohn, M.; Breinbauer, R., The Staudinger ligation - A gift to chemical biology. *Angew. Chem. Int. Ed. Engl.* **2004**, 43, (24), 3106-3116.
3. Gil, M. V.; Arevalo, M. J.; Lopez, O., Click chemistry - What's in a name? Triazole synthesis and beyond. *Synthesis-Stuttgart* **2007**, (11), 1589-1620.
4. Kolb, H. C.; Sharpless, K. B., The growing impact of click chemistry on drug discovery. *Drug Discov. Today* **2003**, 8, (24), 1128-1137.
5. Rostovtsev, V. V.; Green, L. G.; Fokin, V. V.; Sharpless, K. B., A stepwise Huisgen cycloaddition process: copper(I)-catalyzed regioselective "ligation" of azides and terminal alkynes. *Angew. Chem. Int. Ed. Engl.* **2002**, 41, (14), 2596-2599.
6. Agard, N. J.; Prescher, J. A.; Bertozzi, C. R., A strain-promoted [3+2] azide-alkyne cycloaddition for covalent modification of biomolecules in living systems. *J. Am. Chem. Soc.* **2004**, 126, (46), 15046-15047.
7. Rabuka, D.; Hubbard, S. C.; Laughlin, S. T.; Argade, S. P.; Bertozzi, C. R., A chemical reporter strategy to probe glycoprotein fucosylation. *J. Am. Chem. Soc.* **2006**, 128, (37), 12078-12079.
8. Sawa, M.; Hsu, T. L.; Itoh, T.; Sugiyama, M.; Hanson, S. R.; Vogt, P. K.; Wong, C. H., Glycoproteomic probes for fluorescent imaging of fucosylated glycans in vivo. *Proc. Natl. Acad. Sci. U. S. A.* **2006**, 103, (33), 12371-12376.
9. Hanson, S. R.; Hsu, T. L.; Weerapana, E.; Kishikawa, K.; Simon, G. M.; Cravatt, B. F.; Wong, C. H., Tailored glycoproteomics and glycan site mapping using saccharide-selective bioorthogonal probes. *J. Am. Chem. Soc.* **2007**, 129, (23), 7266-7267.
10. Hsu, T. L.; Hanson, S. R.; Kishikawa, K.; Wang, S. K.; Sawa, M.; Wong, C. H., Alkynyl sugar analogs for the labeling and visualization of glycoconjugates in cells. *Proc. Natl. Acad. Sci. USA* **2007**, 104, (8), 2614-2619.
11. Hsu, T.-L.; Wong, C. H., Personal Communication.
12. Link, A. J.; Vink, M. K. S.; Tirrell, D. A., Presentation and detection of azide functionality in bacterial cell surface proteins. *J. Am. Chem. Soc.* **2004**, 126, (34), 10598-10602.
13. Rybak, J. N.; Scheurer, S. B.; Neri, D.; Elia, G., Purification of biotinylated proteins on streptavidin resin: A protocol for quantitative elution. *Proteomics* **2004**, 4, (8), 2296-2299.
14. Murrey, H. E.; Gama, C. I.; Kalovidouris, S. A.; Luo, W. I.; Driggers, E. M.; Porton, B.; Hsieh-Wilson, L. C., Protein fucosylation regulates synapsin Ia/Ib expression and neuronal morphology in primary hippocampal neurons. *Proc. Natl. Acad. Sci. USA* **2006**, 103, (1), 21-26.

15. Wuhrer, M.; Geyer, H.; von der Ohe, M.; Gerardy-Schahn, R.; Schachner, M.; Geyer, R., Localization of defined carbohydrate epitopes in bovine polysialylated NCAM. *Biochimie* **2003**, 85, (1-2), 207-218.
16. Liedtke, S.; Geyer, H.; Wuhrer, M.; Geyer, R.; Frank, G.; Gerardy-Schahn, R.; Zahringer, U.; Schachner, M., Characterization of N-glycans from mouse brain neural cell adhesion molecule. *Glycobiology* **2001**, 11, (5), 373-384.
17. Kojima, N.; Tachida, Y.; Yoshida, Y.; Tsuji, S., Characterization of mouse ST8Sia II (STX) as a neural cell adhesion molecule-specific polysialic acid synthase - Requirement of core alpha 1,6-linked fucose and a polypeptide chain for polysialylation. *J. Biol. Chem.* **1996**, 271, (32), 19457-19463.
18. Gerrow, K.; El-Husseini, A., Cell adhesion molecules at the synapse. *Frontiers Biosci.* **2006**, 11, 2400-2419.
19. Panicker, A. K.; Buhusi, M.; Thelen, K.; Maness, P. F., Cellular signalling mechanisms of neural cell adhesion molecules. *Frontiers Biosci.* **2003**, 8, D900-D911.
20. Doherty, P.; Williams, G.; Williams, E. J., CAMs and axonal growth: A critical evaluation of the role of calcium and the MAPK cascade. *Mol. Cell. Neurosci.* **2000**, 16, (4), 283-295.
21. Baldwin, T. J.; Fazeli, M. S.; Doherty, P.; Walsh, F. S., Elucidation of the molecular actions of NCAM and structurally related cell adhesion molecules. *J. Cell. Biochem.* **1996**, 61, (4), 502-513.
22. Vernon, A. E.; Movassagh, M.; Horan, I.; Wise, H.; Ohnuma, S.; Philpott, A., Notch targets the Cdk inhibitor Xic1 to regulate differentiation but not the cell cycle in neurons. *EMBO Reports* **2006**, 7, (6), 643-648.
23. Moloney, D. J.; Shair, L. H.; Lu, F. M.; Xia, J.; Locke, R.; Matta, K. L.; Haltiwanger, R. S., Mammalian Notch1 is modified with two unusual forms of O-linked glycosylation found on epidermal growth factor-like modules. *J. Biol. Chem.* **2000**, 275, (13), 9604-9611.
24. Rampal, R.; Arboleda-Velasquez, J. F.; Nita-Lazar, A.; Kosik, K. S.; Haltiwanger, R. S., Highly conserved O-fucose sites have distinct effects on Notch1 function. *J. Biol. Chem.* **2005**, 280, (37), 32133-32140.
25. Rampal, R.; Luther, K. B.; Haltiwanger, R. S., Notch signaling in normal and disease states: Possible therapies related to glycosylation. *Curr. Mol. Med.* **2007**, 7, (4), 427-445.
26. Arbuzova, A.; Schmitz, A. A. P.; Vergeres, G., Cross-talk unfolded: MARCKS proteins. *Biochem. J.* **2002**, 362, 1-12.
27. Schmitz, A. A. P.; Ulrich, A.; Vergeres, G., Membrane binding of MARCKS-related protein studied by tryptophan fluorescence spectroscopy. *Arch. Bioch. Biophys.* **2000**, 380, (2), 380-386.
28. Arbuzova, A.; Wang, L. B.; Wang, J. Y.; Hangyas-Mihalyne, G.; Murray, D.; Honig, B.; McLaughlin, S., Membrane binding of peptides containing both basic and aromatic residues. Experimental studies with peptides corresponding to the scaffolding region of caveolin and the effector region of MARCKS. *Biochemistry* **2000**, 39, (33), 10330-10339.
29. Victor, K.; Jacob, J.; Cafiso, D. S., Interactions controlling the membrane binding of basic protein domains: Phenylalanine and the attachment of the myristoylated

- alanine-rich C-kinase substrate protein to interfaces. *Biochemistry* **1999**, 38, (39), 12527-12536.
30. Bahr, G.; Diederich, A.; Vergeres, G.; Winterhalter, M., Interaction of the effector domain of MARCKS and MARCKS-related protein with lipid membranes revealed by electric potential measurements. *Biochemistry* **1998**, 37, (46), 16252-16261.
 31. Vergeres, G.; Ramsden, J. J., Binding of MARCKS (myristoylated alanine-rich C kinase substrate)-related protein (MRP) to vesicular phospholipid membranes. *Biochem. J.* **1998**, 330, 5-11.
 32. Matus, A., MARCKS for maintenance in dendritic spines. *Neuron* **2005**, 48, (1), 4-5.
 33. McLaughlin, R. E.; Denny, J. B., Palmitoylation of GAP-43 by the ER-Golgi intermediate compartment and Golgi apparatus. *Biochim. Biophys. Acta* **1999**, 1451, (1), 82-92.
 34. Liu, Y. C.; Fisher, D. A.; Storm, D. R., Analysis of the palmitoylation and membrane targeting domain of neuromodulin (Gap-43) by site-specific mutagenesis. *Biochemistry* **1993**, 32, (40), 10714-10719.
 35. Gomez, M.; Hernandez, M. L.; Pazos, M. R.; Tolon, R. M.; Romero, J.; Fernandez-Ruiz, J., Colocalization of CB1 receptors with L1 and GAP-43 in forebrain white matter regions during fetal rat brain development: Evidence for a role of these receptors in axonal growth and guidance. *Neuroscience* **2008**, 153, (3), 687-699.
 36. Korshunova, I.; Novitskaya, V.; Kiryushko, D.; Pedersen, N.; Kolkova, K.; Kropotova, E.; Mosevitsky, M.; Rayko, M.; Morrow, J. S.; Ginzburg, I.; Berezin, V.; Bock, E., GAP-43 regulates NCAM-180-mediated neurite outgrowth. *J. Neurochem.* **2007**, 100, (6), 1599-1612.
 37. Metz, G. A.; Schwab, M. E., Behavioral characterization in a comprehensive mouse test battery reveals motor and sensory impairments in growth-associated protein-43 null mutant mice. *Neuroscience* **2004**, 129, (3), 563-574.
 38. Bian, F.; Li, Z.; Offord, J.; Davis, M. D.; McCormick, J.; Taylor, C. P.; Walker, L. C., Calcium channel alpha2-delta type 1 subunit is the major binding protein for pregabalin in neocortex, hippocampus, amygdala, and spinal cord: An ex vivo autoradiographic study in alpha2-delta type 1 genetically modified mice. *Brain Res.* **2006**, 1075, 68-80.
 39. Wei, J.; Zhang, M.; Zhu, Y.; Wang, J. H., Ca²⁺-calmodulin signalling pathway up-regulates gaba synaptic transmission through cytoskeleton-mediated mechanisms. *Neuroscience* **2004**, 127, (3), 637-647.
 40. Tang, T. S.; Tu, H. P.; Chan, E. Y. W.; Maximov, A.; Wang, Z. N.; Wellington, C. L.; Hayden, M. R.; Bezprozvanny, I., Huntingtin and Huntingtin-associated protein 1 influence neuronal calcium signaling mediated by inositol-(1,4,5) triphosphate receptor type 1. *Neuron* **2003**, 39, (2), 227-239.
 41. Baskin, J. M.; Prescher, J. A.; Laughlin, S. T.; Agard, N. J.; Chang, P. V.; Miller, I. A.; Lo, A.; Codelli, J. A.; Bertozzi, C. R., Copper-free click chemistry for dynamic *in vivo* imaging. *Proc. Natl. Acad. Sci. U.S.A.* **2007**, 104, (43), 16793-16797.

42. Laughlin, S. T.; Baskin, J. M.; Amacher, S. L.; Bertozzi, C. R., *In vivo* imaging of membrane-associated glycans in developing zebrafish. *Science* **2008**, 320, (5876), 664-667.

Appendix I

Exploring Synapsin I Regulation and Fucosylation by Small Molecule

Inhibitors

A1.1. Background

The synapsins are a multigene family of neuronal phosphoproteins involved in regulating neurotransmitter release and neuronal development.^{1, 2} There are five known members of the family encoded by three distinct genes: synapsin I, synapsin II, and synapsin III.³⁻⁶ They are the most abundant protein on synaptic vesicles and constitute ~ 1% of total brain protein.⁷⁻⁹ The synapsins are composed of eight different domains termed A-H, and all synapsin members are homologous at the N-terminal domain, which contain the A, B, and C domains.¹⁰ Domains A and C are the most conserved domains.^{1, 11} Domain A contains the only phosphorylation site conserved in all synapsin isoforms, and phosphorylation of this site controls its association with synaptic vesicles. The site is a substrate for both protein kinase A (PKA) and the Ca²⁺/calmodulin-dependent protein kinase I (CAMKI).^{5, 10, 12} Phosphorylation of this site leads to dissociation from synaptic vesicles.¹² The C domain is also highly conserved, and binds ATP in all synapsin isoforms, however, no ATPase activity has been associated with this domain.¹³ Thus, the function of ATP binding remains unknown. The C domain binds to other synapsin C domains, creating homo- and heterodimers, which are important for synaptic vesicle clustering.¹⁴

The synapsins have been most characterized for their role in regulating synaptic vesicle cycling, where they tether synaptic vesicles to the actin cytoskeleton.¹⁵⁻²¹ Because of the homo- and heterodimerization of synapsins, this creates a meshwork of synaptic

vesicle pools as synapsins also interact with the synaptic vesicle membrane.^{1, 22-25} The synapsins are reported to maintain the “reserve pool” of synaptic vesicles that contains a large portion of vesicles clustered away from the plasma membrane near the active zone of presynaptic terminals.²⁶⁻²⁸ There is a small subset of synaptic vesicles, termed the “releasable pool”, that are physically docked to the plasma membrane. Upon Ca^{2+} influx through voltage-gated Ca^{2+} channels, this pool of synaptic vesicles undergoes fusion with the plasma membrane, releasing neurotransmitter into the synaptic cleft.²⁹⁻³² Phosphorylation of synapsins leads to release from synaptic vesicles in the releasable pool in response to increased activity, which can then dock at the plasma membrane for further fusion events. Thus, the synapsins appear to regulate synaptic vesicle cycling, implicating them in the ability to modulate synaptic transmission.

In addition to their roles in regulating neurotransmitter release, the synapsins have also been reported to play a role in mediating neuronal growth as well as the formation and maintenance of synaptic contacts.² They are localized to the growth cones of developing cerebellar granule and hippocampal neurons.³³⁻³⁶ In addition suppression of synapsins I, II, and III expression alters developmental morphology in cultured hippocampal neurons.^{34, 37-39} In fact, hippocampal neurons cultured from synapsin I-deficient mice display stunted neurites and delayed synapsin formation.³⁷ We recently reported that fucosylation of synapsin I is involved in this process (Chapter 2), suggesting a novel mode of synapsin regulation.⁴⁰ Here, we further examine synapsin fucosylation with a panel of deoxy-galactose inhibitors, and demonstrate that only 2-dGal conclusively affects synapsin expression and fucosylation. In addition, we attempt to label synapsin I with ^3H -Fuc in transfected HeLa cells and cortical neurons. However, we were never

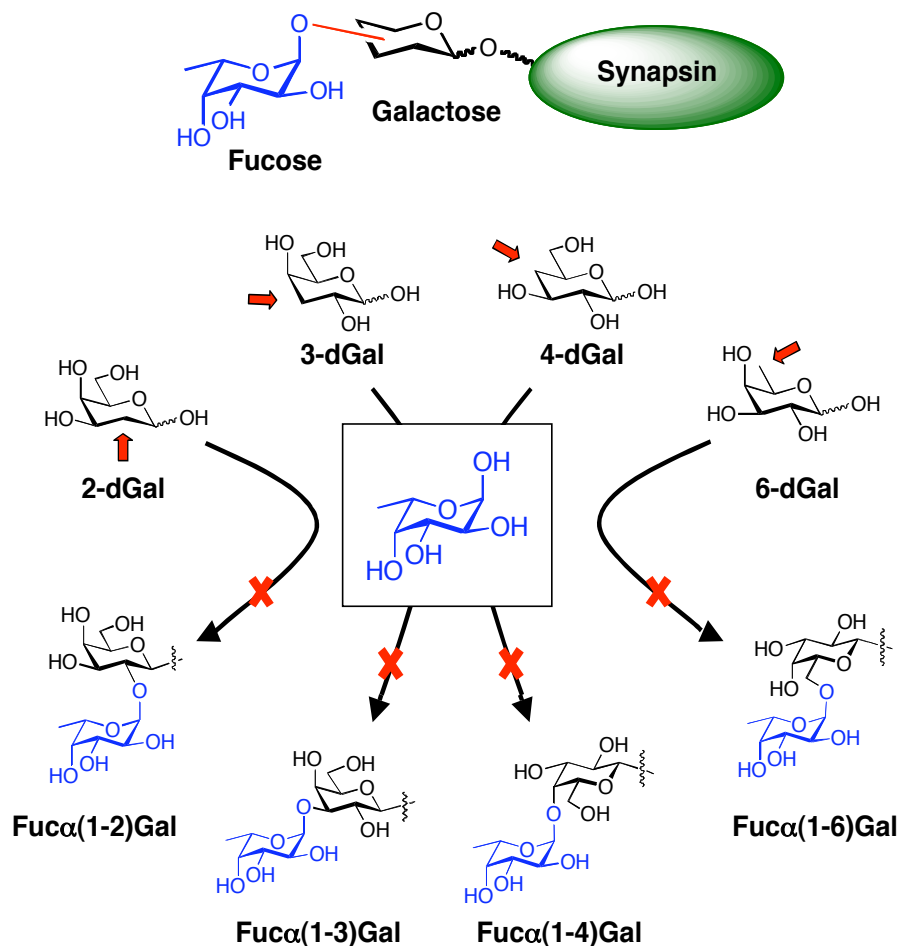


Figure A1.1. Strategy for mapping of Fuc-Gal linkages. Treatment of cells with different deoxy-Gal analogues should inhibit the various Fuc-Gal linkages.

able to detect a fucosylated moiety through tritium labeling. Lastly, we examine inhibitors of glycosylation synthesis, and demonstrate that disruption of Golgi trafficking leads to loss of synapsin expression.

A1.2. Deoxy-Gal Analogues Can Map Fucose Linkages

Traditional methods of elucidating the structure of complex oligosaccharides are time-consuming and challenging. Large quantities of protein, sequential deglycosylation reactions using a series of exo- and endoglycosidases, and advanced MS or NMR

analyses are typically required.⁴¹⁻⁴³ Despite significant progress, many glycoproteins are not amenable to the established methods, and there is a significant need for new approaches to oligosaccharide linkage analysis.

We envisioned exploiting a series of deoxy sugar analogues to map the structure of the oligosaccharide present on synapsin. Our approach stems from the observation that 2-dGal can inhibit protein fucosylation by competing with D-galactose for incorporation into the oligosaccharide chain.^{44, 45} Upon cellular uptake, 2-dGal is converted via the Leloir pathway to the 1-phosphate analogue, which is subsequently converted to the activated uridyl diphosphate (UDP) sugar.⁴⁶ Based upon these observations, we postulated that 3-dGal, 4-dGal and 6-dGal might also be converted into UDP sugars in sufficient quantity to compete with D-galactose. We have previously demonstrated in Chapter 2 that 2-dGal is an efficient substrate for metabolism through the Leloir pathway. While the conversion efficiencies of other deoxy sugars via this pathway have not been systematically examined in mammalian cells, *in vitro* studies using purified enzymes have suggested that substitution at the various positions should be tolerated, with the C4 position least favored.⁴⁷⁻⁴⁹ Subsequent incorporation of the deoxy analogues into glycoproteins would inhibit formation of the corresponding fucose-galactose disaccharide and permit mapping of the precise linkage (Figure A1.1).

We evaluated the relative ability of a series of 2-, 3-, 4- and 6-deoxy-galactose analogues to inhibit formation of the glycosidic linkage on synapsin Ia. The 3-dGal and 4-dGal analogues were synthesized by Stacey Kalovidouris and Callie Bryan using procedures reported by Lowary *et al.*⁵⁰ HeLa cells were pre-treated for 1 h with the deoxy analogues at the concentrations indicated in Figure A1.2. After pre-incubation,

cells were transiently transfected with synapsin Ia, $\alpha(1-2)$ fucosyltransferase H enzyme (FUT1), and β -galactosidase. FUT1 has been shown to catalyze the formation of Fuc $\alpha(1-2)$ Gal linkages on glycoproteins bearing the type 2 Lewis antigen⁵¹ and thus was employed to potentially enhance fucosylation of synapsin. β -Galactosidase was used to normalize each sample for transfection efficiency. Cell lysates were resolved by SDS-PAGE, and the fucosylation and protein levels of synapsin were measured by

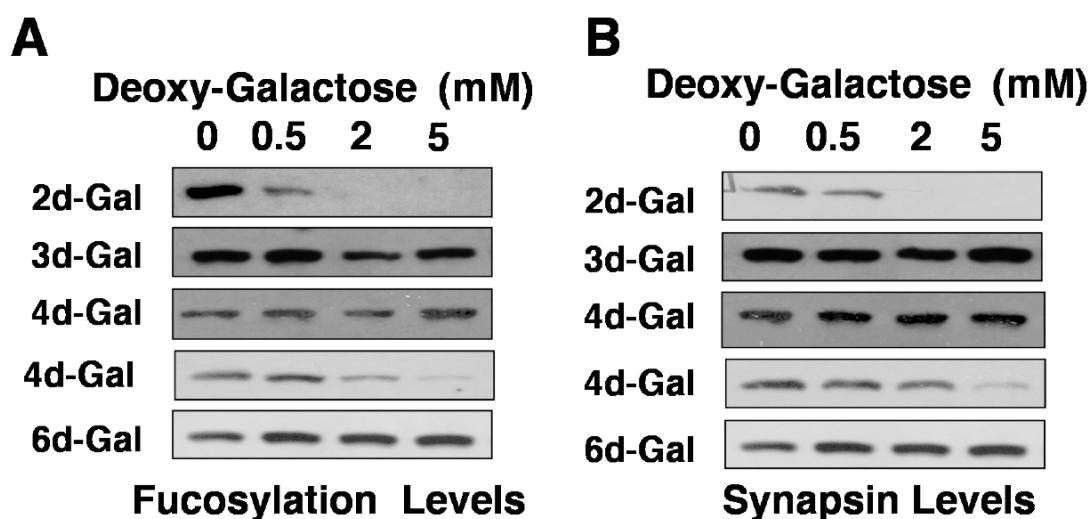


Figure A1.2. Deoxy-Gal treatment can potentially be used to determine oligosaccharide linkages. HeLa cells were treated with deoxy-Gal analogues at the indicated concentrations. Fucosylation levels were determined by Western blotting with antibody A46-B/B10 (A) and expression levels were determined by immunoblotting with anti-synapsin I (B).

immunoblotting.

As anticipated, treatment of mammalian cells with 2-dGal had a dramatic effect on the fucosylation levels (Figure A1.2A) and expression of synapsin (Figure A1.2B). In contrast, 3-dGal and 6-dGal had no observable effect on the fucosylation or expression level of synapsin. In some experiments, we saw no effect with 4-dGal treatment. However, in other experiments, incubation of cells with 4-dGal at higher concentrations

produced effects similar to those observed for 2-dGal in experiments. Thus, the results of 4-dGal treatment are inconclusive.

A1.3. 2-dGal Treatment Affects Synapsin I Deletion Mutants and S579A Synapsin

Once we established that deoxy-Gal sugars can potentially be used to determine oligosaccharide linkages, we sought to address the specificity of 2-dGal treatment using synapsin I deletion mutants and the fucosylation-deficient S579A synapsin I construct. HeLa cells were pre-treated with 2-dGal for 1 h and then transfected with Flag-synapsin

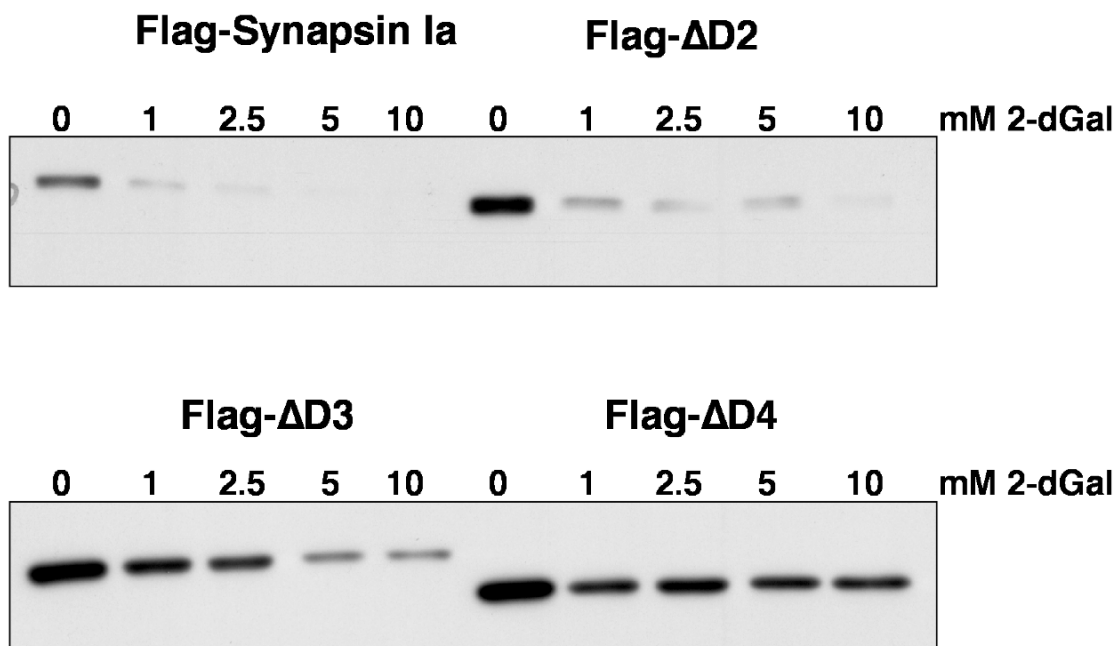


Figure A1.3. Deoxy-Gal affects Synapsin Ia deletion mutants. HeLa cells were transfected with the indicated constructs and treated with increasing concentrations of 2-dGal as indicated above. Flag-synapsin I, Flag-ΔD2, and Flag-ΔD3 exhibited increasing degradation by Western blot analysis with increasing concentrations of 2-dGal. In contrast, the Flag-ΔD4 mutant, which does not contain a Fuc α (1-2)Gal epitope, exhibited an initial decrease in protein expression, followed by stability to increasing concentrations of 2-dGal.

I, Flag-Synapsin I Δ D2, Flag-Synapsin I Δ D3, Flag-Synapsin I Δ D4, or Flag-S579A-Synapsin I. 24 h post-transfection, cells were harvested and resolved by SDS-PAGE and blotted with an anti-Flag antibody to examine protein expression levels. As expected, the Flag-Synapsin I, Flag-Synapsin Δ D2, and Flag-Synapsin Δ D3, which all contain Fuc α (1-2)Gal moieties, exhibited loss of synapsin expression with increasing concentrations of 2-dGal (Figure A1.3). Interestingly, the loss of synapsin I expression was reduced with greater truncations of the D-domain with the Flag-Synapsin I Δ D3 construct being the most stable to 2-dGal treatment. Surprisingly, the Flag-Synapsin I Δ D4 construct, which lacks a Fuc α (1-2)Gal moiety, had a modest reduction in synapsin I expression after treatment with 1 mM 2-dGal, then exhibited stable expression with increasing concentrations of 2-dGal (Figure A1.3). This initial decrease in synapsin expression may suggest that there is another glycan lacking a Fuc α (1-2)Gal that 2-dGal affects in this construct, or may reflect some non-specific effects of 2-dGal treatment. However, after the initial decrease in synapsin expression, the a Flag-Synapsin I Δ D4 construct exhibited no further decrease in expression, consistent with a role for 2-dGal in affecting synapsin I fucosylation and expression via the C-terminal region.

We next explored whether mutation of the putative fucosylation site at Ser 579 rescued synapsin I from 2-dGal-mediated degradation. Mutation of this site to Ala should abolish glycosylation, thus 2-dGal should have no effect on degradation of synapsin if mediated by the Fuc α (1-2)Gal epitope at this site. Interestingly, the Flag-S579A-Synapsin exhibited significant loss of expression upon increasing concentrations of 2-dGal (Figure A1.4), similar to Flag-Synapsin degradation levels. This suggests that 2-dGal-mediated synapsin I degradation is not mediated via this fucosylation site. We

have evidence that a second site of Fuc α (1-2)Gal glycosylation exists in synapsin I (Chapter 2), thus perhaps this alternative glycosylation site is responsible for 2-dGal-induced degradation. Experiments are currently underway to identify this alternate site of glycosylation, and when identified similar experiments will be performed to determine if this site is responsible for synapsin I stability.

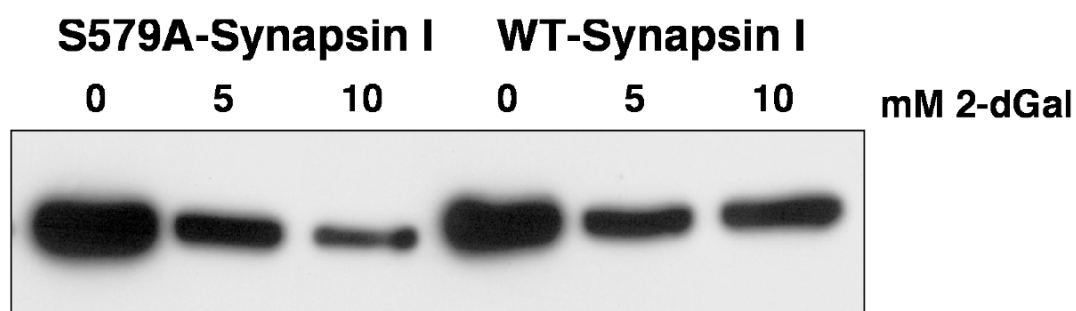


Figure A1.4. S579A-Synapsin I is degraded by 2-dGal treatment. HeLa cells were transfected with Flag-Synapsin I or Flag-S579A-Synapsin I and treated with 2-dGal as indicated above. Lysates were analyzed by immunoblotting with anti-Flag antibody.

A1.4. Flag_S579A-Synapsin may have a Defect in Localization to Synaptic Terminals.

Since S579A-Synapsin I did not appear to be involved in synapsin I degradation from defucosylation with 2-dGal, we next examined whether this fucosylation site might be involved in protein targeting. Wild-type C57BL/6 neurons were transfected at 0 DIV with GFP-Synapsin I or GFP-S579A-Synapsin I and grown for 14 DIV to establish functional synapses. We observed a significant decrease in the amount of synapsin localized to synapses by fluorescence microscopy (Figure A1.5). The data suggest that fucosylation of this site may be involved in synaptic targeting. However, more experiments need to be performed to confirm the result.

A1.5. Examination of Synapsin Fucosylation with ^3H -Fucose

Tritium labeling is the traditional method to detect sugars on glycoconjugates. However, tritium is a weak beta emitter, and exposure times can take weeks to months to detect the sugar. Despite these drawbacks, we explored the ability to label synapsin I with ^3H -Fuc in both transfected Chinese hamster ovary (CHO) cells and neuronal cell cultures. CHO cells were transfected with empty vector (pcDNA 3.1) as a control, with synapsin Ia, or co-transfected with synapsin Ia and FUT1. FUT1 increases the expression of synapsin I in transfected cells (Figure A1.6), and we hoped to enhance synapsin fucosylation with this enzyme. However, despite multiple attempts, we were never able to significantly immunoprecipitate synapsin I from these cells (Figure A1.6). In addition, radiolabeling was very weak of endogenous CHO fucosylated proteins, even after a 2-week exposure time (data not shown). This suggests that radiolabeling of transfected CHO cells was not the optimal system to detect ^3H -Fuc on synapsin I, or significantly longer exposure times would be required.

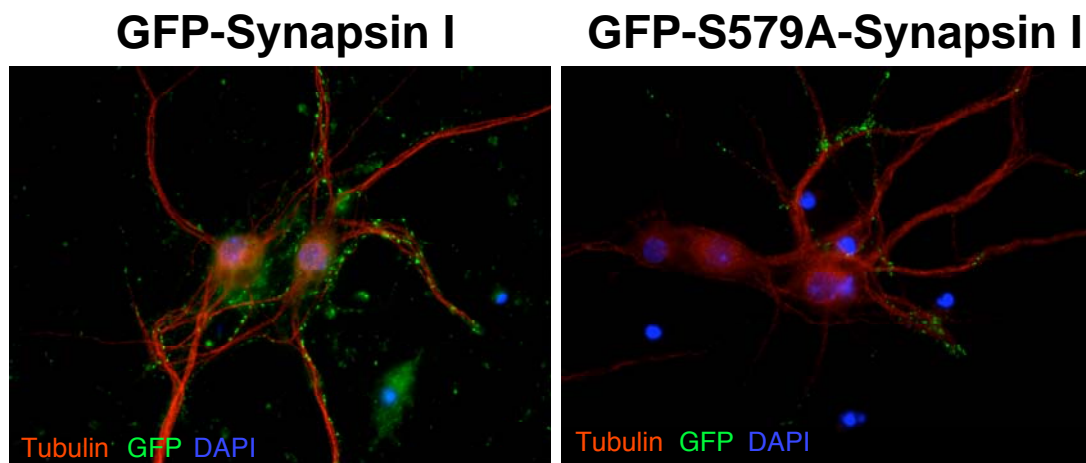


Figure A1.5. GFP-S579A-Synapsin has a defect in localization to synapses. C57BL/6 cortical neurons were transfected at 0 DIV with GFP-synapsin I or GFP-S579A-Synapsin Ia and cultured for 14 DIV, then examined by fluorescence microscopy.

We next turned our attention towards radiolabeling cultured cortical neurons. We first attempted to inhibit fucosylation of endogenous proteins with 2-dGal treatment. Cortical neurons were cultured for 2 DIV, then treated with 15 mM 2-dGal and 200 μ Ci of 3 H-Fuc for 2 more days. Lysates were resolved by SDS-PAGE, and either immunoblotted with antibody A46-B/B10 or exposed to film for tritium detection. We observed complete loss of fucosylated bands detected by the $\text{Fu}\alpha(1-2)\text{Gal}$ antibody after treatment with 2-dGal (data not shown). However, we did not observe any difference in tritium labeling of fucosylated glycoproteins, suggesting that the majority of fucose is incorporated into other linkages in neurons (data not shown). We attempted to label older neuronal cultures in which synapsin expression is prominent, however, we again had problems with the immunoprecipitation and results were inconclusive.

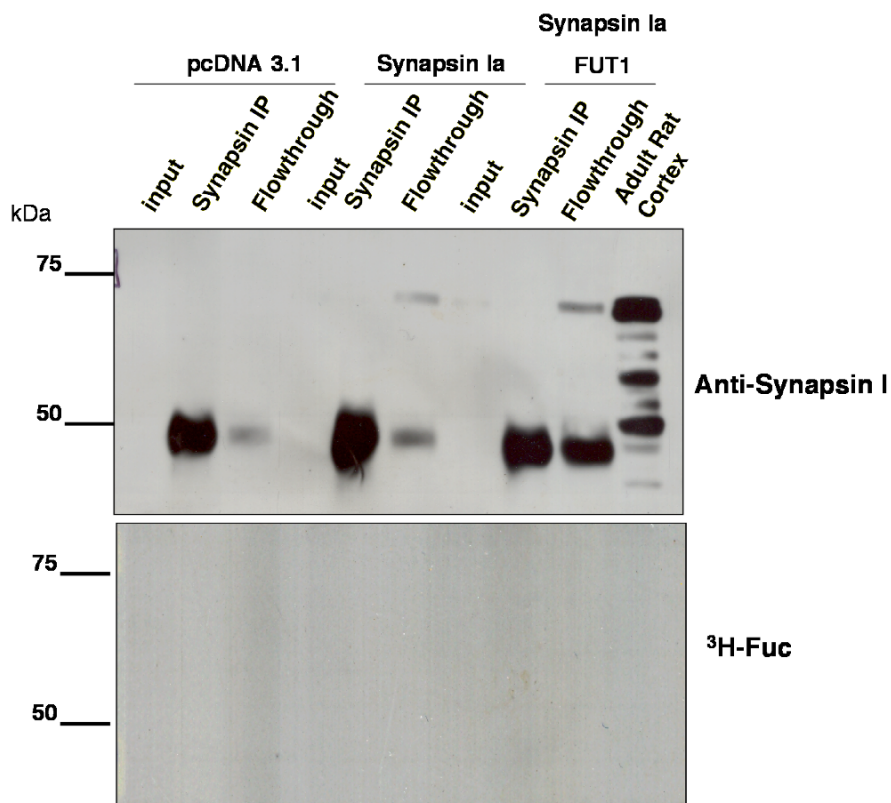


Figure A1.6. Autoradiography fails to detect a fucosylated glycan on synapsin I. Western blot of immunoprecipitated synapsin I (top panel) and autoradiography of immunoprecipitates (bottom panel) from CHO cells transfected as indicated above. Input is 10% of lysate used for immunoprecipitation, synapsin IP is immunoprecipitated synapsin, and flowthrough is 20% of lysate after immunoprecipitation. Co-transfection with FUT1 enhances synapsin I expression, lanes 4 and 7. No synapsin is detected in IP lanes.

A1.6. Synapsin I Expression is Reduced by Inhibitors of Golgi Trafficking

Synapsin I is a cytosolic protein, thus the mechanism of glycosylation is unknown. There is no signal sequence on synapsin to enter the endoplasmic reticulum (ER) for glycosylation reactions, which led us to postulate that perhaps synapsin I is fucosylated in the cytosol via a novel mechanism. We examined synapsin expression in response to the small molecule inhibitor Brefeldin A (Figure A1.8) that inhibits protein translocation from the ER to the Golgi in cultured hippocampal neurons. Neurons were

cultured for 6 DIV, then treated for 1 day with Brefeldin A. Cells were lysed and resolved by SDS-PAGE followed by immunoblotting for synapsin I, Fuc α (1-2)Gal, *N*-cadherin as a control for a known glycoprotein, and tubulin as a control for a known cytosolic protein. We observed a loss of the Fuc α (1-2)Gal signal as recognized by antibody A46-B/B10, consistent with a loss of glycosylation by inhibiting Golgi trafficking (Figure A1.9A). We also observed a decrease in molecular weight of the glycosylated *N*-cadherin protein, consistent with a loss of glycosylation (Figure A1.9B). As expected, we saw no effects on the cytosolic protein tubulin (Figure A1.9B). We were surprised to discover a decrease in synapsin I expression when we inhibited Golgi trafficking (Figure A1.9C). This may suggest that synapsin I is glycosylated via the Golgi apparatus.

A1.7. Discussion

An understanding of the role of Fuc α (1-2)Gal carbohydrates in neuronal communication has been hampered by the lack of information regarding their molecular level functions. Here, we further investigated synapsin I fucosylation through different mechanisms. We attempted tritium labeling of synapsin, yet were unsuccessful due to immunoprecipitation problems. We also examined the ability to map Fuc-Gal linkages using a panel of deoxy-Gal substrates. We consistently observed an effect on synapsin fucosylation and expression with 2-dGal. This is consistent with formation of a Fuc α (1-2)Gal linkage on synapsin I. On occasion, we also saw effects on synapsin I expression with higher concentrations of 4-dGal. While the results with 4-dGal are inconclusive, we have demonstrated in Chapter 2 that there is not a Fuc α (1-4)Gal epitope on synapsin I

through enzymatic deglycosylation with an $\alpha(1-3,4)$ -fucosidase. If 4-dGal affects synapsin I expression and fucosylation, this may suggest an important role for the C4 position of galactose, presumably elsewhere in the oligosaccharide chain. Alternatively, 4-dGal could inhibit enzymes of the Leloir pathway, thus preventing fucosylation of synapsin I. The observation that higher concentrations of 4-dGal are required to abolish glycosylation is consistent with previous reports demonstrating that 4-deoxy analogues are poor substrates for galactosyltransferases and enzymes of the Leloir pathway.^{49, 52} Nonetheless, the 4-dGal analogue may be a competent substrate in mammalian cells. Further experiments are currently underway to confirm incorporation of 4-dGal into the oligosaccharide chain.

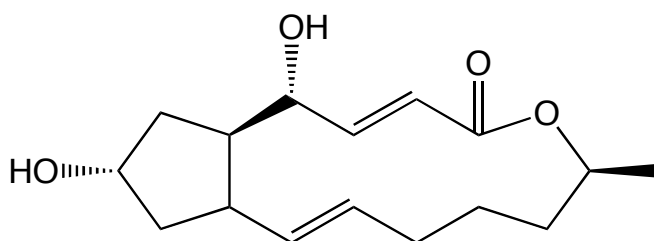


Figure A1.7. Chemical structure of Brefeldin A.

Disruption of the glycosidic linkage in cells led to synapsin Ia turnover. We also observed significant degradation of synapsin I ΔD mutants that contain a $Fuc\alpha(1-2)Gal$ moiety. Surprisingly, we observed a modest decrease of synapsin I expression in the deletion mutant $\Delta D4$, which does not contain a $Fuc\alpha(1-2)$ epitope as determined by Western blotting with antibody A46-B/B10 or UEA1 lectin (Chapter 2). This suggests there may be some non-specific effects of 2-dGal treatment on synapsin I degradation. However, despite this initial decrease in synapsin I degradation, the construct was stable

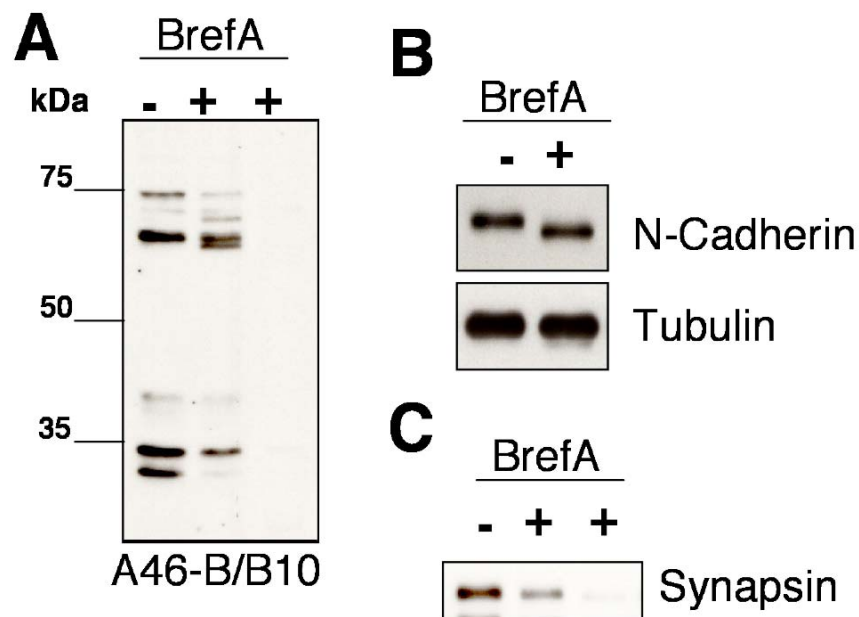


Figure A1.8. Treatment of 6 DIV cortical neurons with the Golgi trafficking inhibitor Brefeldin A for 1 DIV leads to loss of synapsin I expression (C) and expression of the Fuc α (1-2)Gal epitope on glycoproteins (A). Treatment of N-cadherin with Brefeldin A leads to loss of glycan expression and a molecular weight shift whereas treatment of tubulin has no effect (B). Cells were treated with 0.5 to 1 μ g Brefeldin A.

to higher concentrations of 2-dGal, suggesting that defucosylation of synapsin I fucosylation sites is involved in 2-dGal-mediated synapsin degradation. We next tested the identified fucosylation site at Ser 579 for its response to 2-dGal treatment. We observed degradation of S579A-Synapsin I similar to wild-type synapsin I, suggesting that this site is not involved in defucosylation-induced protein degradation, and that it is likely due to another Fuc α (1-2)Gal moiety in synapsin I protein.

We examined the ability of GFP-S579A-Synapsin I to target to presynaptic terminals. While S579A synapsin I was able to target to some terminals as indicated by the green punctate staining in figure A1.5 (right panel), we observed significantly less synapsin I-positive puncta than the wild-type counterpart. This may suggest a problem with S579A synapsin in localization to presynaptic terminals, and would implicate

fucosylation of this site in synapsin I targeting. This data is a preliminary result, and further experiments need to be performed to determine whether the result is not an artifact. In addition, we wish to explore these findings in synapsin I-deficient neurons, to determine if transfection of S579A-Synapsin can rescue neurite outgrowth deficits.

Cumulatively, these results suggest that the Fuc α (1-2)Gal carbohydrate may regulate the expression levels of synapsin I *in vivo*. Interestingly, the targeting of synapsins to presynaptic terminals involves complex interactions within the domains of synapsin and between its different isoforms (Ia/Ib, IIa/b, IIIa-d).⁵³ As the Fuc α (1-2)Gal epitope is not found on synapsin II and III family members (Chapter 2),⁴⁰ glycosylation could influence the differential expression of synapsin I isoforms, as well as the targeting of different synapsin isoforms to the synapse. Alterations in synapsin expression or targeting via fucosylation could affect the clustering of synaptic vesicles, the size of the synaptic vesicle reserve pool, and neurotransmitter release.

Interestingly, synapsin I is a cytosolic protein, and the mechanism of glycosylation is unknown. We observed a significant decrease in synapsin I expression in response to inhibition of ER to Golgi trafficking, suggesting that synapsin I either travels through the normal glycosylation pathway, or interacts with the Golgi in such a manner that disruption of trafficking affects synapsin expression. If synapsin is glycosylated via a Golgi-dependent mechanism, then this would represent a novel pathway for glycosylation as synapsin I does not contain an ER translocation signal sequence. Future studies will address the impact of synapsin fucosylation on neurotransmitter release, neuronal morphology, and protein targeting. A comprehensive

molecular level understanding of Fuc α (1-2)Gal carbohydrates should continue to reveal new insights into the diverse mechanisms of neuronal communication.

A1.8 Materials and Methods

General

Chemicals were purchased from Sigma-Aldrich unless otherwise stated. All reactions were performed in glass round bottom flasks (Pyrex) under an argon atmosphere. Thin-layer chromatography (TLC) was carried out on glass sheets coated with Kieselgel 60 F₂₅₄ Fertigplatten (Merck, Darmstadt, Germany), and plates were inspected by UV light and developed by treatment with a cerium ammonium molybdate stain. Column chromatography was carried out using silica gel 60 (ICN Silitech 32-63 D, 60 Å). High resolution fast atom bombardment mass spectra (FAB-MS) were obtained on a Jeol JMS-600H spectrometer and low resolution electrospray mass spectra (ES-MS) were acquired on a PE Sciex API 365 LC/MS/MS Triple Quadrupole mass spectrometer with a proton nanospray source. ¹H and ¹³C NMR spectra were recorded using a Varian Mercury 300 spectrometer with the solvent or TMS as the internal standard. The chemical shifts are expressed on the δ scale in parts per million (ppm). The following abbreviations are used to explain the observed multiplicities: s, singlet; d, doublet; dd, doublet of doublets; t, triplet; m, multiplet; br, broad.

Treatment of Mammalian Cells with Deoxy-Galactose Analogues

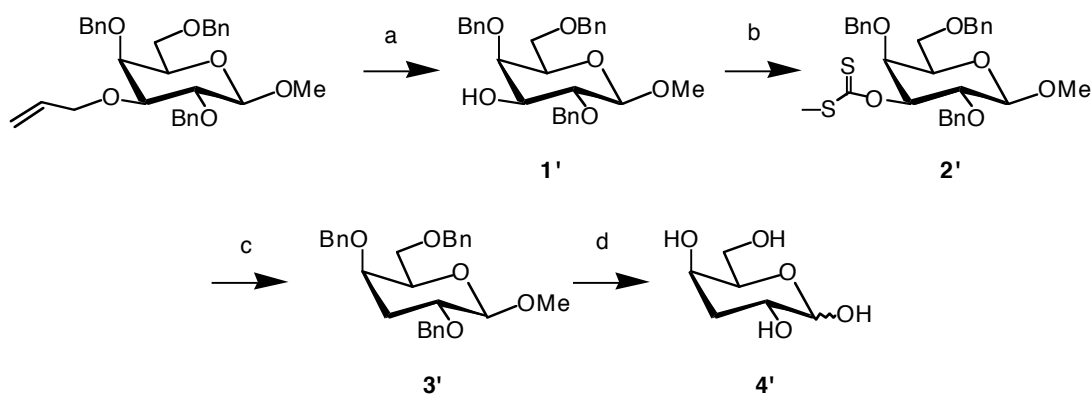
HeLa cells were maintained in Dulbecco's Modified Eagle Medium (DMEM) supplemented with 10% fetal bovine serum (FBS). Cells were seeded at 6×10^5 cells per

60 mm dish and incubated at 37 °C/ 5% CO₂ for 24 h. The cells were then pretreated with the deoxy-galactose analogues (0.5 - 50 mM) for 1h at 37 °C/ 5% CO₂ and transfected at ~60% confluence without changing the media with pcDNA3.1-SynIa, FUT1,²¹ and pSV- β -galactosidase (Promega) using Lipofectamine 2000 (Invitrogen) for deoxy-Gal analogues. Cells were transfected with pCMV-Flag-Synapsin Ia, pCMV-Flag-Synapsin Δ D2, pCMV-Flag-Synapsin Δ D3, pCMV-Flag-Synapsin Δ 4, or pCMV-Flag-S579A-Synapsin I for 2-dGal experiments. After 20-22 h, the cells were harvested, resuspended in PBS (1 mL per plate), and either lysed in 1% boiling SDS (70% of the cells) or analyzed for transfection efficiency using a β -galactosidase assay (30% of the cells). Equivalent amounts of transfected protein were loaded onto SDS-PAGE gels and analyzed by Western blotting.

Synthesis of 3-dGal and 4-dGal

Syntheses were performed by Stacey Kalovidouris and Callie Bryan. The synthetic methods used to prepare 3-dGal and 4-dGal were analogous to those reported by Lowary *et al.*¹ and are described below.

Scheme A1.1 Synthesis of 3-deoxy-D-galactose.



“Conditions: (a) methyl 3-*O*-allyl-2,4,6-tri-*O*-benzyl- β -D-galactopyranoside, EtOH, benzene, H₂O, (Ph₃P)₃RhCl, DABCO, Hg₂O, HgCl₂ (61%) (b) THF, NaH, imidazole, CS₂, MeI (58%) (c) toluene, tributylstanane, AIBN (40%) (d) *i.* H₂, Pd(OH)₂/C, CH₂Cl₂, MeOH *ii.* H₂O, H⁺ (50%).

Methyl 2,4,6-tri-*O*-benzyl- β -D-galactopyranoside (1’): A solution of methyl 3-*O*-allyl-2,4,6-tri-*O*-benzyl- β -D-galactopyranoside² (600 mg, 1.2 mmol), tris(triphenylphosphine)rhodium(I) chloride (160 mg, 0.20 mmol), and 1,4-diazabicyclo[2.2.2]octane (60 mg, 0.54 mmol) in EtOH (10 mL), benzene (4.5 mL) and water (1.5 mL) was refluxed for 20 h. Upon evaporation of the solvents, the resulting residue was dissolved in a solution of acetone (9 mL) and water (1 mL). Mercuric oxide (10 mg) and mercuric chloride (1.5 g) were added to the solution. After 12 h of stirring at rt, the mixture was diluted with CH₂Cl₂ and washed sequentially with a saturated solution of KI, water and then brine. Purification by SiO₂ column chromatography (5:1 hexanes / EtOAc) of the organic layer gave 340 mg of a white solid (61%). ¹H-NMR (300 MHz, CDCl₃): δ = 1.12 (s, 3H, CH₃), 3.40 (d, 1H, *J* = 4.5 Hz, 3-OH), 3.55 (d, 1H, *J* = 7.5 Hz, H-2), 3.59-3.70 (m, 4 H, H-3, H-5, H-6, H-6’), 3.85 (d, 1H, *J* = 3.5 Hz, H-4), 4.33 (d, 1H, *J*=7.5 Hz, H-1), 4.43-4.50 (m, 6H, PhCH₂), 7.20-7.40 (m, 15H, Ph), ¹H-NMR (300 MHz, CDCl₃) in the literature:^{3,4} δ = 1.12 (s, 3H, CH₃), 3.40 (d, 1H, *J* = 4.5 Hz, 3-OH), 3.55 (d, 1H, *J* = 7.5 Hz, H-2), 3.59-3.70 (m, 4 H, H-3, H-5, H-6, H-6’), 3.85 (d, 1H, *J* = 3.5 Hz, H-4), 4.33 (d, 1H, *J*=7.5 Hz, H-1), 4.43-4.50 (m, 6H, PhCH₂), 7.20-7.40 (m, 15H, Ph).

Methyl 2,4,6-tri-*O*-benzyl-3-*O*-[(methylthio)thiocarbonyl]- β -D-galactopyranoside

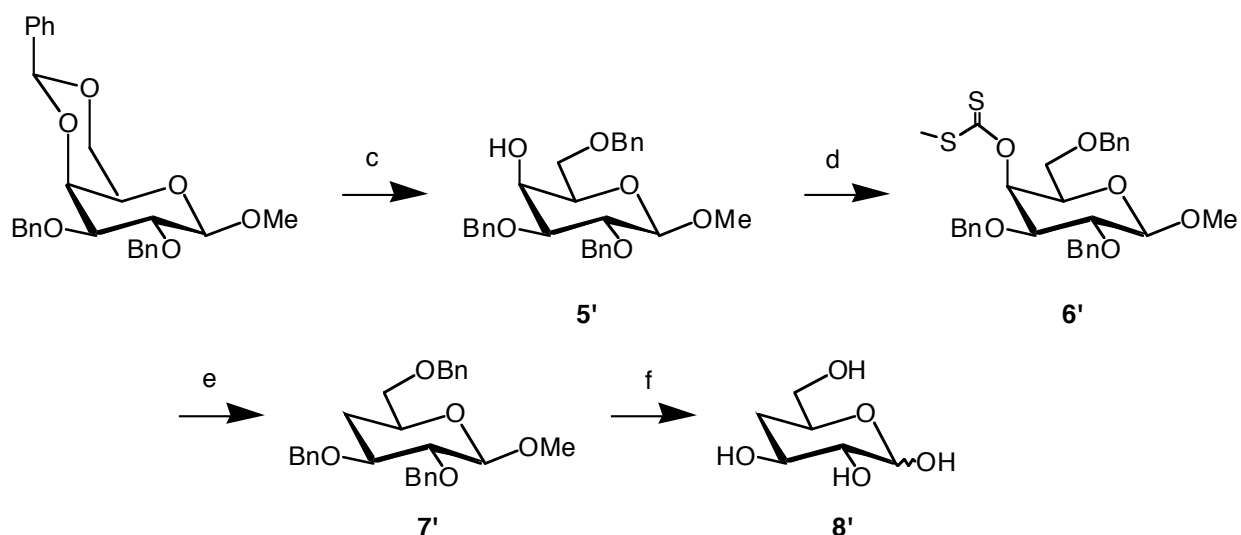
(2'): Sodium hydride, 60% dispersion in oil, (88 mg, 2.1 mmol) and imidazole (5.0 mg, 0.07 mmol) were added to a solution of **1'** dissolved in THF (5 mL) and this solution stirred for 1 h. After this time, CS₂ (450 μ L, 0.07 mmol) was added and the solution stirred for an additional hour. MeI (130 μ L, 0.02 mmol) was subsequently added, and the reaction mixture was stirred for 12 h. The solvent was evaporated *in vacuo*, and the resulting residue was subjected to SiO₂ column chromatography (5:1 hexanes / EtOAc) to yield 234 mg of an oil (58%). ¹H-NMR (300 MHz, CDCl₃): δ = 1.12 (s, 3H, CH₃), 2.54 (s, 3H, SCH₃) 3.55-3.58 (m, 2H, H-6, H-6'), 3.68-3.71 (m, 1H, H-5), 3.95-4.01 (m, 1H, H-2), 4.18 (d, 1H, *J* = 3.0 Hz, H-4), 4.43-4.50 (m, 3H, PhCH₂, H-1), 4.65-4.71 (m, 4H, PhCH₂), 5.75 (d, 1H, *J* = 3.0 Hz, H-3), 7.20-7.45 (m, 15H, Ph). ¹H-NMR (300 MHz, CDCl₃) in the literature:⁵ δ = 1.12 (s, 3H, CH₃), 2.54 (s, 3H, SCH₃) 3.55-3.60 (m, 2H, H-6, H-6'), 3.68-3.73 (m, 1H, H-5), 3.95-4.00 (m, 1H, H-2), 4.18 (d, 1H, *J* = 3.0 Hz, H-4), 4.43-4.50 (m, 3H, PhCH₂, H-1), 4.65-4.71 (m, 4H, PhCH₂), 5.75 (d, 1H, *J* = 3.0 Hz, H-3), 7.20-7.45 (m, 15H, Ph).

Methyl 2,4,6-tri-*O*-benzyl-3-deoxy- β -D-galactopyranoside (3')

To a solution of **2'** (230 mg, 0.42 mmol) in toluene was added tributylstannane (0.37 mL, 1.2 mmol) followed by AIBN (51 mg, 0.31 mmol). This solution was refluxed for 1 h, evaporated *in vacuo*, then purified by SiO₂ column chromatography (10:1 hexanes / EtOAc) to afford 75 mg of an oil (40%). ¹H-NMR (300 MHz, CDCl₃): δ = 1.12 (s, 3H, CH₃), 1.46 (ddd, 1H, *J* = 14.5 Hz, *J* = 2.4 Hz, H-3') 2.36 (ddd, 1H, *J* = 14.5 Hz, *J* = 4.0 Hz, H-3), 3.62-3.68 (m, 5H, H-2, H-4, H-5, H-6, H-6'), 4.36 (d, 1H, *J* = 11.0 Hz, PhCH₂), 4.38 (d, 1H, *J*

= 8 Hz, H-1), 4.65-4.70 (m, 5H, PhCH₂), 7.20-7.45 (m, 15H, Ph). ¹H-NMR (300 MHz, CDCl₃) in the literature:⁶ ¹H-NMR (300 MHz, CDCl₃): δ = 1.12 (s, 3H, CH₃), 1.46 (ddd, 1H, *J* = 14.5 Hz, *J* = 2.4 Hz, H-3') 2.36 (ddd, 1H, *J* = 14.5 Hz, *J* = 4.0 Hz, H-3), 3.60-3.70 (m, 5H, H-2, H-4, H-5, H-6, H-6'), 4.36 (d, 1H, *J* = 11.0 Hz, PhCH₂), 4.38 (d, 1H, *J* = 8 Hz, H-1), 4.65-4.70 (m, 5H, PhCH₂), 7.20-7.45 (m, 15H, Ph).

3-Deoxy-D-galactose (4'): A solution of **3'** (40 mg, 0.09 mmol), Pd(OH)₂/C (40 mg), CH₂Cl₂ (1 mL) and MeOH (4 mL) was stirred at rt under a H₂ atmosphere for 12 h. The mixture was filtered through Celite, evaporated, and then the 12 h reaction and filtration steps were repeated to afford methyl-3-deoxy-β-D-galactoside. The galactoside was then re-dissolved in water (20 mL), Dowex 50X-8 was added to the aqueous suspension, and the reaction mixture was left to reflux for 12 h. After this time, the mixture was filtered, and the filtrate was lyophilized to yield 7.0 mg (50%) of a fluffy amorphous solid. Selected ¹H-NMR (300 MHz, D₂O): δ = 4.55 (d, 1H, *J* = 8.0 Hz, H-1 β-pyranose), 5.18 (d, 2H, *J* = 4.0 Hz, H-1 of α-pyranose and β-furanose), 5.25 (d, 1H, *J* = 1.0 Hz, H-1 of β-furanose) ¹H-NMR (250 MHz, D₂O) in the literature:⁷ δ = 4.55 (d, 1H, *J* = 8.0 Hz, H-1 β-pyranose), 5.18 (d, 2H, *J* = 4.0 Hz, H-1 of α-pyranose and β-furanose), 5.25 (d, 1H, *J* = 1.0 Hz, H-1 of β-furanose).

Scheme A1.2 Synthesis of 4-deoxy-D-galactose.

“Conditions: (a) PhCHO, CH₂Cl₂, ZnCl₂ (65%) (b) DMF, benzyl bromide, NaH (quant.) (c) NaCNBH₃, methyl orange indicator, ethereal HCl, 3 Å MS (75%) (d) THF, NaH, imidazole, CS₂, MeI (83%) (e) toluene, tributylstanane, AIBN (60%) (f) *i.* H₂, Pd(OH)₂/C, CH₂Cl₂, MeOH *ii.* H₂O, H⁺ (80%).

Methyl 2,3,6-tri-O-benzyl-4-deoxy-β-D-galactopyranoside (5'): NaCNBH₃ (265 mg, 4.00 mmol) and methyl orange indicator were added to methyl 2,3-di-O-benzyl-4,6-O-benzylidene-β-D-galactopyranoside (180 mg, 0.40 mmol) dissolved in THF (3.0 mL) containing 3 Å molecular sieves (100 mg). The reaction mixture was cooled to 0 °C and ethereal HCl (~ 1.5 mL of a 1M diethyl ether solution) was added until a red color persisted. The reaction was left to stir rt for 2 days. At that point, the mixture was

quenched with NaHCO₃, diluted with CH₂Cl₂ (100 mL) and washed with water (20 mL) and brine (20 mL). The organic layer was then dried, filtered, evaporated and purified by SiO₂ column chromatography (4:1 hexanes / EtOAc) to afford 130 mg (75 %) of a white solid. ¹H-NMR (300 MHz, CDCl₃): δ = 1.12 (s, 3H, CH₃), 2.45 (d, 1H, *J* = 2.0 Hz, 4-OH), 3.55-3.57 (m, 2 H, H-2, H-5), 3.59 (d, 1 H, *J* = 7.1 Hz, H-3), 3.70 (d, 1H, *J* = 10 Hz, H-6), 3.79 (d, 1H, *J* = 10 Hz, H-6'), 3.99 (d, 1H, *J*=2.0 Hz, H-4), 4.21 (d, 1H, *J* = 8.0 Hz, H-1), 4.43-4.50 (m, 6H, PhCH₂), 7.20-7.40 (m, 15H, Ph). ¹H-NMR (300 MHz, CDCl₃) in the literature:⁸ δ = 1.12 (s, 3H, CH₃), 2.45 (d, 1H, *J* = 2.0 Hz, 4-OH), 3.55-3.57 (m, 2 H, H-2, H-5), 3.59 (d, 1 H, *J* = 7.1 Hz, H-3), 3.70 (d, 1H, *J* = 10 Hz, H-6), 3.79 (d, 1H, *J* = 10 Hz, H-6'), 3.99 (d, 1H, *J*=2.0 Hz, H-4), 4.21 (d, 1H, *J* = 8.0 Hz, H-1), 4.43-4.50 (m, 6H, PhCH₂), 7.20-7.40 (m, 15H, Ph).

Methyl 2,3,6-tri-*O*-benzyl-4-*O*-[(methylthio)thiocarbonyl]-β-*D*-galactopyranoside (6'): Sodium hydride, 60% dispersion in oil, (88 mg, 2.1 mmol) and imidazole (5.0 mg, 0.07 mmol) were added to a solution of **5'** dissolved in THF (5 mL) and this solution stirred for 1 h. After this time, CS₂ (450 μL, 0.07 mmol) was added and the solution stirred for an additional hour. MeI (130 μL, 0.02 mmol) was subsequently added, and the reaction mixture was stirred for 12 h. The solvent was evaporated *in vacuo*, and the resulting residue was subjected to SiO₂ column chromatography (5:1 hexanes / EtOAc) to yield 334 mg of an oil (83%). ¹H-NMR (300 MHz, CDCl₃): δ = 1.12 (s, 3H, CH₃), 2.58 (s, 3H, SCH₃), 3.53-3.57 (m, 4H, H-2, H-3, H-6, H-6'), 3.76-3.82 (m, 1H, H-5), 4.35 (d, 1H, *J* = 7.5 Hz, H-1), 6.48 (d, 1H, *J*= 3.0 Hz, H-4), 4.43-4.44 (m, 2H, PhCH₂), 4.65-4.72 (m, 4H, PhCH₂), 7.20-7.45 (m, 15H, Ph). ¹H-NMR (300 MHz, CDCl₃) in the literature:⁵

$\delta = 1.12$ (s, 3H, CH₃), 2.58 (s, 3H, SCH₃), 3.53-3.60 (m, 4H, H-2, H-3, H-6, H-6'), 3.76-3.85 (m, 1H, H-5), 4.35 (d, 1H, $J = 7.5$ Hz, H-1), 6.48 (d, 1H, $J = 3.0$ Hz, H-4), 4.43-4.45 (m, 2H, PhCH₂), 4.65-4.72 (m, 4H, PhCH₂), 7.20-7.45 (m, 15H, Ph).

Methyl 2,3,6-tri-*O*-benzyl-4-deoxy- β -D-galactopyranoside (7'): To a solution of **6'** (230 mg, 0.42 mmol) in toluene was added tributylstannane (0.37 mL, 1.2 mmol) followed by AIBN (51 mg, 0.31 mmol). This solution was refluxed for 1 h, evaporated *in vacuo*, then purified by SiO₂ column chromatography (10:1 hexanes / EtOAc) to afford 112 mg of an oil (60%). ¹H-NMR (300 MHz, CDCl₃): $\delta = 1.12$ (s, 3H, CH₃), 1.43 (t, 1H, $J = 13.0$ Hz, H-4') 2.12 (t, 1H, $J = 13.0$ Hz, H-4), 3.68-3.72 (m, 5H, H-2, H-3, H-5, H-6, H-6'), 4.21 (d, 1H, $J = 8.0$ Hz, H-1), 4.53 (d, 1H, $J = 11.0$ Hz, PhCH₂), 4.65-4.70 (m, 5H, PhCH₂), 7.20-7.45 (m, 15H, Ph). ¹H-NMR (300 MHz, CDCl₃) in the literature:^{6, 9} $\delta = 1.12$ (s, 3H, CH₃), 1.43 (t, 1H, $J = 13.0$ Hz, H-4') 2.12 (t, 1H, $J = 13.0$ Hz, H-4), 3.68-3.72 (m, 5H, H-2, H-3, H-5, H-6, H-6'), 4.21 (d, 1H, $J = 8.0$ Hz, H-1), 4.53 (d, 1H, $J = 11.0$ Hz, PhCH₂), 4.65-4.70 (m, 5H, PhCH₂), 7.20-7.45 (m, 15H, Ph).

4-Deoxy-D-galactose (8'): A solution of **7'** (40 mg, 0.09 mmol), Pd(OH)₂/C (40 mg), CH₂Cl₂ (1 mL) and MeOH (4 mL) was stirred at rt under a H₂ atmosphere for 12 h. The mixture was filtered through Celite, evaporated, and then the 12 h reaction and filtration steps were repeated to afford methyl-3-deoxy- β -D-galactoside. The galactoside was then re-dissolved in water (20 mL), Dowex 50X-8 was added to the aqueous suspension, and the reaction mixture was left to reflux for 12 h. After this time, the mixture was filtered, and the filtrate was lyophilized to yield 11 mg (80%) of a fluffy amorphous solid.

Selected $^1\text{H-NMR}$ (300 MHz, D_2O): $\delta = 3.49\text{-}3.54$ (m, 3H, α -pyranose, α -/ β -furanose), 4.57 (d, 1H, $J = 7.2$ Hz, H-1 β -pyranose). $^1\text{H-NMR}$ (250 MHz, D_2O) in the literature:¹⁰⁻¹² $\delta = 3.49\text{-}3.55$ (m, 3H, α -pyranose, α -/ β -furanose), 4.57 (d, 1H, $J = 7.2$ Hz, H-1 β -pyranose).

Transfection of Cortical Neurons and ^3H -Fucose Labeling

HeLa cells were maintained as described above. Cells were pretreated with 200 μCi of ^3H -Fucose (Sigma), then transfected with pcDNA 3.1 Synapsin Ia as described above. Cells were lysed in 1% boiling SDS and protein concentrations were determined with the BCA Assay (Pierce). Cortical neurons were prepared as described in Chapter 2. Neurons were grown on 100 mM dishes pre-coated with poly-DL-lysine (Sigma) which were cultured for either 2 DIV or 5 DIV, than treated with 15 mM 2-dGal or PBS + 200 μCi of ^3H -Fucose for 2 more days. Cell lysates were neutralized in NETFD and 1 mg of total lysate was immunoprecipitated with 5 μg of antibody G304. Immunoprecipitates were washed 3 \times 1% NP-40. Lysates and immunoprecipitates were split 10% for Western blotting and 90% for autoradiography, then resolved by SDS-PAGE and transferred to PVDF membranes for Western blotting. Membranes were immunoblotted as described in Chapter 2 with antibody A46-B/B10 or G304. For autoradiography, gels were immersed in Amplify (Amersham). And then dried on a Bio-Rad Gel Dryer. Gels were exposed to autoradiographic film (Amersham) for 2 days up to 3 weeks at -80°C .

Treatment of Neurons with Brefeldin A

Cortical neurons were prepared as described previously (Chapter 2) and cultured in 100 mm dishes coated with poly-DL-lysine. Neurons were cultured for 6 DIV then treated with 0.5 or 1 μ g Brefeldin A or a vehicle control for 1 DIV.

A1.9. References

1. Hilfiker, S.; Pieribone, V. A.; Czernik, A. J.; Kao, H. T.; Augustine, G. J.; Greengard, P., Synapsins as regulators of neurotransmitter release. *Phil. Tran. Royal Soc.* **1999**, 354, (1381), 269-279.
2. Ferreira, A.; Rapoport, M., The synapsins: beyond the regulation of neurotransmitter release. *Cell. Mol. Life Sci.* **2002**, 59, (4), 589-595.
3. Hosaka, M.; Sudhof, T. C., Synapsin III, a novel synapsin with an unusual regulation by Ca^{2+} . *J. Biol. Chem.* **1998**, 273, (22), 13371-13374.
4. Yang-Feng, T. L.; Degennaro, L. J.; Francke, U., Genes for synapsin-I, a neuronal phosphoprotein, map to conserved regions of human and murine X-chromosomes. *Proc. Natl. Acad. Sci. U.S.A.* **1986**, 83, (22), 8679-8683.
5. Kao, H. T.; Porton, B.; Czernik, A. J.; Feng, J.; Yiu, G.; Haring, M.; Benfenati, F.; Greengard, P., A third member of the synapsin gene family. *Proc. Natl. Acad. Sci. USA* **1998**, 95, (8), 4667-4672.
6. Kao, H. T.; Porton, B.; Hilfiker, S.; Stefani, G.; Pieribone, V. A.; DeSalle, R.; Greengard, P., Molecular evolution of the synapsin gene family. *J. Exp. Zool.* **1999**, 285, (4), 360-77.
7. Goelz, S. E.; Nestler, E. J.; Chehrazi, B.; Greengard, P., Distribution of protein-I in mammalian brain as determined by a detergent-based radioimmunoassay. *Proc. Natl. Acad. Sci. U.S.A.* **1981**, 78, (4), 2130-2134.
8. Ueda, T.; Greengard, P., Adenosine 3'-5'-monophosphate-regulated phosphoprotein system of neuronal membranes .1. Solubilization, purification, and some properties of an endogenous phosphoprotein. *J. Biol. Chem.* **1977**, 252, (14), 5155-5163.
9. Browning, M. D.; Huang, C. K.; Greengard, P., Similarities between protein-IIIa and protein-IIIb, 2 prominent synaptic vesicle-associated phosphoproteins. *J. Neurosci.* **1987**, 7, (3), 847-853.
10. Sudhof, T. C.; Czernik, A. J.; Kao, H.-T.; Takei, K.; Johnston, P. A.; Horiuchi, A.; Kanazir, S. D.; Wagner, M. A.; Perin, M. S.; de Camilli, P., Synapsins: mosaics of shared and individual domains in a family of synaptic vesicle phosphoproteins. *Science* **1989**, 245, (4925), 1474-1480.
11. DeCamilli, P.; Benfenati, F.; Valtorta, F.; Greengard, P., The Synapsins. *Ann. Rev. Cell Biol.* **1990**, 6, 433-460.
12. Hosaka, M.; Hammer, R. E.; Sudhof, T. C., A phospho-switch controls the dynamic association of synapsins with synaptic vesicles. *Neuron* **1999**, 24, (2), 377-387.
13. Esser, L.; Wang, C. R.; Hosaka, M.; Smagula, C. S.; Sudhof, T. C.; Deisenhofer, J., Synapsin I is structurally similar to ATP-utilizing enzymes. *EMBO J.* **1998**, 17, (4), 977-984.
14. Hosaka, M.; Sudhof, T. C., Homo- and heterodimerization of synapsins. *J. Biol. Chem.* **1999**, 274, (24), 16747-16753.
15. Chieriegatti, E.; Ceccaldi, P. E.; Benfenati, F.; Valtorta, F., Effects of synaptic vesicles on actin polymerization. *FEBS Lett.* **1996**, 398, (2-3), 211-216.

16. Ceccaldi, P. E.; Grohovaz, F.; Benfenati, F.; Chieriegatti, E.; Greengard, P.; Valtorta, F., Dephosphorylated synapsin-I anchors synaptic vesicles to actin cytoskeleton - an analysis by videomicroscopy. *J. Cell Biol.* **1995**, 128, (5), 905-912.
17. Goold, R.; Chan, K. M.; Baines, A. J., Coordinated regulation of synapsin-I interaction with F-actin by Ca²⁺ calmodulin and phosphorylation - inhibition of actin-binding and bundling. *Biochemistry* **1995**, 34, (6), 1912-1920.
18. Greengard, P.; Benfenati, F.; Valtorta, F., Synapsin-I, an actin-binding protein regulating synaptic vesicle traffic in the nerve-terminal. In *Molecular and Cellular Mechanisms of Neurotransmitter Release*, 1994; Vol. 29, pp 31-45.
19. Ceccaldi, P. E.; Benfenati, F.; Chieriegatti, E.; Greengard, P.; Valtorta, F., Rapid binding of synapsin-I to F-actin and G-actin - a study using fluorescence resonance energy-transfer. *FEBS Lett.* **1993**, 329, (3), 301-305.
20. Valtorta, F.; Greengard, P.; Fesce, R.; Chieriegatti, E.; Benfenati, F., Effects of the neuronal phosphoprotein synapsin-I on actin polymerization .1. Evidence for a phosphorylation-dependent nucleating effect. *J. Biol. Chem.* **1992**, 267, (16), 11281-11288.
21. Benfenati, F.; Valtorta, F.; Chieriegatti, E.; Greengard, P., Interaction of free and synaptic vesicle bound synapsin-I with F-actin. *Neuron* **1992**, 8, (2), 377-386.
22. Fdez, E.; Hilfiker, S., Vesicle pools and synapsins: New insights into old enigmas. *Brain Cell Biol.* **2006**, 35, (2-3), 107-115.
23. Lonart, G.; Simsek-Duran, F., Deletion of synapsins I and II genes alters the size of vesicular pools and rabphilin phosphorylation. *Brain Res.* **2006**, 1107, 42-51.
24. Cousin, M. A.; Malladi, C. S.; Tan, T. C.; Raymond, C. R.; Smillie, K. J.; Robinson, P. J., Synapsin I-associated phosphatidylinositol 3-kinase mediates synaptic vesicle delivery to the readily releasable pool. *J. Biol. Chem.* **2003**, 278, (31), 29065-29071.
25. Mozhayeva, M. G.; Sara, Y.; Liu, X. R.; Kavalali, E. T., Development of vesicle pools during maturation of hippocampal synapses. *J. Neurosci.* **2002**, 22, (3), 654-665.
26. Llinas, R.; McGuinness, T. L.; Leonard, C. S.; Sugimori, M.; Greengard, P., Intraterminal injection of synapsin-I or calcium calmodulin-dependent protein kinase-II alters neurotransmitter release at the squid giant synapse. *Proc. Natl. Acad. Sci. USA* **1985**, 82, (9), 3035-3039.
27. Pieribone, V. A.; Shupliakov, O.; Brodin, L.; Hilfiker-Rothenfluh, S.; Czernik, A. J.; Greengard, P., Distinct pools of synaptic vesicles in neurotransmitter release. *Nature* **1995**, 375, (6531), 493-497.
28. Greengard, P.; Valtorta, F.; Czernik, A. J.; Benfenati, F., Synaptic vesicle phosphoproteins and regulation of synaptic function. *Science* **1993**, 259, (5096), 780-785.
29. Oheim, M.; Kirchhoff, F.; Stuhmer, W., Calcium microdomains in regulated exocytosis. *Cell Calcium* **2006**, 40, (5-6), 423-439.
30. Kittel, R. J.; Hallermann, S.; Thomsen, S.; Wichmann, C.; Sigrist, S. J.; Heckmann, M., Active zone assembly and synaptic release. *Biochem. Soc. Trans.* **2006**, 34, 939-941.

31. Felix, R., Molecular regulation of voltage-gated Ca²⁺ channels. *J. Recep. Signal Transduc.* **2005**, 25, (2), 57-71.
32. Heuser, J. E.; Reese, T. S., Evidence for recycling of synaptic vesicle membrane during transmitter release at frog neuromuscular junction. *J. Cell Biol.* **1973**, 57, (2), 315-344.
33. Harada, A.; Sobue, K.; Hirokawa, N., Developmental-changes of synapsin-I subcellular-localization in rat cerebellar neurons. *Cell Struct. Funct.* **1990**, 15, (6), 329-342.
34. Ferreira, A.; Kosik, K. S.; Greengard, P.; Han, H. Q., Aberrant neurites and synaptic vesicle protein-deficiency in synapsin II-depleted neurons. *Science* **1994**, 264, (5161), 977-979.
35. Ferreira A, K. H., Feng J, Rapoport M, Greengard P, Synapsin III: developmental expression, subcellular localization, and role in axon formation. *J. Neurosci.* **2000**, 20, (10), 3736-44.
36. Fletcher, T. L.; Cameron, P.; Decamilli, P.; Banker, G., The Distribution of synapsin-I and synaptophysin in hippocampal-neurons developing in culture. *J. Neurosci.* **1991**, 11, (6), 1617-1626.
37. Chin, L. S.; Li, L.; Ferreira, A.; Kosik, K. S.; Greengard, P., Impairment of axonal development and of synaptogenesis in hippocampal-neurons of synapsin I-deficient mice. *Proc. Natl. Acad. Sci. USA* **1995**, 92, (20), 9230-9234.
38. Ferreira, A.; Chin, L. S.; Li, L.; Lanier, L. M.; Kosik, K. S.; Greengard, P., Distinct roles of synapsin I and synapsin II during neuronal development. *Molecular Med.* **1998**, 4, (1), 22-28.
39. Ferreira, A.; Kao, H. T.; Feng, J.; Rapoport, M.; Greengard, P., Synapsin III: Developmental expression, subcellular localization, and role in axon formation. *J. Neurosci.* **2000**, 20, (10), 3736-3744.
40. Murrey, H. E.; Gama, C. I.; Kalovidouris, S. A.; Luo, W. I.; Driggers, E. M.; Porton, B.; Hsieh-Wilson, L. C., Protein fucosylation regulates synapsin Ia/lb expression and neuronal morphology in primary hippocampal neurons. *Proc. Natl. Acad. Sci. USA* **2006**, 103, (1), 21-26.
41. Robbe, C.; Capon, C.; Coddeville, B.; Michalski, J. C., Diagnostic ions for the rapid analysis by nano-electrospray ionization quadrupole time-of-flight mass spectrometry of O-glycans from human mucins. *Rapid Commun. Mass Spectrom.* **2004**, 18, (4), 412-420.
42. Kogelberg, H.; Piskarev, V. E.; Zhang, Y. B.; Lawson, A. M.; Chai, W. G., Determination by electrospray mass spectrometry and H-1-NMR spectroscopy of primary structures of variously fucosylated neutral oligosaccharides based on the iso-lacto-N-octaoase core. *Eur. J. Biochem.* **2004**, 271, (6), 1172-1186.
43. Mattu, T. S.; Royle, L.; Langridge, J.; Wormald, M. R.; Van den Steen, P. E.; Van Damme, J.; Opdenakker, G.; Harvey, D. J.; Dwek, R. A.; Rudd, P. M., O-glycan analysis of natural human neutrophil gelatinase B using a combination of normal phase- HPLC and online tandem mass spectrometry: Implications for the domain organization of the enzyme. *Biochemistry* **2000**, 39, (51), 15695-15704.
44. Bullock, S.; Potter, J.; Rose, S. P. R., Effects of the Amnesic Agent 2-Deoxygalactose on Incorporation of Fucose into Chick Brain Glycoproteins. *J. Neurochem.* **1990**, 54, (1), 135-142.

45. Jork, R.; Schnurra, I.; Smalla, K. H.; Greksch, G.; Popov, N.; Matthies, H., Deoxy-galactose mediated amnesia Is related to an inhibition of training-induced increase in rat hippocampal glycoprotein fucosylation. *Neurosci. Res. Commun.* **1989**, 5, (1), 3-8.
46. Holden, H., M.; Rayment, I.; Thoden, J. B., Structure and function of enzymes of the Leloir pathway for galactose metabolism. *J. Biol. Chem.* **2003**, 278, (45), 43885-43888.
47. Yang, J.; Fu, X.; Jia, Q.; Shen, J.; Biggins, J. B.; Jiang, J.; Zhao, J.; Schmidt, J. J.; Wang, P. G.; Thorson, J. S., Studies on the substrate specificity of *Escherichia coli* galactokinase. *Org. Lett.* **2003**, 5, (13), 2223-2226.
48. Hoffmeister, D.; Yang, J.; Liu, L.; Thorson, J. S., Creation of the first anomeric D/L-Sugar kinase by means of directed evolution. *Proc. Natl. Acad. Sci. USA* **2003**, 100, (23), 13184-13189.
49. Timson, D. J.; Reece, R. J., Sugar recognition by human galactokinase. *BMC Biochem.* **2003**, 4, (1), 16-22.
50. Lowary, T. L.; Hindsgaul, O., Recognition Of synthetic deoxy and deoxyfluoro analogs of the acceptor alpha-L-Fucp-(1-]2)-Beta-D-Galp-or by the blood-group-A and blood-group-B gene-specified glycosyltransferases. *Carbohydr. Res.* **1993**, 249, (1), 163-195.
51. Larsen, R. D.; Ernst, L. K.; Nair, R. P.; Lowe, J. B., Molecular-Cloning, Sequence, and Expression of a Human Gdp-L-Fucose - Beta-D-Galactoside 2-alpha-L-fucosyl-transferase cDNA that can form the H-blood group antigen. *Proc. Natl. Acad. Sci. USA* **1990**, 87, (17), 6674-6678.
52. Qian, X. P.; Sujino, K.; Palcic, M. M.; Ratcliffe, R. M., Glycosyltransferases in oligosaccharide synthesis (Reprinted from *Glycochemistry: Principles, Synthesis, and Applications*, pg 535-565, 2001). *J. Carb. Chem.* **2002**, 21, (7-9), 911-942.
53. Gitler, D.; Xu, Y. M.; Kao, H. T.; Lin, D. Y.; Lim, S. M.; Feng, J.; Greengard, P.; Augustine, G. J., Molecular determinants of synapsin targeting to presynaptic terminals. *J. Neurosci.* **2004**, 24, (14), 3711-3720.

Appendix 2

Early Efforts for Identification of the Fuc α (1-2)Gal Glycoproteome

A2.1. Background

Identification of Fuc α (1-2)Gal glycoproteins has been technically challenging due to their low abundance in neuronal tissues and the difficulty of isolation by antibody and lectin affinity chromatography. Here we report our early efforts to identify the Fuc α (1-2)Gal proteome using an antibody affinity column with antibody A46-B/B10. This monoclonal antibody has been shown to be highly specific in binding the blood group H type II and type IV trisaccharides (Fuc α (1-2)Gal β (1-4)GlcNAc and Fuc α (1-2) β (1-3)GalNAc respectively).(1) This antibody interferes with a brightness discrimination task in rats when intrahippocampally injected pre- and post-training. The animals have less retention for the learning paradigm and exhibit amnesia for the event, suggesting that the Fuc α (1-2)Gal epitope is important for the underlying molecular mechanisms of memory formation in mammals.(2)

We tried multiple approaches to identify and purify Fuc α (1-2)Gal glycoproteins such as 1D and 2D-gel electrophoresis. Our studies were hampered by the low binding affinity of the antibody to Fuc α (1-2)Gal disaccharides, and our attempts to identify the proteome led to the isolation of mostly cytosolic proteins. We next employed lectin affinity chromatography using the *Lotus tetragonobolus* lectin (LTL) and were able to isolate cytosolic proteins such as CRMP-2 and Rab-GDI, however, we were never able to confirm the presence of a Fuc α (1-2)Gal moiety on either protein. We developed a successful method for the isolation of Fuc α (1-2)Gal glycoproteins using UEAI lectin

affinity chromatography. Through this approach, we identify tenascin C as a prominent Fuc α (1-2)Gal glycoprotein present in rat cortex and confirm its fucosylation by immunoprecipitation experiments. In addition we find the neural cell adhesion molecule NCAM, the Na⁺/K⁺ ATPase, and multiple heterogeneous ribonucleoproteins.

A2.2. Results

A2.3. Preliminary Attempts to Identify the Fuc α (1-2)Gal Proteome by Antibody A46-B/B10 Enrichment and Lectin Affinity Chromatography

To identify Fuc α (1-2)Gal glycoproteins from the brain, we first sought to use antibody A46-B/B10 which has previously been shown to recognize physiologically relevant epitopes.(2, 3) Antibody A46-B/B10 was covalently cross-linked with dimethylpimelimidate to protein A-sepharose beads. Coupling efficiency was monitored by dot blot analysis. After the column was created, embryonic rat forebrain lysates were fractionated by standard procedures and purified over the anti-Fuc α (1-2)Gal column. A test of different wash conditions suggests that TBST works best to wash away non-specific proteins as opposed to lysis buffer, and we observed the enrichment of many Fuc α (1-2)Gal glycoproteins in column eluates as detected by Western blotting with antibody A46-B/B10 (Figure A2.1, A and B). In particular, we observe enrichment of bands at approximately 200, 180, 120, 105, 75, 55, 40, and 35 kDa from TBST washed columns. We next attempted to isolate and identify proteins from the antibody column by running a Coomassie-stained gel in parallel with the Western blot using antibody A46-B/B10 and overlaying the images. While bands were still present in the fourth wash as indicated by Coomassie staining, further washing of the columns led to loss of

enrichment of fucosylated bands, thus we maintained these mild wash conditions in hopes that we could still identify putative Fuc α (1-2)Gal glycoproteins. However, eluate lanes from Coomassie-stained gels contained the same enriched bands that were in the wash (Figure A2.1 C), suggesting that Fuc α (1-2)Gal enriched bands were too weak to be detected by Coomassie staining. Despite this issue, we attempted to isolate proteins from bands of interest that overlaid with the Western blot in hopes that we could detect them by mass spectrometry. These bands were excised from the Coomassie-stained gel, even if no protein was detected, digested with trypsin, and subjected to MALDI-TOF analysis. The peptides were searched against the nonredundant NCBI protein database. Through this method, we identified pyruvate kinase, the heterogeneous ribonucleoprotein (hnRNP), phosphoenolpyruvate carboxylase (PEPCase), the protein kinase Raf 1, heat shock protein 70, and a mannosidase. We were surprised to isolate mostly cytosolic proteins, suggesting that this methodology was not working properly, and Fuc α (1-2)Gal glycoproteins are not enriched in sufficient quantities for MALDI-TOF analysis.

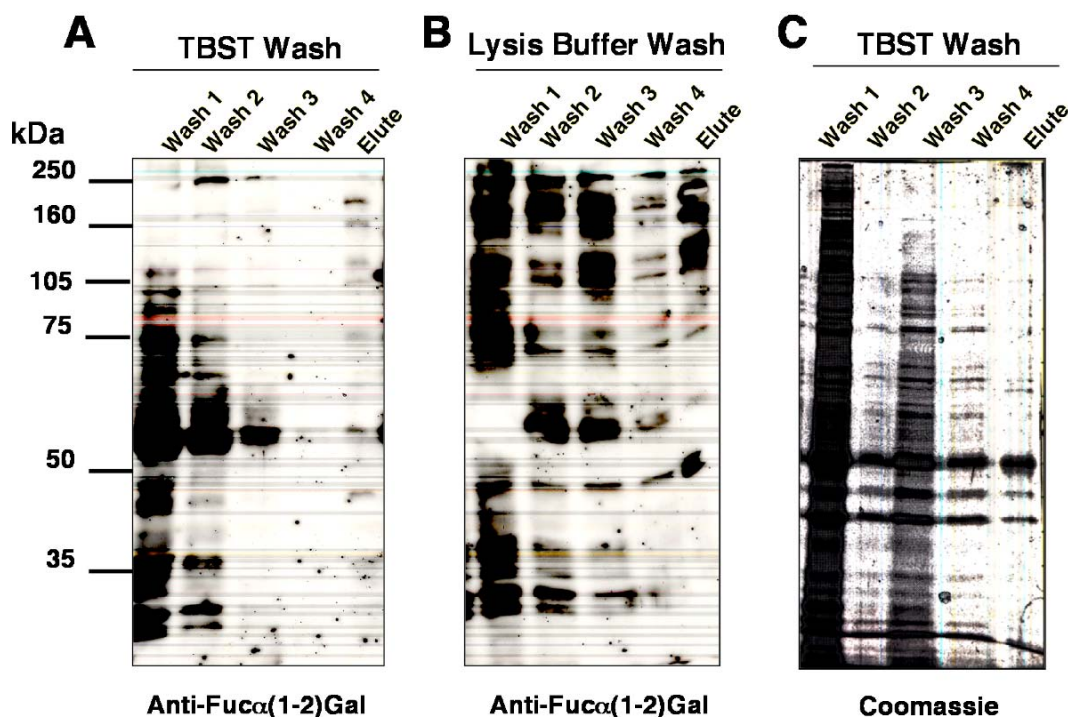


Figure A2.1. Optimization of antibody A46-B/B10 affinity column wash conditions. Western blot using antibody A46-B/B10 of wash conditions with TBST (A), or Lysis buffer wash (B). Coomassie stain of TBST wash conditions (C). Washes 1-4 are 10% (100 μ L) of the total wash and are from sequential washes collected. The elution is 20% of the total eluate from the antibody column in (A) and (B), and 80% in (C).

We next attempted to run 2D gel electrophoresis in an attempt to better separate the proteins for MALDI-TOF analysis. However, we were never able to purify enough Fuc α (1-2)Gal glycoproteins to detect them on the Coomassie-stained gels nor by silver stain. We also tried lysates before purification. Here, we were able to detect more proteins and overlaid the gels with a western using antibody A46-B/B10 to excise bands of interest (Figure A2.2). Again, we saw similar proteins in the MALDI-TOF analysis, suggesting that this methodology was not working properly either.

Joshua Klein, a rotation student in the laboratory, exploited the use of a known fucose-binding lectin LTL, to run in parallel with the antibody A46-B/B10 column.

Column eluates were immunoblotted with antibody A46-B/B10 and he isolated a larger number of proteins from the LTL column, suggesting that this route was more desirable

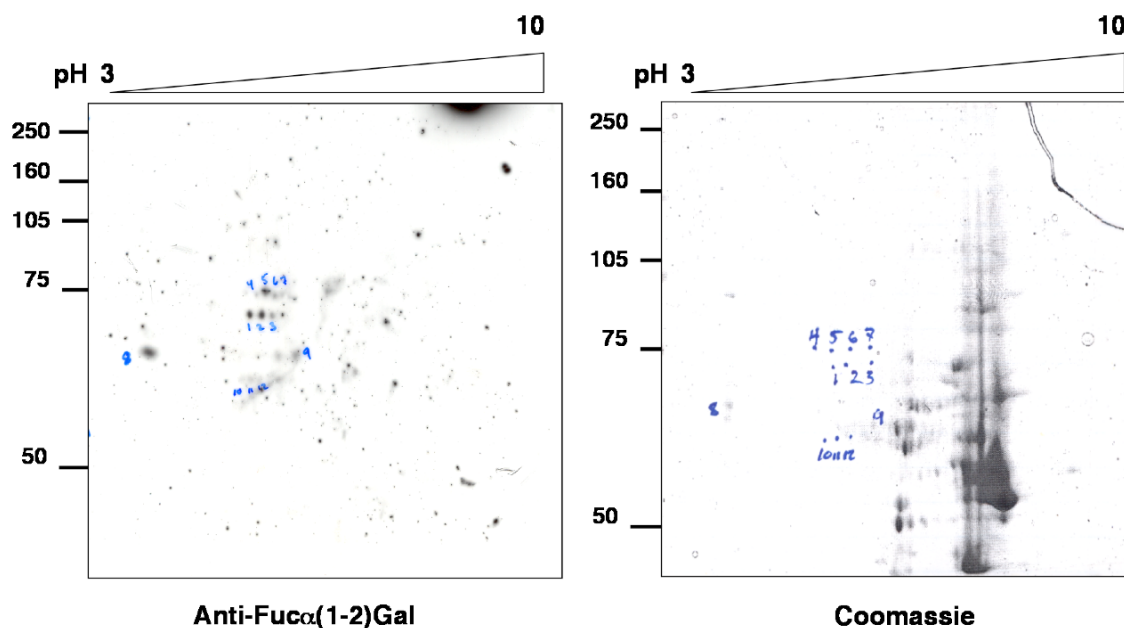


Figure A2.2. 2-Dimensional gel electrophoresis of embryonic rat forebrain lysates. Immunoblotted with antibody A46-B/B10 (left panel) or stained with Coomassie (right panel). Bands excised are indicated above for samples 1-12.

to isolate to Fuc α (1-2)Gal glycoproteins (data not shown). However, many of the proteins eluted from the LTL column were not specifically detected by antibody A46-B/B10, which may suggest the isolation of fucosylated glycoconjugates with other linkages. He was able to isolate a number of proteins including pyruvate kinase, the collapsin-response mediator protein CRMP-2, and Rab-guanine dissociation inhibitor (Rab-GDI). We next tried to confirm some of these proteins by immunoprecipitation studies. CRMP-2, which is 64 kDa protein involved in neuronal development, growth cone collapse and generating neuronal polarity,(4-6) was immunoprecipitated from embryonic rat forebrain, however we were not able to detect fucose in the

immunoprecipitate lane, suggesting that this protein is non-specifically present in the sample (data not shown). We next examined whether we could detect fucose on Rab-GDI, a protein involved in vesicular transport.(7, 8) We immunoprecipitated Rab-GDI from h embryonic and adult rat forebrain. Analysis of the results suggests that Rab-GDI may be glycosylated (data not shown). The bands run very similar, but are too close the antibody band at 50 kDa to be conclusive and the molecular weights are slightly shifted, suggesting that the protein is most likely not fucosylated. Since we had some success with the LTL column in purifying Fuc α (1-2)Gal glycoproteins, we next made attempts to develop a procedure to isolate these glycoproteins with UEAI lectin. UEAI is highly specific for interaction with terminal Fuc α (1-2)Gal disaccharides on glycoconjugates. While LTL also binds fucose, this lectin can be promiscuous in recognizing fucose present in other linkages. Therefore, we developed a novel protocol using UEAI lectin and proteins purified from rat forebrain (containing the cortex, hippocampus, and striatum). Through much experimentation, we developed and optimized a binding protocol specific for UEAI lectin. In addition, we found that protein lysates bound better at room temperature incubations, rather than the standard 4 °C incubation, thus enhancing our capture of Fuc α (1-2)Gal glycoproteins. We also moved towards using LC/MS instead of MALDI-TOP analysis to better separate the peptides in each sample and to enhance sensitivity. We observed that the quantity of glycoproteins eluted from a 100 μ L column was too small to detect by MS analysis when eluted with α -L-fucose. Therefore, we scaled up our columns and created a larger 1 mL lectin column to capture more Fuc α (1-2)Gal glycoproteins. In addition, we concentrated the 10 mL elution down to 100 μ L, so that we could load all proteins isolated onto one lane of an SDS-PAGE gel.

Using this approach, we were successfully able to detect proteins specifically eluted from UEA1 columns. In addition, we used a protein-A-agarose column as a control to detect non-specific binding (data not shown). We did observe a number of proteins bound in

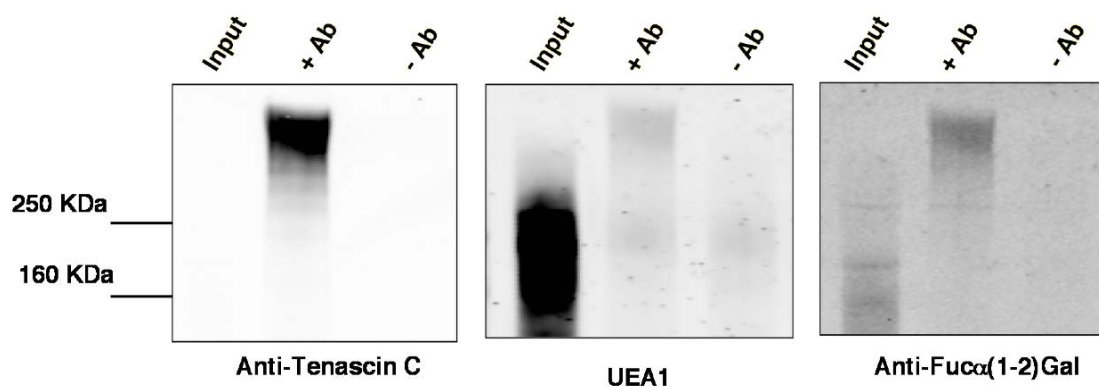


Figure A2.3. Immunoprecipitation confirms that tenascin C is a Fuc α (1-2)Gal glycoprotein. Adult rat forebrain was immunoprecipitated with anti-tenascin C (lanes 2) or no antibody (control, lanes 3) and resolved by SDS-PAGE followed by immunoblotting with anti-tenascin C (left panel) UEA1 (middle panel) or antibody A46-B/B10 (right panel). The input is 10% (100 μ g) of the total IP. 20% of the eluted was loaded for the anti-tenascin C blot, and 40% each was loaded for the UEA1 and antibody A46-B/B10 blots.

the control columns, confirming the importance of using a control. We next excised 22 bands from each lane of the silver-stained gel, and subjected them to LC-MS/MS for identification in collaboration with Dr. Scott Ficarro and Dr. Eric Peters at the Genomics Institute of the Novartis Foundation (GNF). The data was searched against the NCBI non-redundant database, and each sample was analyzed in Bioworks. We were able to isolate a number of proteins from each sample. Any protein identified in the control column was considered non-specific (Table A2.1). We identified a number of proteins including tenascin C, NCAM, the Na⁺/K⁺ ATPase and a number of heterogeneous ribonucleoproteins. Our biggest hit was for the proteins tenascin C. Tenascin C is an extracellular matrix protein involved in central synaptic differentiation.(9) We next

confirmed the presence of tenascin C as a Fuc α (1-2)Gal glycoprotein by immunoprecipitation from rat cortex. We were able to specifically detect fucosylation of tenascin C with both antibody A46-B/B10 and UEA1 lectin, further suggesting that tenascin C is a Fuc α (1-2)Gal glycoprotein (Figure A2.3). However, despite our identification of tenascin C, we still identified a lot of soluble cytosolic proteins in the proteome, which either suggests that a lot of Fuc α (1-2)Gal glycoproteins exist in the cytosol contrary to previous findings, or that these proteins are non-specifically isolated in the UEA1 lectin column eluates. Due to the extensive difficulty we had in identification of the Fuc α (1-2)Gal proteome and potential isolation of non-specific proteins, we sought to development a new method to increase our signal-to-noise ration for identifying the Fuc α (1-2)Gal proteome.

MW Range	Protein	MW (predict)	Function
160+ KDa	Tenascin C	222 KDa	Extracellular matrix protein, cortical defects in KO
	Ubiquitin-protein ligase e3 component n-recognition	193 KDa	ubiquitin ligase (<i>Skp1</i>)
	DEAD/H box polypeptide 9	141 KDa	RNA helicase
	NCA2 NCAM	80 KDa	Cell adhesion molecule, neurite fasciculation, outgrowth
	NCA1 NCAM	94 KDa	Cell adhesion molecule, neurite fasciculation, outgrowth
30-160 KDa	Na+/K+ transporting ATPase	112 KDa	membrane polarization create electrochemical gradient neuro
	DEAD/H box polypeptide 9	141 KDa	RNA helicase
	Tenascin	222 KDa	Extracellular matrix protein, cortical defects in KO
	Splicing factor 3b, subunit 3 (130 Kda)	139 KDa	spliceosome
95-130 KDa	Na+/K+ transporting ATPase	112 KDa	membrane polarization create electrochemical gradient neuro
	hnRNP U	88 KDa	scaffold attachment factor A/RNA binding
	eukaryotic translation elongation factor 2	94 KDa	protein synthesizing machinery
	hnRNP R	70 KDa	complexes polyA-mRNA in neurons
80-95 KDa	doublecortin and CaM kinase-like I	80 KDa	kinase, regulates m-tube org.
	DCK1 ser/thr protein kinase	80 KDa	controls neuronal migration in developing brain
	spermatid perinuclear RNA-binding protein	71.3 KDa	KO has neurologic and sperm effects
	Gry-rbp	68.5 KDa	RNA-binding protein
	hn RNP R	70 KDa	complexes polyA-mRNA in neurons
	polyA-binding protein, cytoplasmic 1	70 KDa	mRNA stabilization
70-80 KDa	78 KD Glucose-Regulated Protein	71.8 KDa	ATP-binding, in ER
	DEAD/H box polypeptide 5	67.5 KDa	RNA helicase (ATP-binding), transcriptional co-activator
	hnRNP L	61.4 KDa	packaging/rprocessing RNA
	Siah binding protein 1	59.5 KDa	RNA metabolism
60-70 KDa	DEAD/H box polypeptide 5	67.5 KDa	RNA helicase (ATP-binding), transcriptional co-activator
	U2 small nuclear RNA auxiliary factor	52.3 KDa	RNA Splicing
	hnRNP ROK	50.9 KDa	polyC binding K protein
50-60 KDa	hnRNP H1	49.4 KDa	polyA-mRNA binding
35-50 KDa	neuronal pentraxin I precursor	47.3 KDa	similar to bp for snake venom toxin taipoxin
	hnRNP A1 beta	35.2 KDa	RNA helix destabilizing protein
	hnRNP A/B	31.4 KDa	Transcription regulator in developing brain
33-35 KDa	ROA2 hnRNP	38.8 KDa	pre-RNA processing
30-33 KDa	ROA2 heterogeneous nuclear ribonucleoprotein	38.8 KDa	pre-RNA processing
	B-cell Receptor-associated protein 37	32.8 KDa	modulates estrogen receptor
	protein kinase, protein activator interferon-inducible RNA	34.4 KDa	protein kinase regulates translation
25-30 KDa	Cleavage and Polyadenylation specific factor 5	24.9 KDa	3' RNA cleavage

Table A2.1 Summary of proteins identified by LC-MS/MS of rat cortical neuronal lysates listed by apparent molecular weights.

A2.4 Discussion

Identification of the $\text{Fuca}(1-2)\text{Gal}$ proteome has suffered from many complications that hinder the isolation of proteins for mass spectrometry. Low abundance of $\text{Fuca}(1-2)\text{Gal}$ glycoproteins and the low affinities of antibody- and lectin-carbohydrate interactions often precluded the ability to identify these proteins. We attempted to identify $\text{Fuca}(1-2)\text{Gal}$ glycoproteins by a variety of techniques, such as antibody affinity chromatography with antibody A46-B/B10, lectin affinity

chromatography with LTL and UEAI lectins, and 1D- and 2D-gel electrophoresis. The only method that yielded successful identification of Fuc α (1-2)Gal glycoproteins was the isolation of glycoproteins with UEAI lectin.

In adult forebrain, the most predominant Fuc α (1-2)Gal glycoprotein identified was the extracellular matrix glycoprotein tenascin C. Tenascin C is present during neuronal development and regulates wound healing and neural regeneration in adult tissues.(10) The tenascins interact with cell adhesion molecules, other Fuc α (1-2)Gal glycoproteins identified by our studies. An important role in nervous system development is the interaction between tenascins and CAMs. These interactions lead to neuronal outgrowth, migration, and pathfinding. Tenascin C knock-out mice display deficits in hippocampal synaptic plasticity.(11) and NCAM is involved in develop and plasticity of the nervous system,(12) which suggests an important role for fucosylated glycoproteins in the molecular events that may underlie synaptic remodeling and plasticity.

In addition to tenascin C, the largest class of proteins identified was the family of heterogeneous ribonucleoproteins (hnRNPs). These molecules are involved in the trafficking of mRNA between the nucleus and the cytosol. Interestingly, nuclear proteins associated with chromatin are reported to be fucosylated and are specifically recognized by UEAI lectin,(13) suggesting that this may represent a novel class of cytosolic Fuc α (1-2)Gal glycoproteins.

Furthermore, we identify the protein doublecortin, which is enriched in the leading process of growth cones in neurons. Defects in doublecortin lead to lissencephaly in humans, which is characterized by defects in neuronal migration that

lead to epilepsy and mental retardation.(14) Finally, we identify neuronal pentraxin I (NPI) as a putative Fuc α (1-2)Gal glycoprotein. NPI is reported to play a role in excitatory synapse remodeling.(15) It has also been shown to mediate neuronal death in the pathogenesis of Alzheimer's disease.(15) Cumulatively, these proteins suggest important roles for Fuc α (1-2)Gal glycoproteins in the molecular mechanisms that may underlie development and synaptic plasticity.

A2.5 Materials and Methods

Animals, Tissue Isolation and Homogenization

C57BL/6 wild-type animals and Sprague-Dawley rats were maintained in accordance with proper IACUC procedures. Adult male mice ages 3-4 months were anesthetized with CO₂ and dissected to remove the forebrain. For Western blotting, dissected tissues were cut into small pieces and placed immediately on ice, then lysed in boiling 1% SDS with sonication until homogeneous (5V:W). For lectin affinity chromatography, the adult rat forebrain was isolated and homogenized in lectin binding buffer (100 mM Tris pH 7.5/ 150 mM NaCl/ 1mM CaCl₂/ 1 mM MgCl₂/ 0.5% NP-40/ 0.2% Na deoxycholate plus protease inhibitors) by passing through a 26G needle 5 times, then sonicated to homogeneity. Samples were clarified by centrifugation at 12,000G x 10 min. Lysates were between 6 to 10 mg/mL total protein concentration as determined by the BCA protein assay (Pierce) for lectin affinity chromatography.

Creation of Antibody-A46-B/B10 Protein A-Sepharose Column

100 μ L of goat IgG anti- μ -specific IgM at 13.6 mg/mL (1.36 mg total IgG) was dialyzed into 100 mM NaHCO₃ pH 8.0 / 500 mM NaCl. Equilibrate protein A-sepharose beads (100 μ L beads) into dialysis buffer. Rotate beads plus goat IgG at 4 °C for 2 days. Spin down bead and wash 3 \times dialysis buffer. Buffer exchange Antibody A46-B/B10 IgM into 0.1 M borate buffer pH 8.2 (concentration 0.78 mg/mL). Wash protein A beads with 0.1 M borate buffer pH 8.2 3 \times 500 μ L. Resuspend in 20 volumes of 100 mM dimethylpimelimidate (Pierce) in 0.2 M triethanolamine and rotate at RT for 45 min. Quench reaction by centrifuging beads, removing supernatant, and resuspending in 100 μ L of 100 mM ethanolamine pH 8.2. Incubate 5 min with rotating at RT. Wash beads with 3 \times 500 μ L 0.1 M borate buffer pH 8.2. Store beads in 0.1 M borate buffer pH 8.2 / 0.02% NaN₃.

Purification of Fuca(1-2)Gal by the Antibody Column

Embryonic rat forebrain was homogenized in lysis buffer (50 mM Tris pH 8.2 / 150 mM NaCl / 0.2% Na deoxycholate / 1% NP-40) supplemented with protease inhibitors. The tissue was passed through a 26G needle 5 times, then sonicated on ice 8 x 5 s pulses. Tissue was spun at 12,000 \times G for 10 min and the supernatant was removed for experiments. Equilibrate goat IgG anti μ -specific IgM protein A-sepharose in lysis buffer. Bind proteins for 3 h in batch at 4 °C with rotating. Wash column with 4 CV of TBST. Elute proteins with 50 mM diethylamine pH 11.5 / 0.5% Na deoxycholate. Proteins were resolved by SDS-PAGE as described previously.(16)

2D Gel Electrophoresis

Embryonic forebrain was lysated in 1.25 × Urea buffer (1.3 × Urea/thiourea / 5% CHAPS ; 0.625% Ampholy resins pH 3-10 (Amersham). Homogenize through 22-G needle 10×, then sonicate on ice 5 × 5 s pulses. Pass through 22-G needle 5×. Spin at 15,000 × G for 10 min. Remove supernatant for 2D gel. Take 200 µL of protein lysate, and add 2 µL of 0.2% bromophenol blue / 10 µL of reducing agent (Amersham) / 38 µL of H₂O. Set up 2D gel using pH 3-10 strips (Amersham). Run isoelectric focusing overnight for ~22 h. Make 15 mL per isoelectric focusing strip of SDS equilibration buffer (50 mM 1.5 M Tris pH 8.8 / 6 M Urea / 30% glycerol / 0.001% bromophenol blue). Split solution in half and add 1% DTT to one half, and 2.5% iodoacetamide to the other half. Equilibrate isoelectric focusing strip in SDS equilibration buffer with DTT for 15 min at RT, followed by SDS equilibration buffer with iodoacetamide for 15 min at RT. After strips have equilibrated, run 10% SDS-PAGE by place strip on the top of the gel and seal with 0.5% low melting agarose in SDS running buffer. Run gels at 0.15 mA/gel until the solution enters the gel, then run at 30 mA per gel for ~ 5 h or until dye front reaches the bottom. Parallel equipments were run to stain one gel with Coomassie brilliant blue and the second gel was transferred for western blotting with antibody A46-B/B10.

Lectin Affinity Chromatography and SDS-PAGE

One mL bed volume of *Ulex europaeus* agglutinin I (UEAI) conjugated to agarose (Vector Labs,) and control Protein A conjugated to agarose (Vector Labs,) columns were packed ~333 µL into 3 minicolumns run in parallel (BioRad). The resin

was equilibrated with 10 column volumes (CV) lectin binding buffer. 3 mL of olfactory bulb lysate at 6-10 mg/mL was bound in batch at RT for 4 h. Columns were repacked and the flowthrough was passed 3 additional times over the column. Columns were washed with 40 CV of lectin binding buffer, followed by 10 CV of lectin binding buffer lacking detergent (NP-40 and Na deoxycholate). Proteins were eluted in 10 CV of lectin binding buffer lacking detergent supplemented with 200 mM α -L-Fuc and protease inhibitors.

Protein eluates were concentrated in 10,000 molecular weight cut-off (MWCO) centricons (Millipore) followed by 10,000 MWCO microcons (Millipore) to 100 μ L. Following concentration, samples were boiled with 35 μ L of 4 \times SDS loading dye and loaded onto 10% SDS gels for electrophoresis as described previously.(16)

Coomassie staining, Peptide Extraction, and In-Gel Tryptic Digests

Coomassie-stained gels were incubated in 300 mL of 1 g Coomassie brilliant blue/ 50% MeOH/ 10% HOAc for 1 h, then destained in the same solution without Coomassie brilliant blue with multiple changes until bands were visible. Peptide extraction and in-gel tryptic digests were as reported in Chapter 2.

LTQ LC-MS Analysis

Approximately 50% of gel extractions were loaded onto a 360 μ m O.D. \times 75 μ m precolumn packed with 4 cm of 5 μ m Monitor C18 particles (Column Engineering) as described previously.(17)

Immunoprecipitation

CRMP was immunoprecipitated from rat embryonic forebrain homogenized in 25 mM sodium phosphate, pH 6.0/ 10 mM 2-mercaptoethanol/ 10 mM tetrasodium pyrophosphate/ 1mM EGTA plus protease inhibitors (0.5 mM phenylmethylsulfonyl fluoride/ 1 μ g/mL leupeptin/ 1 μ g/mL pepstatin/ 1 μ g/mL antipain). Proteins were immunoprecipitated with 4 μ g of C4G antibody (courtesy of Ihara) at 4°C for two hours. 50 μ L of protein A sepharose was added and the immunoprecipitates incubated 4 °C for another two h. Immunoprecipitates were washed 3 \times 500 μ L lysis buffer, boiled in 1X SDS-PAGE loading dye and subjected to SDS-PAGE for blotting with C4G (1:2000) or antibody A46-B/B10 at 5 μ g/mL.

Rab GDI and tenascin C was homogenized in 1% SDS and neutralized with Neutralization buffer. Rab GDI was immunoprecipitated with 4 μ g of antibody (Synaptic Systems) and tenascin C was immunoprecipitated with 4 μ g of antibody (Santa Cruz) for 4 hr at 4 °C, followed by 30 μ L of Protein-A-sepharose for 2 more h.

A2.6. References

1. Karsten U, *et al.* (1988) A new monoclonal-antibody (A46-B/B10) highly specific for the blood group-H type-2 epitope - generation, epitope analysis, serological and histological-evaluation. *Brit. J. Cancer* 58(2):176-181.
2. Jork R, *et al.* (1991) Monoclonal-antibody specific for histo-blood group antigens-H (type-2 and type-4) interferes with long-term-memory formation in rats. *Neurosci. Res. Commun.* 8(1):21-27.
3. Murrey HE, *et al.* (2006) Protein fucosylation regulates synapsin Ia/Ib expression and neuronal morphology in primary hippocampal neurons. *Proc. Natl. Acad. Sci. USA* 103(1):21-26.
4. Christie TL, Starovic-Subota O, & Childs S (2006) Zebrafish collapsin response mediator protein (CRMP)-2 is expressed in developing neurons. *Gene Express. Patt.* 6(2):193-200.
5. Goshima Y, Nakamura F, Strittmatter P, & Strittmatter SM (1995) Collapsin-induced growth cone collapse mediated by an intracellular protein related to unc-33. *Nature* 376(6540):509-514.
6. Li W, Herman RK, & Shaw JE (1992) Analysis of the caenorhabditis-elegans axonal guidance and outgrowth gene unc-33. *Genetics* 132(3):675-689.
7. Chen CY, Sakisaka T, & Balch WE (2005) Use of hsp90 inhibitors to disrupt GDI-dependent rab recycling. *Gtpases Regulating Membrane Targeting and Fusion*, (Methods in Enzymology), Vol 403, pp 339-347.
8. Ricard CS, *et al.* (2001) Drosophila rab GDI mutants disrupt development but have normal rab membrane extraction. *Genesis* 31(1):17-29.
9. Soussand J, Jahke R, Simon-Assmann P, Stoeckel ME, & Schimchowitsch S (2001) Tenascin and laminin function in target recognition and central synaptic differentiation. *Neuroreport* 12(5):1073-1076.
10. Jones FS & Jones PL (2000) The tenascin family of ECM glycoproteins: Structure, function, and regulation during embryonic development and tissue remodeling. *Develop. Dynam.* 218(2):235-259.
11. Evers MR, *et al.* (2002) Impairment of L-type Ca²⁺ channel-dependent forms of hippocampal synaptic plasticity in mice deficient in the extracellular matrix glycoprotein tenascin-C. *J. Neurosci.* 22(16):7177-7194.
12. Ronn LCB, Hartz BP, & Bock E (1998) The neural cell adhesion molecule (NCAM) in development and plasticity of the nervous system. *Exper. Gerontol.* 33(7-8):853-864.
13. Cervoni L, Ferraro A, Eufemi M, & Turano C (1990) Fucose-carrying nuclear glycoproteins - distribution and tissue-specificity. *Ital. J. Biochem.* 39(6):368-374.
14. Feng YY & Walsh CA (2001) Protein-protein interactions, cytoskeletal regulation and neuronal migration. *Nat. Rev. Neurosci.* 2(6):408-416.
15. Abad MA, Enguita M, DeGregorio-Rocasolano N, Ferrer I, & Trullas R (2006) Neuronal pentraxin 1 contributes to the neuronal damage evoked by amyloid-beta and is overexpressed in dystrophic neurites in Alzheimer's brain. *J. Neurosci.* 26(49):12735-12747.

16. Tai H-C, Khidekel N, Ficarro SB, Peters EC, & Hsieh-Wilson LC (2004) Parallel identification of O-GlcNAc-modified proteins from cell lysates. *J. Am. Chem. Soc.* 126:10500-10501.
17. Khidekel N, *et al.* (2007) Probing the dynamics of O-GlcNAc glycosylation in the brain using quantitative proteomics. *Nat. Chem. Biol.* 3(6):339-348.

Appendix 3: Protein Fucosylation in FUT1 and FUT2 Transgenic Knockout Mice

A3.1. Results

Neurite Outgrowth of Cultured FUT1 and FUT2 KO mice

As $\text{Fu}\alpha(1-2)\text{Gal}$ carbohydrates have been implicated in neurite outgrowth pathways, we sought to address whether FUT1 and FUT2 mice, which do not express the $\text{Fu}\alpha(1-2)\text{Gal}$ epitope, had defects in neuronal growth. We cultured hippocampal neurons in a substratum of poly-DL-lysine for 2 days to examine neurite lengths. Surprisingly, we saw no difference between the length of neurites between wild-type, FUT1 or FUT2 KO mice (Figure A3.1). This may suggest that the neurons respond to a $\text{Fu}\alpha(1-2)\text{Gal}$

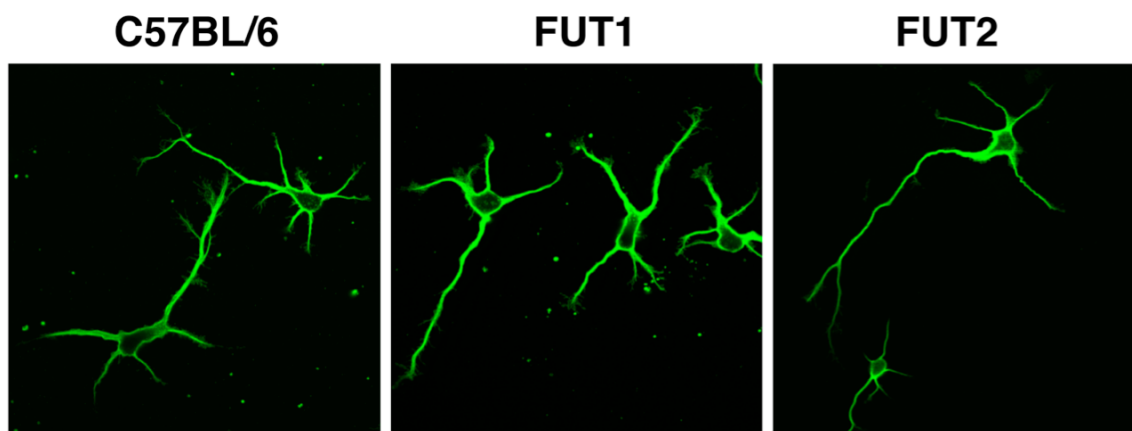


Figure A3.1. Deletion of FUT1 or FUT2 does not affect neurite outgrowth. Cultured hippocampal neurons from wild-type C7BL/6, FUT1, and FUT2 knockout mice were cultured for 2 DIV and stained with tubulin.

epitope secreted or present on other cell types such as glial cells or oligodendrocytes. In addition, there could be compensatory effects from knockdown of one gene, in which case the other fucosyltransferase can take over and synthesize $\text{Fu}\alpha(1-2)\text{Gal}$ glycoconjugates on the cell surface, which has never been investigated in cell culture

experiments. Furthermore, other neuronal growth pathways may compensate for loss of fucosyl expression in mediating neurite outgrowth.

Fut1 Regulates the Fuc α (1-2)Gal Proteome in Murine Olfactory Bulb while FUT2 Regulates Expression of Fuc α (1-2)Gal Glycoproteins in the Hippocampus

We next examined whether FUT1 or FUT2 could regulate the proteome in various adult mouse brain fractions including the cortex, cerebellum, hippocampus, striatum, and olfactory bulb. We first examined recognition by antibody A46-B/B10 in addition to the Fuc α (1-2)Gal-specific lectin UEA1. Surprisingly, we did not see any difference in bands from most brain fractions labeled from antibody A46-B/10, suggesting a redundancy of Fuc α (1-2)Gal expression or compensation by the other enzyme. We did observe a reduction in intensity of bands in the cerebellum of both FUT1 and FUT2 KO animals at ~35, 32, 27, and 25 kDa (Figure A3.2). These data suggest that FUT1 and FUT2 either do not regulate or play redundant functions in the synthesis of the majority of Fuc α (1-2)Gal glycoproteins recognized by this antibody.

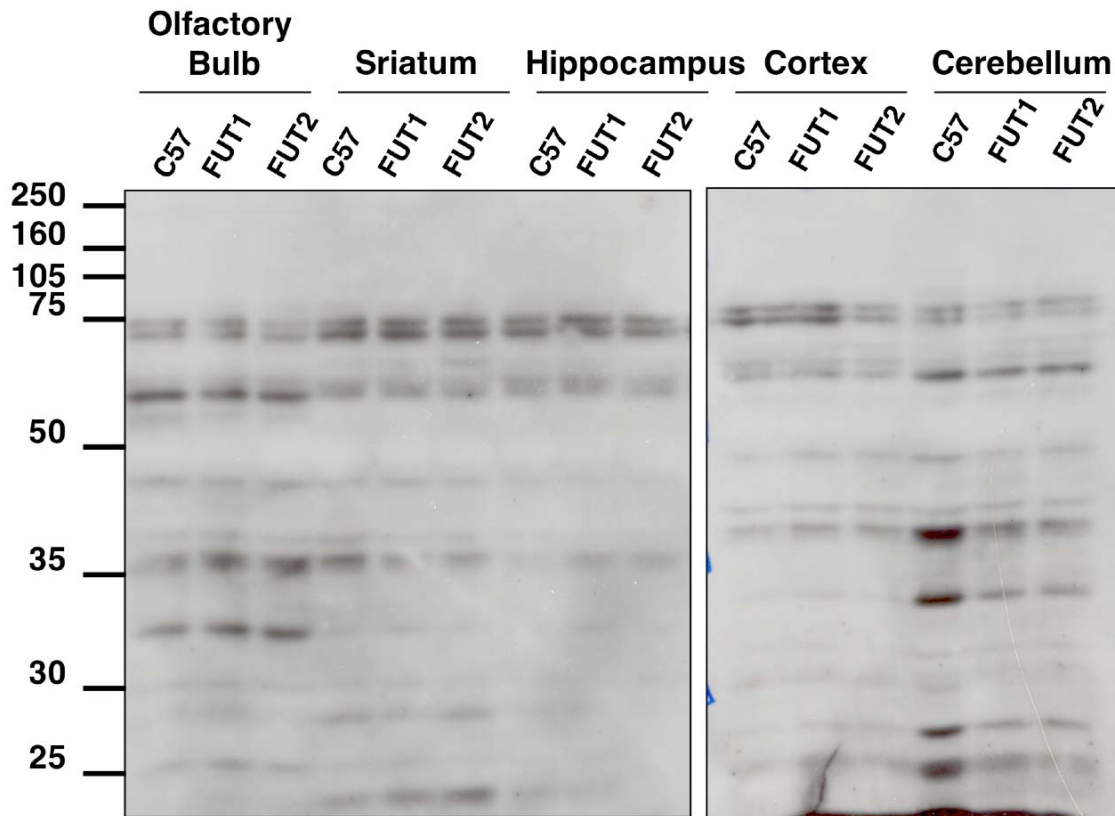


Figure A1.2. Neither FUT1 nor FUT2 regulates the fucose proteome recognized by antibody A46-B/B10. Adult mouse brain fractions from C57BL/6, FUT1, or FUT2 were homogenized, separated by SDS-PAGE, and analyzed by immunoblotting with Fuc α (1-2)Gal-specific antibody A46-B/B10. Neither FUT1 nor FUT2 was found to regulated the majority of glycoproteins, except for several low molecular weight glycoproteins in the cerebellum.

In contrast, we observed a significant loss of staining of Fuc α (1-2)Gal glycoproteins from the olfactory bulb of transgenic FUT1 knockout mice (Figure A1.3). In addition, UEAI lectin largely recognized a different subset of glycoproteins than antibody A46-B/B10. The majority of fucosylated glycoproteins were between 50 and over 250 kDa. Interestingly, in FUT2 KO mice, expression of Fuc α (1-2)Gal glycoproteins is upregulated, suggesting potential cross-talk between FUT1 and FUT2 regulation. In the cerebellum, we observed a decrease in fucosylation of glycoproteins at ~30, 28, 25, and 24 kDa in both FUT1 and FUT2 KO animals. These proteins are similar

in molecular weights to the proteins observed from antibody A46-B/B10, suggesting that they may be the same glycoproteins. In addition, we only observed significant levels of

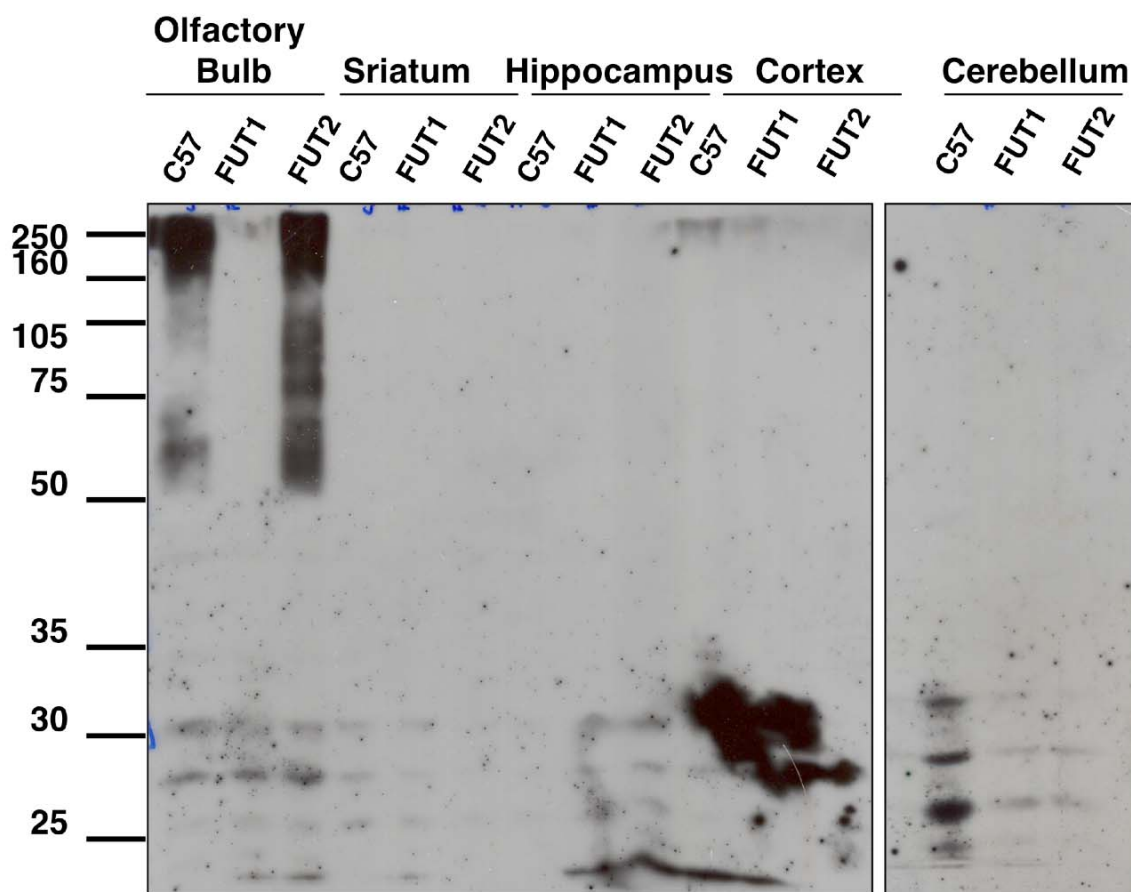


Figure A1.3. The adult mouse olfactory bulb is enriched in expression of $Fucc\alpha(1-2)Gal$ disaccharides and the proteome is regulated by FUT1. In the cerebellum, there is reduced expression of fucose on low molecular weight glycoproteins in both FUT1 and FUT2 KO animals.

$Fucc\alpha(1-2)Gal$ glycoproteins in the olfactory bulb of adult mouse brain, suggesting that this brain region is significantly enriched in this plasticity-relevant epitope and is discussed in Chapter 4.

We also examined darker exposures to see if we could detect $Fucc\alpha(1-2)Gal$ glycoproteins from other brain regions in C57BL/6 and FUT2 transgenic KO animals.

While $\text{Fuc}\alpha(1-2)\text{Gal}$ glycoproteins were highly over exposed from the olfactory bulb, we observed that the hippocampus is the next brain region with enriched expression of $\text{Fuc}\alpha(1-2)\text{Gal}$. Furthermore, expression of $\text{Fuc}\alpha(1-2)\text{Gal}$ was completely ablated in FUT2 knockout mice (Figure A1.4). However, we are still in the process of repeating these experiments with FUT1 KO mice to determine the role of FUT1 in synthesis of fucosyl glycoproteins in the hippocampus.

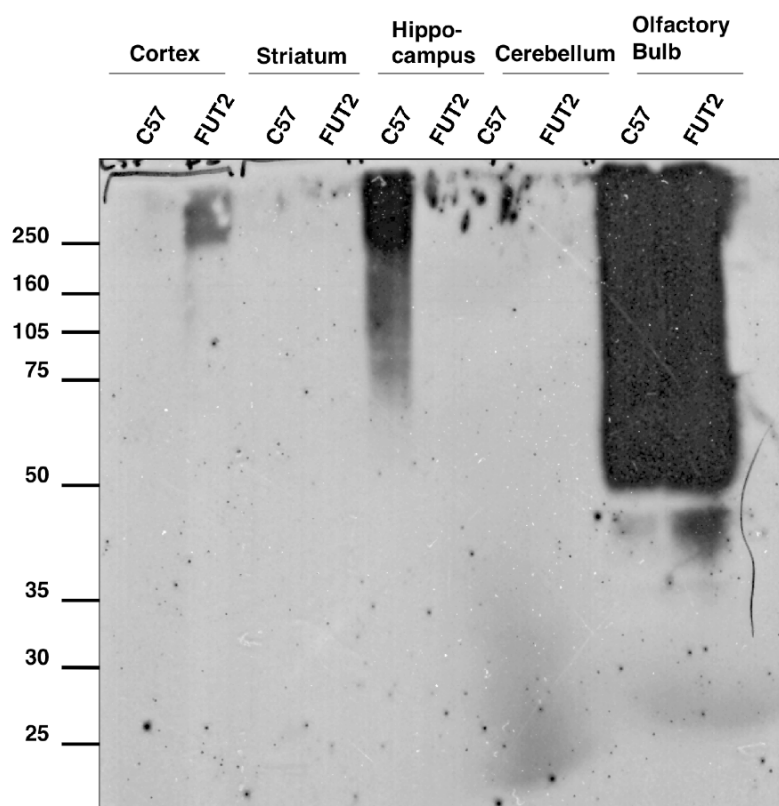


Figure A1.4. The $\text{Fuc}\alpha(1-2)\text{Gal}$ proteome is regulated by FUT2 in the hippocampus of adult mouse brain. Blots were probed with UEAI.

We also examined expression and localization of $\text{Fuc}\alpha(1-2)\text{Gal}$ glycoproteins in olfactory bulb and hippocampal slices of adult mouse brain. We observed staining of the

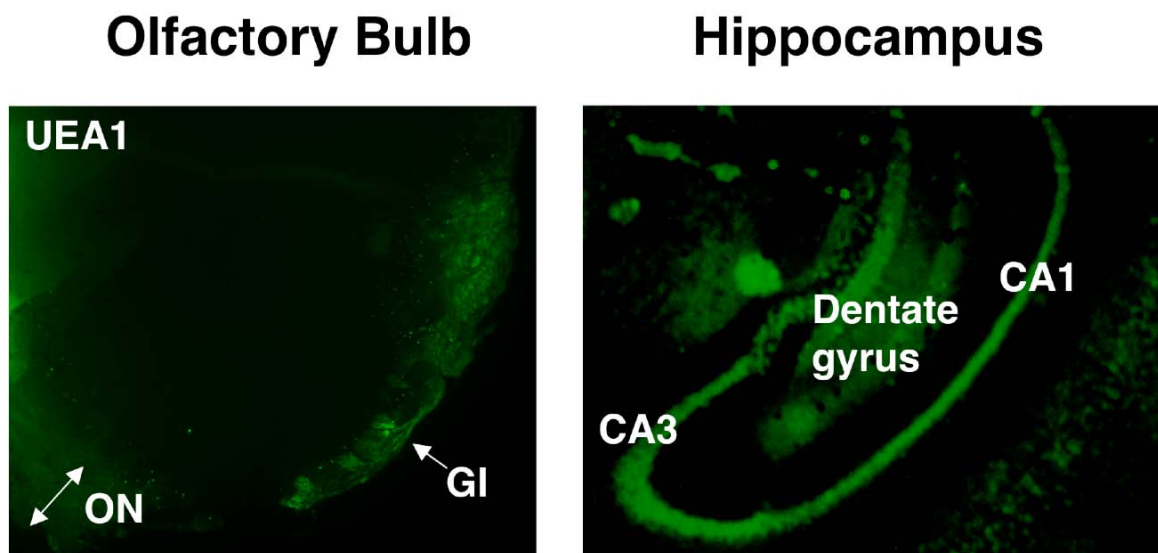


Figure A1.5. Immunohistochemistry of adult mouse brain slices from the olfactory bulb and hippocampus. Sections were labeled with UEA1 conjugated to fluorescein. In the olfactory bulb (left panel), there was strong labeling of the olfactory nerve layer (ON) and glomerular layer (GI). In the hippocampus, $\text{Fuc}\alpha(1-2)\text{Gal}$ glycoconjugates are present in the CA1, CA3, and dentate gyrus regions.

olfactory nerve layer and the glomerular layers in the olfactory bulb of C57BL/6 animals (Figure A1.5, left panel). In the adult hippocampus, we observe staining in the CA1, CA3, and dentate gyrus, consistent with a role for $\text{Fuc}\alpha(1-2)\text{Gal}$ in learning and memory formation (Figure A1.5, right panel).

Discussion

FUT1 and FUT2 transgenic knockout mice have been analyzed in blastocyst adhesion and the gastrointestinal system. Here, we examined the roles of FUT1 and

FUT2 in the brain. While Fuc α (1-2)Gal carbohydrates have been implicated in neurite outgrowth pathways, we did not observe any defects in neurite length of cultured hippocampal neurons. This may suggest that knockout of both Fuc α (1-2)Gal-synthesizing enzymes is necessary to observe any effects on neurite outgrowth. Furthermore, the neurite outgrowth pathways mediated by Fuc α (1-2)Gal may be presented on glia or secreted proteins in the extracellular matrix, in which case hippocampal neuronal culture experiments may not reveal the effects of neurite outgrowth. In addition, there may exist as yet unidentified fucosyltransferases that are responsible for the growth promoting effects of Fuc α (1-2)Gal disaccharides.

The mouse olfactory bulb was found to be the brain region with the highest expression of Fuc α (1-2)Gal, followed next by the hippocampus, two brain regions that retain a high degree of plasticity in the adult animal. Interestingly, FUT1 regulates the Fuc α (1-2)Gal glycoproteome in both adult and neonatal mice whereas FUT2 has no effect, suggesting that FUT1 is the predominant enzyme for the synthesis of Fuc α (1-2)Gal in the olfactory bulb. We also observed a loss of expression of Fuc α (1-2)Gal in the hippocampus of FUT2 transgenic mice, but we were unable to determine whether FUT1 also plays a role in this brain region. Our data suggest that in some tissues, only one enzyme can be active, whereas in other tissues, FUT1 and FUT2 may compensate or have redundant functions such as in blastocyst adhesion.

Materials and Methods

See Chapter 4.